UNIVERSITAT DE BARCELONA

The role of SIRT1 and SIRT6 in epigenetic regulation of genome stability under stress

George Rasti Zaghiyan

Universitat de Barcelona

Facultat de Biologia

Programa de Doctorat en Biomedicina

THE ROLE OF SIRT1 AND SIRT6 IN EPIGENETIC REGULATION OF GENOME STABILITY UNDER STRESS

Thesis presented by George Rasti Zaghiyan in order to obtain the degree of Doctor by Universitat de Barcelona (UB) 2021.

Instituto de Investigación CONTRA LA LEUCEMIA Josep Carreras

UNIVERSITAT DE BARCELONA

PEBC
Cancer Epigenetics and Biology Program
Programa d'Epigenètica i Biologia del Càncer
Programa de Epigenética y Biología del Cáncer

Universitat de Barcelona

Facultat de Biologia

Programa de Doctorat en Biomedicina

THE ROLE OF SIRT1 AND SIRT6 IN EPIGENETIC REGULATION OF GENOME STABILITY UNDER STRESS

Thesis presented by George Rasti Zaghiyan in order to obtain the degree of Doctor by Universitat de Barcelona (UB).

This thesis has been realized under supervision of Dr. Alejandro Vaquero García from the Cancer Epigenetics and Biology Program(PEBC) of IDIBELL and Cancer and Leukemia Epigenetics and Biology Program (PEBCL) of IJC

George Rasti Zaghiyan
Firmado digitalmente por George Rasti Zaghiyan
Fecha: 2021.06.14 23:03:15 +02'00'

Student:
George Rasti Zaghiyan

VAQUERO GARCIA ALEJANDRO - 52461768X
Firmado digitalmente por VAQUERO GARCIA ALEJANDRO - 52461768X
Fecha: 2021.06.01 13:04:41 +02'00'

Director:
Dr. Alejandro Vaquero Garcia

Marta Giralt Oms - DNI 40304679P (TCAT)
Signat digitalment per Marta Giralt Oms - DNI 40304679P (TCAT)
Data: 2021.05.27 14:22:20 +02'00'

Tutor:
Dr. Marta Giralt Oms

This thesis is dedicated to my family

For their endless love and support

INDEX

Abstract

The Sirtuin family of NAD^+-dependent enzymes plays a key role in the maintenance of genome integrity upon stress. Sirtuins coordinate the response to different forms of stress at different levels and have been involved in a wide range of processes directly linked to tumorigenesis such as genome stability, cell cycle regulation, apoptosis, senescence and DNA repair. The main objective of this work was to deepen the role of Sirtuins in genome stability and cancer. This has been fulfilled through the development of two specific objectives: First, to define the factors that contribute to the role of SIRT6 in tumorigenesis. Second, to decipher the role of SIRT1 in DNA damage signaling and repair.

SIRT6 is an important regulator of genome stability and metabolic homeostasis and has been shown to work as a tumor suppressor. This antitumoral activity is directly associated to the epigenetic silencing of a specific set of genes involved in glucose metabolism, but little is known about the partners of SIRT6 in this functional context. Previous studies of the group identified two histone H3K9 specific histone methyltransferases (HMTs) Suv39h1 and G9a, as interaction partners of SIRT6. Both Suv39h1 and G9a are responsible for methylation of H3K9, a hallmark of heterochromatin organization, transcriptional repression, and epigenetic silencing. Several studies have shown correlation of altered expression of Suv39h1 and G9a in cancer. In the first specific objective of the thesis, we studied the functional relationship between SIRT6 and Suv39h1 as well G9a to provide evidence about the mechanism behind the described tumor suppressor activity of SIRT6. Our results support a direct functional link between SIRT6 and Suv39h1 in tumor supression in contrast to G9a.

Sirtuins have been also implicated in the regulation of the DNA damage response (DDR) signaling, and DNA repair, being SIRT1 is the best studied Sirtuin in this functional context. In the second specific objective, we studied the role of SIRT1 in DNA damage signaling. SIRT1-deficient cells show impairment of the DDR, which result in an increased genome instability and decreased levels of γH2AX. Phosphorylation of S139 in histone H2A variant H2AX (γH2AX) is a hallmark of DNA damage signaling. Upon repair completion, γH2AX must be dephosphorylated. Protein phosphatase 4 (PP4) complex dephosphorylates key targets such as γH2AX and RPA2 and it is particularly relevant

because its depletion induces γH2AX hyperphosphorylation and alters DNA damage efficiency. RPA2 is a subunit of the trimeric complex RPA, which binds to single-stranded DNA during the repair of DSB and ssDNA damage. We demonstrated that upon DNA damage SIRT1 interacts specifically with PP4 complex (PP4C, PP4R2 and PP4R3α/β) and promotes its inactivation through deacetylation of the WH1 domain of the PP4R3α/β regulatory subunits. Our findings demonstrated that SIRT1-PP4 interplay regulates γH2AX and RPA2 phosphorylation levels and DDR progression. SIRT1-mediated oxidative stress response and the DNA repair proteins PP4 complex and RPA2 provide a dynamic model of their regulation through SIRT1 to ensure genome stability.

Overall, these findings of this thesis improve our understanding of the functional implications of and SIRT1 and SIRT6 in genome stability and DNA damage signaling and reinforce the key contribution of Sirtuins to genome stability, stress response and cancer.

List of Abbreviations

29-OAADPr	29-O-acetyl-ADP-ribose
29-OMADPr	29-O-malonyl-ADP-ribose
29-OSADPr	29-O-succinyl-ADP-ribose
AceCS2	Acetyl coenzyme A (CoA) synthetase 2
ANK	Ankyrin
ARTDs	ADP-ribosyltransferases
AS	Atherosclerosis
ATG	Autophagy-related gene
ATM	Ataxia–telangiectasia mutated protein kinase
BAT	Brown adipose tissue
BER	Base excision repair
BRCA1	Breast cancer 1
BRD	Bromodomain
BrdU	Bromodeoxyuridine
CBP-1	CREB-binding protein 1
CCBB	Coomsassie-blue
CD	Chromodomain
CH	Constitutive heterochromatin
ChIP-seq	Chromatin immunoprecipitation sequencing
CPS1 or CPSI	Carbamoyl phosphate synthetase 1
CPT	Camptothecin
CSD	C-terminal chromo shadow domain
CTE	C-terminal extension
Cys	Cysteine
DBC1	Deleted in breast cancer 1
DC	Double crosslinking
ddH20	Double distilled water
DDR	DNA damage response
DMSO	Dimethyl sulfoxide
DNA-PK	DNA-dependent protein kinase
DNA–PKcs	DNA–PK catalytic subunit
Doxo	Doxycycline
DSB	Double strand break repair
DSG	Disuccinimidyl glutarate
DUBs	Deubiquitinating enzymes
ECM	Cell-extracellular matrix
eNoSC	Energy- dependent nucleolar silencing complex
ERK	Extracellular signal-regulated protein kinases
Exo1	Exonuclease 1
EZH2	Enhancer of zeste homolog 2
FAO	Fatty acid oxidation
Fapy-G	Formamidopyrimidine
FH	Facultative heterochromatin
FOXO3a	Forkhead box O 3a
FPG	Giemsa
G6PC	Glucose-6-phosphatase catalytic subunit
G6PD	Glucose 6-phosphate dehydrogenase
GDH	Glutamate dehydrogenase
GG-NER	Global genome nucleotide excision repair
GO	Gene ontology
GREAT	Genomic regions enrichment of annotations tool
H2AK119ub	Monoubiquitination of H2A at Lys119
H2BK123ub	Monoubiquitination of H2B at Lys123
H_2O_2	Hydrogen Peroxide

H3K9me3	Trimethylation of H3K9
H3N	N-terminal histone tail of histone H3 Wt
H3ph	Histone phosphorylation
HATs	Histone acetyltransferases
HCC	Hepatocellular carcinoma
HDACs	Histone deacetylases
hESCs	Human embryonic stem cells
HGP	Hepatic glucose production
Hh	Hedgehog
HIF-1α	Hypoxia-inducible factor 1 α
HOCl	Hypochlorous acid
HP1	Heterochromatin protein 1
HR	Homologous recombination
IP	Immunoprecipitation
iPSCs	Induced pluripotent stem cells
IR	Ionizing radiation
IRE1α	inositol requiring kinase enzyme 1α
ISO	Isoproterenol
JNKs	C-Jun N-terminal protein kinases
K	Lysine
KATs	Lysine acetyltransferases
KEGG	Kyoto encyclopedia of genes and genomes
KMTs	Lysine methyltransferases
LCAD	Long-chain acyl-CoA dehydrogenase
LDL	Low-density lipoprotein
LINEs	Long interspersed nucleotide elements
LXRs	Liver X receptors
mADPRTs	Mono-ADP-ribosyltransferase
Mage-a	Melanoma-associated antigen-a
MAPK	Mitogen-activated protein kinase
MCD	Mitochondrial malonyl-CoA decarboxylase
MMC	Mitomycin C
MMR	Mismatch repair
MnSOD	Manganese superoxide dismutase
MRN	MRE11-Rad50-NBS1 complex
NAM	Nicotinamide
NBS1	Nibrin
NER	Nucleotide excision repair
NF-κB	Nuclear factor kappa B subunit
NHEJ	Non-homologous end joining
NI	Non- expressing
NML	Nucleomethylin
NTE	N-terminal extension
OA	Okadaic acid
OAADPR	O-acetyl-ADPribose
OGG1	8-oxoguanine-DNA glycosylase
OTC	Ornithine transcarbamoylase
ox-LDL	Oxidized low density lipoprotein-cholesterol
PAF53	polymerase-associated factor 53
PARP1	Poly-(adenosine diphosphate-ribose) polymerase 1
PCK1	Phosphoenolpyruvate carboxykinase 1
PFA	Paraformaldehyde
PGAM2	Phosphoglycerate mutase 2
PHD	Plant homeodomain
PIKKs	Phosphatidylinositol 3-OH-kinase-related kinases
PKM2	Pyruvate kinase M2
Pol η	DNA polymerase η

PP2A	Protein Phosphatase 2A
PP2AC	PP2A catalytic subunit
PP4	Protein phosphatase 4
PP4C	PP4 catalytic subunit
PP6	Protein Phosphatase 6
PP6C	PP6 catalytic subunit
PPAR-γ	Peroxisome proliferator-activated receptor γ
PPIs	Protein-protein interactions
PPMs	Metal-dependent protein phosphatases
PPP	Phosphoprotein phosphatase
PRB	Phosphatase Reaction Buffer
PRC2	Polycomb repressive complex 2
PRMTs	Protein arginine methyltransferases
PTMs	Post-translational modifications
Q	Glutamine
R	Arginine
Rb	Retinoblastoma
rDNA	Ribosomal DNA
ROS	Reactive oxygen species
RPA	Replication protein A
SAM	S-adenosyl-L-methionine
Scr	Scramble
SINEs	Short interspersed nucleotide elements
Sirt6$^{-/-}$	SIRT6-deficient cells
SOD2	Superoxide dismutase 2
ssDNA	Single-stranded DNA damage
SUMO	Small ubiquitin-related modifier
TC-NER	Transcription-coupled repair
TGF	Transforming growth factor
TLS	Translational synthesis
WAT	White adipose tissue
WNT	Wingless-related integration site
WRN	Werner syndrome ATP-dependent helicase
XP	Xeroderma pigmentosum
XRCC1	X-ray cross-complementing-1
γH2AX	Histone H2A variant H2AX at serine 139
γ-satellite	Major satellite repeats

INTRODUCTION

1. Chromatin structure and organization

In eukaryotic chromatin, the DNA double helix is packed in a nucleoprotein complex named Chromatin. The word chromatin derives from word “chroma” (color in Greek) due to its staining properties in initial cytological studies. The basic unit of chromatin is the nucleosome, which contains 145 to 147 base pairs (bp) of DNA wrapped in 1.67 left-handed superhelical turns around a histone octamer (Lugar et al., 1997; Davey et al., 2002; Ong et al., 2007). Each histone octamer contains two copies of each core histone protein: H2A, H2B, H3 and H4.

Despite the structure of the nucleosome core particles have been solved two decades ago, the structure of the full nucleosome and linker histone H1 structure remains unclear (Zhou et al., 2013; Bednar et al., 2017). The nucleosomes play a key role in regulating all nuclear processes such as replication, transcription, recombination, and DNA repair (Felsenfeld et al., 2003; Kornberg, 2007; Jiang et al., 2009). The core histones are assembled into a spool-like structure into which the core DNA is wrapped, the remaining mass of the core histones includes the largely structurally undefined but evolutionarily conserved domains or histone tails. These domains are localized at the N-terminal of all four core histone proteins and the C-terminus of H2A. They were primarily described by their sensitivity to proteases, indicating their highly dynamic nature referring to the known ‘structured’ domains (Bohm et al., 1984).

Chromatin is structured in a successive hierarchy of orders of organization being the basic string or nucleosomes, also known as beads-on-a-string or 11-nm fibers, the most basic form of chromatin structure. These structures compact *in vitro* into a closed zigzag structure of 30 nm fibers in higher ionic strength and in the presence of histone H1. Interestingly, although the chromatin extracted from diverse cell types under physiological conditions were originally described as mainly present in the form of 30-nm fibers, the *in vivo* existence of the 30-nm chromatin fiber in the vast majority of eukaryotic cells has been questioned by several reports (Fusser et al., 2012; Gan et al., 2013) and is currently under debate. It is openly accepted by many researchers that the 30 nm fibers are absent from many eukaryotic nuclei *in vivo*, and chromatin seems to form irregularly folded chains with zigzag conformations (Scheffer et al., 2011). However, some authors have provided evidences of their existence by cryo-EM in the

nuclei of two specific cell types, starfish sperm and chicken erythrocytes (Woodcock, 1994). Both are terminally differentiated cells with minimal transcriptional activity, which suggests that these structures may exist beyond *in vitro* conditions under very specific conditions (Maeshima et al., 2016).

1.1. Heterochromatin structure and function

The original observation of differential chromosomal staining by Emil Heitz in 1928, forms the basis of the classification of eukaryotic genomes into two main functional states. Lighter stained chromatin, or euchromatin, correlates to a more open and transcriptionally active conformation, while patches of darker stained zones, or heterochromatin, corresponds to a condensed and transcriptionally inactive conformation. Heterochromatin has been further sub classified into facultative and constitutive heterochromatin. Constitutive heterochromatin (CH) has a structural role, encompasses large regions of the genome, harbors a very limited amount of genes and forms stable structures that once established, are maintained through cell generations.

The major bulk of constitutive heterochromatin is found at pericentromeric regions and telomeres. They are mainly formed by tandem repetitions, so called satellites, which vary in size from 5bp to some hundreds bp. In contrast, facultative heterochromatin (FH) corresponds to regions within euchromatin that are established in response to specific conditions, such as development or differentiation. FH are enriched in genes and can involve from few genes to a whole chromosome, such as the mammalian female inactive X-chromosome. In contrast to CH, FH can revert to euchromatin under certain conditions (reviewed in Bizhanova and Kaufman, 2020).

2. Histone post-translational modifications and their functional significance

The N-terminal and C-terminal tails of histones undergo reversible PTMs but many of them take place in the globular domain as well. This forms a complex regulatory network, known as histone code that enables multiple types of crosstalk between different PTMs (reviewed in Eymery et al., 2009). Although the first histone post-translational modifications (PTMs), acetylation and methylation, were discovered more than 50 years ago (Allfrey et al., 1964), their functional significance was not fully

addressed until 30 years later. The discovery of the first enzymes involved in the regulation of acetylation, histone acetyltransferases (HATs) and histone deacetylases (HDACs), and their link to gene expression and transcriptional regulation boosted the characterization of these PTMs. To this data, a wide range of PTMs have been described in addition to lysine acetylation and methylation, such as phosphorylation, SUMOylation, ubiquitination, crotonylation, butyrylation, propionylation, citrullination or ADP-ribosylation, among others (reviewed in Eymery et al., 2009).

Histone PTMs regulate virtually all functions associated to DNA function, expression dynamics and structure. They can regulate these functions through two major mechanisms: First, by inducing directly structural alterations in chromatin. Second, by working as recognition sites of specific mediators that can in turn promote specific regulatory responses. Another interesting feature is that there can be interplay between different histone modifications, allowing further levels of control in regulation of chromatin function. There are three types of factors involved the regulation of dynamics and function of post translational histone modifications: writers, readers and erasers. Writers are the enzymes that deposit these PTMs while erasers are responsible for their removal. Readers are proteins that bind specifically to PTMs through a wide range of protein domains and mediate the functional input of these modifications, such as the regulation of chromatin structure and gene expression.

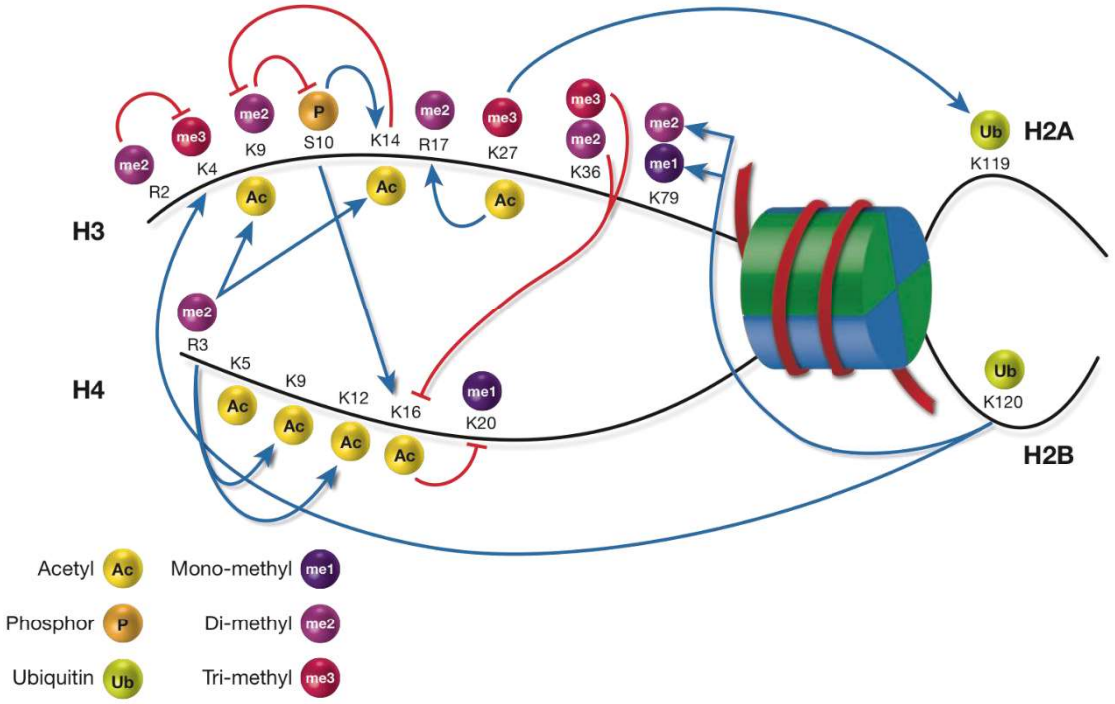

Figure 1. Cross-talk between histone PTMs. Positive and negative interplays between histone modifications. This crosstalk can take place on the same histone tail (cis crosstalk) or between different histone tails (trans crosstalk). Arrows heads and flat heads indicate positive and negative effects, respectively (adapted from Simonet et al., 2016).

They can modulate protein functions in all eukaryotes and have a ubiquitous role in wide range of cellular functions. The most relevant PTMs include acetylation, methylation, ubiquitination, SUMOylation, ADP-ribosylation and phosphorylation (reviewed in Gillette et al., 2015).

2.1. HISTONE LYSINE ACETYLATION

The Nε-acetylation of lysine residues is a major covalent modification involved in gene transcription, chromatin regulation, and DNA repair signaling. Acetylation is unique modification as it's the only PTM that has been shown to regulate directly the folding of the chromatin fiber (Bascom and Schlick, 2017). Acetylation neutralizes lysine's positive charge and weaken the electrostatic interaction between histones and negatively charged DNA which exposes the DNA to regulatory proteins. Therefore, histone acetylation is generally associated with an ''open'' chromatin structure. The importance of acetylation is reflected by the fact that they participate in virtually all chromatin associated functions including transcription, DNA repair, DNA replication, genome structure and architecture, cell cycle and stress response, among others. Despite all

these functional implications, one of the major roles of these PTMs is the control of gene expression. Thus, the genome-wide distribution of histone acetylation monitored by ChIP-seq analysis shows that acetylation tends to be mainly concentrated at promoters and enhancers and, interestingly in several cases, throughout the transcribed region of active genes (Bannister et al., 2011).

Acetylated lysines can also be recognized by specific readers that mediate acetylation-related functional outputs. The main protein domains recognizing acetylation described so far are bromodomains (BRD) , tandem plant homeodomain (PHD) fingers and YEATS domains (Li et al.,2006). Histone acetylation marks are highly dynamic and reversible modifications regulated by the antagonistic activities of two enzyme families, lysine acetyltransferases (KATs), also known as histone acetyltransferases (HATs), and histone deacetylases (HDACs). The antagonism between both factors represents one of the major regulation mechanisms for gene transcription in the cells. Importantly, both KATs and HDACs not only deacetylate histones, but also target many non-histone proteins involved in a wide variety of functions (Yang et al., 2007).

KATs were the first histone modifying enzymes described. They can be classified into two main types: (1) nuclear or type-A, which is localized in nucleus and can be classified into the GNAT, MYST, and CBP/p300 families. (2) Type-B, which are primarily cytoplasmic and modify free histones (Table 1), and KATs were the first enzymes shown to modify histones (Parthun et al., 2007).

HAT family	HAT enzyme	Histone substrates	Cellular related Functions
GNAT	Gcn5	H2B, H3.	Coactivator, DNA replication
	PCAF	H3, H4	Coactivator
	Hat1	H2B, H4 (K5, K12)	Histone deposition, silencing, DNA replication
	Elp3	H3, H4	Transcriptional elongation
	Hpa2	H3, H4	Unknown
	ATF-2	H2B, H4	Sequence specific transcription factor
	Sas2	H4K16	Silencing, DNA replication

MYST	Sas3	H2A, H3, H4	Silencing
	MORF	H3, H4	Transcriptional activation
	TIP60	H2A, H3, H4	Transcriptional activation, DNA repair, apoptosis
	Esa1	H4, H2A	Cell cycle progression, DNA silencing
	MOF	H4K16	Transcriptional activation, DNA repair, Xchromosome hyperactivation
	HBO1	H3, H4	DNA replication
	MOZ	H2A, H3, H4	Transcriptional activation
P300/CBP	P300	H2A, H2B, H3, H4	Coactivator
	CBP	H2A, H2B, H3, H4	Coactivator
SRC	ACTR	H3, H4	Hormone receptor coactivator
	SRC-1	H3, H4	Hormone receptor coactivator
	TIF2	Unknown	Hormone receptor coactivator

Table 1. Summary of HATs members, histone specificity and linked cellular functions. HATs serve many biological roles inside the cell because they target a wide variety of histones and interact with different partners.

HDACs are a family of enzymes that can reverse lysine acetylation and restore the positive charge of the histone tails. There are more than 18 HDACs identified, which have been subdivided into four main classes, depending on sequence homology. Class I (HDAC 1-3 and HDAC8) and class II (HDAC 4-7 and HDAC 9-10) are closely related to yeast scRpd3 and scHda1, while Class III members, also known as Sirtuins, are homologous to yeast scSir2. Class IV contains only HDAC11 (Table 2) (Dell'Aversana et al., 2012). HDACs can be also divided based on the mechanism of deacetylation. Class I, II, and IV HDACs are metalloenzymes that requires a zinc metal ion and release acetyl group to the solution (Table 2). In contrast, Sirtuins share a distinct catalytic mechanism which depends on the catalytic cofactor NAD^+ (see later section 2), and involves the transfer of the removed acetyl group to ADP-ribose from NAD^+, resulting in a release of o-acetyl-ADPribose (OAADPR) to the media (Tanner et al.,2000).

HDAC family	HDAC enzyme	Histone substrates	Function
Class I (Rpd3)	HDAC1	H3ac, H4K16ac	Transcriptional repression
	HDAC2	H3(K56, K9)ac, H4K16ac	Transcriptional repression
	HDAC3	H2Aac, H3 (K9, K14)ac,H4(K5, K12)ac	Heterochromatin, DNA repair, Transcriptional repression, cell cycle
	HDAC8	H2A, HAB, H3, H4	Transcriptional repression, Heterochromatin formation, cell cycle
Class II (Hdal)	HDAC4	H3	Transcriptional repression, DNA repair
	HDAC5	Unknown	Transcriptional repression, heterochromatin formation, DNA replication
	HDAC6	Unknown	DNA repair, cell migration
	HDAC7	Unknown	Transcriptional repression
	HDAC9	H3, H4	Transcriptional repression
	HDAC10	H4	Transcriptional repression
Class III (Sir2)	SIRT1	H1K26ac, H3K9ac,H4K16ac	Transcriptional repression, heterochromatin formation, apoptosis, cell survival, cell cycle, DNA repair
	SIRT2	H4K16ac	Cell cycle, cell survival, DNA repair
	SIRT3	H3K9ac, H4K16ac	Transcriptional repression, DNA repair, cell death
	SIRT4	Unknown	Metabolism
	SIRT5	Unknown	Metabolism
	SIRT6	H3(K9,56)ac	DNA repair, Transcriptional repression, chromatin structure
	SIRT7	H3K18ac	rDNA regulation, Transcriptional repression
Class IV	HDAC11	H3, H4	Replication, Transcriptional repression

Table 2. Summary of HDACs members, histone specificity and related cellular functions. HDACs have different functions because they target a wide variety of histones and bind to many different partners.

2.2. HISTONE METHYLATION

Histone methylation is a reversible modification detected in lysines, arginines and histidines. In lysines, methylation occurs in the Nε-amino group (as acetylation), which could be mono-, di- or trimethylated. There are three types of arginine methylation: monomethyl arginine, asymmetric dimethyl arginine and symmetric dimethyl arginine. Unlike acetylation and phosphorylation, histone methylation does not alter the net charge of mentioned histone residues but increase their basicity and hydrophobicity which allows the selective recruitment of effector proteins (or readers) and transcriptions factors to DNA (Greer et al., 2012). In mammals, methylation of histone lysines typically occurs at Lys4, -9, -27, -36 and -79 of histone H3 and at Lys20 of histone H4 (Jung et al., 2010), while in arginine methylation, the most frequently methylated residues are Arg2, -8, -17 and -26 of histone H3, and Arg3 of histone H4 (Zhang et al., 2001).

The enzymes in charge of histone methylation are lysine methyltransferases (KMTs) and protein arginine methyltransferases (PRMTs). KMTs and PRMTs catalyze the transfer of a methyl group from S-adenosyl-L-methionine (SAM) to the ε-amino group of lysine or to the guanidine group of arginine (Schubert et al., 2003). KMTs have been classified into two main families, the SET-domain family (Cheng et al., 2005), which comprise the vast majority of KMTs, and DOT1 (Feng et al., 2002). The SET-domain family is subdivided into eight subfamilies: SUV39, SET1, SET2, EZ, RIZ, SMYD, SUV4-20 and the orphan members, which contain SET7/9 and SET8 (PR-SET7)(Dillon et al., 2005). PRMTs are classified into two main classes: Type I PRMTs (PRMT1, 2, 3, 4, 6, and 8), which catalyze the formation of both monomethyl arginine and asymmetric dimethyl arginine, and Type II PRMTs (PRMT5 and 7), which catalyze monomethyl arginine and symmetric dimethyl arginine modifications (Bedford et al., 2005).

As in the case of acetylation, histone methylation is involved in many functions from gene expression to chromatin structure. In contrast to acetylation, the functional diversity of methylation is based on the wide range of highly specific readers that recognize specific methylation states (mono-, di- and/or trimethylation in the case of lysines) in a specific residue. This specificity allows methylation to play roles in antagonistic functions. In the case of gene expression and chromatin structure, some

methylation marks participate in active transcription while others have been linked to gene silencing and heterochromatin (Yun et al., 2011). For instance, both H3K4me3 and H3K36me3 are found in active genes while H3K27me3 and H3K79me3 are hallmarks of inactive genes when are found in promoter and gene-body regions. Interestingly, active promoters are rich in H3K9me1, H3K27me1, H3K36me1, H4K20me1 and H2BK5me1 (Barski et al., 2007), whereas H3K4me1 is often related to enhancer function(Heintzman et al., 2007).

Histone methylation also plays an important role in the Heterochromatin structure. A common mark of constitutive heterochromatin is the trimethylation of H3K9 (H3K9me3), in contrast H3K27me3 is typically enriched on facultative heterochromatin. Both marks recruit distinct protein machineries to promote distinct biological features, but the final consequence in both cases is chromatin compaction. The constitutive heterochromatin is maintained by H3K9me3 which is essential for genome stability and for preventing abnormal chromosome segregation (Saksouk et al., 2015).

2.3. HISTONE PHOSPHORYLATION

Histone phosphorylation (H3ph) was first reported in 1960s (Gutierrez and Hnilica, 1967), and the responsible was shown to be a kinase named AMP-dependent kinase (Langan, 1968). Subsequently Shoemaker and Chalkley observed that a cAMP-independent protein kinase phosphorylates histone H3 *in vivo* during metaphase of cell cycle at a single tryptic peptide (Shoemaker and Chalkley, 1978). Paulson and Taylor reported that cAMP-dependent kinase is capable of phosphorylating H3 on Serine 10 (H3S10) *in vitro* (Paulson and Taylor, 1982). Afterwards, a large number of kinases have been identified as histone H3S10 kinases *in vivo*, like PKA and Aurora B. These protein kinases can be classified in signal transduction kinases and mitotic histone kinases, which reflects the importance of Serine 10 phosphorylation in cell cycle control (Wei et al., 1999).

H3ph has been linked to the control of gene expression and mitosis. In this sense, it is often found on genomic regions of transcriptionally active genes where participates in processes requiring opposing chromatin states. Among the main H3ph marks, H3S10

phosphorylation is considered to be a key event for mitosis entry, as a first stage of chromatin hypercompaction. This modification appears in early G2 within the pericentromeric heterochromatin (Hendzel et al., 1997) and spreads by metaphase throughout all chromosomes promoting mitotic chromosome condensation. In addition to H3S10 (Gurley et al., 1978), histone H3 is also phosphorylated during mitosis on H3S28 (Goto et al., 1999). In the context of mitosis, the best described H3 kinases are Aurora kinases A and B, which interact with the H3 tail and can phosphorylate both H3S10 and H3S28. However, Aurora-A seems to be a more efficient H3 kinase than Aurora-B due to diverse signaling requirements of Aurora-B (Giet et al., 2001).

In contrast, histone H2A phosphorylation has been generally linked to DNA Repair. In this sense phosphorylation of histone H2A variant H2AX at serine 139 (γH2AX) is a hallmark of DNA damage and repair in mammals (Rogakou et al., 1998; Sedelnikova et al., 2002). For instance, in the case of hyperoxia, γH2AX depends on two major kinases, ATR and ATM. ATR is the main DNA damage signal transducer under hyperoxia conditions and is also necessary for ATM activation in hyperoxia (Kulkarni et al., 2008).

2.4. HISTONE UBIQUITINATION

Ubiquitin, is a 76-amino acid protein (MW 8KDa) that is covalently attached to lysine residues. The establishment of this mark involves three coupled sequential reactions catalyzed by three different enzymatic activities: 1) activation by an activating enzyme (E1); 2) conjugation by a conjugating enzyme (E2); and 3) attachment of ubiquitin to the protein by an isopeptide ligase (E3) (Ye et al., 2009). Depending of the cellular context, lysines can be either mono- or poly-ubiquitinated. Protein monoubiquitination plays a role in cell-signaling transduction in different functional contexts(Miller et al., 2005), whereas polyubiquitination has been mainly associated with protein degradation via the 26S proteasome. Histone ubiquitination and deubiquitination effects on gene expression have been more studied at histones H2A and H2B than at histones H3, H4 and H1 (Wright et al., 2012). Histone H2A was the first ubiquitinated protein identified. Monoubiquitination of H2A at Lys119 (H2AK119ub) is associated with facultative heterochromatin formation mediated by Polycomb group factors, which includes many genomic regions such as silenced developmental genes and the inactive mammalian X-

chromosome in females (Joo et al., 2007). In contrast, H2B monoubiquitinatio at Lys123 (H2BK123ub) is important for transcriptional elongation by RNA-polymerase II and has been associated with both repressive and active DNA regions, based on their positional context (Batta et al., 2011). Interestingly, H2BK120ub has a very important functional interplay with other PTMs. For instance, this modification is required for the establishment of histone H3K4 methylation, which in turn is inhibited by H2AK119ub (Nakagawa et al., 2008).

Ubiquitination is also a reversible mark. Ubiquitin moieties can be removed from target residues by a class of thiol proteases known as deubiquitinating enzymes (DUBs) (Reyes-Turcu et al., 2009). Different DUBs have been identified, despite there are specific DUBs for H2A (e.g. USP16, 2A-DUB, USP21, BAP1) or H2B (e.g. USP3, USP7, USP12, and USP49) (Zhang et al., 2013), some DUBs display dual specificity for the deubiquitination of either H2Aub or H2Bub suggesting a redundant functions among DUBs (Zhang et al., 2008).

2.5. HISTONE SUMOYLATION

SUMOylation is a reversible PTM that involves covalent ligation of SUMO (small ubiquitin-related modifier) groups at specific lysine residues. The SUMO family members (SUMO-1, -2, -3 and -4) belong to the group of ubiquitin-like protein-modifying enzymes. Compared to ubiquinitation, SUMOylation is a multi-step process that involves: 1) an activating heterodimer enzyme (E1: SAE1/SAE2); 2) a conjugating enzyme (E2: Ubc9); and, 3) a SUMO ligase(E3) (Flotho et al., 2013). Unlike acetylation, methylation, phosphorylation and ubiquitination reactions which occur throughout the cell, SUMOylation mainly takes place in the nucleus. Growing evidence corroborates a link between protein SUMOylation and critical processes, including transcriptional regulation, cell-cycle progression, cellular localization, chromatin organization, genome stability, protein-protein or protein-DNA interactions, and signal transduction. First evidences demonstrated that histone H4 SUMOylation is associated to transcriptional repression, through recruitment of HDAC and HP1 (Shiio et al., 2003). Recent studies in Saccharomyces cerevisiae have identified histone SUMOylation in all four core histones and linked the presence of SUMO with transcriptional repression. In a latter study that

identified more than 4,300 SUMOylation sites in more than 1,600 proteins. Interestingly, many SUMOylated lysines can be subjected to methylation, acetylation or ubiquitination, which suggests cross-talk between SUMOylation and other PTMs (Hendriks et al., 2014).

2.6. HISTONE ADP-RIBOSYLATION

Histone ADP-ribosylation is a reversible post-translational modification that involves the transfer of an ADP-ribose moiety from NAD^+ to specific amino acid residues such as lysine, arginine, aspartate, cysteine, glutamate, asparagine and phospho-serine (Pearson, 1995). Depending on the functional context, histones can be either mono- or poly-ADP-ribosylated. To this date, three main families of ADP-ribosyltransferases have been described. The first family is the diphtheria toxin-like ADP-ribosyltransferases (ARTDs), also known as PARPs, a superfamily of many members that can act as both mono- and poly-ADP-ribosyltransferases. The other two families are the clostridial toxin-like ADP-ribosyltransferases (ARTCs) and the Sir2 family of protein deacetylases (Sirtuins); both of which can catalyze mono-ADP-ribosylation (Messner et al., 2011).

The transferring of a single ADP-ribose group implies the addition of a negative charge to the ADP-ribosylated protein. As a consequence, poly-ADP-ribosylation implicates a considerable increase of negative charge in the substrate, and therefore has more radical functional consequences compared to other PTMs (Messner et al.,2010). As ARTCs are often expressed at the surface of cells or are secreted into the extracellular matrix, only ARTDs and Sirtuins have the potential to target histones. Among all nuclear ARTDs (ARTD1, ARTD2, ARTD3, ARTD5 and ARTD6), ARTD1 (or PARP1) is the most studied member which is responsible for up to 90% of the total cellular poly-ADP-ribosylation.

ADP-ribosylation is recognized by a group of protein domains, the best known of which is the macrodomain (Palazzo et al., 2017). The best known macro-containing protein is the histone H2A variant macroH2A, which is present in three isoforms, macroH2A1.1, macroH2A1.2 and macroH2A2. Of them, macroH2A1.1 is the only one that binds specifically ADP-ribose moieties. Considering the close link between ADPr and the metabolic/energetic state of the cell, as well as the role of mH2A1.1 as a component of

chromatin, this histone variant plays a key role as a sensor of the response to metabolic fluctuations. For instance, macroH2A1.1 seems to tune gene expression to adapt to different metabolic states through by chromatin compaction together with activated ARTD1 (Timinszky et al., 2009).

Despite, the main target of PARP1 is itself; it also targets a wide variety of nuclear proteins including all five histone proteins. It is also involved in many cellular processes, including DNA repair, genotoxic stress response, cell cycle regulation, gene expression and differentiation. In contrast, mono-ADP-ribosyltransferase (ADPRT) activity of Sirtuins is not yet fully understood and so far histones have not been identified as targets of their activity (Rezazadeh et al., 2020).

3. SIRTUINS: master regulators of the cellular stress response

The Sirtuin family of NAD^+-dependent enzymes plays important roles in a wide range of processes, such as maintenance of genome stability, stress response, metabolic homeostasis, cell division, and aging (Guarente et al., 2011; Haigis et al., 2010). The dependence of sirtuins on the cellular levels of NAD^+ links sirtuin activity to cellular redox status, which makes them sensors of cellular energy fluctuations. Thus, the ratio NAD^+/NADH regulates redox balance in energy metabolism. Moreover, NAD^+ is the precursor of $NADP^+$ and NADPH, which protect cells from reactive oxygen species (ROS). NAD^+ is produced by two biologically different pathways: First, the de novo synthesis that uses the essential amino acid tryptophan which is supplied by diet, and is metabolized to form biosynthetic precursors to generate NAD^+; Second, the salvage pathway recycles, where NAD^+ is resynthesized from nicotinamide by NAMPT (nicotinamide phosphoribosyl transferase enzyme) (Imai et al., 2000; Hershberger et al., 2017).

3.1. Mammalian Sirtuin proteins

Mammals harbor seven Sirtuin family members (SIRT1–SIRT7) that show a high degree of functional and catalytic diversification. Although sirtuins are deacetylases, also catalyze other NAD^+-dependent enzymatic activities such as ADPribosyl-transferases, demalonylase, and desuccinylase which are involved in diverse important physiologic processes (Figure 2) (Vassilopoulos et al., 2011).

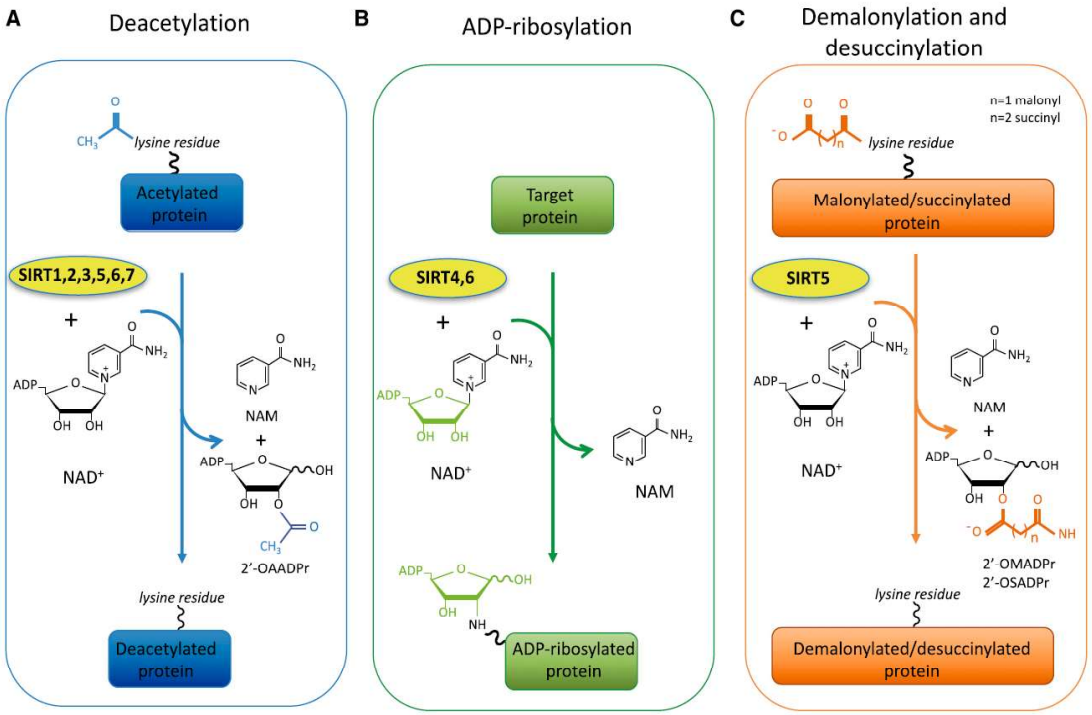

Figure 2. Sirtuins catalyze a wide variety of enzymatic activities. **(A)** Sirtuins (1-7) exhibit a lysine deacetylation activity, where the coenzyme NAD^+ is required as a cofactor in order to generate nicotinamide (NAM) and 29-O-acetyl-ADP-ribose (29-OAADPr). **(B)** SIRT4 exclusively exhibit ADP-ribosyl transferase activity, where NAD^+ is consumed as the donor of the ADP-ribose group to the target proteins. SIRT6 and SIRT7 have also an ADP-ribosyl transferase activity. **(C)** SIRT5 requires NAD^+ as a cofactor to demalonylate and desuccinylate target proteins, resulting in the production of NAM and 29-O-malonyl-ADP-ribose (29-OMADPr) and 29-O-succinyl-ADP-ribose (29-OSADPr), respectively (adapted from Morigi et al., 2018).

New studies performed in mice have shown promising progress regarding lifespan extension effect of sirtuins, especially in the case of SIRT6. Reflecting the key role of Sirtuins as crucial modulators of metabolic adaptive responses upon stress, their alteration has been associated with a broad spectrum of diseases, including neurodegenerative disorders, metabolic abnormalities, cardiovascular diseases, and cancer, all of which are age-associated diseases (reviewed in Liu et al., 2021).

The functional loss of some sirtuins, involved in maintaining genome integrity, may promote tumorigenesis due to their implication in genome stability and DNA repair. On the other hand, cancer cells require sirtuins for the same processes in order to promote proliferation, tumor growth and survival. The mechanisms involved seem to be complex, but it is showed that Sirtuins are bifunctional: acting as both tumor suppressors and oncogenic factors depending on the cellular context and the study conditions (Bosch-Presegué et al., 2011).

3.1.1. SIRT1

SIRT1, the most studied sirtuin, is a ubiquitous nuclear deacetylase that has been associated with longevity, gene silencing, energy homeostasis, cell-cycle control and apoptosis (Yang et al., 2006; Dali-Youcef et al., 2007; Yamamoto et al., 2007). Its main targets are histone (H1, H3, and H4) and non-histone proteins. SIRT1 also has been involved in functions connected to inflammation and neurodegeneration (Yamamoto et al., 2007), and differentiation of muscle cells, adipogenesis, and liver metabolism (Fulco et al., 2003; Picardet al., 2004; Rodgers et al., 2005). SIRT1 is discussed in detail in section 4.1.

3.1.2. SIRT2

SIRT2 is found ubiquitously expressed in all tissues, although it seems to be highly expressed in organs closely linked to metabolism, including liver, brain, pancreas, testes, fat tissue and kidneys. At the cellular level, SIRT2 mainly localizes in the cytoplasm, where it participates in the control of cytoskeleton, metabolism and cell cycle progression. During G_2/M, SIRT2 is shuttled to the nucleus where it deacetylates H4K16ac, allowing the establishment of the antagonist mark H4K20me1 and the compaction of chromatin in metaphase chromosomes (Inoue et al., 2007). SIRT2 is also involved at end of mitosis as a decrease of SIRT2 protein levels is key to allow mitotic exit (Dryden et al., 2003).

SIRT2 also plays a role in the nuclear envelope development, possibly by ANKLE2 deacetylation, which is shown to control nuclear envelope reassembly (Kaufmann et al., 2016).

Several studies have been shown that SIRT2 plays an important role in antioxidant and redox-mediated cellular homeostasis. Among the deacetylation targets of SIRT2 is PGC-1α, a master regulator of mitochondrial biogenesis that is also involved in ROS levels reduction and upregulation of antioxidant enzyme expression (Krishnan et al., 2012).

SIRT2 can target other metabolic enzymes involved in ROS modulation such as transcription factor forkhead box O 3a (FOXO3a), glucose 6-phosphate dehydrogenase (G6PD), phosphoglycerate mutase (PGAM2), or nuclear factor kappa B subunit (NF-κB). FOXO3a is a transcriptional activator of many stress dependent genes such as the ROS scavenger manganese superoxide dismutase (MnSOD), and is deacetylated by SIRT2 in response to oxidative stress and calorie restriction. These evidences suggest that the link SIRT2/FOXO3a may also be important in the described beneficial effects of calorie restriction. SIRT2 has been also showed to activate G6PD through deacetylation under oxidative stress conditions. G6PD is an essential enzyme of the pentose phosphate pathway that produces NADPH in the cytoplasm (Gomes et al., 2015; Wang et al., 2007).

3.1.3. SIRT3

Despite a common origin of SIRT1-3, SIRT3 is mainly located in the mitochondria. SIRT3 is mainly present in a cleaved form, and very limited levels of full-length SIRT3 have also been found in the nucleus. Interestingly, full-length SIRT3 translocate to the mitochondria in response to different kind of stress where it is cleaved by the mitochondrial matrix processing peptidase (Scher et al., 2007). SIRT3 has been described as the main mitochondrial deacetylase, where it targets many proteins involved in mitochondrial metabolism (Weir et al., 2013). For instance, SIRT3 targets acetyl coenzyme A (CoA) synthetase 2 (AceCS2), implicated in acetate recycling (Hallows et al., 2006; Schwer et al., 2006), long-chain acyl-CoA dehydrogenase (LCAD), associated to fatty acid oxidation (Hirschey et al., 2010), and ornithine transcarbamoylase (OTC), which is involved in increasing metabolic flow through the urea cycle (Hallows et al., 2011).

The SIRT3-dependent deacetylation of these activities highlights the important role of SIRT3 in adjusting mitochondrial consumption, and minimizing the effect of increased ROS levels. SIRT3 has also been shown to be responsible for deacetylation of ROS scavenging enzymes and ROS reduction. It protects against oxidative stress-dependent

diseases like aging, cancer, neural degeneration, and cardiac dysfunction (reviewed in Ansari et al., 2017). Overexpression of SIRT3 indirectly promotes an increase in expression of the nuclear genes encoding MnSOD and catalase through deacetylation of FOXO3a, which results in FOXO3a retention in the nucleus (Sundaresan et al., 2009). SIRT3 also targets SOD2 (Superoxide dismutase 2) to promote its antioxidative activity (Chen et al., 2011).

In contrast, SIRT3 depletion is linked to an increased of glycolysis, a hallmark of tumorigenesis. In this regard, the elevated levels of ROS produced due to SIRT3 depletion result in the stabilization of HIF-1α (hypoxia-inducible factor 1 α), involved in activation of the expression of several glycolytic enzymes (Finley et al., 2011). Due to the functional relevance of SIRT3, it has been implicated in a wide range of diseases, including cardiovascular, renal, and neurodegenerative diseases, and cancer. Interestingly, accumulated evidence suggests that SIRT3 is one of the sirtuins more directly involved in the control of human longevity (reviewed in Zhang et al., 2020).

Like the majority of the Sirtuin family members, SIRT3 plays a double-sided role in cancer. SIRT3 is widely known as a functional tumor suppressor (Kim et al., 2010), specially by targeting proteins that decrease ROS levels accumulated as a consequence of fatty acid oxidation. SIRT3 also can act as an oncogene to induce HFD-induced (high fat diet) tumorigenesis in mice (Ahmed et al., 2020) and in cancers that are addicted to oxidative phosphorylation (Baccelli et al., 2019). Thus, the role of SIRT3 in cancer seems to be context-dependent (Torrens-Mas et al., 2017).

3.1.4. SIRT4

SIRT4 is one of the less studied sirtuins. It is located in the mitochondria and is highly expressed in the heart, kidneys, liver, and brain, suggesting that it may have important roles in these tissues. The primary sequence and predicted secondary structure of SIRT4 are quite similar to the rest of mitochondrial sirtuins. Although SIRT4 has a highly conserved NAD^+-binding catalytic domain, it was initially proposed not to have deacetylase activity but to modulate its targets predominately by NAD^+-dependent mono-ADP-ribosylation (Ahuja et al., 2007; Haigis et al., 2006).

One of the best-known targets of SIRT4 is glutamate dehydrogenase (GDH), through which SIRT4 controls glutamine catabolism and metabolic reprogramming in cancer

cells. SIRT4 mono-ADP-ribosylates and downregulates GDH activity which is known to promote the metabolism of glutamate, generating ATP and insulin secretion in insulinoma cells (Jokinen et al., 2017; Min et al., 2019). SIRT4 is also expressed in response to DNA damage and inhibits GLUD1 and negatively regulates anaplerosis by catalyzing mono-ADP ribosylation of GLUD1. This results in the block of glutamine metabolism into tricarboxylic acid cycle and cell cycle arrest. SIRT4 has also been linked to the control of insulin function. Thus, SIRT4 inhibits insulin secretion through ADP-ribosylation of GDH and modulates insulin sensitivity in the pancreas as a deacylase.

Interestingly, SIRT4 also inhibits fatty acid oxidation (FAO) in the muscles and liver, but in a very different way. In the case of liver, SIRT4 overexpression results in repression of SIRT1-dependent activation of PPARα and consequently inhibits hepatic FAO. In contrast, the inhibitory effect of SIRT4 against FAO in muscle and fat cells is regulated by the deacetylation and inhibition of the activity of MCD (mitochondrial malonyl-CoA decarboxylase) which in turn leads to an increase in malonyl-CoA, a key metabolite responsible of inhibition of fat catabolism and fat synthesis induction (reviewed in Min et al., 2019).

3.1.5. SIRT5

Sirtuin 5 (SIRT5) is also localized in the mitochondria, where it is responsible for deacylation of multiple proteins (Park et al., 2013). Thus, in addition to deacetylation, SIRT5 can also catalyze demalonylation and desuccinylation reactions, which are involved in control of ketogenesis (Du et al., 2011; Rardin et al., 2013). SIRT5 is a global regulator of lysine malonylation and an inducer of the energetic flux via glycolysis (Nishida et al., 2015).

SIRT5 is highly expressed in brain, liver, heart and lymphoblasts, where it is found to be accumulated in the intermembrane spaces of the mitochondria (Matsushita et al., 2011). SIRT5 has been involved in cellular metabolism, detoxification, oxidative stress regulation, energy production, and apoptosis pathway. It was originally described as a mitochondrial enzyme that regulates the first step of the urea cycle through deacetylation and direct activation of carbamoyl phosphate synthetase 1 (CPS1 or CPSI) (Tan et al., 2014).

3.1.6. SIRT6

SIRT6 has been involved in several key molecular pathways associated with glycolysis, gluconeogenesis, DNA repair, tumorigenesis, cardiac hypertrophic responses, and neurodegeneration. SIRT6 is tightly bound to chromatin and was initially described as a NAD^+-dependent deacetylase of H3K9ac and H3K56ac (Elhanati et al, 2013; Tao et al., 2013).

Further studies also demonstrated that SIRT6 also targets H3K18ac at pericentric chromatin (Tasselli et al., 2016). Moreover, SIRT6 is also a dual sirtuin as it also harbors a mono-ADP-ribosyltransferase activity towards itself and other proteins (Mao et al., 2011). SIRT6 is discussed in detail in section 4.2.

3.1.7. SIRT7

The last identified member of mammalian sirtuin family, SIRT7, is a nuclear protein mainly localized in the nucleolus where it positively regulates ribosomal DNA (rDNA) transcription. In the nucleolus SIRT7 interacts with the transcription factor UBF, the Pol I subunit PAF53 (polymerase-associated factor 53) and U3–55k. PAF53 deacetylation by SIRT7 leads to increased DNA binding and enhanced pre-rRNA synthesis. SIRT7 also deacetylates U3–55k, a core component of the U3 snoRNP complex facilitating the interaction of U3–55k with U3 snoRNA, hence promoting pre-rRNA cleavage (reviewed in Wu et al., 2018).

Supporting a direct link between SIRT7, nucleolar function and metabolism, its expression is increased in higher metabolic tissues. Overexpression of SIRT7 promotes RNA Pol I-mediated transcription, while knockdown or inhibition of SIRT7 results in a decrease in its transcription (Ford et al., 2006). This effect seems to be related to its ability to regulate subunits of RNA Pol I subunits, especially RPA194 and PAF53 (Chen et al., 2013, Tsai et al., 2012). This action appears to involve NAD^+-dependent activity of SIRT7, which in turn deacetylates RPA194 and PAF53, resulting to increased RNA Pol I activity and rDNA transcription.

Interestingly, SIRT7 has been linked to aging. SIRT7 knockout mice present reduced embryonic viability, accelerated aging phenotype and lethal heart hypertrophy. SIRT7 plays a direct role in DNA repair through SIRT7-mediated H3K18 deacetylation and

genome integrity (Vazquez et al., 2016). Supporting an anti-aging role of SIRT7, its expression inversely correlates with aging. There are several hypotheses to explain this link with aging. One of the most established theories is that these expression patterns and progeroid phenotypes are at least in part due to alterations in rDNA transcriptional regulation. During replicative senescence, SIRT7 has been shown to shuttle between nucleoli, the chromatin and cytoplasm, where it may reduce rDNA transcription (Ford et al., 2006). Another possibility may be related to the proposed role of SIRT7 in DNA repair. Thus, SIRT7 deacetylates histone H3K18 through which regulates cancer cell transformation and NHEJ-mediated DNA repair (Vazquez et al., 2016). Additionally, recent studies of our group have demonstrated that SIRT7 exhibits a mono -ADP-ribosyl transferase (mADPRT) activity which regulates glucose starvation response through mH2A1 (Simonet et al., 2020). It has also been proposed a role for SIRT7 in mitochondrial homeostasis via deacetylation of GABPβ1, one of the subunits of a complex associated with regulating of several essential mitochondrial genes (Ryu et al., 2014).

All together these studies demonstrate that SIRT7 plays a vital role in cellular responses to energy levels, allowing the cells to control simultaneously ribosomal DNA transcription and protein production while protecting genome stability under stress conditions.

4. SIRT1 and SIRT6, two key regulators of genome stability involved in cancer

4.1. SIRT1

SIRT1 has been shown to modulate many central pathways related to genome stability and metabolism upon stress, such as lipid metabolism, insulin secretion, cellular senescence, inflammation, cell cycle, proliferation, stress resistance, cell differentiation, longevity, DNA damage response, and tumorigenesis (Figure 3). SIRT1 carries out its function in part through deacetylation of N-terminus tails of acetylated histones: H1K26ac, H3K56ac, H2A.Zac, H3K9ac and H4K16ac (Vaquero et al., 2004; Vaquero et al., 2007; Bosch-Presegué and Vaquero, 2015). SIRT1 also targets a wide number of key non-histone proteins in numerous tissues, such as liver, muscle, adipose tissue, endothelium and heart (Bolmeson et al., 2011; McArthur et al., 2011). Among these factors are many key stress-associated transcription factors such as p53, forkhead transcription factors,

nuclear receptor coactivator PGC-1α, and NF-κB (Mantel and Broxmeyer, 2008), as will be discussed later on in this section.

Figure 3. Activation and inhibition of cellular processes by SIRT1. SIRT1 performs a wide variety of biological functions in cancer, adipose tissue, cell aging, cellular senescence, neurodegeneration, the response to environmental stress, development and placental cell survival. SIRT1 protects against genotoxic, metabolic and oxidative stresses. Among other functions, SIRT1 also protects against chronic inflammation through the NF-κB signaling pathway, it improves insulin sensitivity, and plays an important role in DNA damage repair and in maintaining genome integrity. SIRT1 is also associated with epigenetic silencing of DNA-hypermethylated tumor suppressor genes (TSGs) in cancer cells (adapted from Rahman et al., 2011).

4.1.1. SIRT1 in heterochromatin formation and genome stability

SIRT1 is involved in the formation of both facultative and constitutive heterochromatin. SIRT1 acts as a master coordinator of heterochromatin formation through different mechanisms including deacetylation of histone and non-histone proteins, as well as recruitment and stabilization of chromatin-associated factors,

among which are enzymes, transcription factors, co-repressors and structural proteins (reviewed in Bosch-Presegue and Vaquero, 2011).

SIRT1 plays a key role in constitutive heterochromatin (CH) through a close functional relationship with Suv39h1 mediated by several mechanisms: First SIRT1 binds to and recruits of Suv39h1 promoting its specific activity by deacetylation of K266, a residue in the catalytic SET domain of Suv39h1. Second, it deacetylates H3K9ac, allowing the deposition of H3K9me3 by Suv39h1. Third, SIRT1 binding to Suv39h1, inhibits its binding to MDM2, the E3 ubiquitin ligase of Suv39h1, thus inhibiting its degradation through the ubiquitination/Proteasome machinery. Under genotoxic stress, SIRT1 increases Suv39h1 levels through this mechanism, which increases the rate of Suv39h1 turnover in CH and ensures the protection of CH structure and stability (Bosch-Presegue et al., 2011).

SIRT1 interacts with several HMTs including Suv39h1, G9a and Enhancer of zeste homolog 2 (EZH2). EZH2 is a H3K27me3-specific histone methyltransferase and catalytic component of PRC2 that can be deacetylated by SIRT1. Acetylation of EZH2 at K348 decreases EZH2 phosphorylation at T345 and T487 to increase EZH2 stabilization and boosts PRC2 capacity in gene repression events (Wan et al., 2015).

SIRT1 also regulates facultative heterochromatin (FH) formation through deacetylation of different histone marks including H4K16ac, H3K9ac, and H1K26ac. Moreover, its deacetylation of H3K9ac also regulates indirectly H3K9me3 deposition by Suv39h1 (Peters et al., 2001; Vaquero et al., 2004). FH formation by SIRT1 has important consequences in the cellular response to stress. In the case of Suv39h1, under oxidative stress conditions, SIRT1 and Suv39h1 work together to promote facultative chromatin formation in rDNA loci and suppressing ribosomal gene expressions (Grummt and Ladurner, 2008; Murayama et al., 2008). The key role of SIRT1 in FH goes beyond rDNA regulation and is crucial to the expression program controlled by master regulators of stress such as p53, FOXO proteins, NF-κB, and many others. SIRT1 binds to and deacetylates p53, a keystone of cell cycle regulation, apoptosis, and tumorigenesis (Luo et al., 2001; Vaziri et al., 2001). Other important players in the stress response modulated by sirtuins are the members of the forkhead-box (FOXO) family of transcription factors, which key regulators of apoptosis, energy metabolism, and oxidative stress resistance (Accili et al., 2004). In response to oxidative stress, FOXO proteins, translocate from the cytoplasm to the nucleus to gain stress resistance by

activating genes involved in oxidative detoxification, such as MnSOD and catalase. The c-Jun N-terminal protein kinases (JNKs), a mitogen-activated protein kinase (MAPK) family that play a critical role in the regulation of stress, cell differentiation, and apoptosis, are involved in this process (Balaban et al., 2005). Acetylation of FOXO reduces its binding to DNA and enhances its phosphorylation which leads to FOXO inactivation (Matsuzaki et al., 2005). SIRT1 deacetylates FOXO proteins, inducing transcription of FOXO targets associated to stress resistance and inhibition of transcription in the case of apoptosis-related genes (Kobayashi et al., 2005).

4.1.2. SIRT1 and DNA repair

SIRT1 plays a key role in DNA damage response, through deacetylation of histone and non-histone proteins at DNA damage sites. It has been associated to the regulation of several pathways involved in the repair of single-stranded DNA damage (ssDNA) and double strand breaks (DSB). In the case of DSB repair, SIRT1 is involved in activation of key components of the DNA repair machinery, including Ku proteins, nibrin (NBS1) and Werner helicase (WRN) (Yuan et al., 2007; Li et al., 2008). Although SIRT1 participates in both DSB major repair pathways, non-homologues end joining (NHEJ) and Homologous recombination (HR) pathways, evidences suggest a closer functional relationship with the latter.

The effective recruitment of SIRT1 to damaged sites requires ataxia–telangiectasia mutated protein kinase (ATM) and γH2AX foci formation. Additionally, SIRT1 may be activated in CHK1-dependent phosphorylation on Thr530 and Thr540 residues (Sasaki et al., 2008). SIRT1-deficient cells display diminished levels of γH2AX, BRCA1, NBS1 and RAD51 foci formation following DNA damage, which results in impaired capability of damage repair in these cells when exposed to damaging agents (Wang et al., 2008). This in turn results in the formation of numerous translocations and chromosomal fusions (Oberdoerffer et al., 2008).

SIRT1 has also been involved in several repair pathways of single strand DNA damage such as base excision repair (BER), nucleotide excision repair (NER) and DNA mismatch repair (MMR). In the case of BER, SIRT1 deacetylation of the APE1 endonuclease promotes its binding to X-ray cross-complementing-1 (XRCC) and DNA repair activity (Yamamori et al., 2010; Madabushi et al., 2013). The SIRT1-dependent deacetylation of

xeroderma pigmentosum protein XPA in Lys63 and Lys67 enhances the ability of ATR to phosphorylate XPA at Ser-196, a molecular event critical to cAMP-enhanced NER. In the case of MMR, downregulation of SIRT1 leads to cell death and increased genome instability in human embryonic stem cells (hESCs), but not in differentiated cells. This increased genome instability is partially due to decreased levels of DNA mismatch repair enzymes such as MSH2, MSH6, and APEX1 (Fan et al., 2010; Ming et al., 2010).

4.1.3. SIRT1 and metabolism

A growing body of evidence indicates that SIRT1 regulates glucose and lipid metabolism through its deacetylase activity. SIRT1 improves insulin sensitivity in liver, skeletal muscle and adipose tissue and protects the functional pancreatic β-cell mass. On the other hand, several studies suggest the beneficial effect of SIRT1 on metabolic diseases because of its ability to suppress NF-κB activity, the master regulator of cellular inflammatory response, in macrophages. SIRT1 deacetylates the RelA/p65 subunit of NF-κB at lysine 310, attenuating the NF-κB transcriptional activity, thus reducing production of pro-inflammatory cytokines and anti-apoptotic genes expression (Yeung et al., 2004).

SIRT1 is an important modulator of both white adipose tissue (WAT) and brown adipose tissue (BAT) which play important role in energy homeostasis, body temperature regulation and body insulation. WAT and BAT originate from the differentiation of lipoblasts, and one of the primary factors involved in this process is the nuclear receptor PPAR, the master regulator of adipogenesis (Tontonoz et al., 2008). SIRT1 represses PPARγ, in WAT thereby suppressing the expression of adipose tissue markers, such as the mouse aP2 gene (Picard et al., 2004). Therefore, SIRT1 action is necessary to adapt gene transcription in WAT to changes in systemic nutrient levels. SIRT1-mediated deacetylation of PPARγ is needed to recruit the BAT coactivator Prdm16 to PPARγ, causing selective induction of BAT genes and repression of WAT genes (Qiang et al., 2012). SIRT1 may promote BAT differentiation directly via repressing of the MyoD-dependent myogenic gene expression and promoting PGC-1α-mediated mitochondrial gene expression (Timmons et al., 2007).

Numerous reports have shown that SIRT1 is an important regulator of hepatic glucose metabolism. Hepatic SIRT1 is a master modulator of gluconeogenesis in response to fasting. SIRT1 inhibits TORC2, a CREB-regulated transcription coactivator that is important for cAMP/CREB-dependent activation of gluconeogenesis genes, resulting in reduced gluconeogenesis (Liu et al., 2008). Besides TORC2 and PGC-1α, SIRT1 also deacetylates and activates FOXO1, that ultimately leading to increased gluconeogenesis (Frescas et al., 2005). Therefore, effect of SIRT1 on the regulation of gluconeogenesis is determined by the interactions between multiple factors at different phases of fasting and/or feeding.

SIRT1 may also regulate hepatic lipid metabolism through deacetylation of SREBPs, critical regulators of lipogenesis and cholesterolgenesis. Thus, it can deacetylate SREBPs, inducing fasting-dependent attenuation of SREBPs (Walker et al., 2010; Ponugoti et al., 2010). Several nuclear receptors regulated by acetylation and deacetylation are also involved in lipid metabolism. SIRT1 directly deacetylates LXRs (Liver X receptors), resulting in increased LXRs turnover and enhanced target gene expression. LXRs are nuclear receptors that work as cholesterol sensors and promote lipid homeostasis through regulating the expression of multiple genes involved in the efflux, transport, and excretion of cholesterol (Li et al., 2007).

4.1.4. SIRT1 and Cancer

The involvement of SIRT1 in cancer is complex and often controversial as it has been shown to be upregulated or downregulated in different types of cancer which lead to define SIRT1 as both a tumor suppressor and a tumor promoter. In one hand, SIRT1 is frequently overexpressed in human prostate cancer (Ruan et al., 2018), acute myeloid leukemia (Bradbury et al., 2005), primary colon cancer (Stunkel et al., 2007) and non-melanoma skin cancers (Lim et al., 2006), among others. On the other hand, SIRT1 expression is decreased in for instance, bladder carcinoma, glioblastoma, prostate carcinoma, and ovarian cancers (Wang et al., 2008). Based on these observations, the effect of SIRT1 is considered to be context-specific. This has led to hypothesize that SIRT1 does not play a direct role in the onset of carcinogenesis, but in some cases is upregulated by the tumor cells to promote survival and growth advantages (Deng, 2009).

Interestingly, SIRT1 regulates the tumor suppressor activity of different transcription factors such as p53, p73, E2F1, and FOXO, but also various factors with oncogene properties including STAT3, Survivin, p65/RelA subunit of NF-κB, and β-Catenin. SIRT1 can also upregulate the activity of other oncogenes such as c-Myc and HIF-1α (Vaziri et al., 2001; Dai et al., 2007; Yeung et al., 2004; Wang et al., 2008; Laemmle et al., 2012).

Interestingly, several potential tumor suppressors, including HIC1, microRNA34a, and DBC1 (deleted in breast cancer 1), regulate p53-dependent apoptosis by directly suppressing SIRT1 expression and/or activity (Zhao et al., 2008; Chen et al., 2005). DBC1 gene was originally found to be deleted in chromosome 8p21 in a breast cancer cell line. Downregulation or silencing of DBC1 has also been showed in other type of cancers such as non-small cell lung cancers, bladder cancers and leukemia (Izumi et al., 2005; San José-Enériz et al., 2006). Co-immunoprecipitation assays demonstrated that DBC1 binds SIRT1 and disrupts the interaction between SIRT1 and p53. DBC1-dependent suppression of SIRT1 induces hyperacetylation of p53, thus facilitating its functions in DNA repair, cell cycle arrest, and apoptosis (Chen et al., 2005). In contrast, DBC1 downregulation improves SIRT1-dependent stress resistance and cell survival (Kim et al., 2008; Zhao et al., 2008). On the other hand, DBC1 induces Suv39h1-SIRT1 complex disruption leading to inactivation of both enzymes (Li et al., 2009). Tumor suppressor HIC1 induces promoter hypermethylation and epigenetic repression in a wide number of human cancers. HIC1 binds to SIRT1 to form a transcriptional repression complex (SIRT1/HIC1) which is recruited to the SIRT1 promoter to repress SIRT1 transcription.

SIRT1 also inhibits survivin in BRCA1 (breast cancer 1)-associated breast cancers. Survivin is a small anti-apoptotic protein that is highly expressed in various cancers and embryonic tissues and has been targeted in anti-cancer drug development (Altieri et al., 2008). BRCA1-associated breast cancers exhibit decreased levels of SIRT1 and higher levels of survivin. Wild-type BRCA1 is localized at the SIRT1 promoter in breast cancer cell lines promoting SIRT1 expression. SIRT1 represses survivin expression by deacetylation of histone H3 at the survivin promoter (Wang et al., 2008).

SIRT1 confers chemoresistance to lung cancer cells by stabilizing X-ray cross-complementing-1 (XRCC1). SIRT1 interacts and deacetylates XRCC1 at lysine K260, K298 and K431, disrupting the acetylation dependent interaction of XRCC1 with β-TrCP E3 ligase which prevents it from β-TrCP-dependent ubiquitination. XRCC1 interplays with

other factors such as TP53 to promote cancer development. Hence, targeting SIRT1 might be a novel treatment option to combat the chemoresistance of lung cancer, and likely other cancers (Yousafzai et al., 2019).

4.1.5. SIRT1 and differentiation

SIRT1 has been involved in regulating cell differentiation of many cell types (Firestein et al., 2008). Among the most relevant of them are tissues controlled by SIRT1 are those very dependent on metabolic/energy levels such as muscle, WAT or neural system. For instance, SIRT1 expression negatively regulates the differentiation of both myocytes and white adipocytes (Fulco et al., 2003; Picard et al., 2004). SIRT1 also modulates neuronal differentiation through its nuclear translocation by repressing Notch1-Hes1 signaling pathway (Hishara et al., 2008).

In addition, SIRT1 promotes keratinocyte differentiation through calcium-mediated signal transduction pathways, which are potent inducers of keratinocyte differentiation. Nicotinamide, a Sirtuin inhibitor, suppresses expression of keratinocyte differentiation markers, whereas a SIRT1 activator, resveratrol increases expression of keratinocyte differentiation markers (Blander et al., 2009).

4.1.6. SIRT1 and Autophagy

SIRT1 is a master regulator of autophagy (Salminen and Kaarniranta, 2009) and it has been associated with several autophagy-related diseases, such as neurodegenerative diseases and retinal degenerative disorders (Luo et al., 2019; Wu et al., 2011). In this functional context, SIRT1 deacetylates diverse autophagy-related proteins, including LC3 and other autophagy-related gene (ATG) family members (Lee et al., 2008; Hariharan et al., 2010; Huang et al., 2015). Autophagy may play an important role in SIRT1-dependent response to stress. For instance, the protective effect of SIRT1 in cardiomyocytes upon hypoxia is directly caused by autophagy activation. In that case, SIRT1 induces activation of AMPK and a decrease in apoptosis via the IRE1α (inositol requiring kinase enzyme 1α) pathway (Luo et al., 2019).

4.2. SIRT6

In vivo studies in mice models have demonstrated the functional relevance of SIRT6 activity in organismal health, as SIRT6-deficient mice exhibit shortened lifespan, accelerated aging phenotype, metabolic alterations and higher probability of developing cancer. Consistently, elevated levels of SIRT6 have been shown to have protective effects. For instance, in mice SIRT6 over-expression protects against metabolic disorders related to diet-induced obesity and leads to a slight increase in lifespan in male mice (Kanfi et al., 2010). Moreover, SIRT6 expression is induced in mice under fasting or calorie restriction conditions (Kanfi et al., 2008). As these mice have reduced serum IGF-1 and increased IGFBP-1 levels, gene expression changes can be cause or consequence of changes associated to the endocrine regulatory axis (Swindell et al., 2009). Biochemical characterization of SIRT6 identified two major catalytic activities: deacetylation and mono-ADP-ribosylation (Table 3). A complete characterization of the C-terminal extension (CTE) and N-terminal extension (NTE) of SIRT6 revealed additional important functional roles in the cells. The CTE of SIRT6 contains the nuclear localization signal 345 PKRVKAK 351 that is dispensable for enzymatic activity facilitates its proper sub-cellular localization. On the other hand, the NTE of SIRT6 is critical for its intrinsic deacetylase activity in cells and also for its binding to chromatin. Lack of the NTE drastically decreases the deacetylase activity of SIRT6. Moreover, both NTE and CTE of SIRT6 play a key role for nucleosome binding along with its enzymatic activities (Tennen at al., 2010).

In contrast to other sirtuins, SIRT6 can bind NAD^+ in the absence of an acetylated substrate which makes SIRT6 a NAD^+ sensor. The histone deacetylation activity of SIRT6 *in vitro* is quite weak and is estimated to be three orders of magnitude lower than SIRT1 enzymatic activity (Feldman et al., 2013, Jiang et al., 2013). Interestingly, SIRT6 activity increases significantly toward nucleosomes and is boosted in the presence of fatty acid activators (Feldman et al., 2013). SIRT6 deacetylase activity targets specifically several marks in histone H3 tail, including acetylated lysines K9, K56 and K18 (H3K9ac, H3K56ac, and H3K18ac) (Tasselli et al.,2016; Michishita et al.,2008; Michishita et al.,2009; Yang et al.,2009). It also mono-ADP-ribosylates PARP1, KDM2A and BAF170 (Mao et al., 2011; Rezazadeh et al., 2019; Rezazadeh et al.,2020).

Activity	Substrates		SIRT6-linked cellular functions	References
Deacetylation	Histones	H3K9ac	Telomere stability, transcriptional regulation, DNA damage response	(Michishita et al.,2008)
		H3K56ac	Telomere stability, transcriptional regulation, DNA damage response	(Michishita et al.,2009)
		H3K18ac	Heterochromatin silencing	(Tasselli et al.,2016)
		H3K27ac	Unknown	(Wang et al.,2016)
	Non-Histones	CTIP	Regulation of DSB processing and Homologous Directed Repair	(Kaidi et al.,2010)
		NPM1	Potential link to cellular senescence	(Lee et al.,2014)
		PKM2	Regulation of PKM2 localization and oncogenic functions	(Bhardwaj et al.,2016)
		GCN5	Regulation of GCN5 acetyltransferase activity	(Dominy et al.,2012)
		FOXO3a	Modulation of chemotherapy resistance in breast cancer	(Khongkow et al.,2013)
De-fatty-acylation	Histones	H3K9myristoyl	Unknown	(Feldman et al.,2013)
		H3K9dodecanoyl	Unknown	(Feldman et al.,2013)
		H3K9decanoyl	Unknown	(Feldman et al.,2013)
		H3K9octanoyl, H3K18octanoyl, H3K27octanoyl	Unknown	(Feldman et al.,2013)
		H3K9hexanoyl	Unknown	(Feldman et al.,2013)

	Non-Histones	TNFαK19myr, TNFαK20myr	Regulation of TNFα secretion	(Jiang et al.,2013)
Mono-ADP-ribosylation	Non-Histones	SIRT6	Unknown	(Liszt et al.,2005)
		PARP1	Regulation of PARP1 poly-ADP-ribosyltransferase activity and DSB repair	(Mao et al.,2011)
		KAP1	Regulation of KAP1 interaction with HP1α, and L1 silencing	(Van Meter et al.,2014)
		KDM2A	Transient transcriptional repression and recruitment of NHEJ factors	(Rezazadeh et al.,2019)
		BAF170	Transcriptional activation and formation of active chromatin loop	(Rezazadeh et al.,2020)

Table 3. List of SIRT6 activities, substrates and corresponding cellular functions.

Furthermore, SIRT6 has been described to preferentially hydrolyze long-chain fatty acyl groups (myristoyl and palmitoyl) over acetyl groups. For example, it has shown that the demyristoylation activity of SIRT6 is approximately 300-fold higher than its deacetylation activity *in vitro* (Jiang et al., 2013).

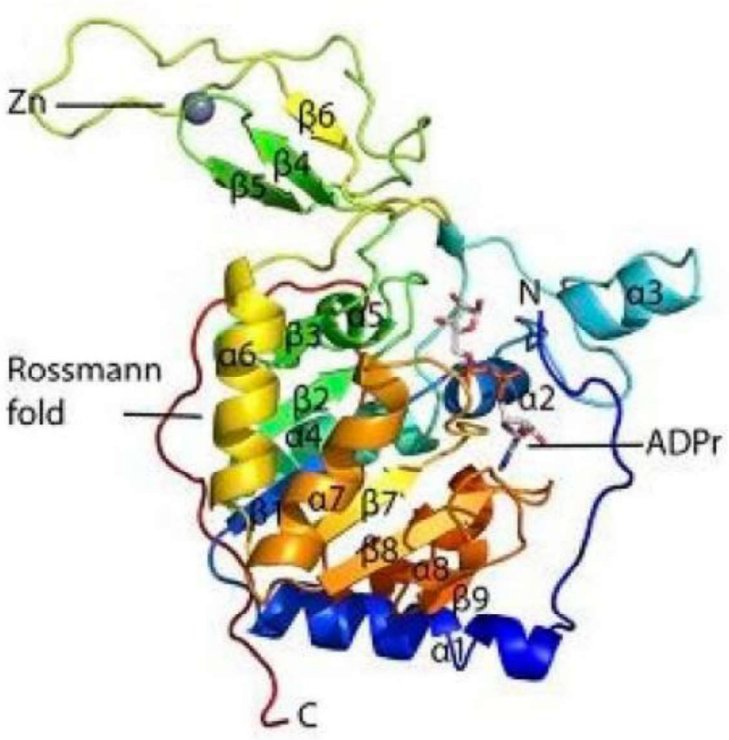

Figure 4. Global view of the SIRT6 monomer structure showing the location of Rossmann fold. The human SIRT6 contains 355 amino acids. Lysine is deacetylated through the coupling of SIRT6 with NAD^+ hydrolysis yielding O-acetyl-ADP (adenosine 5′-diphosphoribose), nicotinamide, and a deacetylated substrate. SIRT6 possess the catalytic core region of the sirtuin family, N-terminal extensions (NTE) and C-terminal extensions (CTE). Further catalysis is promoted by the presence of large and structurally homologous Rossmann-fold domain for NAD^+ binding. Additionally, SIRT6 contains an ADPr binding site and its catalytic core region also contains a more structurally assorted zinc-binding domain. SIRT6 presents an open conformation where the zinc-binding motif is separated from the Rossman-fold domain. The formation of hydrogen bonds between the Rossman-fold and the zinc-binding motif leads to stabilization of the structural conformation of SIRT6 (adapted from Li et al., 2018).

4.2.1. SIRT6, Genome stability and DNA repair

SIRT6 function is intimately related to the protection of genome stability. Basically, SIRT6 promotes genome integrity through two major mechanisms. The first one is associated to the protection of constitutive heterochromatin regions, including telomeres and PCH. SIRT6-dependent histone deacetylation at telomeres is required for binding of Werner syndrome ATP-dependent helicase (WRN) and stabilization of repressive heterochromatin at sub-telomeric regions. This in turn ensures transcription repression of telomere-proximal genes which are associated to cellular changes in aging (Tennen et al., 2011). In *Sirt6*$^{-/-}$ cells, telomere dysfunction results in genomic instability and cellular senescence of primary human fibroblasts (Michishita et al., 2008). SIRT6 also maintains PCH silencing through deacetylation of H3K18ac. In SIRT6-deficient cells,

accumulation of pericentric transcripts plays a role in genomic instability, cellular senescence, and mitotic errors. PCH silencing by SIRT6 is also linked to the epigenetic factor KAP1. Thus, H3K18ac deacetylation by SIRT6 leads to KAP1 retention at pericentric satellite repeats, and in *Sirt6*$^{-/-}$, H3K18 hyperacetylation results in KAP1 release and transcriptional silencing. The second mechanism involves a direct role in DNA damage signaling and repair. SIRT6 has been also involved in ssDNA BER pathway, but its main role is associated to DSB repair pathways, HR and NHEJ. The protein kinase JNK becomes activated under stress conditions and phosphorylates SIRT6 on Ser10 (Van Meter et al., 2016). This post-translational modification facilitates the recruitment of SIRT6 to DNA damage sites, where SIRT6 modulates double strand break repair upon oxidative stress in a PARP1- dependent manner. *Sirt6*$^{-/-}$ MEFs show a 2.6-fold lower NHEJ efficiency compared to wild type MEFs, and siRNA-mediated downregulation of SIRT6 in human fibroblasts results in a 2.2-fold reduction in HR efficiency after paraquat treatment. Accordingly, SIRT6 overexpression improves the efficiency of NHEJ by 3.3-fold and HR by 3.4 fold (Mao et al., 2011).

SIRT6 overexpression results in faster recruitment of repair factors 53BP1 and NBS1 to DNA break sites. Mutants lacking the mono-ADP-ribosyltransferase and/or deacetylase activities reduce the efficiency of DSB repair suggesting that both enzymatic activities play a role in DSB repair (Mao et al., 2011).

Interestingly, SIRT6 was shown to be one of the earliest factors recruited to sites of DSBs. SIRT6 recruits the ISWI chromatin remodeler, SNF2H to DSBs via deacetylation of H3K56. Either SIRT6 or SNF2H are necessary to make chromatin more open and accessible in a local manner, allowing the efficient cascade of repair factor recruitment, including BRCA1, 53BP1, and RPA (Toiber et al., 2013). This early response and involvement of repair factors, suggests a role for SIRT6 in both HR and NHEJ. In separate studies, the SIRT6/SNF2H complex was shown to mediate transient H2AX stabilization. Upon DSB formation, the SIRT6/SNF2H complex and ATM jointly blocks the poly-ubiquitinating E3 ligase HUWE1 and allow the phosphorylation of H2AX at Ser 139 (Atsumi et al., 2015), further confirming the previous studies by Toiber and colleagues. In the case of HR, SIRT6 promotes chromatin relaxation and homologous recombination through CHD4. SIRT6 is required for recruiting CHD4 to DNA damage sites facilitating

chromatin relaxation and proper homologous recombination in G_2 phase. Interestingly, the SIRT6-dependent recruitment of CHD4 requires ATM activity (Hu et al., 2020).

SIRT6 protein promotes NHEJ DNA repair by repressing transcription transitorily. Specifically, SIRT6 mono-ADP-ribosylates the lysine demethylase JHDM1A/KDM2A resulting in displacement of KDM2A from chromatin, and an increase in H3K36me2 levels at DNA damage sites. H3K36me2 promotes subsequent H3K9 tri-methylation through HP1α binding which in turn leads to transient suppression of transcription initiation by RNA polymerase II and recruitment of NHEJ factors to DSBs (Rezazadeh et al., 2020). In the case of mouse induced pluripotent stem cells (iPSCs), SIRT6 directly interacts with Ku80 to facilitates the binding between Ku80 and catalytic subunit of DNA-PK (DNA-PKc) and stabilization of the DNA-dependent protein kinase (DNA-PK) at DNA double-strand breaks. The subsequent phosphorylation of DNA-PKcs at residue Ser2056 results in a more efficient NHEJ. Interestingly, DNA-PKcs levels at the chromatin in SIRT6 knockdown cells remain intact in response to DNA damage signaling (McCord et al., 2009).

4.2.2. Cellular Metabolism and Metabolic Diseases

Despite the involvement of SIRT6 in a wide variety of biological processes, one of its pivotal roles is the maintenance of metabolic homeostasis. Several studies have demonstrated a key function of SIRT6 in glycolysis regulation, triglyceride synthesis, and fat metabolism through deacetylation of histone H3K9 and other chromatin factors (Figure 5). Early studies reported that SIRT6-deficient mice exhibit lethal hypoglycemia early in life providing the first evidence for SIRT6 role in glucose homeostasis (Mostoslavsky et al., 2006). Thereafter, other studies demonstrated that SIRT6 negatively regulates glycolysis through co-repressing HIF-1α, a critical transcription factor in regulation of the response to nutrient deprivation (Zhong et al., 2010). SIRT6 deacetylates histone H3K9 at the promoters of key glycolytic genes such as GLUT1, PDK1, and LDHA, inhibiting their expression. By repressing multiple glycolytic genes in a coordinated manner, SIRT6 switches pyruvate towards the mitochondrial TCA cycle for efficient ATP production, avoiding the conversion of pyruvate into lactate, a feature that suggests that SIRT6 can act as a tumor suppressor (Zhong et al., 2010; Sebastian et al., 2012).

Other studies reveal that SIRT6 can also regulate glucose homeostasis by suppressing gluconeogenesis (Figure 5). SIRT6 suppresses hepatic glucose production (HGP) by deacetylating, and subsequently activating, the acetyltransferase GCN5 (Dominy et al., 2012), which in turn promotes PGC-1α acetylation and inhibition of gluconeogenesis. In a separate study using cancer cell lines, SIRT6 deacetylation of the transcription factor forkhead box protein O1 (FOXO1) resulted in downregulation of gluconeogenesis (Zhang et al., 2014). In this process, p53 mediates the activation of the SIRT6 which subsequently facilitates FOXO1's deacetylation and nuclear exclusion. FOXO1 activates gluconeogenesis by binding to the promoters of glucose-6-phosphatase (G6PC) and phosphoenolpyruvate carboxykinase (PCK1), promoting their expression. Hence, SIRT6-mediated deacetylation facilitates the inactivation of FOXO1 and the downregulation of G6PC and PCK1, both critical enzymes in gluconeogenesis.

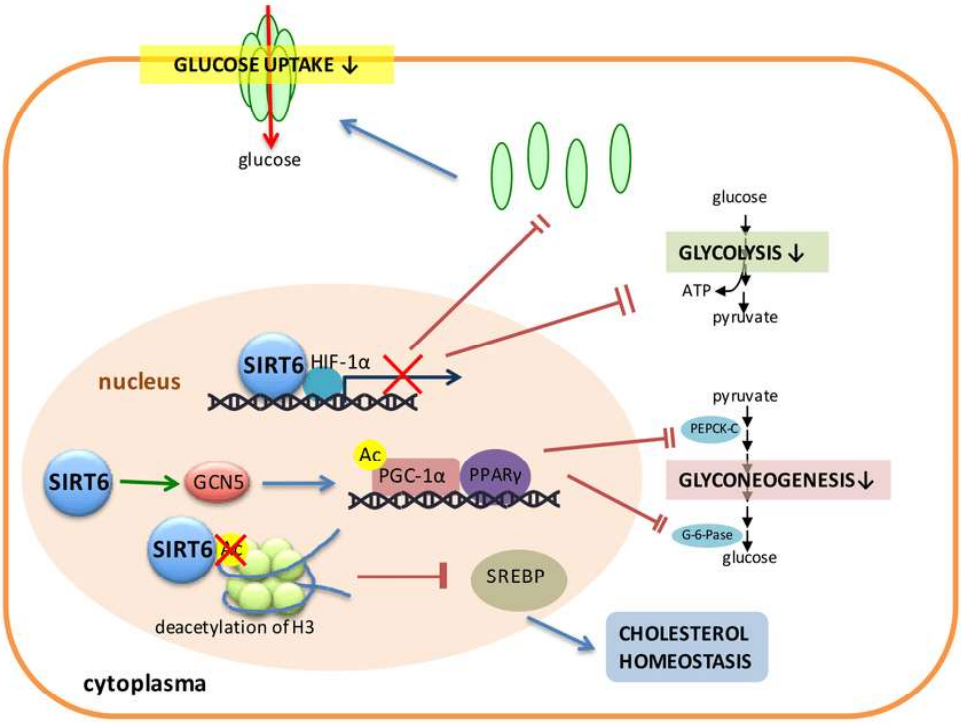

Figure5. SIRT6 plays an importantant role in metabolic homeostasis. SIRT6 interacts with HIF-1α and inhibits the expression of glycolytic enzymes and GLUT1. SIRT6 promotes GCN5 activation, leading to PGC-1α acetylation and activation of PPARγ to downregulate the expression of gluconeogenesis-related enzymes including G6P, and subsequently inhibits this pathway. SIRT6 also is in charge of deacetylating of H3 and inhibition of SREBP expression to modulate the cholesterol homeostasis (adapted from Ye et al., 2017).

SIRT6 also regulates lipid metabolism (Figure 5). Mice with liver-specific SIRT6 deficiency display reduced β-oxidation, more triglyceride accumulation and fatty liver formation (Kim et al., 2010). In addition, SIRT6 negatively regulates the lipogenic transcription factors SREBP1 and SREBP2 (Elhanati et al., 2013) which modulate cholesterol biosynthesis through controlling the expression of several genes, including 3-hydroxy-3-methyl-glutaryl-CoA reductase (Horton et al., 2002).

Along with downregulation of SREBP1 and SREBP2, SIRT6 downregulates peroxisome proliferator-activated receptor γ (PPAR-γ) target genes, and genes related with lipid storage, such as adipocyte fatty acid-binding protein, angiopoietin-like protein 4, and diacyglycerol acyltransferase 1. Thus, overexpressing SIRT6 mice fed with HFD present lower levels of visceral fat, triglycerides and low-density lipoprotein (LDL) cholesterol compared with wild type (Kanfi et al., 2010).

4.2.3. Complex role of SIRT6 in Cancer

As in the case of SIRT1, SIRT6 seems to play a dual role in cancer. Despite this duality, the majority of studies have reported a tumor suppressor role for SIRT6. Consistently, low SIRT6 expression levels are associated with poor prognosis (Sebastian et al., 2012). SIRT6 levels are reduced in a many cancer cell types such as hepatocellular carcinoma, pancreatic cancer, colon adenocarcinoma and squamous cell carcinoma (Sebastian et al., 2012; Min et al., 2012; Bhardwaj & Das, 2015).

The tumor suppressor activity of SIRT6 is directly dependent on SIRT6 enzymatic activities as all infrequent point mutations in SIRT6 identified in cancer cell lines destabilized or inactivated SIRT6 (Kugel et al., 2015). SIRT6 protective effect on tumorigenesis is exerted through a wide range of mechanisms. For instance, SIRT6 can inhibit the activity of different oncogenes. Thus, in the context of regulation of ribosomal metabolism, SIRT6 co-represses the transcription factor c-MYC to inhibit cell growth (Sebastian et al., 2012). SIRT6 suppression is regulated by the c-Jun/c-Fos pathway in liver cancer cells. c-Fos induces SIRT6 transcription and prevents liver tumorigenesis while inhibition of c-Fos by c-Jun promotes the survival of liver cancer cells (Min et al., 2012).

Another important link between SIRT6 and tumor suppression is its close relationship with the control of metabolism. Cancer cells modify their metabolism to promote survival, proliferation, growth, and long-term cell maintenance which is so called the Warburg effect. The main feature of this altered metabolism is increased glucose uptake and glucose to lactate fermentation which is conducive to tumorigenesis. It has been reported high expression levels of pyruvate kinase M2 (PKM2), an isoform that boosts aerobic glycolysis and tumor growth under hypoxic conditions, in hepatocellular carcinoma (HCC) (Yang et al., 2012). SIRT6 binds to and deacetylates the K433 residue of nuclear PKM2 leading to nuclear export of PKM2 via exportin 4 and the disruption of the oncogenic functions of PKM2. Furthermore, SIRT6 overexpression in HCC inhibits tumor growth by blocking extracellular signal-regulated kinases (ERK) 1/2 signaling pathway (Bhardwaj and Das, 2015).

In agreement with this metabolic role, SIRT6 has an important tumor suppressor role in liver cancer through different mechanisms: First, by repressing the oncogene survivin which results in reduced levels of H3K9ac and NF-κB. SIRT6 has an important tumor suppressor role in liver cancer through different mechanisms: First, by repressing the $onco_1$ phase, which deters tumorigenesis. Second, both SIRT6 and miR-122 oppositely regulate a similar set of genes related to metabolism and fatty acid β-oxidation and they both act as tumor suppressors (Elhanati et al., 2016). In fact, the overexpression of miR-122 or SIRT6 in hepatocellular carcinoma (HCC) cells reduces the expression levels of HCC-related genes AFP, H19, GPC3, and IGF2 (Marquardt et al., 2013; Elhanati et al., 2016).

Although most of its tumor suppressive functions relate to its metabolic roles, SIRT6 evolved to act as a tumor suppressor in pancreatic cancer, breast cancer and melanoma through separate mechanisms. For example, in pancreatic ductal adenocarcinoma (PDAC), SIRT6 deficiency resulted in histone hyperacetylation at the promoter of the oncofetal RNA-binding protein Lin28b, a negative regulator of the let-7 microRNA. Let-7 targets genes including HMGA2, IGF2BP1, and IGF2BP3 which promote tumorigenesis. In fact, low levels of both SIRT6 and high Lin28b are associated with poorer prognosis in PDAC patients, and SIRT6 downregulation resulted in a highly aggressive metastatic disease in a mouse model of pancreatic cancer (Kugel et al., 2016).

Interestingly, in some specific cases, SIRT6 may also play a pro-oncogenic role. For instance, in Hepatocellular carcinoma (HCC) SIRT6 overexpression is required for induction of transforming growth factor (TGF)-β1 and H2O2/HOCl (hypochlorous acid) reactive oxygen species that promote tumorigenesis. TGF-β1 stimulates SIRT6 expression inducing the activation of ERK and Smad pathways, altering the effect of these proteins on cellular senescence (Feng et al., 2015; Ran et al., 2016).

4.2.4. SIRT6 in cellular senescence, aging and oxidative stress response

SIRT6 overexpression in male transgenic mice significantly extends mean lifespan representing the first example of a mammalian sirtuin capable of lifespan extension in mice. The overexpression of SIRT6 causes reduced IGF1 blood levels, and increased levels of IGF-binding protein 1 and alterations in phosphorylation levels of components of the IGF1 signaling. Such mechanisms have been proposed SIRT6 as a driver in the longevity phenotype (Kanfi et al., 2012).

Moreover, increased levels of SIRT6 delay replicative senescence through attenuation of NF-κB signaling. Specifically, SIRT6 prevents NF-κB-dependent transcription through its H3K9ac deacetylase activity. Upon stress induced by TNF-α, SIRT6 redistributes to new gene promoters through its interactions with RelA/p65. The redistribution promotes de-repression of genes like Mapk2 and Fbxo4, and repression of a group of genes, among which are aging-associated Cdkn2a and Lmna (Kawahara et al., 2009; Kawahara et al., 2011). Moreover, SIRT6 induces the monoubiquitination of cysteines (Cys) in the pre-SET domain of Suv39h1, inducing the eviction of Suv39h1 from the gene IκBα, a general repressor of the NF-κB pathway. This in turn negatively regulates the NF-κB pathway (Santos-Barriopedro and Vaquero, 2018; Santos-Barriopedro et al., 2018).

In contrast, SIRT6 depletion results in accelerated cell senescence and hyperactive NF-κB signaling in *Sirt6*$^{-/-}$ mice. Consistently, calorie restriction can extend lifespan of aged mice through SIRT6 activation and thus the repression of NF-κB signaling (Zhang et al., 2016). In cellular senescence conditions, increased p27 acetylation levels promote its protein stability and senescent phenotypes. SIRT6 reduced the acetylation levels of p27, which results in protein destabilization by inducing proteasome-dependent degradation (Zhao et al., 2016).

Other studies reported that the C. elegans homolog of SIRT6, SIR-2.4, regulates stress response through preventing CBP-1 (CREB-binding protein 1)-mediated acetylation (Chiang et al., 2012). The decreased acetylation levels of DAF-16, the FOXO ortholog in C. elegans, triggers DAF-16-mediated transcriptional activities and DAF-16 nuclear localization upon stress. SIR2.4-dependent DAF-16 activation results in longevity, fat storage, and stress tolerance (Yen et al., 2011).

Moreover, SIRT6 recruits and mono-ADP-ribosylates BAF170, a subunit of BAF chromatin remodeling complex which plays a key role for activation of a subset of NRF2 responsive genes upon oxidative stress. SIRT6 mediated binding of BAF170 to enhancer region of the Heme oxygenase-1 locus and recruitment of RNA polymerase II (Rezazadeh et al., 2019).

4.2.5. Role of SIRT6 in cardiovascular system

SIRT6 has an important role in the cardiovascular system as well. Cardiomyocyte-specific SIRT6-KO mice develop spontaneous cardiac hypertrophy at around 8–12 weeks of age (Sundaresan et al., 2012). SIRT6 deficiency has been reported in failing human hearts and in mice subjected to hypertrophic stimuli, while SIRT6 overexpression protects against cardiac hypertrophy under stress conditions in mice (Alcendor et al., 2007). Recent studies confirmed the protective role for SIRT6 against heart diseases through inhibition of various pro-hypertrophic pathways including NF-κB, STAT3 and IGF-Akt. It prevents oxidative stress and cardiac fibrosis through inhibition of the NF-κB and the AMPK/angiotensin-converting enzyme 2 pathways (Kawahara et al.,2009; Yu et al., 2013; Shen et al., 2016; Zhang et al., 2016; Wang et al., 2016; Zhang et al., 2017). Furthermore, SIRT6 reduced the formation of foam cells associated with early atherosclerosis (AS) in an autophagy-mediated manner. The oxidized form of low-density lipoprotein-cholesterol (ox-LDL) is one of primary drivers of atherosclerosis imitation and progression (Mitra et al., 2011). Upon ox-LDL conditions, macrophage foam cell formation is decreased by SIRT6 via induction of autophagy and cholesterol efflux. Indeed, SIRT6 overexpression in foam cells increases levels of ABCA1 and ABCG1 and decreases miR-33 levels activating cholesterol efflux.

SIRT6 also significantly reduce cardiac hypertrophy caused by isoproterenol (ISO) through the activation of autophagy. ISO suppresses autophagy and causes cardiac hypertrophy in primary neonatal rats. SIRT6-dependent autophagy attenuates ISO-mediated cardiomyocyte hypertrophy. SIRT6 regulates cardiac autophagy in a FOXO3-mediated manner by repression of Akt signaling (Lu et al., 2016).

5. Histone methyltransferases and cancer

The important role of histone methylation in gene expression and genome organization placed histone methyl transferases in a central position in cancer epigenetics. KMTs and KDMs are capable to reprogram gene expression in response to cellular metabolism changes. Thus, it has been hypothesized, that KMTs and KDMs could contribute to metabolic control through transcriptional regulation of various metabolic enzymes (Teperino et al., 2010).

As discussed above, Suv39h1 and H3K9me3 are linked to heterochromatin organization, structure, and transcriptional silencing at constitutive and facultative heterochromatin regions. Several studies have shown correlation of altered Suv39h1 expression with cancers (Summarized in section 5.1.6). On the other hand, G9a specifically associates with euchromatin where is involved in the formation of facultative heterochromatin and repression of active promoters (Tachibana et al., 2005). G9a has been found to be overexpressed in a number of cancers. Consistently, G9a methylates the tumor suppressor p53, leading to its inactivation. Considering these observations, targeting of G9a and Suv39h1 should result in re-expression of various tumor suppressor genes in tumorigenesis (Huang et al., 2010). In this section, the role of these two important methyltransferases, Suv39h1 and G9a, will be discussed, focusing on its functional role in regulation of gene expression as well as its functional roles in cancer initiation and progression.

5.1. Suv39h1

The Su (var) or suppressor of variegation group of genes encode a wide number of factors involved in the maintenance of heterochromatin including HDACs, HMTs, and protein phosphatases. One of the most relevant members of this group is Su(var)3-9, that was originally identified in *D. melanogaster* and *S. pombe*. In 2000, Rea et al

identified the corresponding human (SUV39H1) and murine (Suv39h1) homologues, respectively. These enzymes showed to be histone methyltransferases specific for H3K9 (Rea et al., 2000).

5.1.1. Molecular structure and function

Members of SU(VAR)3-9 family proteins contain two evolutionarily conserved chromatin regulating motifs, the N-terminal "chromo" (chromatin organization modifier) and the C-terminal "SET" signature domain (Figure 6).

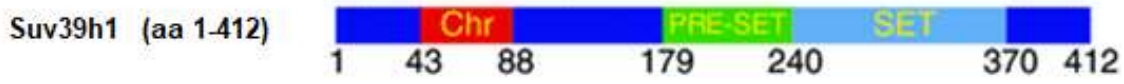

Figure 6. Suv39h1 structure is characterized by a catalytic SET domain at C-terminal, responsible for the enzymatic activity. In addition to the SET domain, two adjacent cysteine-rich regions, preSET and postSET are necessary for its proper enzymatic activity (adapted from Santos-Barriopedro et al., 2018).

The catalytic SET domain was initially identified in the three founding members of regulatory genes SU(VAR)3-9, the polycomb protein E(Z) and the trithorax-protein TRX. So far, this domain has been found in more than 140 proteins in eukaryotes. In addition to the SET domain, two adjacent cysteine-rich regions (preSET and postSET) are required for a proper enzymatic activity. This requirement is restricted to only a number of SET domain proteins like the Suv39h family members or *Crl4* (yeast homologue) (Melcher et al., 2000).

5.1.2. Constitutive heterochromatin formation

Constitutive heterochromatin is typically enriched in repetitive sequences, including tandem repeats, such as the minor and major satellite repeats (γ-satellite), DNA transposons like long interspersed nucleotide elements (LINEs) and short interspersed nucleotide elements (SINEs) (Saksouk et al.,2015). The selective methylation of H3K9 (H3K9me3) in these regions catalyzed by Suv39h1 creates a dynamic binding site for heterochromatin protein 1 (HP1) contributing to the establishment and maintenance of stable heterochromatic regions. HP1 binds to H3K9me3 through its N-terminal chromo domain (CD) and recruits Suv39h1 through its sequence-related C-terminal chromo

shadow domain (CSD) to the next nucleosome, spreading this mark and contributing to heterochromatin formation (Smothers et al., 2000). Subsequently, H4K20me3-specific HMT activities Suv4-20h1/2 are recruited by both HP1 and Suv39h1 promoting the deposition of H4K20me3 in these regions. H4K20me3 has, like H3K9me3, an important role in gene silencing and chromatin compaction, particularly through a specific functional relationship with cohesins (Fioriniello et al., 2020).

The role of Suv39h1 in heterochromatin goes beyond chromatin structure. For instance, in the case of telomeres and telomeric heterochromatin, Suv39h1 also governs proper telomere capping. Depletion of both enzymes result in a decrease in di- and tri-methylated H3K9 and HP1 levels and an abnormal telomere length (Petti et al., 2015).

As mentioned earlier, SIRT1 is the main Sirtuin involved in pericentromeric heterochromatin (PCH), as its loss has been linked to a loss of PCH foci and de-repression of the underlying γ-satellites (Oberdoerffer et al., 2008). Under stress conditions SIRT1 promotes *in vivo* upregulation of Suv39h1, which provides a direct link between the stress response and Suv39h1 expression levels in heterochromatin structure as a mechanism of genome protection (Bosch-Presegué et al., 2011).

5.1.3. Facultative heterochromatin formation

As mentioned, Suv39h1 is also associated with facultative heterochromatin formation of different regulatory pathways such as NF-κB, Retinoblastoma or p53-dependent signaling. In these regions Suv39h1 associates with other proteins involved in transcriptional repression, such as HDAC1 and HDAC2, but also SIRT1 and SIRT6 (Santos et al., 2018). Suv39h1 binds to HDAC1 and HDAC2 through its N-terminal domain in order to promote gene silencing. It has been linked to the core histone deacetylase complex formed by HDAC1, HDAC2, RbAp48 and RbAp46 and other subunits. For instance, Runx1 interacts with the repressor complex Sin3 (which comprises HDAC1 and HDAC2), Suv39h1 and HDAC3 to induce gene repression (Reed-Inderbitzin et al., 2006). Retinoblastoma (Rb) protein is recruited to promoters by sequence-specific transcription factors such as E2Fs, which preferentially recruits Suv39h1, HDAC1/2 repressor complex and HP1 to silence target key genes such as cyclin E and

cyclin A gene (S-phase genes) (Vandel et al., 2001; Nielsen et al., 2001). Additionally, Cabin-1 triggers MEF2-target genes silencing by interacting with Suv39h1 and the Sin3 complex leading to the inhibition of interaction between MEF2 with coactivator p300 (Youn et al., 2000).

Suv39h1 also interacts with other HMTs such as GLP. Thus, both HMTs form a complex with MDM2 which binds to p53 target promoters. While GLP inactivates p53 through methylation, Suv39h1 methylates and represses p53 target genes (Chen et al., 2010). The functional relationship between SIRT1 and Suv39h1 goes beyond PCH and is also relevant in facultative heterochromatin. For instance, both SIRT1 and Suv39h1 are components of the nucleolar silencing complex (eNoSC) associated with rRNA transcription regulation in response to glucose deprivation (Murayama et al., 2008). Under glucose starvation conditions, another component of eNOSC, nucleomethylin (NML), inhibits rRNA synthesis through recruiting SIRT1 and Suv39h1 to rDNA promoters, which results in the spreading of heterochromatin marks throughout the rDNA repeat (reviewed in Yang and Chen 2014).

5.1.4. Cell cycle and Suv39h1

Given its key role in chromatin condensation and organization, Suv39h1 plays a key role in cell cycle progression. Furthermore, the levels of H3K9me3 in PCH, are important not only for chromatin compaction, but also to promote an efficient dynamic establishment of other epigenetic marks, such as H4K12ac and H3S10P. For instance, H3K9me3 inhibits H3S10 phosphorylation mediated by kinase Aurora-A. H3S10 phosphorylation by Aurora-A occurs in G2/M phase and is necessary for chromatin condensation during mitosis (Ribeiro-Mason et al., 2012). Suv39h1 is dynamically distributed in mitotic chromatin during cell cycle. It is found in centromeres from prometaphase to anaphase. H3K9ac levels decrease from G2 to metaphase, while the levels of H3K9me3 and the HMTs, Suv39h1 and SETDB1 increase in centromeres, to promote chromosome condensation (Loyola et al., 2009).

Among the many Suv39h1 interacting proteins, retinoblastoma (Rb) is of particular interest. Suv39h1 is bound to Rb in a complex with HP1γ, which predominantly localizes

to euchromatic regions, and contains a chromodomain capable of recognizing methylated lysine 9 on histone H3 (Nielsen et al., 2001). Suv39h1 is phosphorylated in G1/S phase, and this phosphorylation is increased when Sbf1, a phosphatase inhibitor, is overexpressed. This in turn inhibits the Suv39h1-mediated ability of Rb to block E2F transcription of cyclin E promoter in the G1/s checkpoint (Firestein et al., 2000). During S-phase of cell cycle CDK2 phosphorylates Suv39h1 at S391 residue to facilitate dissociation of Suv39h1 from chromatin and demethylase JMJD2A recruitment allowing a correct replication of heterochromatin. Moreover, it has been shown that Suv39h1 deficiency induces hypersensitivity to replicative stress and DNA replication impairment (Park et al., 2014).

5.1.5. Suv39h1 and DNA repair

Suv39h1 also plays a direct role in DNA repair, as transient formation of repressive chromatin is crucial for stabilization of the damaged chromatin and chromatin remodeling, which provides an efficient template for the DNA repair machinery. Upon DNA damage SET7/9 (H3K4 histone methyltransferase) binds to the Suv39h1 chromodomain and methylates it at K105 and K123. Methylated Suv39h1 shows a decreased activity which induces a loss in H3K9me3 levels and as consequence promotes heterochromatin relaxation and genomic instability (Wang et al., 2013). After DNA damage, the recruitment of the complex Suv39h1/Kap1/HP1 to DSB foci induces an increase in H3K9me3, which spreads along the damage site, activating the Tip60 HAT which in turn acetylates and activates ATM. Activated ATM immediately phosphorylates KAP-1, leading to release of the repressive Suv39h1/Kap1/HP1 complex from the chromatin. Thus, ATM activation functions as a negative feedback loop to eliminate repressive Suv39h1 complexes at DSBs, which may interfere in DSB repair. Suv39h1/KAP1/HP1 recruitment to DSBs provides a mechanism for transiently increasing H3K9me3 levels in open chromatin domains that lack H3K9me3 to ensure an efficient activation of both Tip60 and ATM in these regions (Liu et al., 2013; Ayrapetov et al., 2014).

5.1.6. Suv39h1 and Cancer

A number of studies have been correlated Suv39h1 de-regulation with cancers. As in the case of SIRT1 and SIRT6, Suv39h1 has been assigned a pro-tumorigenic and tumor suppressor role, depending on the functional context. Suv39h1/H3K9me3 attenuates sulforaphane-induced apoptotic signaling in PC3 prostate cancer cells (Watson et al., 2014) and is frequently upregulated in human hepatocellular carcinoma (HCC) (Cai et al., 2011). Another study demonstrated that Suv39h1 promotes HCC progression and is negatively regulated by microRNA-125b (Fan et al., 2013). As a tumor suppressor, the link between Suv39h1 and Rb protein in the progression of the cell cycle, seems to be important for Rb-associated tumor suppression.

5.2. G9a

G9a (KMT1C/EHMT2) and its closely related homolog, GLP (KMT1D/EHMT1) are responsible for the H3K9 mono and di-methylation in mammals. Additionally, G9a targets many non-histone proteins including itself. H3K9me2 is a hallmark of gene silencing in euchromatin and, as in the case of H3K9me3, is a recognition site for heterochromatin protein 1 (HP1). Despite H3K9me2 is the primary product of G9a methylation, the G9a complex (contains GLP) has also been showed to methylate histone H1 and contributes to the H3K27 methylation as well (Tachibana et al.,2001; Ta chibana et al.,2002; Shankar et al., 2013). PRC2 interacts physically and functionally with G9a and GLP. In fact, PRC2 and G9a/GLP share a considerable number of genomic targets and regulate expression of a subset of developmental and neuronal genes. This regulation is dependent on G9a enzymatic activity which is involved in PRC2 recruitment (Mozzetta et al., 2014).

5.2.1. G9a structure and function

G9a is composed of different domains and repeats: i) an N-terminal region containing the NLS sequence; ii) a protein domain containing ankyrin (ANK) repeats, which are involved in protein-protein interaction; and iii) the catalytic SET domain, flanked by a preSET and a postSET domains (Figure 7).

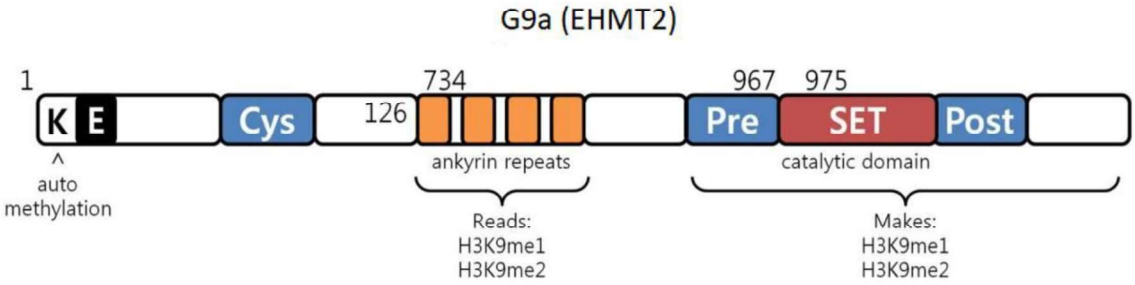

Figure 7. G9a structural organization. G9a structure is characterized by an auto-methylation site at its N-terminal end, ankyrin repeats which recognize mono and dimethylated histone H3K9 and by a catalytic SET domain, responsible for the enzymatic activity (adapted from Collins et al., 2010).

G9a depletion results in embryonic lethality due to activation of repressed genes (Estève et al., 2005). Loss of G9a induces a significant decrease in H3K9me2 dimethylation and a subsequent hyperacetylation of H3K9 in euchromatin regions, which in turn promotes hypermethylation of H3K4me3 (Peters et al., 2003; Rice et al., 2003). G9a has a stronger *in vitro* specific activity than Suv39h1. Although G9a induces in general gene repression through its catalytic activity, it can also induce gene repression through a catalytic-independent mechanism, which involves the specific interaction with additional chromatin modifiers (Bittencour et al., 2012).

There are many examples of G9a functional relevance. For instance, G9a depletion in embryonic stem (*G9a*$^{-/-}$ ES) cells leads to H3K9me2 loss at the Mage-a (Melanoma-associated antigen-a) promoter, a gene that encodes tumor antigens. In turn, this results in general repression of Mage-a-target genes (Tachibana et al., 2002). Recruitment of G9a and induction of H3-K9 methylation at antigen receptor gene segments blocks their germline transcription and V(D)J recombination (Osipovich et al., 2004). Moreover, G9a-dependent H3K9me2 has also been involved in silencing of developmentally regulated genes through interaction with CDP/cut (Nishio and Walsh, 2004), the plasma cell transcription factor Blimp-1 (Gyory et al., 2004), and the neuron-restrictive silencing factor NRSF/REST (Roopra et al., 2004).

As mentioned before, G9a forms a complex with GLP which contains Wiz, a zinc finger protein that is essential for heterodimerization and stability of G9a/GLP complex. Wiz

has two CtBP co-repressor binding sites, which are responsible of G9a/GLP association with the CtBP co-repressor complex (Shi et al., 2003). Wiz may recruit diverse types of transcriptional repressors other than CtBP, to promote gene silencing.

G9a interacts with the E2F1/PCAF complex and enhances PCAF occupancy and histone acetylation marks at E2F1-target promoters. G9a also prevents cell cycle exit by transcriptionally repressing p21 and Rb1 in a methyltransferase activity-dependent manner. These evidences suggest that G9a functions both as a co-activator and a co-repressor to enhance cellular proliferation and inhibit myogenic differentiation (Rao et al., 2016). As mentioned earlier, G9a/GLP also play a role in PRC2 recruitment and the establishment of H3K27me3, which has a key role in the repression of a subset of genes involved in development and differentiation (Mozzetta et al., 2014).

5.2.2. The role of G9a in tumorigenesis

G9a is upregulated in different types of cancer such as liver, colon, ovarian, bone marrow, prostate and bladder cancer. Consistently, increased levels of G9a have been directly associated to poor prognosis. In recent years, the mechanism of action of G9a in tumorigenesis has aroused great interest among scientist community. In human hepatocellular carcinoma, G9a knockdown resulted in reduction of H3K9me2 levels and impairment of both HCC cell growth and sphere formation (Yokoyama et al.,2017). In breast cancer cells, G9a is a key mediator of a wide range of oncogenic processes, including cell growth *in vitro* and *in vivo*, by repressing ferroxidase hephaestin and regulating cellular iron homeostasis (Wang et al., 2017).

Under hypoxic conditions, the stability of G9a protein increases due to decreased proline hydroxylation, which results in a decrease in proteasome degradation efficiency as well as an increase in H3K9me2. Consistently, inhibition of G9a activity induces a block in proliferation and migration of tumor cells *in vitro* and tumor growth *in vivo*. Moreover, an increase in G9a levels is a key factor mediating hypoxia response through the downregulation of several specific genes, such as ARNTL and CEACAM7. This down-regulation can be also modulated by small molecule inhibitors of G9a. Interestingly, these findings can be used as a diagnostic biomarker (Casciello et al., 2017). Other studies revealed that G9a promotes the development of lung cancer by inhibiting CASP1, a cysteine-containing aspartate proteolytic enzyme present in the cytoplasm and is

important in the activation of pyroptosis and inflammasome. Thus, G9a inhibits the expression of the CASP1 gene by methylating its promoter region. CASP1 overexpression inhibits the invasion and migration of lung cancer cells. However, a reduction in CASP1 expression can partially restore the invasion and migration ability of G9a-deficient lung cancer cells, which suggests that the interaction of cytokine and its receptor might be one of the pathways of lung cancer initiation. Furthermore, the expression of CASP1 and G9a correlate negatively in a large number of lung non-small cell lung cancer samples, and high expression of G9a or low expression of CASP1 are significantly associated with poor prognosis in non-small cell lung cancer (Chen et al., 2018).

Altogether, the available evidence suggests that Suv39h1 and G9a play important roles in tumorigenesis at different levels. For this reason, both HMT activities are regarded as a very promising therapeutic targets for cancer treatment. Current efforts to develop novel Suv39h1 and G9a inhibitors, together with EZH2 inhibitors, will probably shape the landscape of cancer epigenetic treatment in the future.

6. Protein phosphorylation

Protein phosphorylation is recognized as one of the most common and versatile mechanisms in cell signaling (Li et al., 2013). Reversible protein phosphorylation plays a key role in control of signal transduction and cellular functions via modulation of protein-protein interactions (PPIs), protein activity and localization. As in the case of other PTMs, protein kinases and phosphatases act in opposition promoting a dynamic control of protein phosphorylation levels. Although proteins are phosphorylated on three main residues (serine, threonine and tyrosine), over 95% of phosphorylation occurs on serine/threonine residues (Nestler et al., 1999). Phosphorylation can alter the modified protein in three important ways: First, it adds two negative charges that can cause a major conformational change in the protein; second, it can be specifically recognized by protein readers; third, the mark can also obstruct protein-protein interaction (Lee et al., 2016).

6.1. Serine/Threonine-Specific Phospho-Protein Phosphatases (PPP) family

Serine/threonine phosphatases can be classified into three main families: the metal-dependent protein phosphatases (PPMs) like PP2C, the aspartate-based phosphatases, and the phosphoprotein phosphatases (PPP) such as PP1, PP2A, PP2B, PP5 and PP7. Members of PPP family catalyze more than 90% of all protein dephosphorylation reactions in eukaryotic cells. The PPP family can be subdivided into various groups: PP1, PP2/PP2A, PP3/PP2B (exclusively in animals), PP4, PP5, PP6, PP7, PPKL/Kelch (exclusively in plants and alveolates), and bacterial-like protein phosphatases (SLP, RLPH, ALPH) (Maselli et al., 2014; Uhrig et al., 2013). Compared with other PPP family members PP2A, PP4, and PP6 are phylogenetically distinct by cluster which is indicative of a common ancestor (Uhrig et al., 2013). The members of the PPP family are usually found in multimeric complexes. For example, in the case of PP2A family is found in dimeric or trimeric complexes containing catalytic and regulatory subunits which confer substrate specificity and tissue- and cell type-specific targeting (Virshup et al., 2009).

6.1.1. Protein Phosphatase 2A (PP2A) and Protein Phosphatase 6 (PP6)

6.1.1.1. PP2A

PP2A plays a key role in various cellular pathways, such as replication, DNA damage repair, cell growth, transcription, protein synthesis, and differentiation (Janssens et al., 2001; Van Hoof et al., 2003; Eichhorn et al., 2008). PP2A activity or expression levels of its catalytic (PP2Ac) or regulatory subunits are downregulated in a variety of cancer cell lines which have led PP2A to be classified as a tumor repressor (Mumby et al.,2007). PP2Ac dysregulation has been reported in other human diseases, including diabetes and Alzheimer's disease (Clark et al., 2019; Martin et al.,2013). In Alzhei mer's disease and other pathologies related to tau protein dysfunction, PP2A is usually downregulated, as it is one of the essential tau phosphatases (Braithwaite et al., 2012).

6.1.1.2. PP6

PP6C, the catalytic subunit of the phosphatase complex, is ubiquitously expressed and its deficiency is embryonic lethal. PP6 has a wide range of functions in cell cycle, genome

stability and cell signaling conserved through evolution. Sit4 (Yeast PP6C homolog) plays a key role in G_1 to S phase progression (Sutton et al., 1991, Stefansson et al., 2007), response to mtDNA damage, TOR signaling, and ER-to-Golgi transport (Bhandari et al., 2013). In higher eukaryotes, PP6 is involved in regulating DNA damage repair, mitosis, autophagy, cell death, and inflammatory signaling (Garipler et al., 2014; Douglas et al., 2010; Zenget al., 2010; Wengrod et al., 2015; Kajino et al., 2006). PP6 activity is essential in DNA repair, specifically in DSBs pathways, HR and NHEJ via its interactions with SAPS-containing regulatory subunits (Douglas et al., 2010; Douglas et al., 2014; Mi et al., 2009).

Like other members of PP2A family, PP6 forms different holoenzyme complexes consisting of a catalytic subunit (PP6C) and at least one regulatory protein. Knockdown or loss-of-function mutations of PP6 lead to increased mutation rates and in consequence increased tumor incidence. For instance, PP6C conditional knockout increases tumorigenesis when the cells are exposed to either dimethyl benzanthracene or UVB radiation (Kato et al., 2015). Additionally, PP6 also suppresses cancer metastasis through regulation of E-cadherin surface expression (Ohama et al., 2013).

6.1.2. Protein Phosphatase 4 (PP4)

Protein phosphatase 4 (PP4), a PP2A-like phosphatase, is one of the most conserved phosphatase activities across metazoans (Mendoza et al., 2007). As PP6, it is involved in a number of cellular processes as diverse as DNA damage response, cell cycle, embryo development, organelle assembly, chemotaxis, and metabolism (Toyo-oka et al., 2008; Mourtada-Maarabouni et al., 2003; Su et al., 2013; Liu et al., 2012). Consistently, it has been linked to several key signaling pathways such as JNK (Huang and Xue, 2015; Zhou et al., 2002), Insulin-like growth factor (Mihindukulasuriya et al., 2004) and developmental signaling pathways such as Hedgehog(Hh) (Jia et al., 2009).

6.1.2.1. PP4 regulatory subunits and holoenzyme complexes

Five main regulatory subunits of PP4 have been identified so far including PP4R1, PP4R2, PP4R3α, PP4R3β, and PP4R4 (Hastie et al., 2000). These subunits are distinct from PP2A subunits, which suggests that they provide the functional specificity of the

complex. In addition to these subunits, some PP4 complexes also harbor other subunits shared with PP2A family such as Alpha4 and TIPRL1 (Gingras et al., 2005, Kloeker et al., 2003) (Figure 8).

The PP4/PP4R2 complex is shown to participate in p53 checkpoint signaling via dephosphorylation of DBC-1 resulting in apoptosis inhibition (Lee et al., 2015) and activation of KAP1 which leads to repression of p21 transcription (Shaltiel et al.,2014). PP4 complex also dephosphorylates HDAC3 inhibiting its enzymatic activity (Zhang et al., 2005), which is showed to be involved in several regeneration-associated signaling pathways (Heinz et al., 2010).

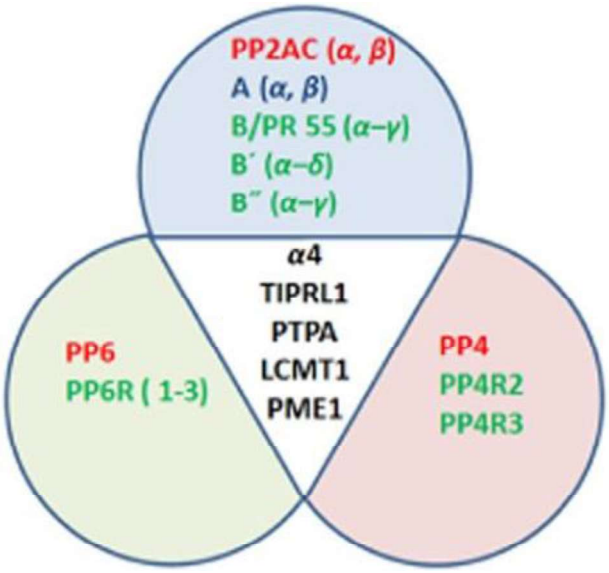

Figure 8. PP2A, PP4 and PP6 subunits and regulatory subunits in Homo sapiens. Catalytic subunits are shown in red, canonical subunits in blue and regulatory subunits are in green. Putative interactor proteins shared by PP2A, PP4 and PP6 are shown in black (adapted from Lillo et al., 2014).

As we will detail below, PP4 has an important role controlling phosphorylation of key proteins including H2AX, RPA2 and KAP1 especially in early DNA damage response (DDR), which is also crucial to double strand break repair, apoptosis and cell cycle arrest (Lee et al., 2010).

Despite the important roles of PP4, the mechanisms by which its activity is regulated are poorly understood, and no specific modulators of PP4 activity or PP4-dependent dephosphorylation have been identified up to this date.

6.1.2.2. PP4 roles in DNA repair

PP4 regulates multiple aspects of the DNA damage response, including DNA repair, DNA damage checkpoint and cell cycle recovery. In DNA repair, PP4 regulates the steady-state phosphorylation of multiple factors implicated in response to replication stress and DNA damage. PP4 is also responsible of H2A dephosphorylation in both yeast and human cells to promote a more efficient recovery from the DNA damage checkpoint arrest (Keogh et al., 2006; Chowdhury et al., 2008; Nakada et al., 2008). It has also been involved in the recruitment of 53BP1 to chromatin during formation of DNA lesions (Lee el al., 2014) and facilitating recovery from the G_2/M arrest by dephosphorylation of KAP1 (Lee el al., 2012). Additionally, as PP1 and PP2C, PP4 can dephosphorylate Rad53 after MMS (methylmethane sulfonate) treatment which results in increased ROS levels (O'Neill et al., 2007). The role of PP4 in the DDR is not only restricted to checkpoint recovery as in human and yeast it also induces DSB repair by homologous recombination (Kim et al., 2011).

6.2. The replication protein A (RPA)

Single-stranded DNA binding proteins (SSBs) are conserved throughout evolution. All prokaryotes and eukaryotes contain SSBs, which bind specifically to regions of single stranded DNA through multiple binding domains. This specific recognition is essential for many conserved processes including DNA repair, replication and recombination (Ashton et al., 2013; Flynn et al., 2010). Replication Protein A (RPA) is the most abundant SSB in eukaryotes, which contain from 50000 to 240000 RPA complexes per cell (Iftode et al., 1999). RPA is a heterotrimeric protein complex composed of three subunits RPA1, RPA2, and RPA3 with molecular masses of 14, 32, and 70 kDa, respectively (Figure 9). All three subunits have been identified in all eukaryotic organisms studied so far from mammals to yeast suggesting that this protein complex is one of the most conserved eukaryotic SSBs (Binz et al., 2004; Fanning et al., 2006). Each subunit of RPA complex is crucial for viability in *S. cerevisiae* (Brill et al., 1991) reflecting the essential role of RPA proteins *in vivo*. Interestingly, humans, appear to harbor an additional RPA2 homologue, termed RPA4, which is preferentially expressed in the placenta and colon, but the role of this protein in other cellular processes is unknown (Keshav et al., 1995).

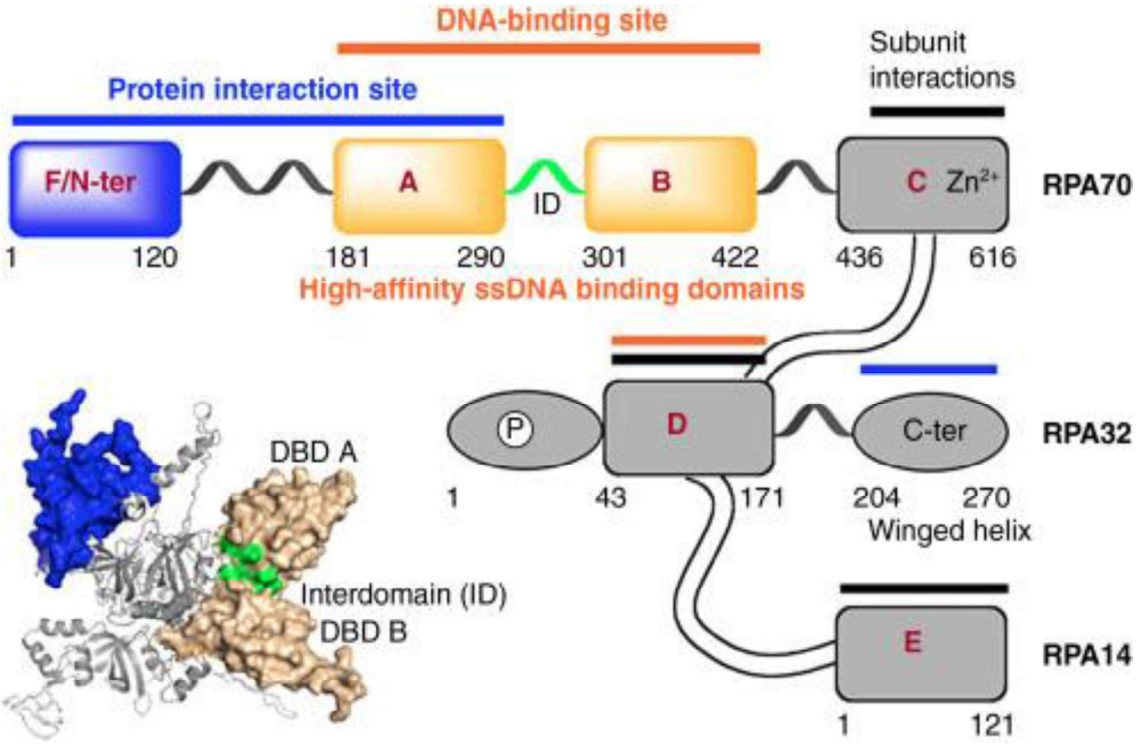

Figure 9. Schematic picture representing RPA heterotrimeric subunits (70, 32, and 14 kDa) and OB-fold domains (A–F). The RPA heterotrimer structure is colored according to the schematic diagram. The sites of DNA interactions are shown in the orange bars, subunit interaction sites in the black bars and domains associated with other proteins binding in the blue bars (adapted from Gavande et al., 2016).

RPA is known to be phosphorylated upon exposure to stress and binding to ssDNA. Although no phosphorylation has been identified in RPA1, nine potential phosphorylation sites have been identified in the N-terminal domain of RPA2 (Niu et al., 1997; Anantha et al., 2007; Liu et al., 2005). RPA2 becomes phosphorylated in both cell cycle and DNA damage-dependent manner. Cyclin-dependent kinase phosphorylates RPA2 at serine residues 23 and 29 in mitosis. Cyclin-dependent kinase 2 (CDK2) is in charge of S phase-dependent phosphorylation of RPA2. DNA damage-induced phosphorylation of RPA2 is so-called RPA2 hyperphosphorylation includes phosphorylation of threonine 21, serines 4, 8 and 33 and at least one phosphoserine in residues 11–13. These modifications are mediated by the phosphatidylinositol 3-OH-kinase-related kinase (PIKKs) family, which includes ATM (Ataxia-telangiectasia mutated), ATR and DNA-PK (DNA-dependent protein kinase) (Binz et al., 2004). A novel DNA damage-induced phosphorylation site at Thr-98 in RPA2 was also recently identified (Nuss et al., 2005) (Figure 10).

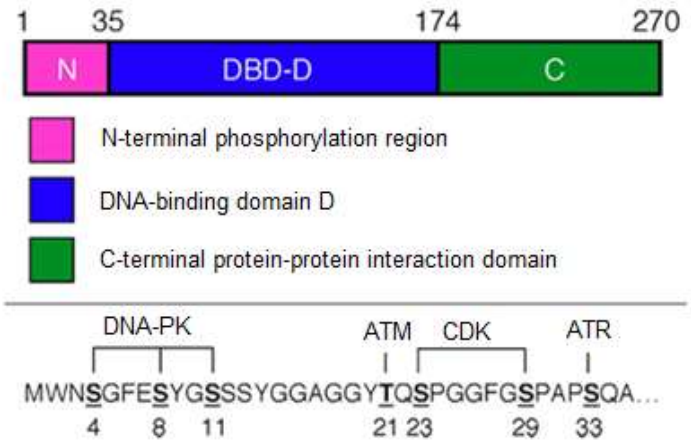

Figure 10. Key domains of RPA2 and its phosphorylation sites. (Upper panel) An schematic picture of RPA2. This subunit is composed of 270 residues. It contains an N-terminal phosphorylation region, a central DNA-binding domain (termed DBD-D), and a C-terminal region. (Lower panel) RPA2 phosphorylation sites are shown in bold, with the principal responsible kinases indicated above each residue. Some residues can be phosphorylated by more than one kinase (e.g., T21 by ATM and DNA-PK) (adapted from Binz and Wold, 2008).

As mentioned above, PP4 efficiently dephosphorylates phospho-RPA2 *in vitro*, and interestingly, silencing of PP4R2 in cells alters the kinetics and pattern of RPA2 phosphorylation (Lee et al., 2010).

7. DNA damage response pathways and Repair mechanisms

Based on its origin, DNA damage can be classified into endogenous and exogenous damage. The origin of majority of the endogenous DNA damage is caused by the chemically active DNA involved in oxidative reactions with water producing reactive oxygen species (ROS). In contrast, exogenous DNA damage is caused by environmental, physical and genotoxic agents that can damage the DNA. These agents include UV and ionizing radiation, crosslinking agents (e.g., mitomycin C, cisplatin) and alkylating agents (Visconti and Grieco, 2009; Reuter et al., 2010; Perrone et al., 2016). For almost each type of damage, the cell has one or more specialized pathways to repair DNA and prevent cell death (Figure 11).

The cells have different mechanisms of protection against exposure to ionizing radiation and subsequent oxidative stress caused by ROS or free radicals. The pathways which are responsible of clearance of ROS and repairing DNA damage play a critical role

in cell viability and survival. DNA repair pathways use an excision mechanism to remove the short single-stranded DNA segment that contains the lesion and use the other strand as template to re-synthesize it. Thus, double-strand breaks are more detrimental and if unrepaired can result in cell death and genomic instability. More than 150 genes have been found to be involved in repair mechanisms so far.

The DNA repair pathways can be classified into six major multistep pathways: base excision repair (BER), nucleotide excision repair (NER), mismatch repair (MMR), homologous recombination (HR), non-homologous end joining (NHEJ) and the translesional synthesis (TLS) (Natarajan et al., 2016). The majority of them are associated with the repair of radiation-induced DNA damage.

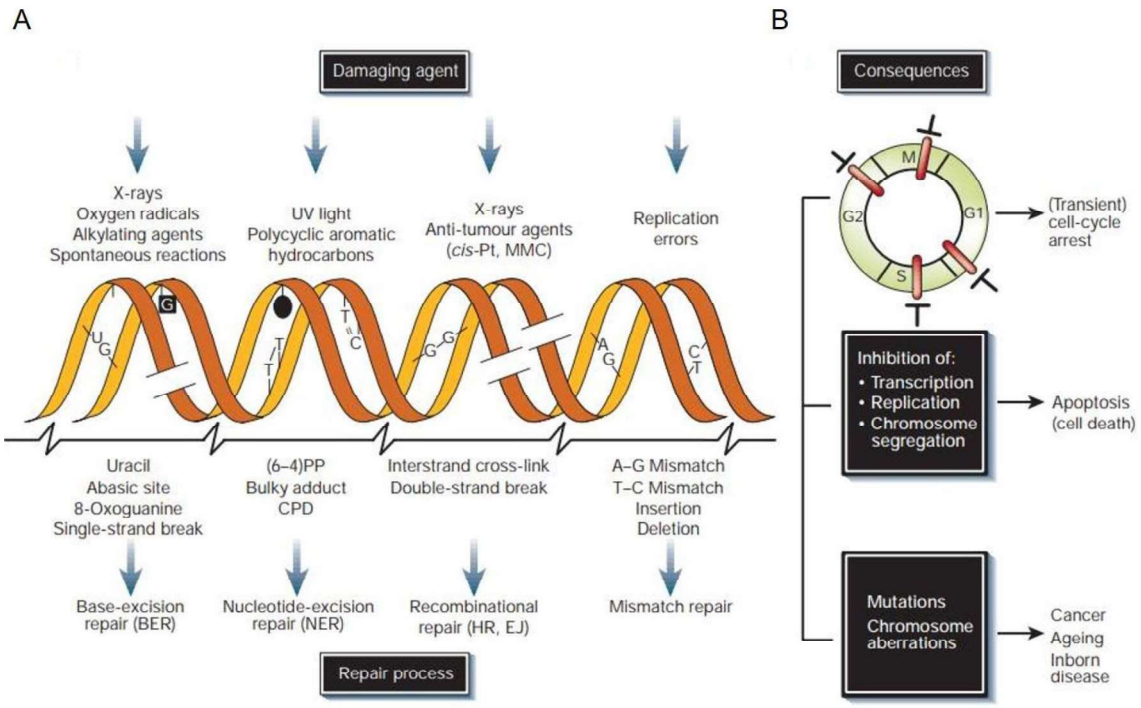

Figure 11. DNA damage, repair mechanism and their consequences. **(A)** DNA damaging agents (top); examples of induced DNA lesions (middle); and DNA repair mechanism responsible for the removal of the lesions (bottom). **(B)** The effects of DNA damage on cell-cycle progression, DNA metabolism (middle) and long-term consequences of DNA damage (bottom) and their biological consequences. Abbreviations: Cis-Pt and MMC, cisplatin and mitomycin C, respectively (both DNA-crosslinking agents); (6–4) PP and CPD, 6–4 photoproduct and cyclobutane pyrimidine dimer, respectively (both induced by UV light); BER and NER, base- and nucleotide-excision repair, respectively; HR, homologous recombination; EJ, end joining. (adapted from Hoeijmakers et al., 2001)

7.1. Double-strand break repair

DNA double-strand breaks (DSBs) are considered to be the most damaging lesions. DNA-damaging agents such as ionizing radiation (IR), some chemicals or endogenously produced ROS can cause DNA double-strand breaks. DSBs can promote genotoxic effects and cell death; they also may contribute to tumor initiation and progression through genome rearrangements and point mutations (Cannan et al., 2016).

Two main interrelated pathways can repair DSB: homologous recombination (HR) and non-homologous end-joining (NHEJ). NHEJ functions during the entire cell cycle and allows a fast DNA repair. However, it is a highly error-prone mechanism, because it only joins the ends of double stranded DNA together, hence it is susceptible to produce genetic alterations. In contrast, homologous recombination is a slower and more efficient process restricted to S and G_2 phases of the cell cycle in which the homologous DNA strand is used as a template for repair (Brandsma and van Gent, 2012).

The decision about which repair pathway is used depends on several factors, including the cell cycle stage or the origin of the damage. For instance, two-ended double strand breaks caused by ionizing radiation can be repaired either by NHEJ or HR. Once one-ended DSB, which may occur when a replication fork runs into an unrepaired SSB will be generally repaired by HR (Figure 12).

7.1.1. Homologous recombination (HR)

During homologous recombination, the undamaged sister chromatid is used to repair the DNA damage. The repair is initiated by 5’ to 3’ nucleolytic resection of the DSB end and by the MRE11-Rad50-NBS1 (MRN) complex to generate 3’-single-stranded DNA tails. The recruitment of the MRN complex is promoted by the binding of NBS1 to yH2AX. After strand resection and protein binding, the resulting complex accesses the complementary sequence of the sister chromatid and catalyzes strand-exchange events which displace one strand as a D-Loop in the end. This process requires the activity of BRCA2 and RAD51 (Figure 13).

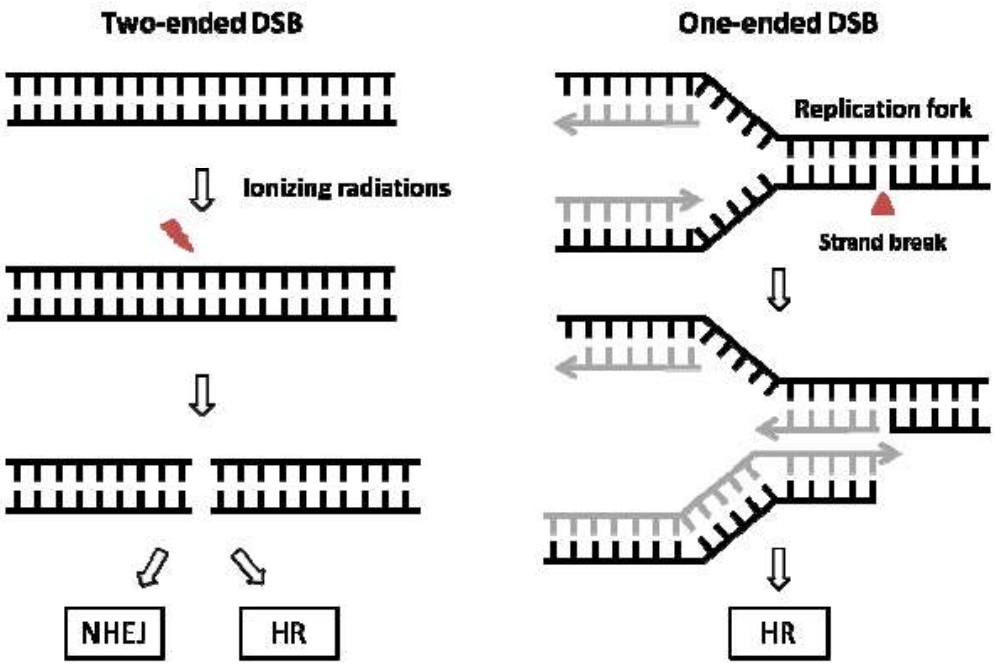

Figure 12. Double-strand breaks (DSBs) in DNA can form as a result of exposure to stress. A one-ended DSB generated by replication stress when only one strand of double-stranded DNA is interrupted and normally is repaired by HR. A two-ended DSB generated by ionizing radiations is broken into two pieces and can be repaired either by HR or NHEJ.

The main function of BRCA2 in recombination is controlling the recombinase activity of RAD51 and its assembling onto ssDNA. RAD51 is assisted by a number of protein factors including BRCA1, RAD52, and RAD54. After D-loop formation, the annealed 3'-end is extended by repair synthesis beyond the original break site to restore the missing sequence information (Cheng et al., 2004; Cheng et al., 2006; Baynton et al., 2003; Otterlei et al., 2006).

Although HR is the most effective error-free DSB repair, the requirement of an undamaged sister chromatid as a repair template for the genetic exchange of DNA between two homologues restricts this pathway to S and G_2 phases. In Figure 13, HR is initiated by the displacement of the Ku complex and recruitment of the heterotrimeric MRN complex for DSB recognition (Chanut et al, 2016).

7.1.2. Non-homologous end joining (NHEJ)

NHEJ is the predominant double-strand break (DSB) repair pathway at all cell cycle stages and especially active in G_2/M. It probably evolved as the main repair pathway for

DSBs during evolution due to its robustness, versatility and reduced limitations such as cell cycle stage (Mao et al., 2008).

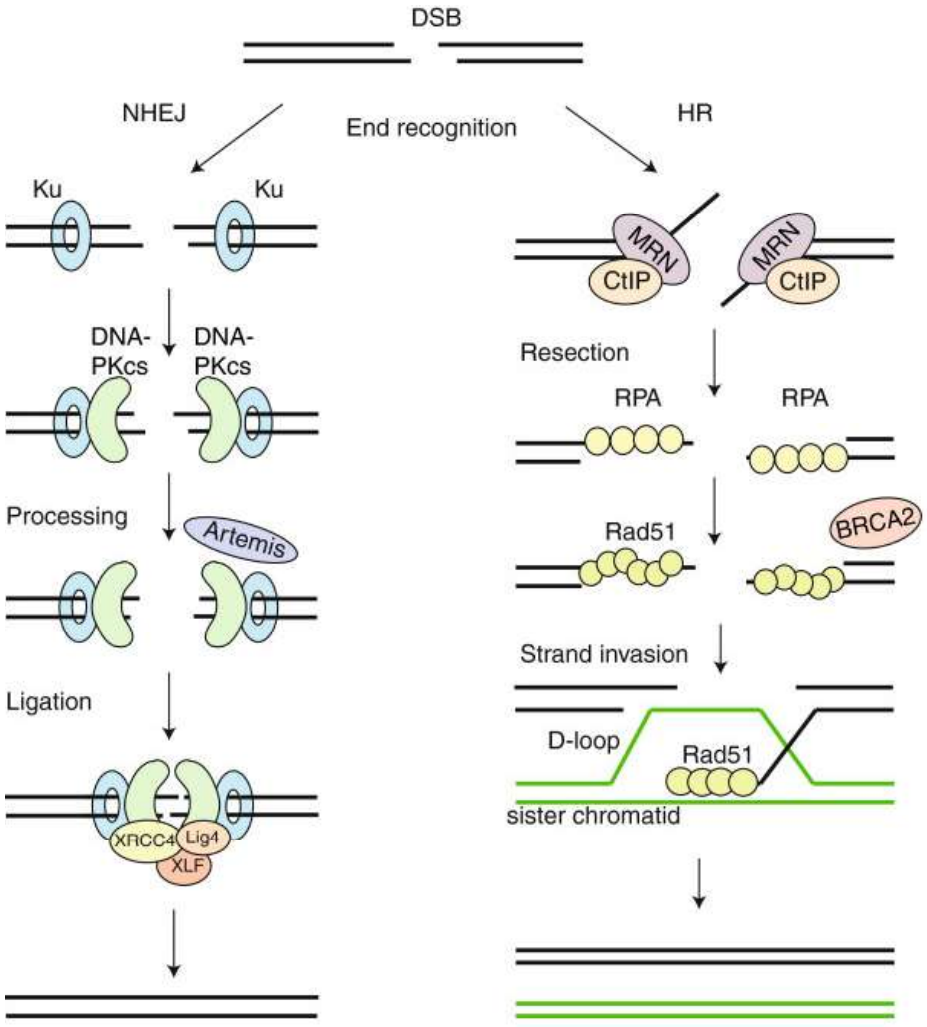

Figure 13. Homologous recombination (HR) and Non-homologous end-joining (NHEJ). NHEJ starts with recognition of the DNA ends by the Ku70/80 heterodimer through recruiting DNA-PKcs. If the ends are incompatible, nucleases such as Artemis can cut the ends and XRCC4-DNA Ligase IV-XLF ligation complex can seal the break. In the case of HR, the MRN-CtIP-complex starts resection on the breaks to generate ssDNA. After resection the break can be repaired by NHEJ. The ssDNA is first covered by RPA, which is subsequently replaced by Rad51 by means of BRCA2. Rad51 nucleoprotein filaments promote strand invasion on the homologous template. D-loop extension and capture of the second end result in break repair (adapted from Brandsma and van Gent, 2012).

This can explain the presence of Ku in all eukaryotic cells and the presence of its homologs in prokaryotes (Bowater et al., 2006).

Six core components are required in NHEJ: DNA- dependent protein kinase catalytic subunit (DNA-PKcs), Ku70, Ku80, DNA ligase IV (LIG4), XLF and XRCC4. Two blunt ended

DSB is a substrate for NHEJ. If end processing is not required, the heterodimeric complex Ku70/80 tightly binds to the both ends of damaged DNA; it recruits the DNA–PK catalytic subunit (DNA–PKcs) which is activated once bound to DNA. DNA-PKs undergo autophosphorylation, which results in kinase inactivation and dissociation. It makes the DNA ends become more accessible for LIG4, XRCC4, and XLF, which all together form an efficient ligase complex and seal the DNA ends (Figure 13). The ligase complex cannot re-ligate directly the majority of the DSBs. If DNA breaks, first the ends need to be processed by the MRN complex to facilitate subsequent DNA repair. MRN complex has both exonuclease and helicase activity against single-stranded DNA and prepares it for the ligation complex. The joining of DNA end configurations with 3'- and 5' overhangs, flaps, gaps or hairpins requires an extra processing before sealing. This is carried out by another protein named Artemis, which functions in a complex with DNA-PKcs. Upon Artemis phosphorylation by DNA-PKcs, its endonuclease activity is activated, to degrade DNA single-strand overhangs and modify them for sealing (Pawelczak et al., 2011).

7.2. Base excision repair (BER)

The base excision repair (BER) pathway is in charge of repairing most endogenous base lesions like, AP sites, abnormal bases such as formamidopyrimidine (Fapy-G) and 8-oxoguanine (8-oxoG) in the genome. BER is also linked to the repair of DNA single-strand breaks. Compared to NHEJ and HR, it is considered to be the main pathway involved in the repair of radiation-induced DNA damages. The great majority of damages repaired through BER are caused by ROS. However, the functional significance of BER in the prevention of diseases is not clear yet (Dizdaroglu et al., 1993; Kasprzak et al., 1997; Mori et al., 1993).

BER is initiated by the excision of a damaged base by DNA glycosylases. Several distinct DNA glycolases exist in mammalian cells. Each recognizes a limited, partially overlapping number of damaged bases or lesions. The glycolases generates an abasic site (apurinic/apyrimidinic, AP site) due to the cleavage of the N-glycosidic bond. An abasic site can also occur spontaneously by hydrolysis. The following steps depend on activity associated with each DNA glycosylase and can be grouped in APE and APEX1-independent repair. DNA glycosylases are in charge of cutting out the damaged region of DNA. They can be classified in monofunctional and bifunctional DNA glycosylases.

Monofunctional glycosylases have only glycosylase activity whereas the bifunctional glycosylases are specific for oxidized base lesions and have an additional intrinsic AP lyase activity that permits them to cut the phosphodiester bond of DNA (Kim et al., 2012). Collectively these enzymes perform base excision repair of a large number of base lesions, each recognized by one or more DNA glycosylases with overlapping functions.

7.3. Nucleotide excision repair (NER)

The nucleotide excision repair (NER) pathway detects a broad range of DNA lesions, mainly generated from exogenous sources, by recognizing abnormal structures of DNA. Among them are helix-distorting intra-strand crosslinks, bulky adducts, minor base damages induced by alkylating and oxidizing agents, UV-light induced photolesions and cyclobutane pyrimidine dimers. In addition, NER is considered to be a backup system for BER to remove oxidative stress induced DNA damage. Several proteins from other repair pathways are also involved in removal of oxidative DNA lesions. In yeast, BER acts synergistically with NER to repair endogenously induced oxidative damage (Dusinská et al., 2006). NER is involved in the repair of 8-oxoG (Boiteux et al., 2002) and It was further shown that NER capacity and the expression of NER related genes may be modulated by oxidative stress (Langie et al., 2007).

NER subunit xeroderma pigmentosum (XP) groups A, C, and G (XPA, XPC, XPG), and DNA glycolases NTH1 and OGG1 (8-oxoguanine-DNA glycosylase) are the main factors involved in NER. XPC acts as a cofactor in BER by stimulating the activity of the DNA glycosylase OGG1 (Melis et al., 2012), XPG serves as a cofactor for the efficient function of human NTH1 and XPA might have a role in the repair of oxidized bases (Schärer et al., 2008).

NER pathway involves more than 30 proteins and can be subdivided into two sub-pathways: the global genomic repair (GG-NER) and the transcription-coupled repair (TC-NER). GG-NER removes lesions from whole genome, whereas the TC-NER repairs polymerase-blocking damage on DNA strands of actively transcribed genes. Both pathways share the same mechanism but differ in their DNA damage recognition step. Upon the recognition of the damage, a multiprotein complex is recruited at the damaged site. Then, the DNA is incised 5’ and 3’ several nucleotides away from the lesion. The

damage containing part is eliminated, and the resulting gap is filled by a DNA polymerase and finally a DNA ligase seal the newly synthesized strand (Tubbs et al., 2009; Latypov et al., 2012).

7.4. Mismatch repair (MMR)

MMR is an evolutionarily conserved pathway which detects and repairs non-Watson–Crick base–base mismatches and short insertion or deletions caused by mis-incorporation of bases during DNA replication. The main function of MMR is to correct errors made in newly synthesized strand during DNA replication, including mispaired bases, and nucleotide loop outs that can lead to insertion or deletion mutations (insertion if loops located on the nascent strand, and deletion if located on the template strand). It also repairs mismatched bases formed in heteroduplex homologous recombination, and prevents HR between divergent DNA sequences (Iyer et al., 2006).

The MMR pathway functions through mispair detection by the partially redundant MutS-related complexes (MSH2-MSH6 and MSH2-MSH3). Eukaryotic MMR consists of three main steps: 1) mispaired bases recognition by MutS-related complexes and recruitment downstream proteins like Mlh1-Pms1. 2) excision of the error-containing nascent DNA strand; and 3) re-synthesis of the excised DNA strand properly. MMR involves both EXO1-dependent pathway that relies on DNA excision by EXO1, and a less studied EXO1-independent pathway. Exonuclease 1 (Exo1) acts as a 5’ to 3’ double stranded DNA exonuclease consisting of a N-terminal nuclease domain and a C-terminal, an unstructured domain which is the unique exonuclease identified in eukaryotic MMR pathways so far.

Defects in MMR cause significantly elevated mutation rates that in turn can drive tumorigenesis. Lynch syndrome is a hereditary disease caused by heterozygous MMR defects that is often characterized by early onset colorectal cancers and some other types of cancer (Goellner et al., 2018).

7.5. Translesion DNA synthesis (TLS)

Translesion DNA synthesis (TLS) is the simplest process through which DNA lesion blocks are bypassed during DNA replication. It is catalyzed by specialized low-fidelity

DNA polymerases such as Rev1, Pol η, Pol ι, Pol ζ, and Pol κ (Vaisman et al., 2017; Sale et al., 2012). Due to their large active site (often contain more than one active site) and lack of proofreading activity, these polymerases are fragment inserters and allow incorporation of a nucleotide or a block of nucleotides opposite the damaged site. One of the most studied of these DNA polymerases is DNA polymerase η (Pol η), in charge of error-free bypassing of UV-induced DNA damage. The other TLS polymerases (Pol ι, Pol κ, REV1, and Pol ζ) members have been studied mainly *in vitro* but their *in vivo* role is under extensive investigation (Masutani et al., 2000).

OBJECTIVES

The main objective of the PhD project was to study the role of SIRT1 and SIRT6 in the protection of genomic integrity upon different types of genotoxic stress such as oxidative stress and IR. Specifically, our purpose was to identify and characterize novel mechanisms regulated by SIRT1 and SIRT6 in the context of these types of stress, to define specific partners involved and their implications in DNA damage signaling, and cancer. We fulfilled this objective through the development of two main objectives:

CHAPTER I

OBJECTIVE 1:

In the first part of the thesis, we studied the tumor suppressor role of Sirtuin 6. This project was aimed to define the role of two important chromatin factors such as Suv39h1 and G9a, in the epigenetic silencing promoted by SIRT6 and their contribution to the tumor suppressor activity of SIRT6. The development of this project should provide key evidence to understand the role of SIRT6 in cancer.

-Sub-objective 1.1. To determine the functional relationship between SIRT6 and Suv39h1 as well G9a to provide evidence about the mechanism behind SIRT6-dependent silencing.

-Sub-Objective 1.2. To define the contribution of both HMTs Suv39h1 and G9a to the tumor suppressor activity of SIRT6, from *in vitro* and cell culture level to *in vivo* nude mice xenograft models.

CHAPTER II

OBJECTIVE 2:

In the second Part of the thesis, we studied the role of SIRT1 in DNA damage signaling through its interaction with the PP4 complex.

-Sub-Objective 2.1. Characterization of the identified interaction among SIRT1, PP4 complex and RPA2 using a combination of molecular biology, cell biology and biochemistry techniques.

-Sub-objective 2.2. The effect of SIRT1 interaction on the respective enzymatic activity of PP4 complex by enzymatic assays.

-Sub-objective 2.3. Determination of the functional implications of the SIRT1-PP4 complex on downstream targets (RPA2) using biochemistry and cell biology techniques.

These findings improve our understanding of the functional implications of SIRT6 and SIRT1 in genome stability and DNA damage signaling.

Materials and Methods

1. Chemicals and Antibodies

All chemicals and reagents, unless otherwise stated, were from Sigma-Aldrich (St. Luis, MO). We obtained hydroxyurea, okadaic acid from Calbiochem and puromycin from Invivogen. The following western blot antibodies were used in this study: HA (Sigma-Aldrich, H6908), FLAG (Sigma-Aldrich, F1804), c-Myc (Cell Signaling, 2276S), actin (Sigma-Aldrich, A1978), α-tubulin (Sigma-Aldrich, T6199), SIRT1 (Millipore, 07-131), SIRT6 (Abcam, AB62739), histone H3 (Cell Signaling, 9715), GFP (Merck, MAB2510), RPA32 (Cell Signaling, 2208), PP4R2 (Bethyl, A300-838A), PP4R3α (Bethyl, A300-840A), PP4R3β (Bethyl, A300-842A), PP4C (Abcam, ab171870), Anti-phospho-Histone H2A.X (Ser139)(abcam ab 2893 and Merck Millipore, JBW301), phospho-RPA2 (Ser33) (Novus, NB100-544 and Bethyl, A300-246A), phospho-RPA2 (Ser4/8) (Sigma, PLA0071), G9A (Cell Signaling Technology, C6H3), Suv39h1 (Cell Signaling , D11B6) and SIRT6 (Abcam, ab62739).

2. Cell lines

Human Embryonic Kidney (HEK) 293T and Hela cells were cultured in Dulbecco's modified Eagle's medium (DMEM) (GIBCO, Invitrogen, Carlsbad, CA, USA) supplemented with 10% (v/v) heat-inactivated FBS (fetal bovine serum), 100 U/ml penicillin and 100 µg/ml streptomycin. *Wt, Sirt1*$^{-/-}$*, and Sirt6*$^{-/-}$ mouse embryonic fibroblasts (MEFs) were cultured in DMEM supplemented with 20% (v/v) fetal bovine serum, Pen-strep (10000 IU/mL, 10 mg/mL), non-essential amino acids and sodium pyruvate according to the manufacturer's instructions. All the cells were grown at 37ºC in an atmosphere containing 5% CO2, and 100% humidity.

3. Cell Treatments

At 48 hours of transfection (If indicated) the cells were treated with the following conditions before harvesting at indicated times: 2mM of H_2O_2 (Merck) for 1 hour, 5mM hidroxyurea (Sigma-Aldrich) for 4 hours, 1 µM campthotecin (Sigma-Aldrich) for 1 hour and irradiation with X rays at 7.5 and 10 Gy. The cells were exposed to different concentrations of EX527(1 and 10 µM) or OSS128167(200 µM) during 24 hours.

METHODS:

4.Plasmid Transfection

One day before transfection, cells were plated in 100-mm dishes at 40-50% confluence. After one-day growth, transfections were performed with Polyethylenimine (PEI, Sigma, St. Louis, MO, USA) using 4µL PEI (stock, 1mg/mL) per µg of DNA in serum free medium and incubated for 5 min at room temperature. The mix was added to the cell culture and allowed to grow at 37ºC, in the incubator humidified 5% CO2 atmosphere for 48 hours.

5. Retroviral generation and infections

The packing cells Platinum A were used to produce retrovirus. Platinum A cells were cultured as per manufacturer's protocol. Platinum A cells were seeded into culture dishes a day before transfection in DMEM supplemented with 10% FBS. The cells were co-transfected with 2 µg of pVSVG plasmid and 8 µg of the retroviral vector. After 24h and 48h the supernatant media containing the retrovirus was collected and stocked at -80ºC. For the infection, one day before cells were plated in 6-well plate. The next day the media was replaced by the stocked supernatant containing the retrovirus and incubated for 16 hours, thereafter the media was replaced by fresh media and after 24 hours, the cells were selected with puromycin.

6.Lentiviral infection

For shRNA knockdown, HEK293T cells were co-transfected with pMD2.G and pPAX2 (Addgene) together with pLKO-shRNA constructs (PLKO-ShRNA PP4C) or a non-targeting pLKO-shRNA (pLKO-ShRNA Scramble). Viral supernatants were harvested after 48 h. For infections, SIRT1 MEF cells were incubated with viral supernatants in the presence of 8 µg /ml polybrene. After 48 h, puromycin (5µg /ml) as selection was added to the medium. Cells were grown in presence of selection for 4 days to select for stable knockdown cells.

7.Site-directed mutagenesis and polymerase chain reactions

PCR reactions were performed using 5-15 ng of templates DNA in 25µL of GoTaq mix, 0.3 µM of each primer and H20 (Milli-Q) added up to 50 µl. The DNA was amplified during 35 cycles of denaturation at 95ºC for 30 seconds; annealing temperature was approximately 5ºC lower than calculated Tm of the primers, extension at 72ºC for 60 seconds per 1 kb. The final extension was performed at 72ºC for 7 minutes and final hold, 4°C. The non-mutated DNA was digested with 3 units of DpnI restriction enzyme for 1h at 37ºC. Following, the reactions was transformed and positive clones selected. PCR products were verified by sequencing.

8. Whole cell extract

Cells were harvested using a cell scraper, nuclear and cytoplasmatic extracts were prepared as previously described by Dignam (Dignam et al., 1983). Briefly, cells were washed two times with PBS and lysed in buffer A (10 mM Tris, pH 7.8, 1.5 mM $Mgcl_2$, 10 mM KCl, 0.1 mM PMSF, 0.5 mM DTT, protease inhibitor cocktail (Sigma-Aldrich) for 10 minutes on ice, centrifuged at 12,000 x g for 1 minute at 4°C. The supernatant (the cytoplasmatic fraction) was transferred into a clean tube. The nuclear fraction was lysed in buffer C (10 mM Tris, pH 7.8, 1.5 mM $Mgcl_2$, 0.42 mM NaCl, 25% glycerol, 0.2% EDTA, 0.1 mM PMSF, 0.5 mM DTT, protease inhibitor cocktail (Sigma-Aldrich) during 20 minutes on ice. The nuclear fraction was harvested by centrifuging the lysate at 12,000 x g for 3 minutes at 4°C, used or stored separately at -80ºC until further use.

9. Total denaturing protein extraction (Phosphorylated proteoins)

MEFs or human cell lines were collected after cold PBS wash by scraping in Lysis 2X SDS Buffer (4% SDS, 20% Glycerol, 120mM Tris-HCl pH 6.8, 1x protease (Roche) and phosphatase inhibitors (Sigma-Aldrich) on ice. Lysates were sonicated at medium-high intensity for 10 minutes in a Bioruptor Standard (Diagenode) placed at 4ºC and subsequently boiled for 10 minutes at 90ºC.

10. Co-immunoprecipitation (CoIP)

For immunoprecipitation experiments, cell extracts were incubated with either α-FLAG, or α-HA resin (Sigma-Aldrich) overnight. Beads were washed three times with BC100 buffer (10mM Tris pH 7.8, 0.5 mM EDTA, 0.1mM PMSF, 0.1 mM DTT, 10% glycerol, 100 mM KCl) then, 3 times with BC500 buffer (10mM Tris pH 7.8, 0.5 mM EDTA, 0.1mM PMSF, 0.1 mM DTT, 10% glycerol, 500 mM KCl). Thereafter, the proteins were eluted with 0.2 M Glycine pH 2.0 or by incubation with the corresponding competing peptides for enzymatic assay or mass spectrometry analysis.

11. SDS-PAGE and western blot analysis

Protein samples were mixed with 5x Laemmli sample buffer (supplemented with 10% β-Mercaptoethanol) and boiled at 95ºC for 2 minutes before loading. Protein extracts were fractionated by SDS-PAGE (10% polyacrylamide) and then transferred to nitrocellulose membrane in transfer buffer (500 mM glycine, 50 mM Tris-HCl, 0.01% SDS, 20% methanol). The membrane was blocked with 5% (w/v) nonfat milk (in Tris-buffered saline, containing 0.01% Triton-X-100), and then the membrane was incubated with primary antibodies for 1h to overnight at 4ºC, after washing the membranes with washing buffer (0.1% Tween and PBS1X) three times for 5 minutes each, followed by incubation with appropriate secondary for 30 minutes. Afterwards, the membrane was washed again with washing buffer three times for 5 minutes each, finally antibody binding was visualized with an ECL chemiluminescence system (Millipore detection kit) and short exposure of the membrane to X-ray films or iBright® Imaging Systems (Thermo Fisher Scientific).

12. Phospho-H2AX-enriched Histone extraction

Hela cells were treated with 2mM of H_2O_2 (Merck) for 1 hour, then the cells were scraped down by a cell scraper, washed with PBS and pelleted by centrifugation at 4,000 x g for 1 minute. Subsequently, the cells were resuspended in buffer A (10 mM Tris, pH 7.9, 1.5 mM $Mgcl_2$, 10 mM KCl, 0.1 mM PMSF, 0.5 mM DTT, supplemented with protease inhibitor) for 10 minutes on ice, and centrifuged at 12,000 x g for 1 minute. The pellet (nuclear fraction) was resuspended with 0.5 M HCl (500 µL/10 cm^2 plate). The samples

were resuspended by vortex and then incubated on ice for 15 minutes. After centrifugation at 14,000 x g for 10 minutes at 4ºC, the supernatant (soluble acid proteins) was collected and precipitated with TCA in final concentration of 20% and incubate on ice for 1 hour. After centrifugation at 14,000 x g for 10 minutes at 4ºC, the pellet was washed with 100% ice-cold acetone and then centrifuged at 14,000 x g for 10 minutes at 4ºC. After drying the pellet in RT, it was resuspended with BC100 and stored at -80ºC.

13. Phosphatase assay

PP4 complex subunits were overexpressed in HeLa cells or SIRT1 MEFs and purified using FLAG resin to immunoprecipitate the catalytic subunit (PP4C). The bound proteins were eluted by competition with a large excess of free FLAG peptide (0.4 mg/ml). Eluted PP4 complex were dialyzed to BC100 and stored at -80ºC.

For *in vitro* phosphatase assay, the purified proteins were first equilibrated with PRB for 10 minutes at 37°C followed by addition of phospho-H2AX-enriched histone as a substrate and incubation at 37ºC for 30 minutes in Phosphatase Reaction Buffer (PRB, 50 mM Tris pH 7.2, 0.1 mM $CaCl_2$, 5 mM $MnCl_2$ and 0.2 mg/ml BSA).The reactions were stopped by adding Laemmli sample buffer (supplemented with 10% B-Mercaptoethanol) and separated by SDS-PAGE and the phosphorylation level of H2AX was monitored by immunoblotting with a specific antibody toward γH2AX.

14. *In vitro* deacetylase assay

HA-SIRT1 and PP4 complex subunits were expressed separately in Hela cells, immunoprecipated and purified using HA and FLAG peptides in BC100 buffer according to the immunoprecipitation protocol previously described. Deacetylation assays were performed in deacetylation buffer (50 mM Tris-HCl pH 8, 100mM NaCl, 2mM DTT, 5% Glycerol) with or without 5 mM of NAD^+. SIRT1 was first equilibrated with deacetylation buffer for 10 minutes at 37°C. Then, hyperacetylated histone substrate were added to the reaction mixture and incubated at 37°C for 1h. The reactions were stopped by adding 5x Laemmli sample buffer (10% β-Mercaptoethanol) and were then separated by SDS-

PAGE. The H4K16 acetylation status of histones was monitored by immunoblotting with a specific antibody to H4K16ac.

15. Immunofluorescence assay (IF) and high-throughput microscopy (HTM)

The cells were placed on glass coverslips in a 6-well plate 1 day before treatment and immunofluorescence assay was performed as follows. Cells were washed two times with PBS (pH 7.4) and fixed with freshly prepared 4% paraformaldehyde (in PBS) for 7 minutes at room temperature (RT). In the case of SIRT1 MEFs, before fixation, the cells were treated with pre-extraction buffer (25 mM Hepes, pH 7.4, 50 mM NaCl, 1 mM EDTA, 3 mM $MgCl_2$, 300 mM sucrose, and 0.5% Triton X-100) for 10 minutes on ice. Fixed cells were then washed two times for 5 minutes in cold PBS and permeabilized in Buffer B (3% BSA, 0.2% Triton-X-100 in PBS) and incubated with Blocking buffer (3% BSA diluted in PBS) for 1 hour at room temperature. Thereafter, the cells were washed three times in blocking buffer and incubated with appropriate primary antibody overnight. Subsequently, the cells were washed three times in blocking buffer and incubated with appropriate secondary antibody conjugated to Alexa Fluor dyes, 488 (green), 594(Texas Red), or 647 (red) (Invitrogen) for 30 minutes at RT in the dark. For DNA staining, DAPI stain was used (1:10000 in PBS1X). DAPI-stained cells were incubated for 5 minutes at RT after last wash of secondary antibody, followed by two more washes with PBS. After staining, coverslips were mounted in Mowiol and allowed to dry overnight before imaging. Images were viewed and captured on a Leica SP5 microscope (Leica, Milton Keynes, UK). Primary antibodies and dilutions were: RPA32 (Cell signalling) at 1:150, anti-Phospho RPA32(Novus) and anti-Phospho RPA32 (S4/S8) (Sigma-Aldrich) at 1:200, Phospho-yH2AX (Abcam) at 1: 500. In the case of high-throughput microscopy (HTM) immunofluorescence, SIRT1 MEFs were grown in LabTek II Chamber slides (Nunc, Thermo Fisher Scientific) and stained using the procedure mentioned above. For HTM, 48 images were automatically acquired per well with a Scan^R (Olympus) with an oil immersion objective at × 40 magnification and non-saturating conditions. Automated image segmentation of DAPI-stained nuclei was generated from which the corresponding signals were calculated using Fiji Software (https://fiji.sc/) and a package based on the Cell Profiler.

Confocal fluorescence images were obtained on a Leica DM2500 SPE confocal system. Images were taken with 40x NA 1.15 oil or 63x NA 1.3 oil objectives and the standard LAS-AF software. Possible crosstalk between fluorochromes was avoided by carefully adjusting laser intensities and HyD gain, thus avoiding false-positive colocalization signals. For high-throughput microscopy (HTM), 24-48 images were automatically acquired from each well with a robotized fluorescence microscopy station (ScanR; Olympus) at 40× magnification and non-saturating conditions. Images were segmented using the DAPI staining to generate masks matching cell nuclei from which the corresponding signals were calculated using an in-house–developed package based on Cell Profiler (www.cellprofiler.org), an open source software program. In collaboration with the Advanced Digital Microscopy Facility at IRB Barcelona, we developed a pipeline to load the stack of 8-bit images with 3 channels, generate nuclear masks with the DAPI channel and measure mean intensity of the two additional channels. Nuclei had a typical diameter of 60-150 pixel units, and background fluorescence in DAPI images below an absolute threshold of 0.20-0.35 was set to 0. These results were exported to Excel for further analysis and GraphPad-Prism was used for graphical representation.

16.Chromatin immunoprecipitation assay (ChIP)

The cells were washed twice with PBS and double cross-linking was performed. The cells first were cross-linked with DSG (Di-Succinimidyl Glutarate; Pierce) at a final concentration of 2 mM in PBS for 45 minutes at RT, then were washed three times with PBS and further cross-linked using 1% (vol/vol) paraformaldehyde (Sigma) for 15 minutes at 37°C as described in (Nowak et al., 2005). Subsequently, the cells were washed three times with cold PBS (supplemented with protease inhibitors), then adherent cells were scraped and collected from dishes. Cells were centrifuged and supernatant discarded. First, cells were re-suspended in lysis Buffer 1 (5 mM Hepes, 85 mM KCl, 0.5% NP-40 and protease inhibitors) and incubated for 5 minutes on ice to disrupt cellular membrane. After centrifugation, obtained nuclei were re-suspended in lysis Buffer 2 (1% SDS, 10 mM EDTA, 50 mM Tris-HCl pH 8.0 and protease inhibitors) and incubated for 20 minutes on ice. Chromatin then sonicated with the Covaris instrument to an average fragment size of 300 bp. Samples were then centrifuged at 12,000 x g, 4°C for 15 minutes and supernatants were collected and

quantified by nanodrop. 60 µg chromatin for each ChIP (SIRT6, G9a and Suv39h1) was taken and the lysate was diluted 10 times with ChIP dilution buffer (0.01% SDS, 1.1% Triton X-100, 1.2 mM EDTA and 16.7 mM Tris-HCl, pH 8.0). Briefly, nuclear extracts were pre-cleared with protein-A and Protein-G coupled magnetic beads (Dyna beads, life technologies) for 1h at 4°C and immunoprecipitated overnight at 4°C with 7.5 µg of corresponding antibodies (SIRT6, G9a and Suv39h1). Beads were then washed 5 times with ice cold RIPA buffer (1%NP-40, 0.7% Na deoxycholate, 50 mM Tris-HCl, pH 8.0, 1mM EDTA, 500 mM $LiCl_2$) and twice with modified TE (0.1 mM EDTA, 10 mM Tris-HCl, pH 8.0). Chromatin was eluted using 2 successive rounds of incubation in 100µl of elution buffer (0.1 m $NaHCO_3$, 1% SDS) for 6h at 60°C.The DNA-chromatin complexes were de-crosslinked by adding NaCl (4M) to final concentration of 0.2 M and Incubate at 65°C overnight, followed by proteinase K treatment (0.1 M EDTA, 0.4 M Tris-HCl, pH 6.8, 0.4 mg/ml proteinase K). Heat at 45 °C for at least for 1h in a termoshaker and purified using a Macherey-Nagel™ NucleoSpin™ Gel and PCR Clean-up Kit. The purified samples were analyzed by quantitative PCR performed using the SYBR-based Quantitative PCR (Applied Biosystems). The values shown represent the percent of DNA specifically ChIPs normalized to the amount of DNA found in the input subtracting their IgG background.

17.ChIP-Seq Analysis

Sequencing reads were trimmed for Illumina adapter sequence with cutadapt, aligned to the mouse reference genome (mm10 v92) with bowtie and exclude PCR duplicates with samtools MarkDuplicates tool. Peaks were called with HOMER2 and params '-region -size 250 -minDist 1000 -inputtbp 0 -tbp 0'. Consesus peaks were created with peaks that were detected in all replicates and any condition for each IP. Peaks were also annotated with HOMER2 (Heinz et al., 2010; Langmead et al., 2009; Li et al., 2009; Martin et al., 2011).

18. Sister Chromatid Exchange (SCE) protocol

This protocol is divided in two parts: preparation of metaphase chromosome spreads and sister chromatid exchange assay. After metaphase chromosome spreads preparation and further processing, SCEs are visualized under the microscope.

A. preparation of metaphase chromosome:

The cells were grown for two days in BrdU (10µM). After 24 hours, Mitomycin C was added to a final concentration of 100nM-250nM. Subsequently, colcemid was added to a final concentration of 100 ng/ml and incubated for 1 hour at 37°C. The supernatant was aspirated and left 1 ml in the tube and the pellet was resuspended by pipetting. 10 ml of KCl was added and mixed by inverting and incubated in a 37 °C water bath for 15 minutes. 5 drops of fresh fixative were added and mixed by inverting. Then, it was centrifuged at 300 x g for 10 minutes at 4°C. The supernatant was aspirated and left 1 ml in the tube for resuspending pellet by pipetting up and down. Afterwards, 5 ml of fresh fixative was added drop by drop while tapping or pulsing on a vortex. Next, an additional 10 ml of fixative was added and incubated for 30 minutes at RT. Then. It was centrifuged at 300 x g for 10 minutes at 4°C. The supernatant was aspirated and the pellet were resuspended in leaving 1 ml in tube by pipetting. Next, 14 ml of fresh fixative was added and centrifuged at 300 x g for 10 minutes at 4°C. 14 ml of fresh fixative (Methanol: Acetic Acid Glacial (3:1)) was added and the caps were sealed with parafilm and stored overnight at -20°C (environmental chamber to 22.9 °C and 52% humidity). The fixed cells were centrifuged at 300 x g for 10 minutes at 4°C. The fixative was aspirated and leaving 200 µl in the tube was resuspended by pipetting. Labeled slides were placed in the humidity chamber at a 35° angle. 35 µl of resuspended cells was dropped onto a slide and drop two slides per sample. The slides were allowed to dry in the humidity chamber for 30 minutes then the slides were stored in a slide box at 37°C.

B. Sister Chromatid Exchange assay

The slides were placed in coplin jar with 2xSSC for 5 minutes while shaking. The slides were stained with 10 µg/ml Hoechst 33342 in PBS for 20 minutes, shaking. The slides were rinsed in MacIlvaine solution (164 mM Na_2HPO_4, 16 mM citric acid, pH 7.0) in

Coplin jar for 10 minutes. The backs of slides were wiped, leaving top wet with MacIlvaine solution, and slides were covered with 24x60 cover slips. The slides were UV irradiated for 1 hour on transilluminator (low setting). The cover slips were removed and were incubated with fresh pre-warm 1x SSC at 55°C for 15 minutes. The slides were incubated in ddH20 (double distilled water) for 15 minutes in a Coplin jar while shaking. The slides were located back to back in 50 ml Falcon tubes, 2 slides per tube, with 25 ml of working Giemsa stain (1:12 in 3% methanol), and they were allowed to rock for 20 minutes. They were rinsed with water in Coplin jar for 5 minutes while shaking.

19. Proliferation Assay

500 cells were plated in triplicates in 12-well plates and cultured and incubated at 37 °C, 5% (v/v) CO2. Cells were trypsinized and counted every day by trypan blue-exclusion method in Neubauer Counting Chamber.

20. Colony formation assay

Cells were plated in triplicates in 6-well plates at low density (50 cells per plate) and cultured in complete medium. The culture medium was replaced with fresh medium twice a week. After three weeks, the colonies were fixed with 4% paraformaldehyde (PFA) for 30 minutes, stained with crystal violet for 30 minutes, and washed with distilled water. The dishes were scanned and photographed using a binocular magnifier MZ16 F (Leica) equipped with a Nikon Digital Sight DS-L camera.

21. Anchorage-Independent Cell Growth

Assays were performed in 6-well plates with cells (n = 3 per group) embedded in 0.4% agarose in culture medium (700 cells per well) seeded on top of a layer of 1% agarose. Colonies were fixed with formaldehyde and photographed after three weeks as explained above in 20 (Colony formation assay).

22. Generation of tumor xenografts

3.5×10^6 cells in 250 µl of 50% matrigel (and 50% PBS1X) were injected subcutaneously into the flanks of nude (Foxn1nu/ Foxn1nu) mice (Jackson Laboratories). The SIRT6-HA expression (Tet-on system) was induced by doxycycline (2 mg/mL in drinking water) 3 days after injection. Mice were checked for the appearance of tumors and the volume was measured every other day from the beginning of the treatment with the following formula: (small diameter)2 × (large diameter)/2. The tumors were harvested when they reached ~10 mm in diameter. The study was approved by the hospital ethics committee.

23.The Tumor Digestion

Fresh tissues were mechanically dissected with a McIlwain tissue chopper andenzymatically digested with appropriate medium (DMEM F-12, 0.3% Collagenase A, 2.5 U/mL dispase, 20 mM HEPES and antibiotics) for 30 minutes at 37°C. Samples were washed with Leibowitz L15 medium containing 10% fetal bovine serum (FBS) between each step. Erythrocytes were eliminated by treating samples with hypotonic lysis buffer (Lonza Iberica). Single epithelial cells were isolated by treating with trypsin (PAA Laboratories) for 2 minutes at 37°C. Cell aggregates were removed by filtering the cell suspension with a 40-µm filter and counted.

24. Histopathology

Tissues were fixed in 4% formaldehyde overnight at RT and embedded in paraffin. 4 µm paraffin embedded sections were first deparaffinized in xylene. Histological sections of whole tumors were stained by hematoxylin and eosin, and high-resolution low-magnification images were taken of the whole tumor area. Images were acquired with a LEICA DM4000B microscope equipped with LEICA DC500 digital camera.

25. Animals

Wild-type, *Sirt6*$^{-/-}$and *Suv39h1*$^{-/-}$ mice, on a C57BL/6 background (>10 backcross), were housed at the Animal facility of IDIBELL research institute. For Xenograft experiments, we used male mice 6–8 week old, BALB/c nu/nu (BALB/c nude). The animals were

maintained at a constant temperature of 22°C, 12 h light/dark cycle, and given standard chow and water fed ad libitum.

26.Statistical analysis

Statistical analysis of the data was performed using two-tailed Student's t test (α = 0.05) in Microsoft Excel (Microsoft, Redwood, CA). Each experiment was repeated three times each with triplicate samples, unless indicated otherwise.

27.Primers

Gene name	Forward Primer (5' to 3')	Reverse Primer (5' to 3')
Glut1	ATGGATCCCAGCAGCAAG	CCAGTGTTATAGCCGAACTGC
Ldha	AGGCTCCCCAGAACAAGATT	TCTCGCCCTTGAGTTTGTCT
Ldhb	AGGGAATGTACGGCATTGAG	CCTCATCGTCCTTCAGCTTC
Pdk1	GGCGGCTTTGTGATTTGTAT	ACCTGAATCGGGGGATAAAC
INTERGENIC	AAGGGGCCTCTGCTTAAAA	AGAGCTCCATGGCAGGTAGA
HMGA2	GGCAAGCAGGCATGCAA	GCACCATCGTGTGTCTGGTAGT
SAT1/2	GACGACTTGAAAAATGACGAAATC	CATATTCCAGGTCCTTCAGTGTGC
NFKBLA	GCCATGGAGCAAACCCATAG	ATTCCATAGCGGGAGGTGTCT
CDKNIA	TCTTCCAGTCCTTGGAGACC	GCACCTGGAATCCCTAGAAA
PP4R3AK64	CTAACACTGCATACCAGAGACAACAGGACACTCTG	CAGAGTGTCCTGTTGTCTCTGGTATGCAGTGTTAG
PP4R3AK64Q	GCA TAC CAG CAA CAA CAG GAC ACT CTG	GTC CTG TTG TTG CTG GTA TGC AGT GTT AGG
PP4R3BK64R	CAAATACTGCATATCAGAGACAACAGGATACATTAATTG	CAATTAATGTATCCTGTTGTCTCTGATATGCAGTATTTG
PP4R3AK64Q	GCA TAC CAG CAA CAA CAG GAC ACT CTG	GTC CTG TTG TTG CTG GTA TGC AGT GTT AGG
PP4R3AK642R	GAAAGGCAAGATAATCCCAGACTTGACAGTATGCG	CGCATACTGTCAAGTCTGGGATTATCTTGCCTTTC
PP4R3A2K64Q	CATACCAGCAACAACAGGAAGATGAAAAATTTC	CTTCCTGTTGTTGCTGGTATGCAGTGTTAGG
PP4R3BK806R	CTAATGGATCCTCTTCCAGAACCACAAACTTGCC	GGCAAGTTTGTGGTTCTGGAAGAGGATCCATTAG
PP4R3BK806Q	CTAATGGATCCTCTTCCCAAACCACAAACTTGCC	GGCAAGTTTGTGGTTTGGGAAGAGGATCCATTAG
mG9A	CACAAGCACATCGATGTGATT	ATGGTAGTTGACAGCATGGAG
mSUV39H1	AAAGGTTGCAGTGTGTGCTG	TCCTGCTCACGGATCTTCTT

Table 4. Primers used for mutagenesis, qRT-PCR and ChIP-PCR

RESULTS

CHAPTER I: UNDERSTANDING THE TUMOR SUPRESSOR ACTIVITY OF SIRT6: THE ROLE OF THE EPIGENETIC FACTORS SUV39H1 AND G9A

1.1. PREVIOUS WORK

Previous data in our lab identified two H3-K9 specific histone methyl transferases (HMTs) Suv39h1 and G9a, as novel interaction partners of SIRT6 (Figure 14). These experiments were the starting point of this objective.

These previous experiments were performed using an unbiased approach to test whether SIRT6 purified from mammalian cells co-fractionates with an HMT activity. They subsequently performed an *in vitro* histone methylation assay (see material and methods) using core histones as the substrate and [^{3}H]-SAM as the methyl donor (Figure 14A). Interestingly, the activity was specific to histone H3 as the band labeled with radioactivity compared to Coomassie-blue staining of the membrane (Figure 14B). Next, they identified histone H3 residue methylated by SIRT6 performing another *in vitro* HMT assay, but in this case, using recombinant proteins formed by GST fused to the N-terminal histone tail of histone H3 WT(H3N) or containing specific mutations of K4, K9 or K27 to R, as well as different combinations of them, as showed (Figure 14C-D). They concluded that the H3 is methylated only when lysine 9 is not mutated and they demonstrated that SIRT6 co-fractionates with an H3K9 histone methyl transferase (H3K9MTases) activity. In order to identify this H3K9 methyl transferase, they tested the interaction between SIRT6 and four main H3K9MTases: Suv39h1, G9a, GLP and SETDB1 by immunoprecitation. They found that SIRT6 specifically interacts with G9a and Suv39h1 (Figure 14E).

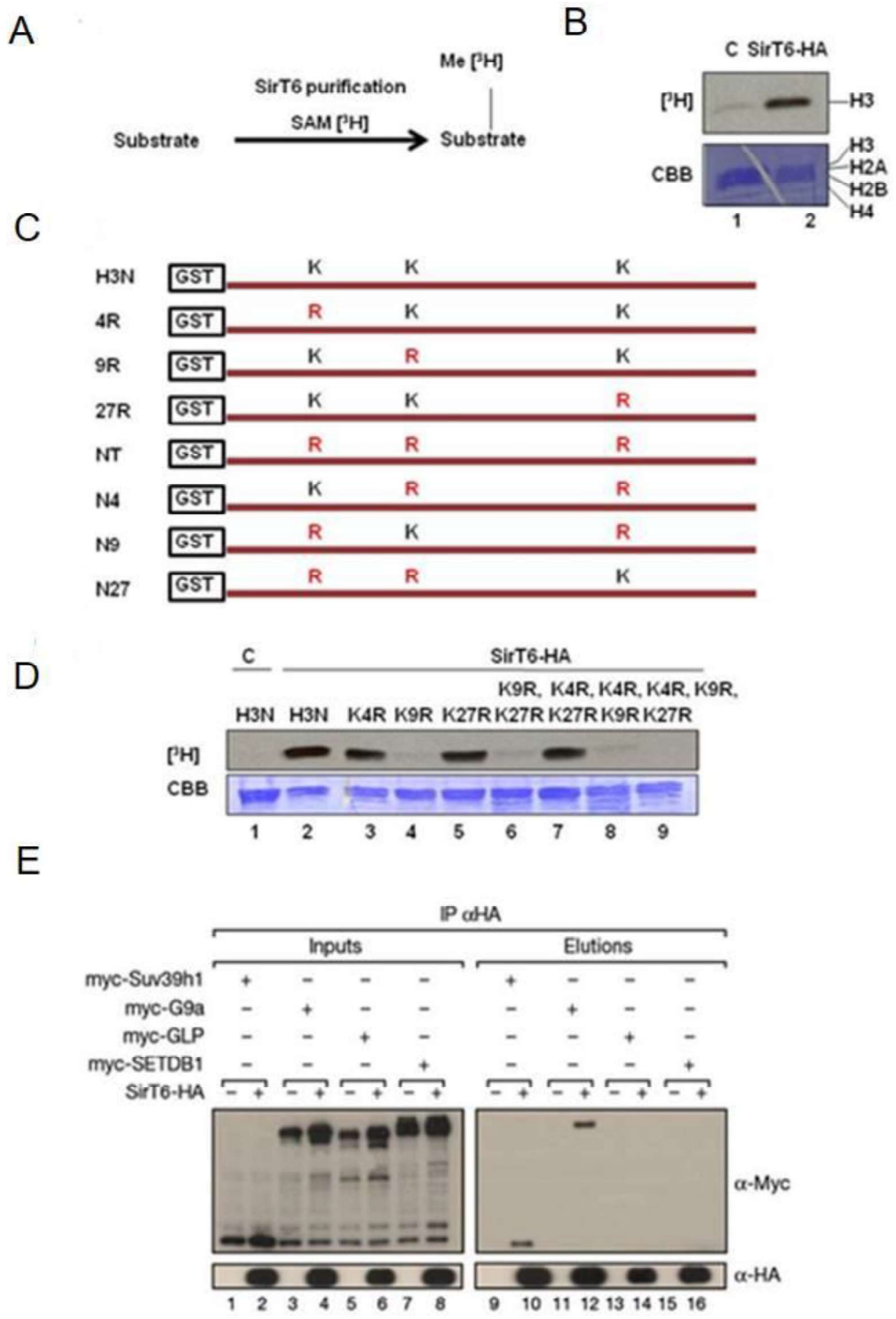

Figure 14. SIRT6 specifically interacts with G9A and Suv39h1. **(A)** Reaction scheme for the *in vitro* Histone methyltransferase (HMT) assays performed. **(B)** HMT assay of SIRT6-HA affinity purified elutions (HA resin) from HeLa nuclear extracts. HeLa core histones were used as substrates. Lower bands: Coomassie-blue staining of the same membrane. **(C)** Scheme of recombinant H3 N-terminal tails. **(D)** Histone methyltransferase (HMT) assay of the same elution as in (B). Recombinant proteins GST fused to histone H3 histone tail (1-30 residues) and modified in indicated ways: Lane 1: Control elution from A. Lanes 2-9 SIRT6-HA elutions. H3N: whole N-terminal tail of H3; KXR: Substitution of the specific residue/s to arginine. Lower panel: Coomassie staining of the same membrane. **(E)** Immunoprecipitation (IPs) experiments in HeLa cells with HA resin between SIRT6-HA and the different H3K9 methyltransferases (Suv39h1, G9a, GLP and SETDB1) tagged with Myc.

RESULTS

1.2. Interaction between SIRT6, Suv39h1 and G9a

Our first approach was to confirm that both Suv39h1 and G9a interact specifically with SIRT6 by immunoprecipitation experiments. We carried out these experiments under two different stress conditions: oxidative stress and IR (ionizing radiations). Interestingly, we found that while the interaction between SIRT6 and Suv39h1 does not change upon stress (15, lanes 2, 4, 6), the interaction with G9a was mainly observed specifically upon oxidative stress (Figure 15, lane 10). This suggested that G9a participates in SIRT6-dependent response to oxidative stress.

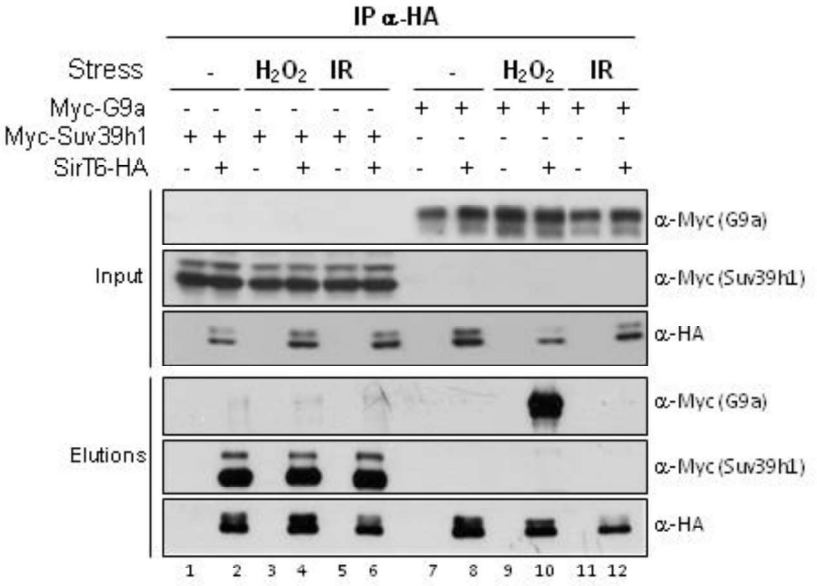

Figure 15. Interaction between SIRT6 and either Suv39h1 or G9a. Immunoprecipitation experiments using anti-HA resin between SIRT6-HA and Myc-Suv39h1 (lanes 1-6), or Myc-G9a (lanes 7-12) under regular conditions, oxidative stress (5 mM H2O2 for 1h) or IR (5 Gy with 1h of recovery) as indicated. Data are representative of three independent experiments.

1.3. SIRT6 may regulate G9a and Suv39h1 post-translationally

Following the characterization of the functional relationship between SIRT6 and both HMTs, we also studied whether loss of each of these factors has any impact on the other two at the level of RNA and protein. Thus, we determined the RNA (qPCR) and protein (Western-blot) levels of SIRT6, Suv39h1 and G9a in MEFs derived from Wt and KO for Suv39h1/2 and SIRT6.

Interestingly, our results showed that upon loss of SIRT6 both G9a and Suv39h1 protein levels decrease significantly (Figure 16A, lanes 2 and 4). In the case of G9a, the analysis of mRNA levels in these cells did not show any alteration, suggesting that the downregulation of G9a was taking place at the protein level (Figure 16B, right column). However, in the case of Suv39h1, both protein and mRNA levels were altered in SIRT6-deficient cells, indicating that SIRT6 may regulate Suv39h1 either at level of RNA, or at both levels (Figure 16B, middle column). Interestingly, neither protein nor mRNA levels of SIRT6 were clearly altered in *Suv39h1/2*$^{-/-}$ MEFs (Figure 16B, left column), indicating that SIRT6 is upstream of Suv39h1.

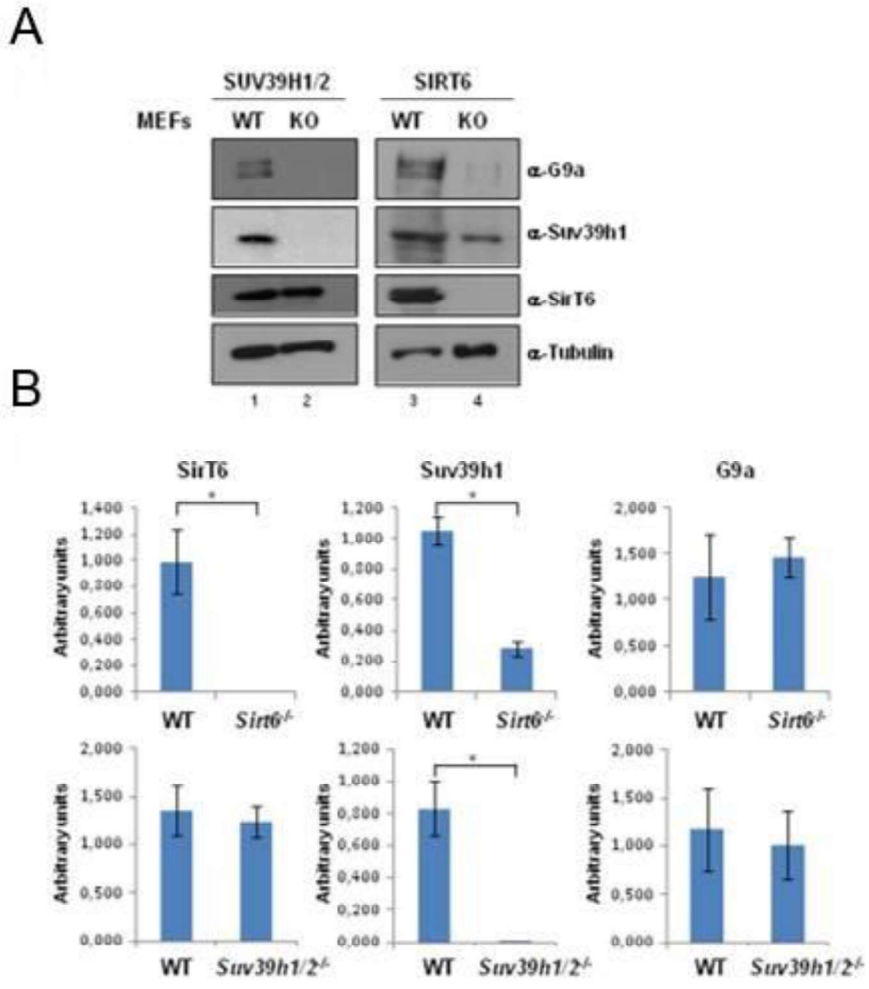

Figure 16. Loss of SIRT6 downregulates Suv39h1 and G9a levels. **(A)** Western-blot of the protein levels of endogenous G9a, Suv39h1 or SIRT6 in MEFs *Wt*, *Suv39h1/2*$^{-/-}$ or *Sirt6*$^{-/-}$. **(B)** Quantitive RT-qPCR analysis (n=3, sd) of mRNA of the three factors in the same cells used in (A). (*): statistically significant differences with $p<0.05$.

1.4. SIRT6 activity is not affected by HMTs, Suv39h1 and G9a

We also tested, whether any of these HMTs regulagte the enzymatic activity of SIRT6. For that purpose, we performed *in vitro* deacetylation activity of an H3 peptide acetylated in K18 using SIRT6, Suv39h1 or G9a -/+ NAD^+ and -/+ the methyl donor S-Adenosyl methionine (SAM). The results showed that incubation of both HMTs decreased the levels of H3K18ac, suggesting that both proteins were associated with other non-Sirtuin HDACs. Nevertheless, no clear effect of these HMT activities was observed on SIRT6 catalytic activity (Figure 17A). We also tested whether SIRT6 deacetylation activity modulates Suv39h1 or G9a histone methyltransferase (HMT) activity. For that purpose, we performed *in vitro* HMT activity using [^{3}H]-labelled SAM with purified G9a or Suv39h1 together with SIRT6 in presence or absence of NAD^+. The results clearly indicate that despite the direct interaction with both HMTs, SIRT6 does not seem to modulate significantly their activity (Figure 17B and data not shown).

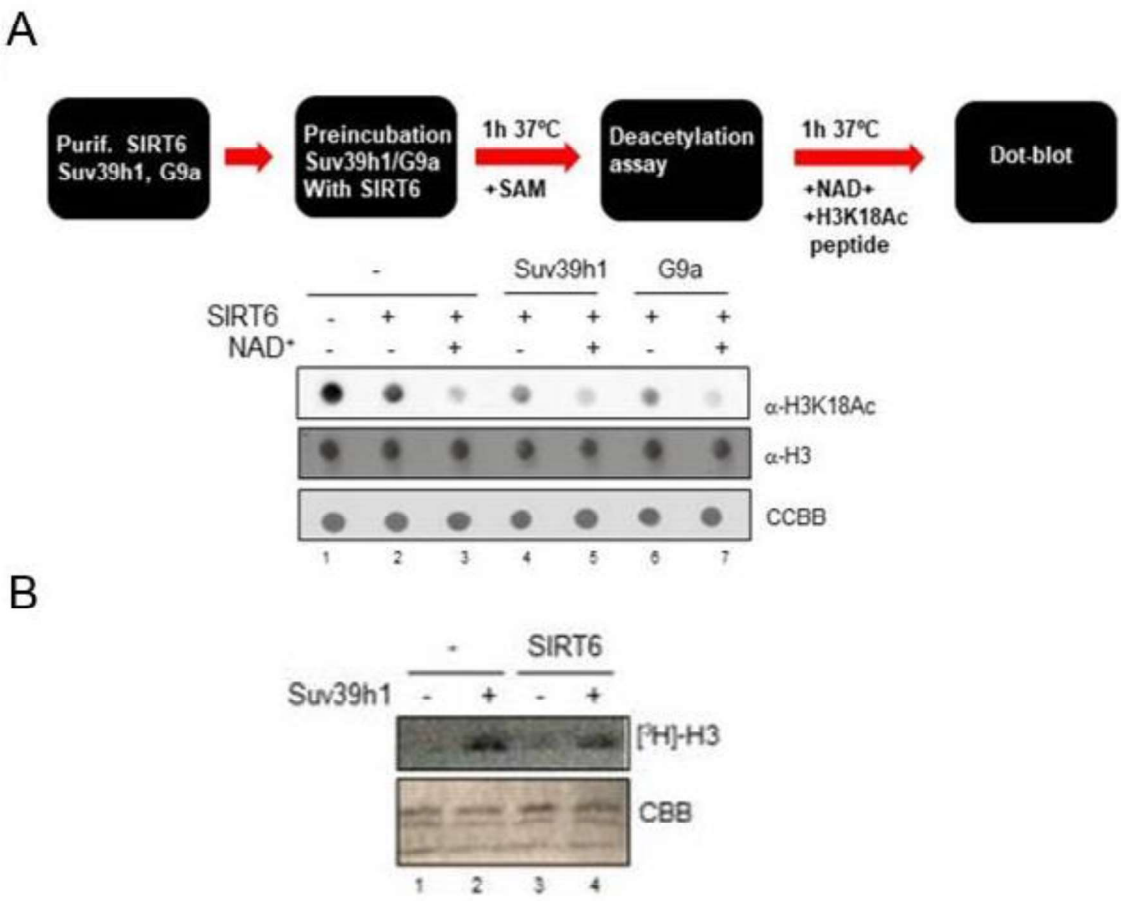

Figure 17. SIRT6 activity is not regulated by HMTs, SUV39H1 or G9a. **(A, upper panel)** Schematic diagram of the assay to test the effect of both HMTs on SIRT6 deacetylation activity. The purified proteins were incubated as indicated with SAM in an HMT buffer for 1h 37ºC. After that deacetylation buffer containing histone H3 K18ac-peptide (3-22aa) -/+ NAD+ was added and incubated again before performing a dot-blot with the reactions. **(A, lower panel)** Representative experiment, H3K18ac and H3 signal is shown. Coomsassie-blue (CCBB) is also shown as a marker of total protein in the Dot blots. **(B)** HMT assay with Suv39h1 using [^{3}H]-SAM as a methyl donor and purified HeLa core histones as substrate. Before the HMT reaction, Suv39h1 was incubated in deacetylation buffer as indicated with SIRT6 -/+ NAD^+. Labelled [^{3}H]-histone H3 and coomassie-blue (total core histones) is shown. All Data are representative of three independent experiments.

1.5. Suv39h1 and G9a loss have distinctive effects on proliferation and viability of SIRT6 MEFs

We also studied the effect of both Suv39h1 and G9a in cell viability. For that purpose, we used MTT assays, which provides a precise measure of cell viability, and to a lesser extent, of proliferation ability. In first place, we aimed to study whether viability defects described in SIRT6-deficient cells (*Sirt6*$^{-/-}$ MEFs) can be rescued by re-introduction of SIRT6. Our first results indicate that this is the case (Figure 18A). On the other hand, we have also optimized the chemical inactivation of Suv39h1 (with 50nM chaetocin) and G9a (50nM UNC0646) in either *Sirt6*$^{-/-}$ MEFs rescued or not with SIRT6-HA (Figure 18B-C). No clear effect was observed until 48h of drug treatment. However, at that time, chaetocin showed a significant effect on viability, which suggests that Suv39h1 may be somehow involved in SIRT6-dependent cell viability and survival.

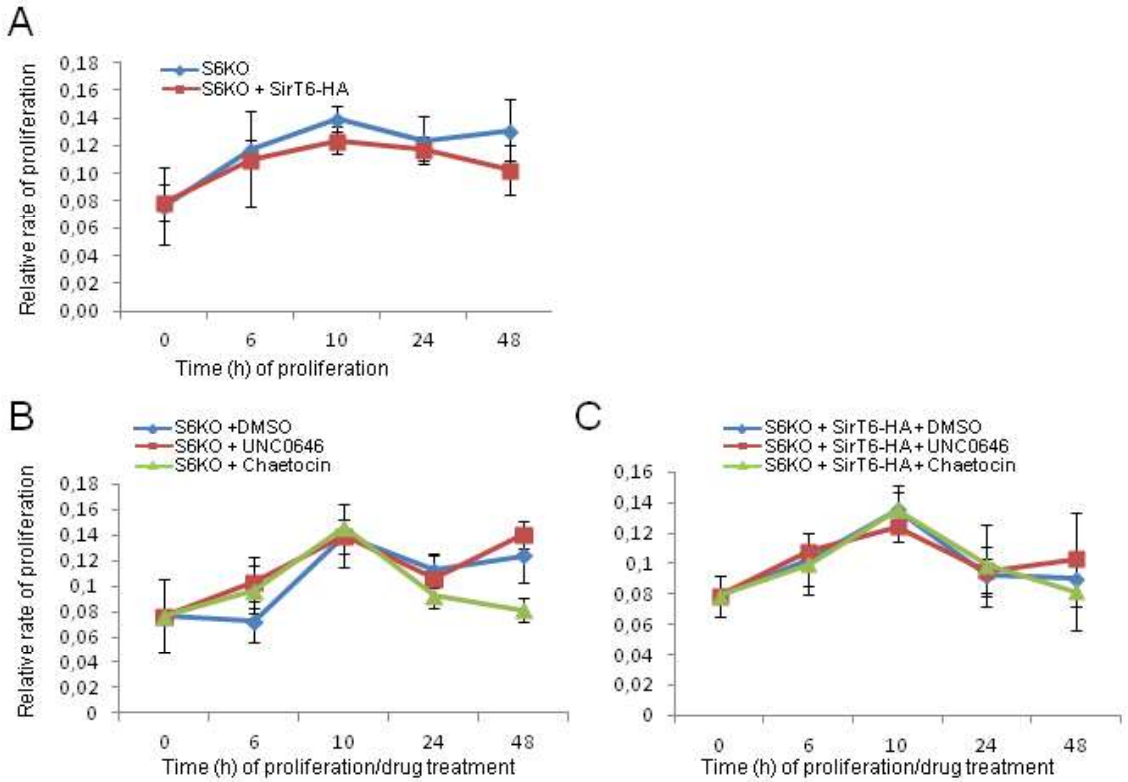

Figure 18. SIRT6-dependent regulation of proliferation. (A) SIRT6 KO MEFs infected either with retrovirus containing empty vector or SIRT6-HA expression vector were plated in 96-well plates and allowed to proliferate during the indicated times and subjected to MTT assay. **(B)** and **(C)** same experiment as in (A) but adding at 0h of proliferation Dimethyl sulfoxide (DMSO, as control) or 50nM of either chaetocin (inhibitor of Suv391) or UNC0646 (inhibitor of G9a) as indicated. Data shown are the mean and s.d. (n=3).

In order to understand the contribution of Suv39h1 and G9a to tumorigenesis, we first designed specific shRNAs to downregulate efficiently Suv39h1 and G9a. We introduced these shRNAs together with a Scramble control shRNA in retroviral vectors and infected *Sirt6*$^{-/-}$ MEFs, selected with puromycin for several days until we obtained a homogenous population of cells expressing the shRNAs. With this procedure we were able to obtain an almost complete downregulation of both HMTs (Figure 19A-B).

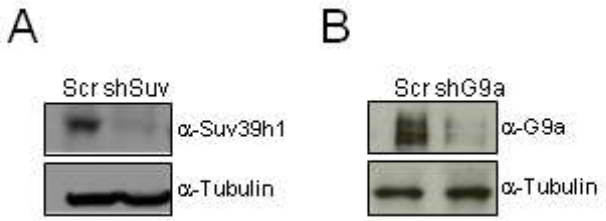

Figure 19. Efficiency of lentiviral shRNA for Suv39h1 and G9a. Western-blot of *Sirt6*$^{-/-}$ MEFs infected with retrovirus expressing shRNA Scramble (Scr), **(A)** ShSuv39h1 or **(B)** ShG9a.

We next generated stable cell lines with these shRNAs in *Sirt6*$^{-/-}$ MEFs cell lines previously engineered to express SIRT6-HA constitutively or empty vector. Once generated, we studied the rate of metabolism, survival and proliferation with a MTT assay of these cell lines (Figure 20).

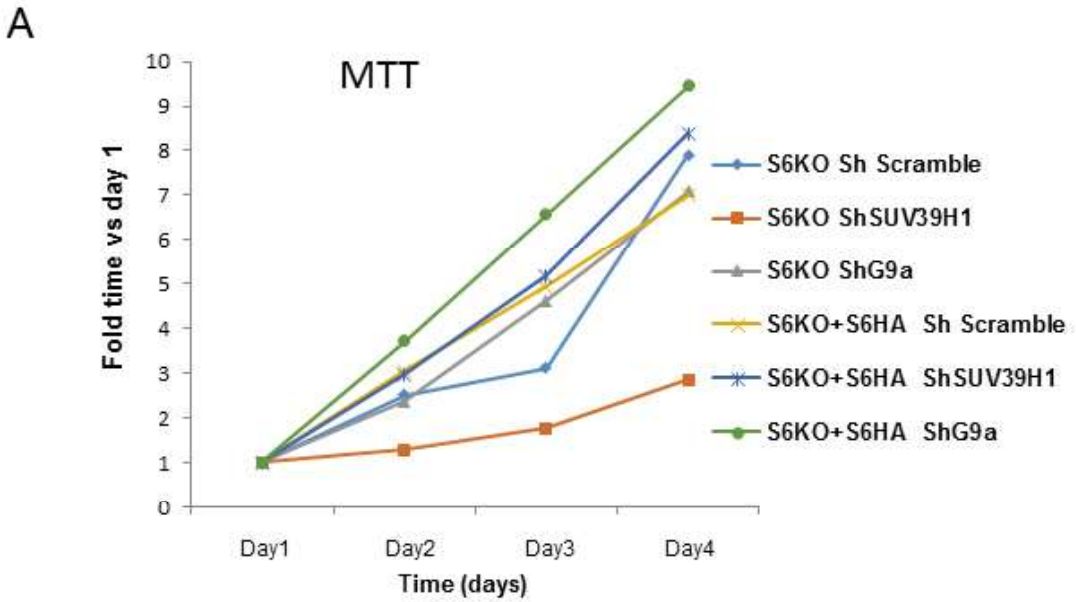

Figure 20. MTT assay of MEFs SIRT6KO rescued or not with SIRT6-HA and expressing ShScramble, ShG9a or ShSuv39h1. 1.5x103 cells were plated and grown for 4 days. MTT levels were measured by absorbance at 595nm every 24h. The levels of each condition are presented related to the MTT levels on day 1. Data shown are the mean (n=3 independent experiments).

As expected, the SIRT6 KO rescued with SIRT6-HA increased the rate of MTT conversion, although for some reason after 4 days, the curves of both cell lines were almost equal. Interestingly, loss of Suv39h1 or G9a had an opposite effect on these cells. While loss of Suv39h1 in SIRT6KO cells decreased significantly MTT signal (SIRT6KO ShSuv39h1 vs SIRT6KO ShScramble), rescue of SIRT6 brought back the MTT curve to the same rate as the rescued with ShScramble. In contrast, G9a loss in the SIRT6KO did not alter the MTT curve compared to ShScramble, but rescue of SIRT6 increased the slope of the MTT rate (Figure 20). This suggested that the relationship between both HMTs and SIRT6 in metabolism, viability and proliferation is not the same. To confirm these results, we also inhibited specifically these HMTs with the inhibitors described earlier. As expected, MTT rate of *Wt* MEFs was much lower than the rate of SIRT6KO cells. Interestingly, inhibition of Suv39h1 activity did not have any effect on the MTT rate of *Wt* cells, but decreased significantly in the SIRT6KO. In

contrast G9a inhibition did not seem to have any clear effect in MTT rate either in *Wt* or KO cells. These results suggested a more direct functional link between Suv39h1 and SIRT6 than G9a (Figure 21).

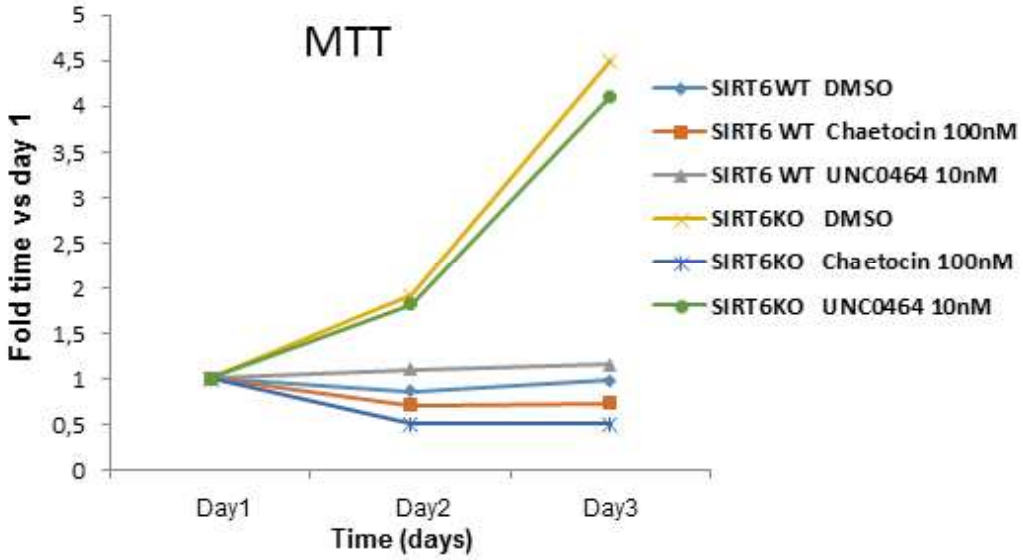

Figure 21. MTT assay of *Wt* or SIRT6KO MEFs incubated with the indicated inhibitors and conditions. 10^3 cells were plated and grown for 3 days. Inhibitors were added on Day 1 and MTT levels were measured by absorbance at 595nm every 24h. The levels of each condition are presented related to the MTT levels on day 1. The data are presented as the mean from three independent experiments.

The experiments shown above aimed to understand the functional relationship between SIRT6 in both HTMs in viability and proliferation. To determine the importance of this interplay in the tumor suppressor role of SIRT6, we decided to transform Wt and *Sirt6*$^{-/-}$ MEFs and characterize the contribution of Suv39h1 or G9a to the role of SIRT6. For that purpose, we first transformed these MEFs with retroviral infection of two vectors, one expressing H-Ras (G12V) and another one harboring shRNA against p53. After several rounds and selection, we infected the cells with the shRNA of Scramble, Suv39h1 and G9a.

A

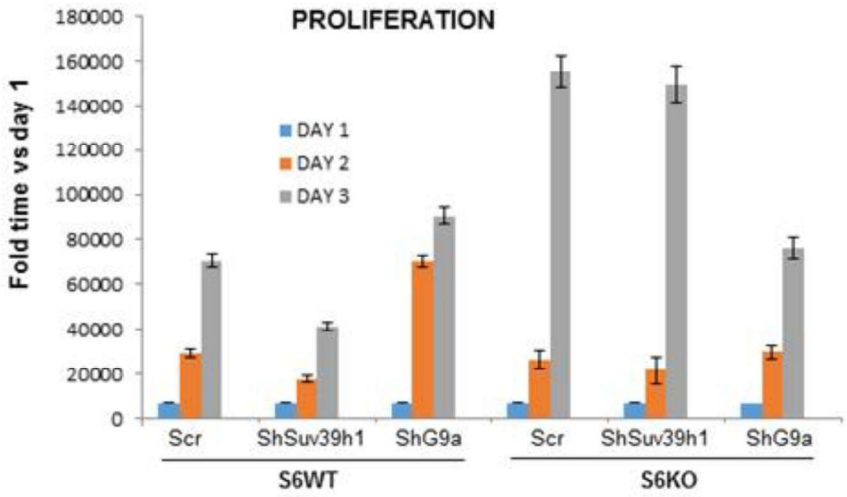

B

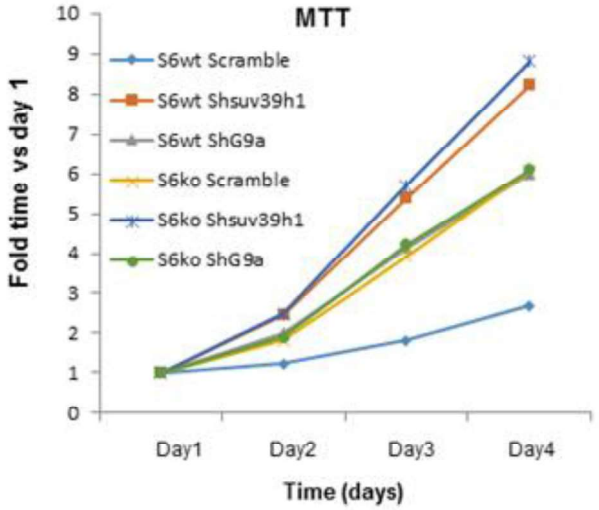

Figure 22. Proliferation and MTT assays of transformed MEFs. *WT* and SIRT6KO MEFs were transformed with retroviral infection of H-Ras(G12V) and Shp53. After transformation, cells were infected with shRNA Scramble, shG9a or shSuv39h1 and selected with puromycin**. (A)** Proliferation rate of these cells. $7x10^4$ cells were plated and the number of cells was counted daily during 3 days. **(B)** MTT assay. $1.5x10^3$ cells were plated and grown for 4 days. MTT levels were measured by absorbance at 595nm every 24h. The levels of each condition are presented related to the MTT levels on day 1. All Data are representative of three independent experiments.

Our first approach was to perform classical proliferation and MTT assays. As expected, loss of SIRT6 induced higher proliferation and MTT rate. Interestingly, loss of Suv39h1 decreased proliferation in *Wt* but not in SIRT6KO cells while increased MTT

rate in *Wt* but not SIRT6KO cells. The fact that in both cases (proliferation and MTT) the effect of Suv39h1 downregulation was specific of *Wt* cells suggested that the effect of Suv39h1 in both assays was related to SIRT6. The case of G9a was more difficult to interpret as it seemed to act in opposition to SIRT6 since G9a loss increased proliferation in *Wt* and decreased in the SIRT6KO, and in the case of MTT increased as Suv39h1 loss, the MTT rate in the *Wt*, but did not changed MTT curve in the SIRT6KO (Figure 22).

1.6. Loss of Suv39h1 increases both the anchorage independent ability and the colony assay formation only in *Wt* cells

To understand better the contribution of both HMTs to the tumor suppression ability of SIRT6, we also performed with these cells two key assays directly associated to the features of cancer cells: the ability to grow in an anchorage independent way and to form individual colonies in cell plates starting from a single cell. These assays are considered two of the gold standard methods to assess the tumorigenic nature of cells *in vitro*. Thus, we performed these assays with the transformed cells tested before. As expected in both assays, loss of SIRT6 associates with higher oncogenic behavior measured by formation of colonies in both cases, reflecting increased tumorigenic capacity.

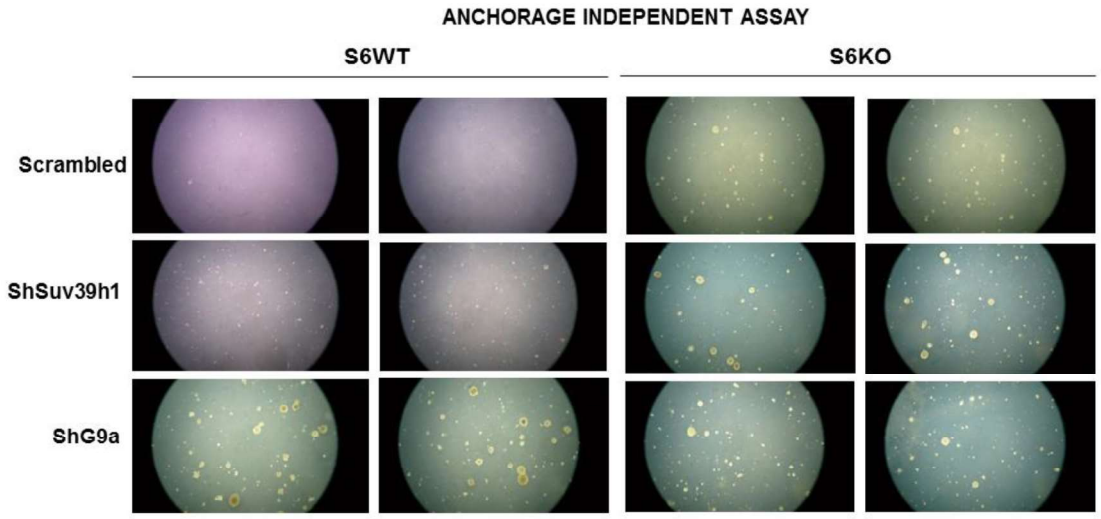

Figure 23. Anchorage independent assays. 700 cells of each type were grown in soft agar plates. The cells were resuspended in 0.4% agar and plated in triplicates in 6cm-plates containing a 1% base agar layer. After 3 weeks, Colonies were fixed with formaldehyde and photographed. Images are representative for at least three independent experiments.

Strikingly, as we found in the proliferation/MTT assays, the increased growth in both assays upon Suv39h1 loss was detected only in *Wt* cells but not in *Sirt6*$^{-/-}$ cells. Thus, in cells lacking SIRT6, loss of Suv39h1 did not have a significant effect. In contrast, loss of G9a in both *Wt* or *Sirt6*$^{-/-}$ cells induced a strong growth effect in these assays, but did not have any specific effect in *Wt* cells vs *Sirt6*$^{-/-}$. Altogether, this strongly suggest that Suv39h1 directly collaborates with SIRT6 in tumor suppression and cell proliferation, while G9a would seem to have a more general SIRT6-independent effect (Figures 23-24).

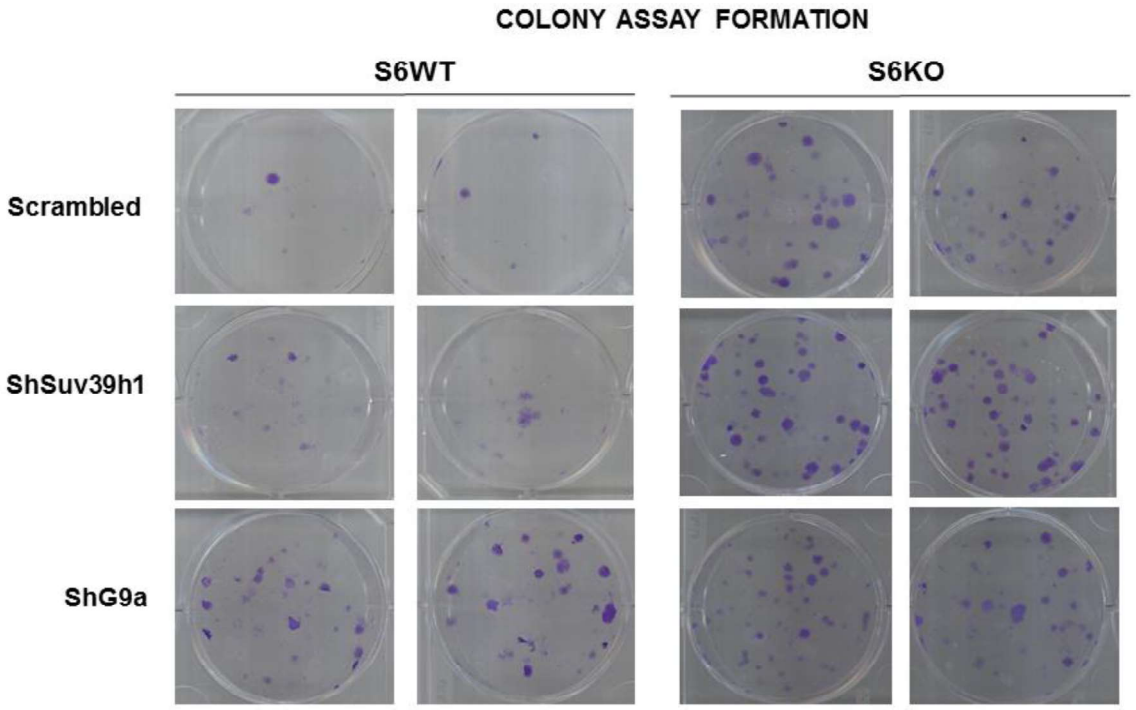

Figure 24. Colony formation assay with the transformed MEFs. 50 cells were plated as a single-cell suspension at low densities and allowed to adhere as single cells. They were grown in 6-well plates for 3 weeks and then, cells were fixed with formaldehyde and stained with crystal violet solution. Images represent at least three independent experiments.

1.7. Suv39h1 downregulation increases the tumorigenic ability of only *Wt* cells

We next, aimed to confirm whether Suv39h1 has a specific role in SIRT6-dependent tumor suppression *in vivo*. For that purpose, we injected these immortalized MEFs in mouse xenografts (BALB/c nude (nu/nu)) and studied the formation of tumors in these

animals. We measured the tumor volume during the process and the final weight of the tumor after the animal sacrifice.

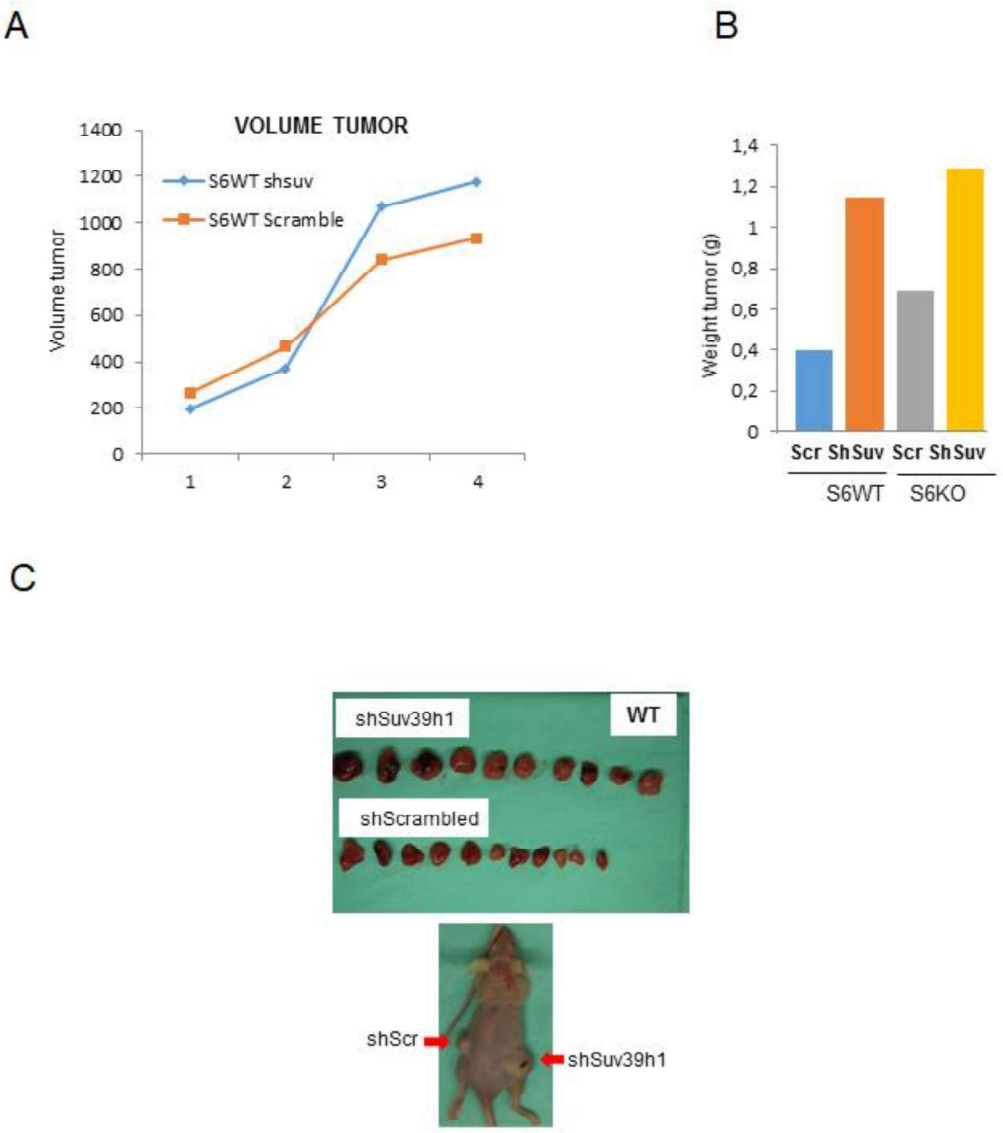

Figure 25. Xenograft analysis of transformed Wt or SIRT6KO MEFs expressing ShScramble, or ShSuv39h1. (A) $3x10^6$ cells were injected subcutaneously in 10 animals for each condition. In every case, ShScramble cells (control) were injected in one side of the body and the shRNA of Suv39h1 in the other one. When possible, volume tumor was measured periodically. **(B)** After sacrifice, the tumor was isolated and weighted. **(C)** Representative image of ShSuv39h1 and ShScramble Xenografts in Wt cells. Each data *set is* representative of three independent experiments.

As expected, SIRT6 KO cells generated bigger tumors than *WT* cells. As observed in figure 26, our analysis strongly suggests that loss of G9a had a strong effect on tumor growth, as it induced a significant increase in both the tumor volume and weight, the observed effect was complex. In the one hand, G9a downregulation induced tumor growth in both *Wt* and *Sirt6*$^{-/-}$ cells suggesting that the effect of G9a is SIRT6 independent. In the other hand, the increase of G9a loss in the tumor weight was lower in *Sirt6*$^{-/-}$ vs *Wt* cells, which may indicate a link between both in this context. Unexpectedly, loss of Suv39h1 induced an increase in tumor growth in both *Wt and Sirt6*$^{-/-}$ MEFs (Figures 25).

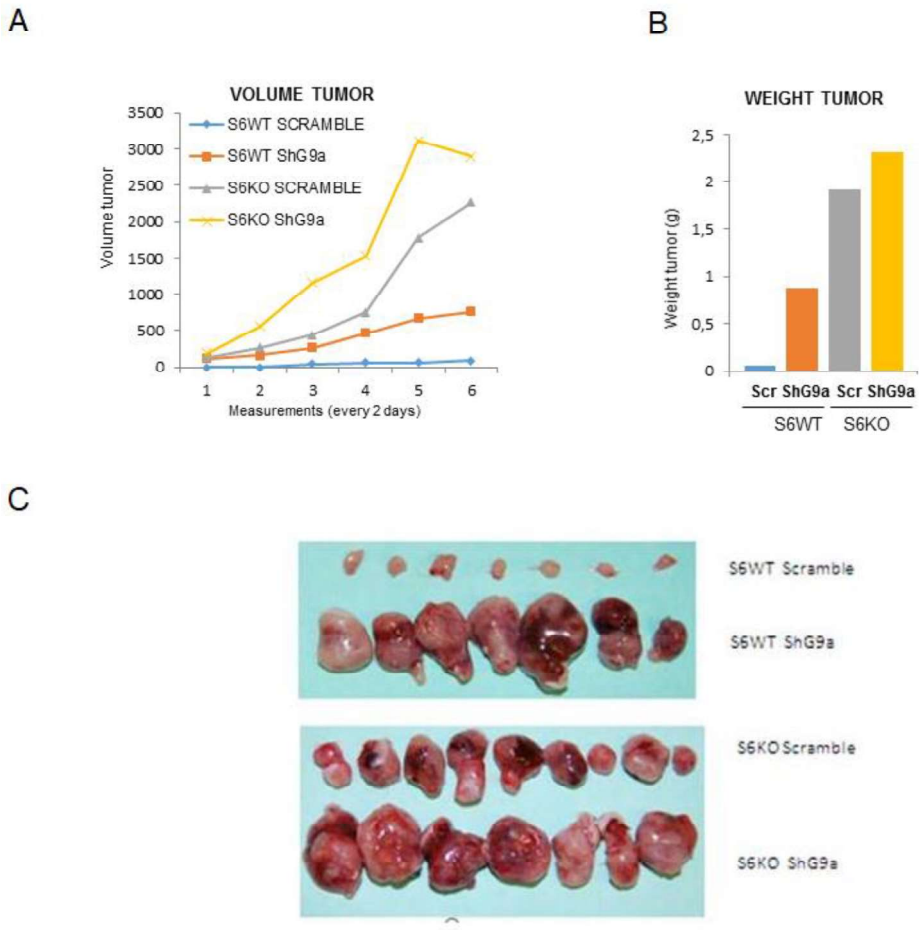

Figure 26. Xenograft analysis of transformed *WT* or SIRT6KO MEFs expressing ShScramble, or ShG9a. **(A)** 3x10^6 cells were injected subcutaneously in 10 animals for each condition. In every case, ShScramble cells (control) were injected in one side of the body and the shRNA of G9a in the other one. When possible, volume tumor was measured periodically. **(B)** After sacrifice, the tumor was isolated and weighted. **(C)** Representative image of ShScramble and shG9a xenografts in in *Wt* and *Sirt6*$^{-/-}$ cells. Each data *set is* representative of three independent experiments.

To understand these observations, we collected the tumors from these animals and they were analyzed at a pathological level in collaboration with Dr Alberto Villanueva (ICO-IDIBELL) and Dr August Vidal (Hospital de Bellvitge). According to the pathological report, all the tumor sections originated from transformed *Wt* cells looked like a pleomorphic sarcoma with disordered growth. In the case of tumor sections originated from *Wt* ShScramble, they present haphazardly distributed epithelioid cells with brisk mitotic activity, while the tumor sections originated from *Wt* ShSuv39h1 cells show predominantly epithelioid areas with some spindle fascicles and irregular nuclei with prominent nucleoli and atypical mitotic figures. In the case of the tumor sections originated from *Wt* ShG9a, we observed fascicular and storiform growth pattern with spindle, epithelioid and pleomorphic cells (Figure27).

On the other hand, all the tumor sections originated from transformed *Sirt6*$^{-/-}$ cells resemble a fibrosarcoma structure (spindle cell sarcoma). The cells are arranged in fascicles that intersect each other at acute angles resulting in a herringbone appearance. In the case of *Sirt6*$^{-/-}$ ShScramble and upon downregulation of either Suv39h1 or G9a, all three tumors show a fascicular pattern with homogeneous spindle cells (Figure 27). The tumor sections originated from transformed *Wt* cells compared to *Sirt6*$^{-/-}$ cells, are more pleomorphic and tend to show a disordered growth pattern. This suggested that *Sirt6*$^{-/-}$ tumor sections were better differentiated and less aggressive. Interestingly, while in *Wt* cells, we observed differences upon depletion of Suv39h1 or G9a, downregulation of both HMTs in *Sirt6*$^{-/-}$ did not have a clear evident effect on the observed features of the tumor sections. This somehow seems to suggest that Suv39h1 or G9a may collaborate in the *in vivo* tumor suppressor activity of SIRT6.

We considered the possibility that the discrepancies between our previous results and these tumorigenesis assays may be due to the fact that *Wt* and *Sirt6*$^{-/-}$ are different cell lines, immortalized independently, which may have unexpected and unrelated stochastic effects on the *in vivo* tumorigenesis growth. In order to avoid the problem of working with different cell lines, and to clarify the contribution of both HMTs *in vivo*, we decided to change the strategy in the tumorigenesis assays. As we did previously in the cell culture assays, to have a more comparable set of cell lines, we decided to focus on

Sirt6$^{-/-}$ cells reconstituted or not with SIRT6-HA expression. For that purpose, we used the *Sirt6*$^{-/-}$ MEFs transformed with H-Ras (G12V)/shp53 and engineered to induced SIRT6-HA expression upon doxocycline treatment. We generated an inducible Tet-on system in *Sirt6*$^{-/-}$ cell lines expressing ShScramble, ShSuv39h1 or ShG9a (Figure 28). Incubation of these cells with doxycycline induced SIRT6-HA expression.

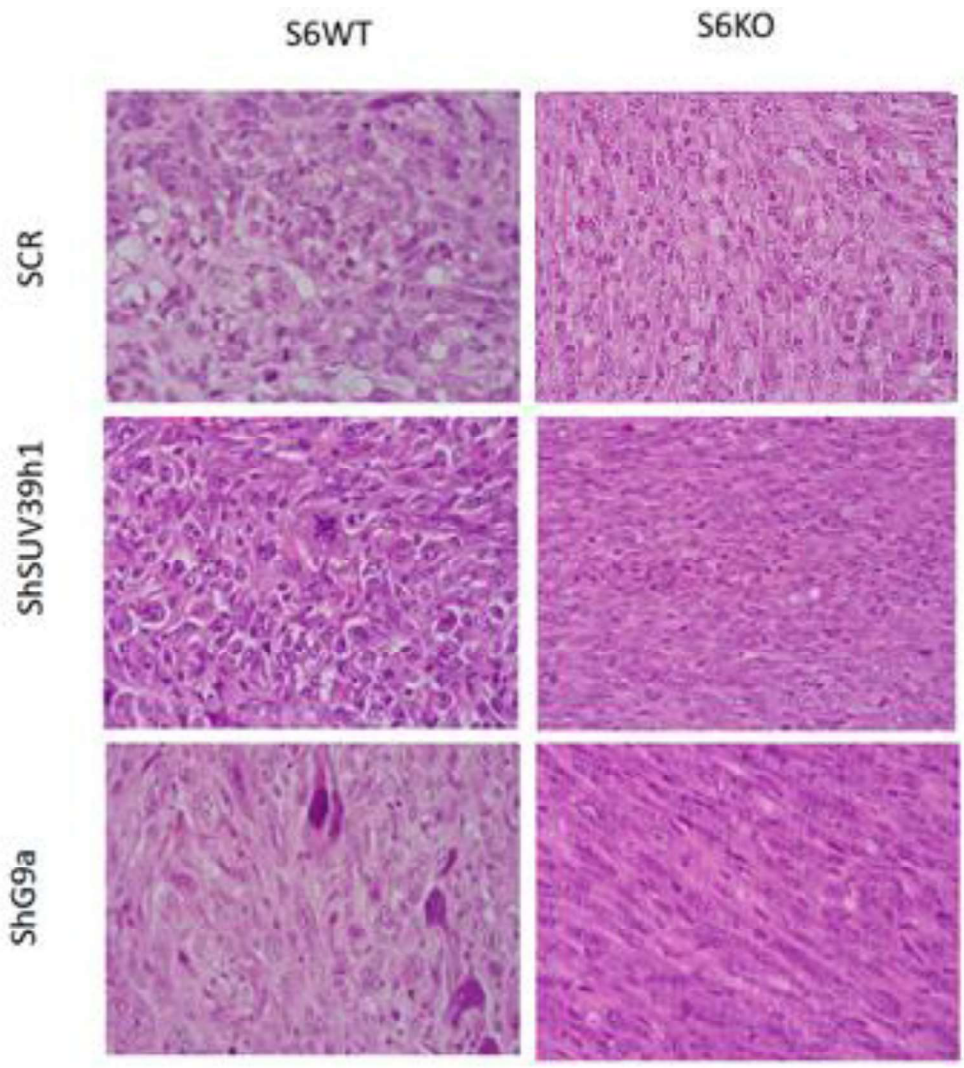

Figure 27. **Representative microscopic findings by hematoxylin and eosin staining**. The tumor sections originated by injection of the indicated transformed Wt and SIRT6 KO MEFs. Tumors were fixed in 4% formaldehyde overnight embedded in paraffin. 4 μm paraffin embedded sections were deparaffinized in xylene and histological sections of whole tumors were stained by hematoxylin and eosin, and the images were acquired with a LEICA DM4000B microscope. Each image is representative of three independent experiments.

We used 60 animals in total, 10 animals for each condition: non-induced (ShScramble, shSuv39h1, shG9a) + Induced (ShScramble, shSuv39h1, shG9a) (Figure 28A). Supporting our previous observations, we observed that the tumor growth generated by *Sirt6*$^{-/-}$ MEFs shScramble was significantly inhibited upon doxocycline -dependent induction of SIRT6-HA expression (Figure 28B-C). However, as expected, this time shG9a tumors behaved exactly as ShScramble tumors upon Doxo induction. Interestingly, the decrease in tumor growth observed upon SIRT6-HA induction was reduced significantly upon Suv39h1 loss. This was in agreement with our previous studies (colony formation, anchorage independent, and proliferation assays), which pointed to an important contribution of Suv39h1, but not of G9a, to the SIRT6 tumor suppression activity. It also suggested that the previous observed results in the first tumorigenesis assays, there was a clear SIRT6-independent factor that contributed to the observed effect of G9a downregulation. In fact, we did observe in these experiments a considerable overgrowth of the tumors in shG9a tumors at the time we induced SIRT6-HA expression, which may explain the limited effect of SIRT6 re-expression in *Sirt6*$^{-/-}$ tumors.

Altogether, these results suggest that to render a full inhibitory effect on tumor growth, SIRT6 requires Suv39h1. In the other hand, G9a downregulation had a strong effect on tumorigenesis, but this seems to be SIRT6-independent. In order to characterize better the SIRT6/ Suv39h1 link, the tumors were collected from these animals and were analyzed at pathological level just in case these cells showed a specific phenotype that could be helpful to decipher this functional link. Pathological analysis of *Sirt6*$^{-/-}$ tumors not expressing (NI) or expressing (I) SIRT6-HA showed clear histological changes between them which include different grade of polymorphisms, necrosis, differentiation, and vascularization (Figure 29).

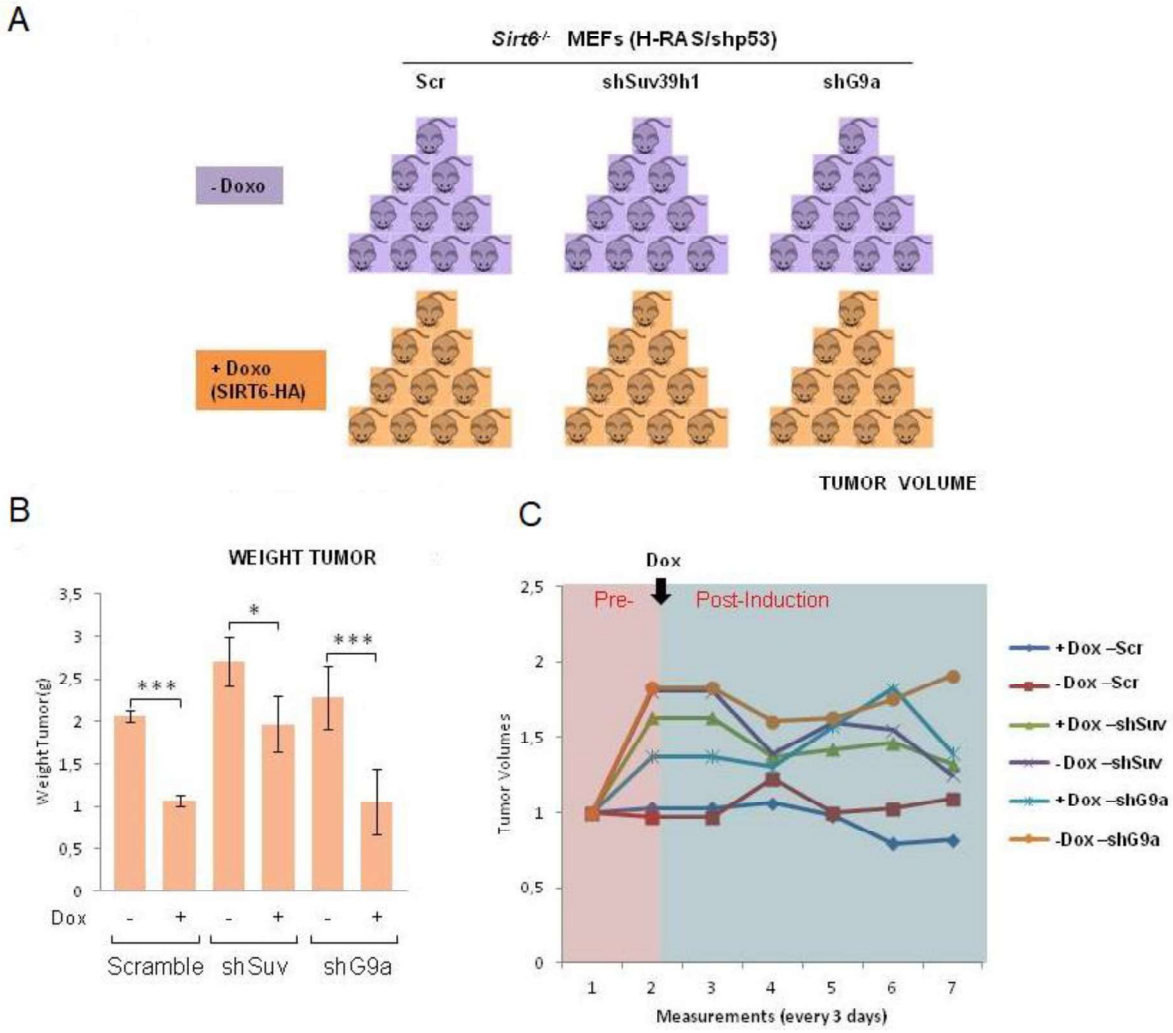

Figure 28. SIRT6 requires Suv39h1 to act as a tumor suppressor. **(A)** Schematic representation of the Tet-on experiment performed. 10 animals were used in each condition. **(B)** Rate of Tumor growth in each condition. Data are expressed as mean ± SD (n = 3), Standard deviation is shown (*: p<0.05; ***: p<0.005). **(C)** Rate of tumor volume pre and post Doxo induction in the same tumors as in (B). All the values are indicated relative to their initial measurement. Data are representative of three independent experiments.

Tumor cells originated from non-induced *Sirt6*$^{-/-}$ ShScramble (S6KO NI) showed haphazard, storiform and fascicular growth pattern which is composed of abundant highly pleomorphic epithelioid cells. They also showed irregular vesicular nuclei with one to three large eosinophilic irregular nucleoli. In contrast, tumor cells originated from Sirt*6*$^{-/-}$ ShScramble cells expressing ectopically SIRT6 (S6KO I) grow in a fascicular arrangement and present long fascicles. The nuclei are relatively homogeneous with oval shape, vesicular chromatin, and focal nucleoli. The non-induced tumors are more pleomorphic whereas induced tumors tend to show a fascicular relatively homogenous

growth pattern which indicates that they are more differentiated. Considering that pleomorphic tumors tend to be much more aggressive, these results indicate, in agreement with the previous results, that reintroduction of SIRT6-HA in *Sirt6*$^{-/-}$ cells decreased the tumorigenicity of these cells.

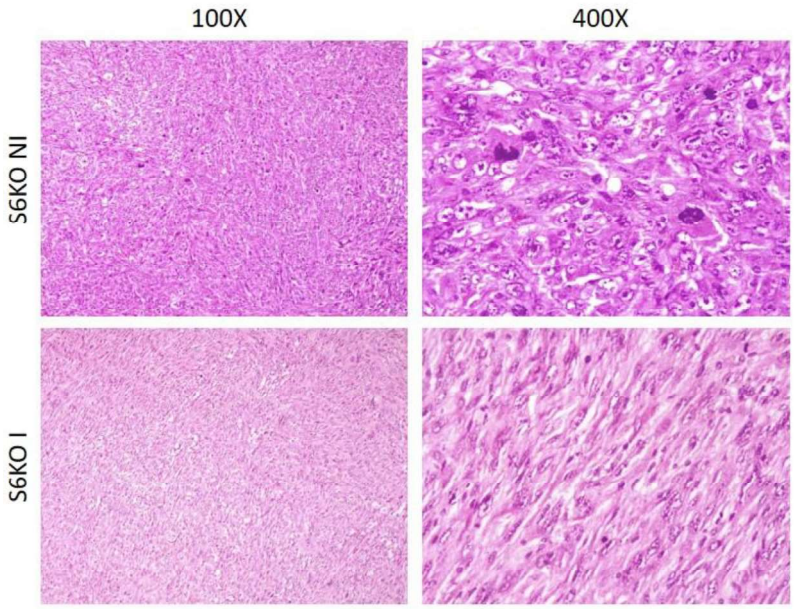

Figure 29. Histological sections of hematoxylin and eosin stained Xenografts. The tumor tissue (magnification, ×100 ×400) from the tumors derived from SIRT6KO ShScramble transplanted into mice in absence of induction (S6KO NI) or upon induction (S6KO I). These sections were obtained from Xenograft tumors developed subcutaneous. Each image is representative of three independent experiments.

The tumor sections originated from uninduced *Sirt6*$^{-/-}$ cells upon depletion of Suv39h1 (SIRT6KO ShSuv39h1 NI), were composed of relatively homogeneous epithelioid cells with round nuclei, and small nucleoli. Reintroduction of SIRT6 (SIRT6KO ShSuv39h1 I), induced a conformation formed by short fascicles of uniform spindle cells with oval nuclei, finely granular chromatin and inconspicuous nucleoli.

We observed a gradual maturation from a pleomorphic SIRT6KO ShScramble non-induced (S6KO NI) to the SIRT6KO ShSuv39h1 (S6KO ShSuv39h1 NI) that shows a predominantly epithelioid but homogeneous morphology without significant pleomorphism. And also, from them to the SIRT6KO ShSuv39h1 induced (S6KO ShSuv39h1 I) which is more differentiated spindle tumor. We observed minimal pathological alteration and they display similar levels of necrosis (Figure 30).

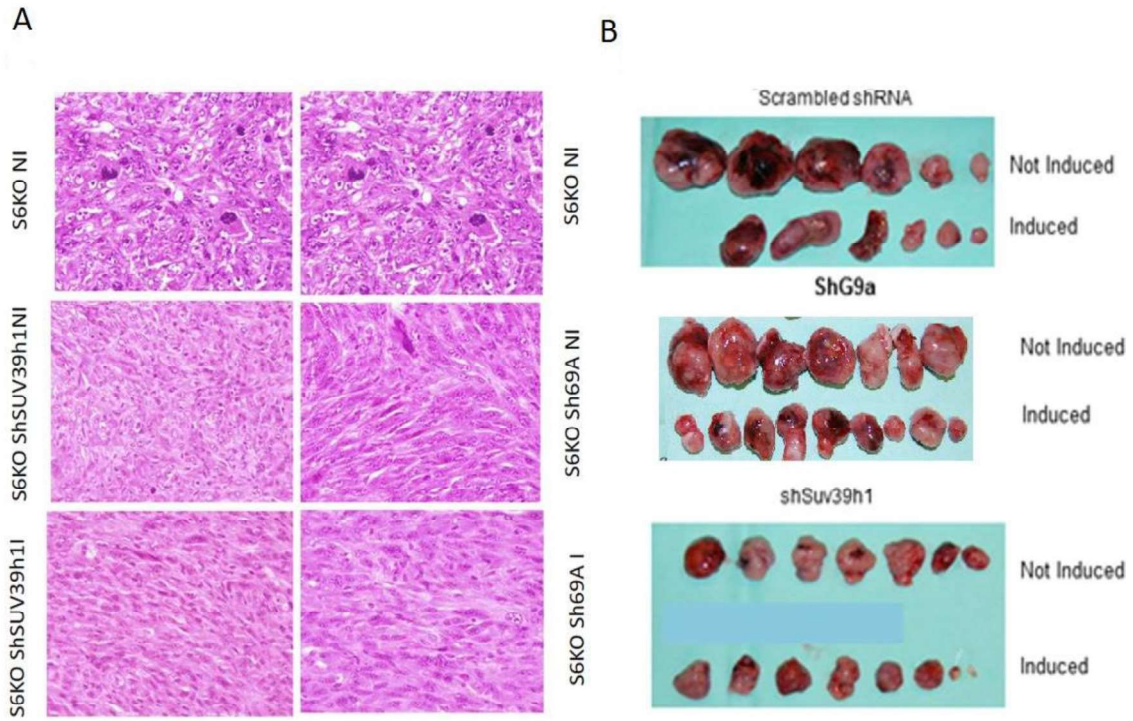

Figure 30. Representative Hematoxylin and Eosin Staining of Xenogrfts. **(A)** The tumor Sections originated by injection of the indicated transformed SIRT6 KO MEFs -/+ doxocyclin induction (SIRT6-HA expression). **(B)** Representative image of ShScramble, ShSuv39h1 and ShG9a Xenografts in *Sirt6*$^{-/-}$ cells lines with or without induction. Each image is representative of three independent experiments.

In contrast, the tumor sections originated SIRT6KO upon depletion of G9a (S6KO ShG9a NI), or even after induction and re-expression of SIRT6 (S6KO ShG9a I) didn't exhibit significant alterations. Both of them, present short fascicles of uniform spindle cells with oval nuclei, finely granular chromatin and inconspicuous nucleoli. In the case of SIRT6KO ShG9a NI tumors can be seen as sparse pleomorphic cells (Figure 30). There is a trend towards "maturation and differentiation" from de pleomorphic SIRT6KO ShScramble non-induced tumor to the induced one which indicates us that G9a is not necessary for the tumor suppressor activities of SIRT6.

Upon overexpression of SIRT6 in Suv39h1 depleted tumors, we observe minimal pathological alteration and they display similar necrosis levels but in the case of G9a depleted tumors we observed that levels of differentiation have been increased in SIRT6KO ShG9a induced tumors. These evidence indicated that SIRT6 needs Suv39h1 in order to carry out its tumor suppressor activities while its effect is G9a independent. Altogether, pathological analysis confirmed that all we observed in other *in vitro* and *in*

vivo studies that SIRT6 and Suv39h1 collaborate together in tumorigenesis suppression while G9a is not essential for tumor suppressor activities of SIRT6.

1.8. Chromatin immunoprecipitation sequencing (ChIP-seq) analysis of SIRT6, Suv39h1 and G9a in tumor xenografts

In order to understand the mechanism through which Suv39h1 contributes to SIRT6 tumor suppressor functions, we next collected the xenograft tumors generated, digested them and sorted them in FACS by GFP signal, since the retroviral vector used to express the shRNA also expresses GFP. After sorting, cells were cultured for several rounds of further selection, which resulted in the successful establishment of the stable cell lines derived from these tumor xenografts. Considering the role of SIRT6, Suv39h1 and G9a in chromatin regulation, we studied the specific interplay of them at genome level, with the purpose of defining i) the effect of Suv39h1 in SIRT6 genomic distribution related genomic functions that could help to explain their interplay in tumorigenesis; ii) the contribution of G9a to SIRT6 chromatin functions; and, iii) to the identification of a number of different SIRT6 targets upon tumorigenesis. For that purpose, we performed a ChIP-seq analysis of these cells derived from tumor xenografts *Wt* (ShScramble, ShSuv39h1, ShG9a) and *Sirt6*$^{-/-}$ (ShScramble, ShSuv39h1, ShG9a) (Figure 31A). The ChIP-seq experiment included the analysis of SIRT6, G9a and Suv39h1 in these cells. We first optimized the ChIPs for all three factors. For that purpose, we performed all three ChIPs (G9a, Suv39h1, SIRT6) under regular 1% formaldehyde fixing conditions or upon double crosslinking (Formaldehyde 1% + 2mM DSG). Strikingly we observed that under double crosslinking (DC), all three endogenous proteins were efficiently detected in specific target genes compared to single formaldehyde treatment (F) (Figure 31, B-D)

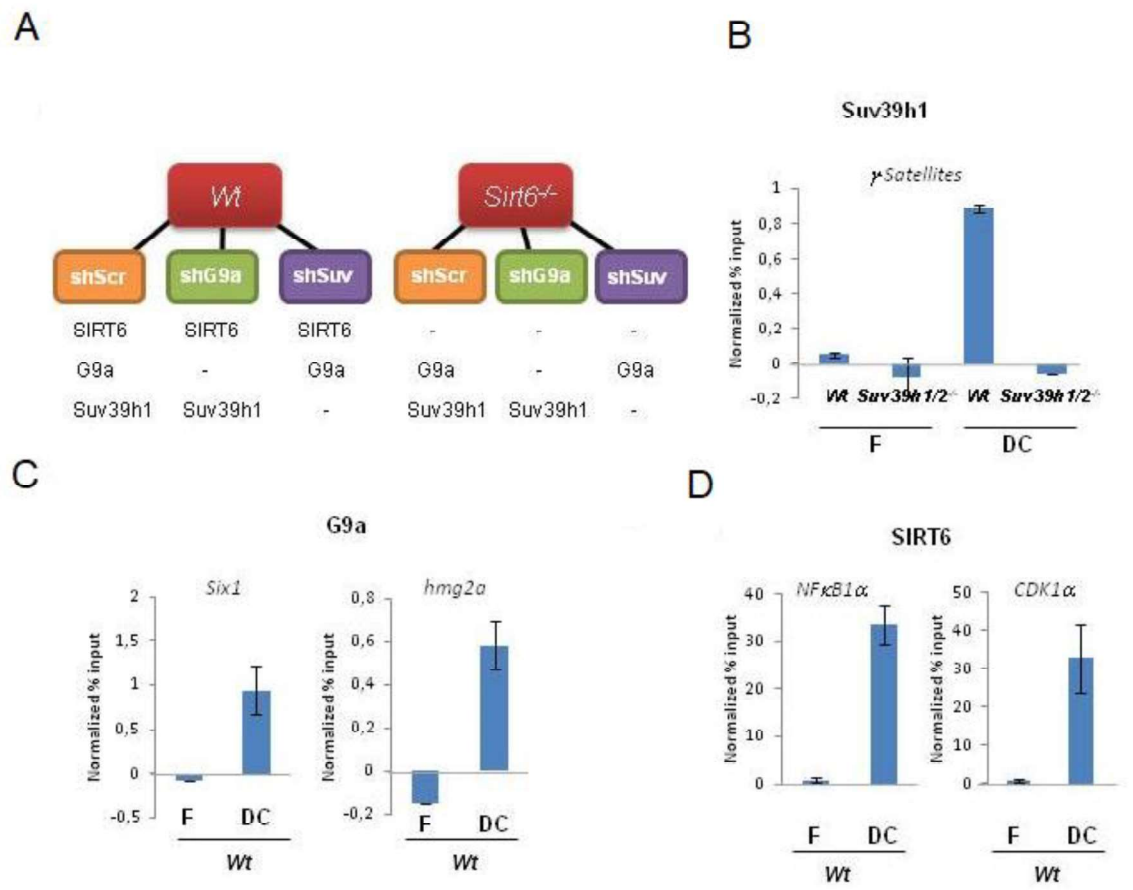

Figure 31. ChIP analysis of the transformed MEFs derived xenografts. **(A)** Schematic diagram of the ChIP-seq experiment. The MEFs used are indicated in boxes. We had 6 different cell lines: *Wt* or *Sirt6*$^{-/-}$ expressing each of them ShRNA Suv39h1 (ShSuv), or ShRNA G9a (ShG9a). Below the boxes, are indicated the specific ChIP performed in each cell line. **(B)** Endogenous Suv39h1 ChIP in pericentric γ-satellites of *Wt* or *Suv39h1/2*$^{-/-}$ MEFs performed under single Formaldehyde 1% crosslinking (F) or double Formaldehyde 1% + 2mM disuccinimidyl glutarate (DSG) crosslinking (DC). **(C)** G9a ChIP performed under single (F) or double (DC) crosslinking in two positive genes in *Wt* MEFs. **(D)** SIRT6 ChIP of two positive genes in *Wt* MEFs performed as in (B) and (C). Each data set is representative of three independent experiments. Data are expressed as mean ± SD (n = 3).

Once we established the conditions for the ChIP of all three factors, we next studied the whole genome distribution of SIRT6 performing chromatin immunoprecipitation followed by sequencing (ChIP-seq) under double crosslinking conditions in triplicate for all three factors in the established cell lines from xenograft tumors. We performed i) SIRT6 ChIP-seqs in *Wt* ShScramble (WS6E), *Wt* ShSuv39h1 (WUSE) and *Wt* ShG9a (WGSE); ii) Suv39h1 ChIP-seq analysis in *Wt* ShScramble (WSUE) and *Sirt6*$^{-/-}$ ShScramble (KSUE); and iii) G9a ChIP-seqs in *Wt* ShScramble (WSGE) and *Sirt6*$^{-/-}$ ShScramble (KSGE). Once completed, the ChIP-seqs were analyzed at the CNIC bioinformatics unit.

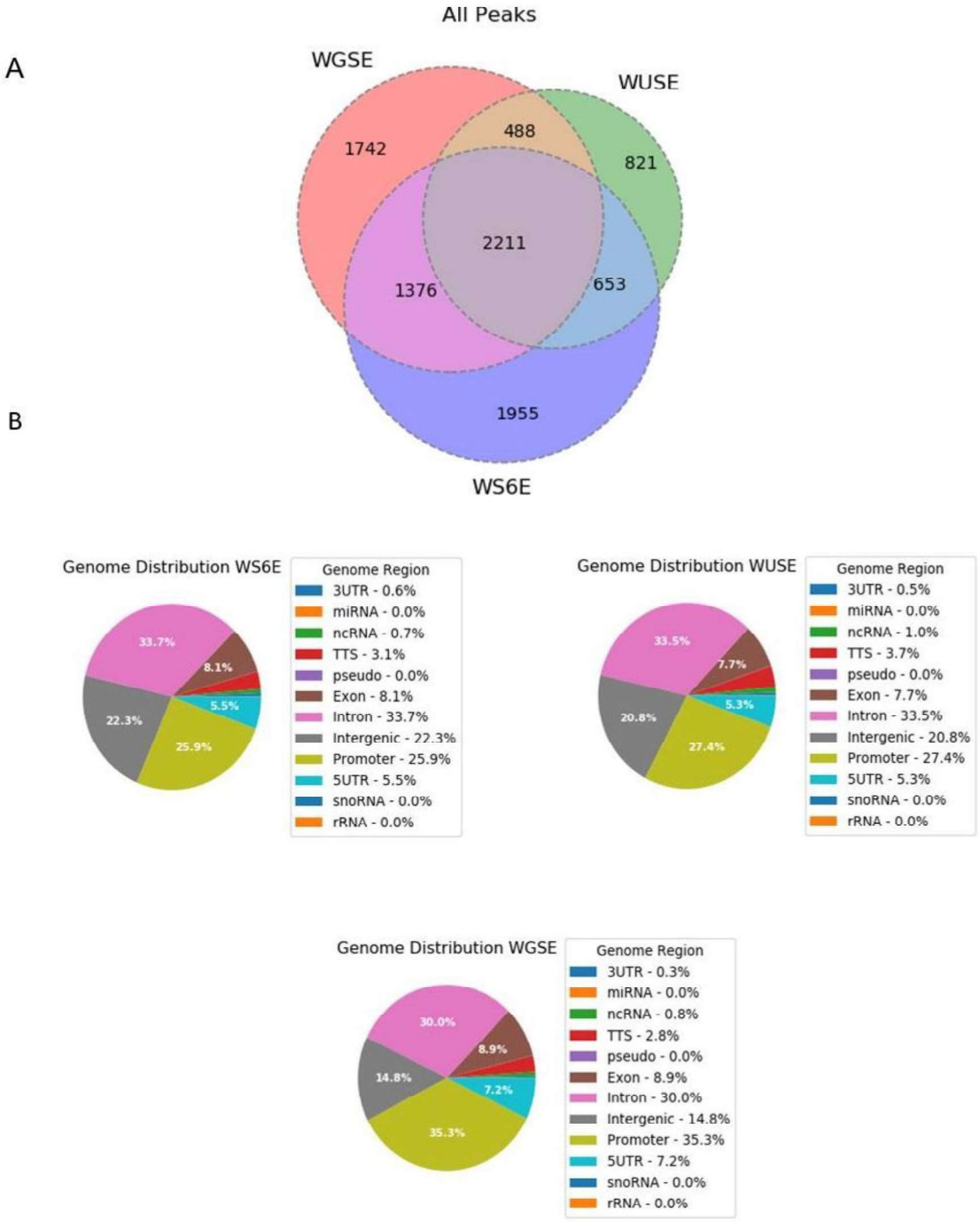

Figure32. Overview of SIRT6 binding sites. **(A)** Venn diagrams showing the intersection of SIRT6-associated genes in WS6E, WUSE and WGSE. **(B)** Genomic distribution of ChIP-seq peaks for SIRT6 in each indicated cell lines, ShScramble, ShSuv39h1 and ShG9a. The genomic locations of peaks detected by ChIP-Seq subdivided into twelve sub-genomic regions. Each pie chart contains sub-genomic regions including promoters, exons, introns, intergenic regions, and others. Each sub-genomic locus was indicated by using a different color. Each data set is representative of three independent experiments.

In our first analysis, we compared the genomic distribution of ChIP-seq peaks of SIRT6 in *Wt* ShScramble, *Wt* ShSuv39h1 and *Wt* ShG9a (Figure 32). We identified 9246 peaks associated to SIRT6. Of them, 2221 were identified in all conditions. Loss of either Suv39h1 or G9a resulted in a common loss of 1955 peaks of SIRT6 and a common gain of 488 peaks. Interestingly, loss of G9a or Suv39h1 resulted in the gain of 1742 or 821 unique SIRT6 peaks, respectively. Overall, this suggested that both Suv39h1 and G9a regulate SIRT6 genomic distribution.

In *Wt* ShScramble, the majority of SIRT6 binding sites (56%) were located within intronic and intergenic regions, while 8.1% was located in exons and 25.9% in promoters. The SIRT6 binding sites have almost similar distributions across the whole genome in the case of Wt ShScramble and *Wt* ShSuv39h1, but depletion of G9a induced a significant change in genome wide distribution of SIRT6. In that case, only 44.8% remained locating within intronic and intergenic regions and SIRT6 displaced toward 5'-UTR (7.2%) and promoter regions (35.5%). These results suggest that, in contrast to Suv39h1, G9a negatively regulates the access of SIRT6 to promoter regions which may suggest an antagonistic effect of G9a in gene expression.

In order to understand better the impact of Suv39h1 and G9a to SIRT6 function we performed a GREAT (Genomic Regions Enrichment of Annotations Tool) analysis, a popular web-based tool to link biological functions to genomic regions. GREAT analysis associated these regions with specific genes, suggesting that the sequences correspond to introns, intergenic regions, and promoters. Many of the SIRT6-associated genes mapped by GREAT were associated by Kyoto Encyclopedia of Genes and Genomes (KEGG) analysis with cell signaling, the majority of which directly or indirectly participate in the regulation of cell cycle and metabolic homeostasis. The main use of the GO is to perform enrichment analysis on gene sets based on biological processes. Gene ontology (GO) analysis revealed more than 20 biological process subcategories in the case of SIRT6 (Figure 34).

To compare the functions of SIRT6 upon downregulation of Suv39h1 or G9a, KEGG analysis and GO enrichment analyses were performed. We explored overrepresented pathways and biological functions of SIRT6 in *Wt* Scramble affected by depletion of Suv39h1 or G9a. KEGG pathway analysis showed that SIRT6 in *Wt* ShScramble were

significantly enriched in MAPK signaling pathway, axon guidance, focal adhesion and Rap1 signaling pathway (Figure 33A). In the case of SIRT6 in *Wt* ShSuv39h1 cell line, KEGG pathway analysis showed that enrichment mostly in proteoglycans in cancer, ECM-receptor interaction, cell cycle and signaling pathways regulating pluripotency of stem cells (Figure 33B). In the case of *Wt* ShG9a cell line, SIRT6 were mostly enriched in Hippo signaling pathway, Wnt signaling pathway, adherens junction and gastric cancer (Figure 33C).

A

Wt Scramble

Index	Name	Combined score
1	MAPK signaling pathway	20.78
2	Axon guidance	18.94
3	Focal adhesion	17.53
4	Rap1 signaling pathway	14.73
5	Ras signaling pathway	14.61
6	Regulation of actin cytoskeleton	12.83
7	Arrhythmogenic right ventricular cardiomyopathy (ARVC)	11.00
8	Proteoglycans in cancer	10.68
9	PI3K-Akt signaling pathway	9.40
10	Cortisol synthesis and secretion	9.26

B

Wt ShSuv39h1

Index	Name	Combined score
1	Proteoglycans in cancer	37.96
2	ECM-receptor interaction	33.21
3	Cell cycle	22.62
4	Signaling pathways regulating pluripotency of stem cells	22.15
5	TGF-beta signaling pathway	19.99
6	Melanoma	17.15
7	Mucin type O-glycan biosynthesis	17.14
8	Fluid shear stress and atherosclerosis	11.81
9	Pyrimidine metabolism	11.69
10	Rap1 signaling pathway	11.42

C

Wt ShG9a

Index	Name	Combined score
1	Hippo signaling pathway	42.81
2	Wnt signaling pathway	34.24
3	Adherens junction	30.95
4	Gastric cancer	29.61
5	Prostate cancer	29.05
6	Pathways in cancer	27.06
7	Acute myeloid leukemia	24.88
8	Signaling pathways regulating pluripotency of stem cells	24.64
9	Thyroid cancer	24.64
10	Colorectal cancer	24.19

Figure 33. **KEGG pathway analysis of the target genes bound by SIRT6 in tumor derived xenograft cells**. **(A)** KEGG pathway analysis for SIRT6 binding genes in *Wt* ShScramble cell line. **(B)** KEGG pathway analysis for SIRT6 binding genes in *Wt* ShSuv39h1 cell line. **(C)** KEGG pathway analysis for SIRT6 binding genes in *Wt* ShG9a cell line. Kyoto Encyclopedia of Genes and Genomes (KEGG) analyses were performed by using Enrichr platform (maayanlab. cloud/Enrichr).

In the case of SIRT6 in *Wt* ShScramble, the pathway with most gene enriched is Mitogen-activated protein kinase (MAPK) signaling pathway. It not only modulates a wide variety of cellular processes but also, amplifies and integrates signals from a broad spectrum of stimuli and elicits an appropriate physiological response such as, differentiation, development, proliferation and apoptosis (Zhang et al., 2002). We also observed the other important gene enriched pathways like Ras signaling pathway and PI3K -AKT signaling pathway both of the play an important role in cell cycle control and tumorigenesis. Upon downregulation of Suv39h1, KEGG analysis showed that the signaling pathway with most SIRT6 enriched is Proteoglycans in cancer. Proteoglycans provide a contact link between the cell membrane and the surrounding cell-extracellular matrix (ECM), thereby playing a central role in regulating cancer cell adhesion and migration (Gorges et al., 2012). KEGG analysis showed that upon G9a downregulation, the signaling pathway associated to SIRT6 enrichment are Hippo and Wnt signaling pathways. The Hippo signaling pathway is an evolutionarily conserved pathway involved in control organ size and development (Halder and Johnson, 2011). The Wnt (Wingless related integration site) pathway is a highly conserved signaling pathway, which was first discovered due to its role in carcinogenesis (Nusse et al., 1982) and body axis formation during embryonic development (Klaus et al., 2008).

The genes recognized by SIRT6 were classified into different functional categories by GO ontology analysis. The genes recognized by SIRT6 in *Wt* ShScramble were involved in diverse physiological processes, such as regulation of cell-matrix adhesion (GO:0001952), regulation of cell migration involved in sprouting angiogenesis (GO:0090049), regulation of vascular endothelial growth factor receptor signaling pathway (GO:0030947) and mitochondrial translational elongation (GO:0070125) (Figure 34A). The genes bounded by SIRT6 in *Wt* ShSuv39h1 participated in different functional categories such as negative regulation of cell differentiation (GO:0045596), negative regulation of transcription, DNA-templated (GO:0045892), positive regulation of heart rate (GO:0010460) and response to laminar fluid shear stress (GO:0034616) (Figure 34B).The genes targeted by SIRT6 in *Wt* ShG9a mainly enriched in regulation of transcription from RNA polymerase II promoter (GO:0006357), negative regulation of transcription, DNA-templated (GO:0045892), negative regulation of transcription from

RNA polymerase II promoter (GO:0000122) and proteasome-mediated ubiquitin-dependent protein catabolic process (GO:0043161)(Figure 34C).

A

Wt Scramble

Index	Name	Combined score
1	regulation of cell-matrix adhesion (GO:0001952)	119.99
2	regulation of cell migration involved in sprouting angiogenesis (GO:0090049)	73.66
3	regulation of vascular endothelial growth factor receptor signaling pathway (GO:0030947)	73.66
4	mitochondrial translational elongation (GO:0070125)	73.66
5	positive regulation of epithelial cell migration (GO:0010634)	73.66
6	translational termination (GO:0006415)	73.66
7	regulation of embryonic development (GO:0045995)	73.66
8	positive regulation of developmental process (GO:0051094)	73.66
9	positive regulation of cell differentiation (GO:0045597)	73.66
10	negative regulation of cellular response to growth factor stimulus (GO:0090288)	71.69

B

Wt ShSuv39h1

Index	Name	Combined score
1	negative regulation of cell differentiation (GO:0045596)	220.57
2	negative regulation of transcription, DNA-templated (GO:0045892)	119.57
3	positive regulation of heart rate (GO:0010460)	119.57
4	response to laminar fluid shear stress (GO:0034616)	119.57
5	negative regulation of cellular macromolecule biosynthetic process (GO:2000113)	119.57
6	wound healing (GO:0042060)	119.57
7	negative regulation of transmembrane receptor protein serine/threonine kinase signaling pathway (GO:0090101)	119.57
8	negative regulation of transforming growth factor beta receptor signaling pathway (GO:0030512)	80.95
9	positive regulation of keratinocyte migration (GO:0051549)	80.95
10	endoplasmic reticulum tubular network organization (GO:0071786)	80.95

C

Wt ShG9a

Index	Name	Combined score
1	regulation of transcription from RNA polymerase II promoter (GO:0006357)	96.93
2	negative regulation of transcription, DNA-templated (GO:0045892)	82.41
3	negative regulation of transcription from RNA polymerase II promoter (GO:0000122)	82.41
4	proteasome-mediated ubiquitin-dependent protein catabolic process (GO:0043161)	82.41
5	endochondral bone morphogenesis (GO:0060350)	67.71
6	regulation of apoptotic process (GO:0042981)	66.00
7	regulation of lamellipodium organization (GO:1902743)	53.56
8	proteasomal protein catabolic process (GO:0010498)	52.74
9	negative regulation of gene expression (GO:0010629)	52.74
10	stress-activated MAPK cascade (GO:0051403)	52.74

Figure 34. **GO category of the target genes bound by SIRT6 in tumor derived xenograft cells**. **(A)** GO ontology categories for SIRT6 binding genes in *Wt* ShScramble cell line. **(B)** GO ontology categories for SIRT6 binding genes in *Wt* ShSuv39h1 cell line. **(C)** GO categories and pathway analysis for SIRT6 binding genes in *Wt* ShG9a cell line. Gene Ontology (GO) enrichment analyses were performed by using Enrichr platform (maayanlab. cloud/Enrichr).

As mentioned, in the case of SIRT6 in *Wt* ShScramble gene ontology analysis revealed that the most enriched clusters were composed of genes involved in regulation of cell-matrix adhesion and regulation of cell migration involved in sprouting angiogenesis. Regulations of both processes play a key in tumorigenesis and may be connected to tumor suppressor activities of SIRT6. Suv39h1 downregulation caused significant changes in enriched clusters related to many important functions and the SIRT6 bounded genes have a significant enrichment in cluster related to negative regulation of cell differentiation and transcription which is essential for cancer cells in order to acquire the capability to sustain proliferative signaling and it is hallmark of cancer initiation. In contrast, G9a downregulation led to SIRT6 enrichment in the GO categories regulation of transcription from RNA polymerase II promoter and negative regulation of transcription, DNA-templated. This may indicate that G9a downregulation resulted in SIRT6 recruitment of Pol II and regulation of transcription from RNA polymerase II promoter. On the other hand, SIRT6 is known as a deacetylase to modulate transcriptional pausing and elongation. It interacts with Pol II and inhibits transcription elongation by decreasing intragenic levels of acetylated H3K9 and H3K56 to regulate recruitment of specific transcription factors. The negative regulation of transcription is essential for the establishment of the temporal patterns of gene expression and is also associated with the regulation of gene expression in response to changes in the micro-environment of the cell (Etchegaray et al., 2019). Besides, the negative regulation of transcription pathway has been showed to be connected to proliferation and apoptosis of cancer cells (Lin and Gregory, 2015). This can explain at least partially, the phenotype we observed in ShG9a tumor xenografts.

We next analyzed the impact of SIRT6 loss in Suv39h1 distribution in these tumor cells. We identified 1055 peaks of Suv39h1, a lower number compared to SIRT6, probably reflecting a) that the vast majority of Suv39h1 is present in CH, which are underrepresented in this analysis for technical reasons; and b) the limited ability of Suv39h1 antibody in immunoprecipitation studies. Interestingly, loss of SIRT6 induced a loss of 849 peaks of Suv39h1 and induced the gain of 163 unique peaks (Figure 35A).

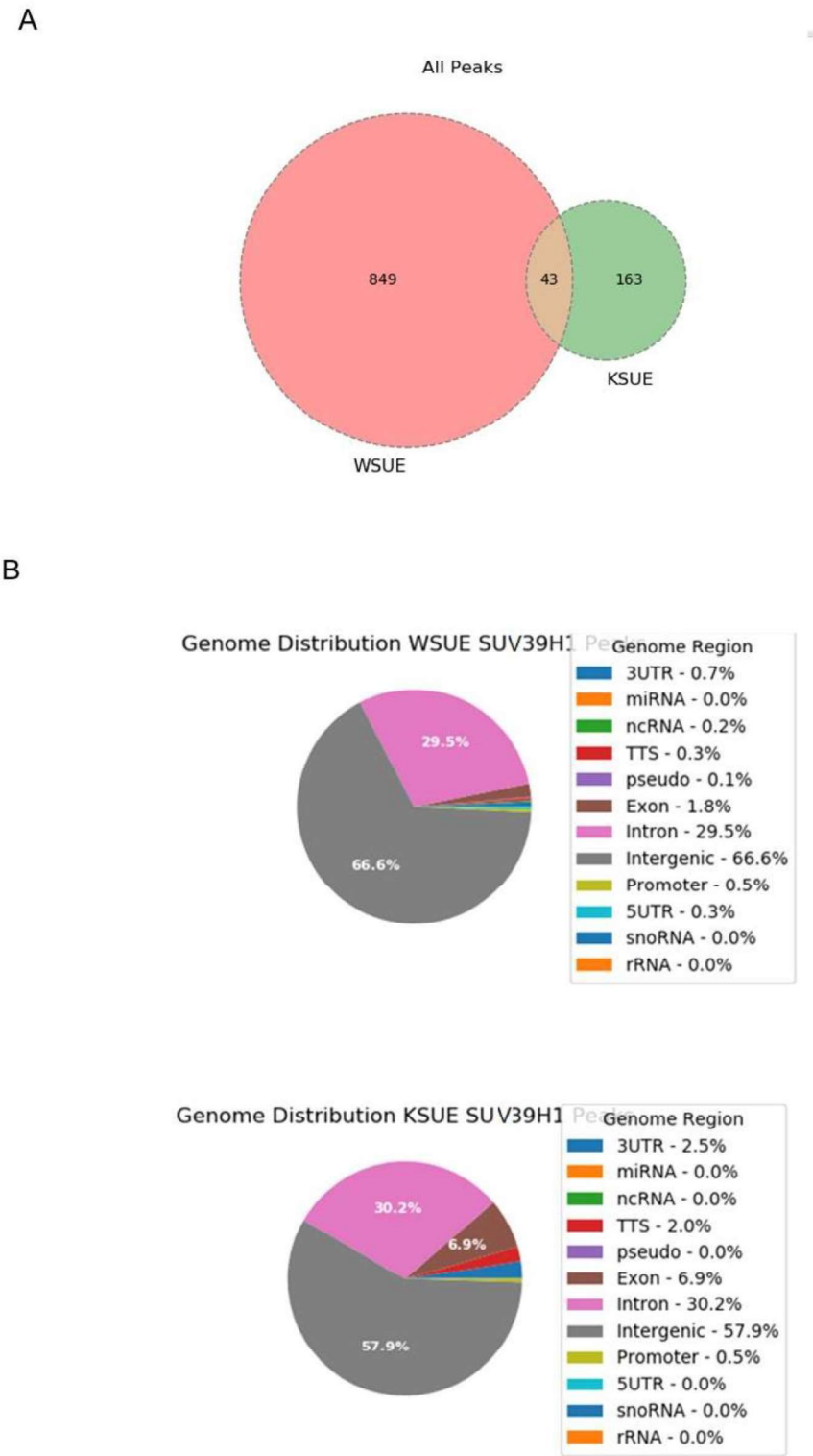

Figure 35. Overview of Suv39h1 binding sites. **(A)** Venn charts showing the intersection of Suv39h1-associated peaks in *Wt* ShScramble (WSUE) and *Sirt6*$^{-/-}$ ShScramble (KSUE). **(B)** Genomic distribution of ChIP-seq peaks for Suv39h1 in each indicated cell lines, *Wt* ShScramble (left) and *Sirt6*$^{-/-}$ ShScramble (right). The genomic locations of peaks detected by ChIP-Seq subdivided into twelve sub-genomic regions. Each sub-genomic locus was indicated by using a different color. Each data set is representative of three independent experiments.

In the case of Wt ShScramble, 96.1% of Suv39h1 binding sites were located in intergenic and intronic regions, 1.8% in exons and 0.5% in promoter regions. Interestingly, loss of SIRT6 displaced Suv39h1 from intergenic and intronic regions (96.1% vs 88.9%). This is a very interesting finding, as it may indicate a role for SIRT6 in Suv39h1 localization in CH. Total number of genes with Suv39h1 occupancy specifically or commonly altered upon depletion of SIRT6 was 43 genes. We observed upon depletion of SIRT6, global genome distribution of Suv39h1 altered, especially in Exon regions, TTS and 3UTR. For instance, exon bounded Suv39h1 increased from 1.8% in the case of Wt shScramble to 6.9% in Wt shSuv39h1 (Figure 35B).

KEGG analysis showed that Suv39h1 in *Wt* were significantly enriched for other types of O-glycan biosynthesis, Phenylalanine, tyrosine and tryptophan biosynthesis, N-Glycan biosynthesis and TGF-beta signaling pathway (Figure 36A). In the case of Suv39h1 in *Sirt6*$^{-/-}$ Scramble, KEGG analysis showed that enrichment mostly in phenylalanine, tyrosine and tryptophan biosynthesis, herpes simplex virus 1 infection, Arginine biosynthesis and MAPK signaling pathway (Figure 36B). In the case of overlapped genes Suv39h1 were mostly enriched in Primary bile acid biosynthesis, VEGF signaling pathway and lysine degradation (Figure 36C).

A

Wt ShScramble

Index	Name	Combined score
1	Other types of O-glycan biosynthesis	24.35
2	Phenylalanine, tyrosine and tryptophan biosynthesis	23.55
3	N-Glycan biosynthesis	16.30
4	Taurine and hypotaurine metabolism	14.31
5	TGF-beta signaling pathway	11.23
6	Hedgehog signaling pathway	7.35
7	Proteasome	6.78
8	Pantothenate and CoA biosynthesis	6.51
9	Malaria	6.03
10	Arginine biosynthesis	5.95

B

***Sirt6*$^{-/-}$ ShScramble**

Index	Name	Combined score
1	Phenylalanine, tyrosine and tryptophan biosynthesis	80.92
2	Herpes simplex virus 1 infection	40.12
3	Arginine biosynthesis	23.07
4	Other types of O-glycan biosynthesis	18.58
5	Phenylalanine metabolism	17.39
6	Chronic myeloid leukemia	13.30
7	MAPK signaling pathway	11.92
8	Cell adhesion molecules (CAMs)	8.77
9	Alanine, aspartate and glutamate metabolism	8.43
10	Tyrosine metabolism	7.45

C

Overlapped genes

Index	Name	Combined score
1	Primary bile acid biosynthesis	157.77
2	VEGF signaling pathway	27.28
3	Lysine degradation	26.63
4	Non-small cell lung cancer	22.70
5	Fc epsilon RI signaling pathway	21.75
6	B cell receptor signaling pathway	20.03
7	Inositol phosphate metabolism	19.63
8	Glioma	18.88
9	Renin secretion	18.52
10	ErbB signaling pathway	16.00

Figure 36. KEGG cell signaling pathways for Suv39h1-associated genes mapped by GREAT analysis in (A) Wt, **(B)** *Sirt6*$^{-/-}$ and **(C)** overlapped genes.

KEGG pathway analysis didn't show significant gene changes in the case Suv39h1 upon depletion of SIRT6. GO biological process analysis showed that in both *Wt* and *Sirt6*$^{-/-}$ cells, Suv39h1 was significantly enriched for cell-cell adhesion mediated by cadherin (GO:0044331). In the case of overlapped genes, Suv391 were mostly enriched in vascular smooth muscle contraction (GO:0014829) (Figure 37C).

The gene ontology analysis (GO) showed that Suv39h1 were in presence or absence of SIRT6 mostly enriched in biological functions related to cell-cell adhesion mediated by cadherin. Cadherins are transmembrane proteins that are well characterized adhesion molecule that plays a key role in epithelial cell adhesion. Cadherins, especially E-cadherin, are frequently inactivated or functionally inhibited in epithelial cancers, and they have been described as a tumor suppressor in pathogenesis of many human epithelial cancers (Reddy et al.,2005). It may indicate that Suv39h1 performs at least

part of its tumor suppressor activities through regulation of cell-cell adhesion mediated by cadherin where SIRT6 is not required.

A

Wt ShScramble

Index	Name	Combined score
1	cell-cell adhesion mediated by cadherin (GO:0044331)	379.57
2	positive regulation of extrinsic apoptotic signaling pathway via death domain receptors (GO:1902043)	216.49
3	mesenchymal to epithelial transition involved in metanephros morphogenesis (GO:0003337)	216.49
4	homophilic cell adhesion via plasma membrane adhesion molecules (GO:0007156)	137.67
5	cell morphogenesis (GO:0000902)	111.12
6	regulation of organ morphogenesis (GO:2000027)	105.98
7	calcium-dependent cell-cell adhesion via plasma membrane cell adhesion molecules (GO:0016339)	86.03
8	adherens junction organization (GO:0034332)	76.21
9	regulation of protein glycosylation (GO:0060049)	65.72
10	fatty acid transport (GO:0015908)	51.07

B

***Sirt6*$^{-/-}$ ShScramble**

Index	Name	Combined score
1	cell-cell adhesion mediated by cadherin (GO:0044331)	226.58
2	embryonic digit morphogenesis (GO:0042733)	147.44
3	regulation of epithelial to mesenchymal transition involved in endocardial cushion formation (GO:1905005)	123.50
4	vocal learning (GO:0042297)	123.50
5	regulation of mitotic spindle checkpoint (GO:1903504)	123.50
6	ventricular compact myocardium morphogenesis (GO:0003223)	123.50
7	negative regulation of interleukin-6 secretion (GO:1900165)	123.50
8	negative regulation of meiotic cell cycle (GO:0051447)	123.50
9	positive regulation of podosome assembly (GO:0071803)	123.50
10	mesenchymal to epithelial transition involved in metanephros morphogenesis (GO:0003337)	123.50

C

Overlapped genes

Index	Name	Combined score
1	vascular smooth muscle contraction (GO:0014829)	482.58
2	protein maturation by iron-sulfur cluster transfer (GO:0097428)	482.58
3	sterol catabolic process (GO:0016127)	341.79
4	negative regulation of circadian rhythm (GO:0042754)	341.79
5	cholesterol catabolic process (GO:0006707)	341.79
6	peptidyl-lysine dimethylation (GO:0018027)	296.32
7	alcohol catabolic process (GO:0046164)	260.59
8	chromatin silencing at rDNA (GO:0000183)	260.59
9	negative regulation of blood vessel diameter (GO:0097756)	260.59
10	vasoconstriction (GO:0042310)	231.84

Figure 37. GO biological process for Suv39h1-associated genes mapped by GREAT analysis in (A) *Wt* , **(B)** *Sirt6*$^{-/-}$ **(C)** and overlapped genes .

In the case of G9a, its binding sites in the case of *Wt*, show that 88.1% of G9a binding sites were located in intronic and intergenic regions, 1.6% in exons and 7.1% in the promoter. Whereas, the SIRT6 depletion caused displacing G9a from introns to intergenic regions and we also observed lower enrichment of G9a on promoters (7.1%

vs 6.4%). Total number of genes with G9a occupancy specifically or commonly altered upon depletion of SIRT6 was 6058 (Figure 38).

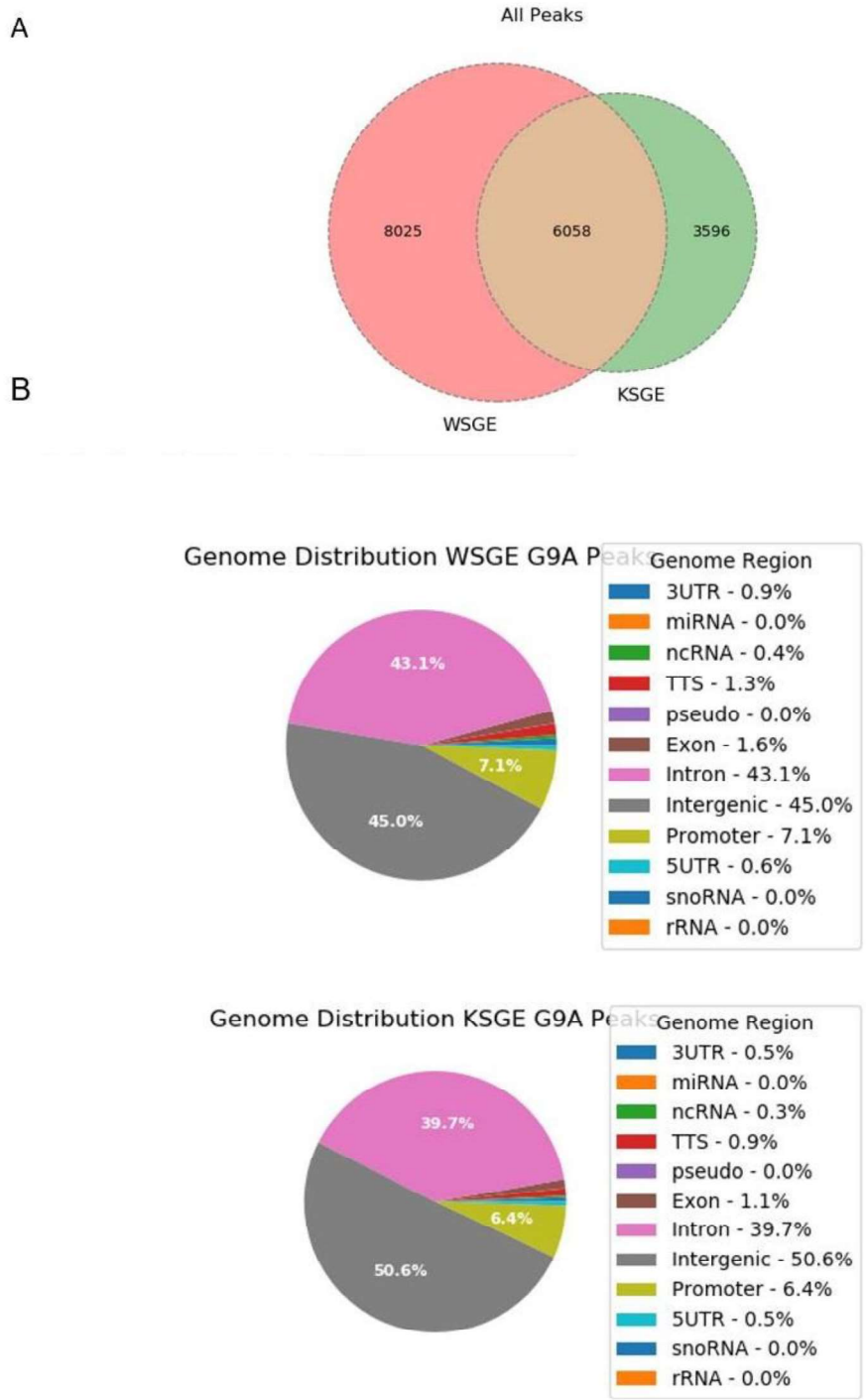

Figure38. Overview of G9a binding sites. **(A)** Venn charts show the distribution of G9a in the genome in *Wt* ShScramble and *Sirt6*$^{-/-}$ ShScramble. **(B)** Genomic distribution of ChIP-seq peaks for G9a in each

indicated cell lines, *Wt* ShScramble (left) and *Sirt6*$^{-/-}$ ShScramble (left). The genomic locations of peaks detected by ChIP-Seq subdivided into twelve sub-genomic regions. Each sub-genomic locus was indicated by using a different color. Each data set is representative of three independent experiments.

KEGG analysis showed that G9a in *Wt* ShScramble cells were significantly enriched in focal adhesion, proteoglycans in cancer, ECM-receptor interaction and pathways in cancer (Figure 39A). In the case of *Sirt6*$^{-/-}$ Scramble cell line, KEGG analysis showed G9a enrichment mostly in Rap1 signaling pathway, adherens junction, PI3K-Akt signaling pathway and ECM-receptor interaction (Figure 39B). In the case of overlapped genes G9a were mostly enriched in focal adhesion, adherens junction, Rap1 signaling pathway and ECM-receptor interaction (Figure 39C).

A

Wt ShScramble

Index	Name	Combined score
1	Focal adhesion	104.40
2	Proteoglycans in cancer	49.61
3	ECM-receptor interaction	73.88
4	Hippo signaling pathway	38.08
5	Pathways in cancer	22.23
6	Arrhythmogenic right ventricular cardiomyopathy (ARVC)	43.36
7	PI3K-Akt signaling pathway	21.89
8	Hypertrophic cardiomyopathy (HCM)	34.08
9	Small cell lung cancer	32.52
10	Regulation of actin cytoskeleton	21.71

B

***Sirt6*$^{-/-}$ ShScramble**

Index	Name	Combined score
1	Rap1 signaling pathway	38.77
2	Adherens junction	32.04
3	PI3K-Akt signaling pathway	21.46
4	Estrogen signaling pathway	20.46
5	ECM-receptor interaction	20.09
6	Sulfur metabolism	20.01
7	Focal adhesion	18.48
8	Arginine biosynthesis	18.37
9	Axon guidance	17.76
10	TNF signaling pathway	17.59

C

Overlapped genes

Index	Name	Combined score
1	Focal adhesion	45.57
2	Adherens junction	26.23
3	Rap1 signaling pathway	25.19
4	ECM-receptor interaction	24.50
5	Proteoglycans in cancer	24.39
6	PI3K-Akt signaling pathway	20.68
7	MAPK signaling pathway	17.47
8	Aldosterone synthesis and secretion	16.75
9	Arrhythmogenic right ventricular cardiomyopathy (ARVC)	15.38
10	AGE-RAGE signaling pathway in diabetic complications	12.86

Figure 39. KEGG pathway analysis of the target genes bound by G9a in tumor derived xenograft cells. **(A)** Pathway analysis for G9a binding genes in *Wt* ShScramble cell line. **(B)** Pathway analysis for G9a binding genes in *Sirt6*$^{-/-}$ Scramble cell line. **(C)** Pathway analysis for overlapping G9a binding genes for both *Wt* ShScramble and *Sirt6*$^{-/-}$ ShScramble cell lines.

According to KEGG analysis, in the case of G9a in *Wt* ShScramble, focal adhesion and ECM-receptor interaction are the most enriched pathways. Focal adhesion is a cell-substrate junction that anchors the cell to the extracellular matrix and structural proteins. It is hypothesized that immature focal adhesion sites are physically fragile in the case of *in vivo* cancer environments and may interfere with cancer cell invasion (Advani et al., 2018). ECM-receptor interaction pathways play an important role in the process of tumor adhesion, degradation, movement and hyperplasia (Andersen et al., 2018). Upon SIRT6 depletion, G9a is displaced to other pathways, including Rap1 signaling pathway and adherens junction. Ras-associated protein-1 (Rap1) involved in the regulation of wide number of key events in tumorigenesis including cell migration, invasion, and metastasis (Gloerich et al., 2016). Adherens junctions (AJs) are major intercellular adhesive structures in the cells and development of metastatic carcinoma is normally associated with deregulation of adherens junctions, composed of E-cadherin/β- and α-catenin complexes (Hage et al., 2009).

The genes recognized by G9A were classified into different functional categories by GO analysis. The genes recognized by G9a in *Wt* ShScramble were involved in diverse physiological processes, such as regulation of platelet-derived growth factor receptor-beta signaling pathway (GO:2000586) and regulation of transcription from RNA polymerase II promoter involved in myocardial precursor cell differentiation (GO:0003256) (Figure 40A).The genes bound by G9a in absence of SIRT6 participated in activation of protein kinase activity (GO:0032147) and regulation of cell migration (GO:0030334) (Figure 40B).The overlapped genes targeted by G9a in both cases mainly focused on promoting tumorigenesis, such as negative regulation of cell differentiation (GO:0045596) and extracellular matrix organization (GO:0030198).

A

Wt ShScramble

Index	Name	Combined score
1	regulation of platelet-derived growth factor receptor-beta signaling pathway (GO:2000586)	220.57
2	regulation of transcription from RNA polymerase II promoter involved in myocardial precursor cell differentiation (GO:0003256)	119.57
3	negative regulation of platelet-derived growth factor receptor-beta signaling pathway (GO:2000587)	119.57
4	vascular endothelial growth factor signaling pathway (GO:0038084)	119.57
5	positive regulation of cell migration by vascular endothelial growth factor signaling pathway (GO:0038089)	119.57
6	positive regulation of cardiac muscle cell differentiation (GO:2000727)	93.90
7	response to chemokine (GO:1990868)	80.95
8	negative regulation of meiotic cell cycle (GO:0051447)	80.95
9	regulation of chemokine-mediated signaling pathway (GO:0070099)	80.95
10	cellular response to chemokine (GO:1990869)	80.95

B

Sirt6$^{-/-}$ ShScramble

Index	Name	Combined score
1	activation of protein kinase activity (GO:0032147)	23.45
2	regulation of cell migration (GO:0030334)	20.59
3	positive regulation of endothelial cell migration (GO:0010595)	35.06
4	axon guidance (GO:0007411)	23.31
5	regulation of endothelial cell migration (GO:0010594)	30.64
6	axonogenesis (GO:0007409)	15.79
7	transforming growth factor beta receptor signaling pathway (GO:0007179)	22.39
8	regulation of small GTPase mediated signal transduction (GO:0051056)	17.38
9	positive regulation of epithelial cell migration (GO:0010634)	20.17
10	cellular response to transforming growth factor beta stimulus (GO:0071560)	17.85

C

Overlapped genes

Index	Name	Combined score
1	negative regulation of cell differentiation (GO:0045596)	28.38
2	extracellular matrix organization (GO:0030198)	24.54
3	enzyme linked receptor protein signaling pathway (GO:0007167)	30.86
4	sprouting angiogenesis (GO:0002040)	43.62
5	integrin-mediated signaling pathway (GO:0007229)	34.97
6	positive regulation of endothelial cell migration (GO:0010595)	29.19
7	positive regulation of angiogenesis (GO:0045766)	24.43
8	positive regulation of epithelial cell migration (GO:0010634)	27.84
9	axon guidance (GO:0007411)	20.50
10	regulation of cell migration (GO:0030334)	13.67

Figure 40. GO analysis of the target genes bound by G9a in tumor derived xenograft cells. (A) GO categories for G9a binding genes in *Wt* ShScramble cell line. **(B)** GO categories for G9a binding genes in *Sirt6*$^{-/-}$ Scramble cell line. **(C)** GO categories and pathway analysis for overlapping G9a binding genes for both *Wt* ShScramble and *Sirt6*$^{-/-}$ ShScramble cell lines.

Gene ontology analysis showed that the G9a bounded genes in *Wt* ShScramble have a significant enrichment effect on positive regulation of platelet-derived growth factor receptor beta which is a protein that in humans is encoded by the PDGFRB essential for vascular development (Andrae et al., 2008). G9a is enriched as well in genes related to regulation of transcription from RNA polymerase II promoter, which imply changes in the recruitment of Pol II to promoters and increased transcription initiation. We observed that following SIRT6 depletion, G9a enriched in genes associated with regulation of cell migration and metabolic processes. GO analysis showed that the activation of protein kinase activity and regulation of cell migration are two most enriched by G9a upon depletion of SIRT6. A wide number of phosphorylation correlates

with carcinogenesis. Overlapped genes were mostly enriched within clusters of negative regulation of cell differentiation which indicates preventing, or reducing the cell differentiation and it is known that poor differentiation is an important hallmark of cancer cells. Thus, these evidence suggested that SIRT6 depletion doesn't affect on tumorigenic functions of G9a.

1.9. Establishment of double KO colony of Suv39h1 KO SIRT6 inducible KO skin specific mouse model

Based on the functional relationship between SIRT6 and Suv39h1 in tumorigenesis, in the late part of the PhD work, we started a long-term project to try to confirm the interplay between both factors *in vivo* using knock-out mouse models of Suv39h1 and SIRT6. To do that, we generated a conditional SIRT6 KO mice in a Suv39h1 KO background. SIRT6 KO will be induced in skin by crossing the animals with a Skin-expressed Cre recombinase. With these animals we wanted to perform a DMBA/TPA skin induced tumorigenesis assay and study the development of papillomas and tumors in the animals under loss of Suv39h1 vs *W*t. On the other hand, we had plans to isolate primary keratinocytes from these animals and study the growth potential, and rate of transformation either spontaneous or under induced conditions (by treatment of H-Ras(G12V)/shp53). Unfortunately, we had an important delay with the establishment of the mouse Suv39h1 KO and SIRT6 inducible KO in our animal facility. The case of the Suv39h1KO animals was even more problematic, not only because these animals had a serious problem of fertility and embryonic viability, but also because they mice were C129, which forced us to backcross these animals with *Wt* C57/BL6 to get >99%. C57/BL6 genetic background purity and avoid influence of genetic background before crossing them with the SIRT6/Cre KO animals with C57/BL6 background (Figure 41 A, C). In the case of SIRT6, meanwhile we had to cross these animals with the CRE skin-specific strain CreK14-ERtam, which took even longer (Figure 41 B, D). finally, we had finally been able to establish definitively conditional SIRT6 KO mice in a Suv39h1 KO background and now we are amplifying the colonies to get enough animals of each genotype to perform all the *in vivo* experiments planned (Figure 41E).

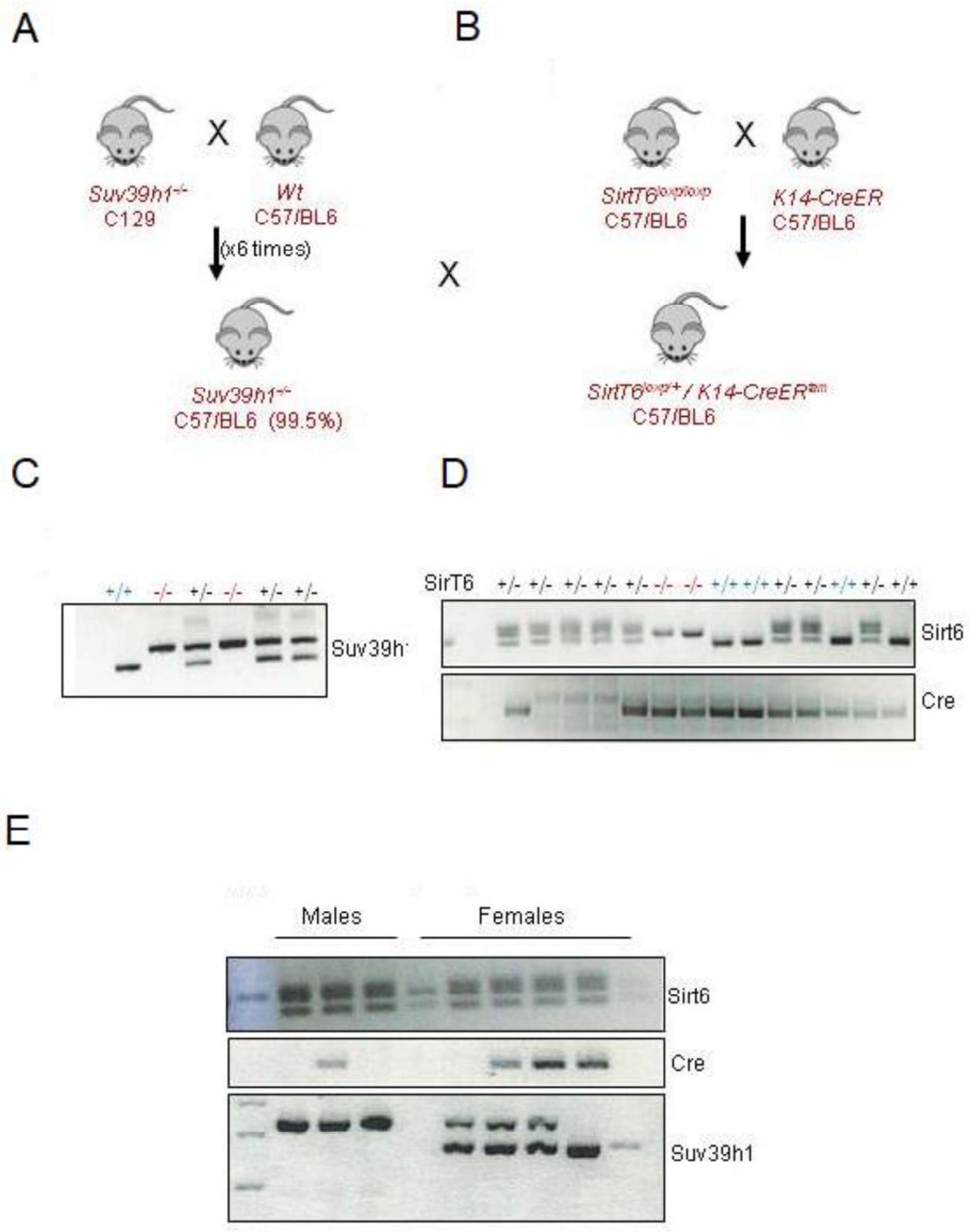

Figure 41. (A)-(B) Schematic representation of the crosses to generate **(A)** *Suv39h1*$^{-/-}$ mice in C57/BL6 strain, and **(B)** SIRT6-K14-Cre inducible KOs. **(C)-(E)** PCR of the representative genotypes generated in the indicated crosses: **(C)** *Suv39h1*$^{-/-}$, **(D)** SIRT6-K14-Cre inducible KOs and **(E)** *Suv39h1*$^{-/-}$ / SIRT6-K14-Cre inducible KOs.

CHAPTER II: SIRT1 REGULATES DNA DAMAGE SIGNALING THROUGH THE PP4 PHOSPHATASE COMPLEX

PREVIOUS WORK

2.1. Identification of DNA repair-associated phosphatase PP4 complex as a novel SIRT1 interactor

Previous studies set up an endogenous SIRT1 purification pipeline from HeLa S3 nuclear extracts through a sequence of chromatographic purification steps, as previously described in Vaquero et. al, 2007. It was found that the SIRT1 is mainly present in homotrimers, with an approximate molecular weight of 434 kDa. In our lab, additional refinement of the purification methodology was performed. Subsequently, they re-adjusted the initial affinity purification steps and focus the attention in less abundant form of SIRT1 in order to identify other SIRT1-containing complexes (Figure 42A). The analysis after several steps of chromatography resulted in the identification of a stable heteromultimeric complex containing SIRT1. The proteins present in the complex were identified by mass spectrometry and corresponded to PP4C, PP4R2, PP4R3α and PP4R3β, subunits of the PP4 complex (Figure 42B).

Interestingly, among the different PP4 complexes described so far, the PP4C-PP4R2-PP4R3α-PP4R3β complex has been specifically associated with DNA repair (Chowdhury et al.,2008). These findings suggested that SIRT1 may be a novel component of this mentioned PP4 complex, through which could collaborate with PP4 complex in the regulation of DNA repair.

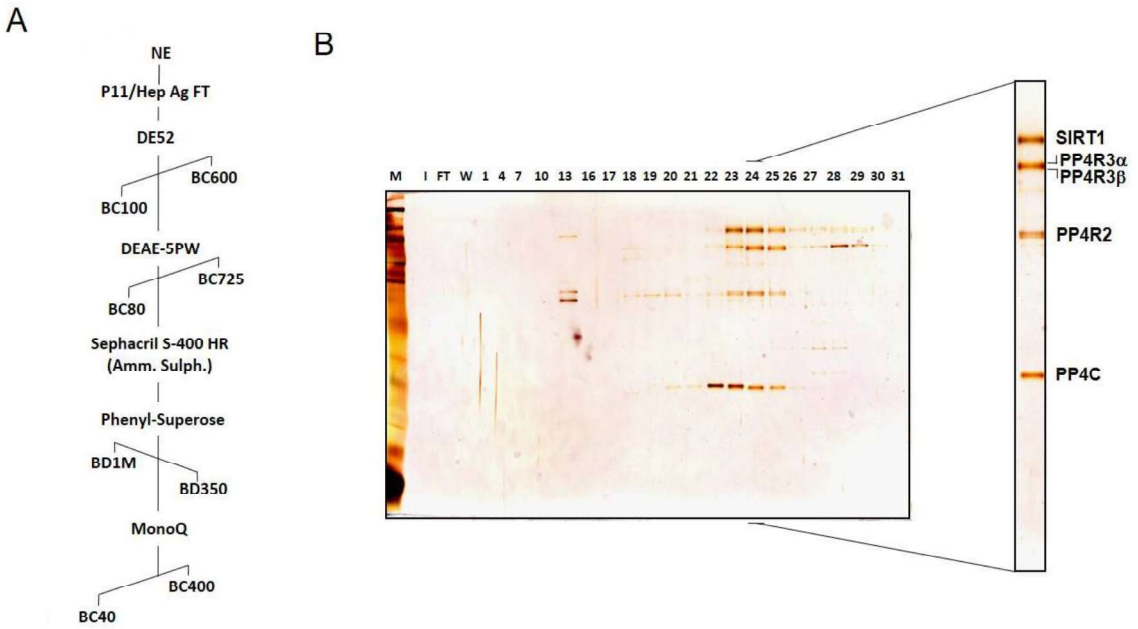

Figure 42: Identification of PP4 as a SIRT1 interaction partner. (A) SIRT1 from HeLa nuclear fractions was purified by several chromatographic steps indicated in the purification scheme. **(B)** The last step of the purification (MonoQ) was resolved on a silver-stained gel.

2.2. SIRT1 interacts with PP4 complex under stress conditions

The interaction between SIRT1 and the PP4 complex was further confirmed. Unexpectedly, FLAG-SIRT1 was able to immunoprecipitate the catalytic subunit of PP4 complex (PP4C) specifically under oxidative stress (Figure 43A), proposing a direct link between this novel complex and stress response. Unexpectedly, other regulatory subunits, PP4R2, PP4R3α and PP4R3β, strongly interacted with SIRT1 even in the absence of stress, indicating that they may play a role in PP4 interaction with SIRT1 (Figure 43B). The enzymatic activity of SIRT1 did not affect this interaction as SIRT1 WT and the catalytically dead point-mutant H363Y (SIRT1m), and both of them were able to immunoprecipitate PP4C (Figure 43C, lanes 4-6). The interaction seemed to be specific for SIRT1, as no PP4C did not seem to interact with other members of Sirtuin family, such as SIRT6, under the same conditions (Figure 43C, lanes 7-9).

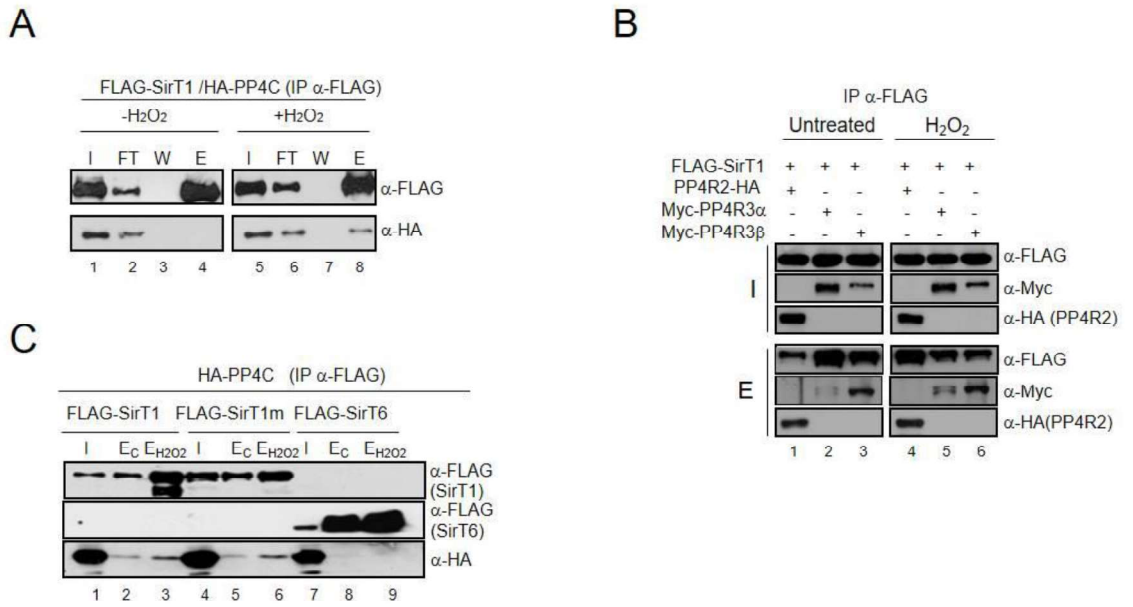

Figure 43: SIRT1 interacts with PP4C in response to oxidative stress. (A) Immunoprecipitation from HeLa cells co-expressing FLAG-SIRT1 and PP4C-HA. **(B)** Immunoprecipitation from HeLa cells where FLAG-SIRT1 and PP4R2, PP4R3α and PP4R3β. **(C)** Co-immunoprecipitation experiment of SIRT1, SIRT1mut and SIRT6. In all cases, HeLa cells were treated with 2mM H_2O_2 for 1h or left untreated. Whole-cell lysates were immunoprecipitated with anti-FLAG antibody, and precipitated proteins were detected with the indicated antibodies.

2.3. PP4 decreases SIRT1 deacetylase activity

In the context of the functional antagonism between SIRT1 and PP4, it is also considered the possibility that PP4 regulates SIRT1 deacetylase activity. For that purpose, they set up an in vitro deacetylate assay as described before (Vaquero et al., 2004) where they used one of the best SIRT1 described substrates, the histone mark H4K16ac as a substrate. They treated the HeLa cells with 5mM nicotinamide for 24h and Trichostatin A (TSA) 5µM for 3 hours. Then, they purified the hyperacetylated histones enriched in H4K16ac by acid extraction methodology (See Materials & Methods). SIRT1 enzymatic activity was measured as a decrease of levels of H4K16 acetylation by western blot analysis. In accordance with previous data SIRT1 deacetylates H4K16ac in the presence of NAD^+ (Vaquero et al., 2004).

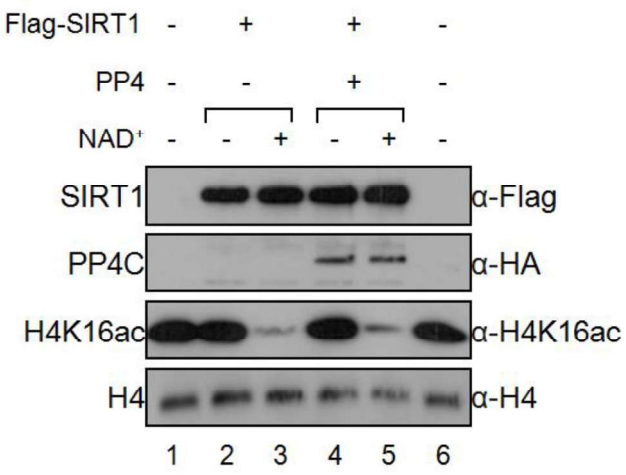

Figure 44. PP4 inhibits SIRT1 deacetylase activity in vitro. SIRT1 was purified alone or with PP4 complex. In vitro Deacetylase reactions were performed, by adding either purified SIRT1 or SIRT1-PP4 complex in presence or absence of NAD^+ to decaetylation reaction buffer and hyperacetylated histones. It was followed by immunoblotting and probed with the corresponding antibodies.

We observed that formation of the PP4/SIRT1 complex has a mild inhibitory effect on SIRT1 enzymatic activity upon addition of NAD^+ (Figure 44). This evidence suggests that PP4 may also play an important role in SIRT1 functions out of the DDR context.

2.4. The SIRT1-PP4 complex interacts with RPA2

RPA2 is one of the best-known targets of PP4 which has been identified in DNA damage signaling pathways. In our lab previously was hypothesized that SIRT1-PP4 complex may contain RPA2, as Lee and colleagues showed that PP4 complex is an important regulator of RPA2 function in DNA repair (Lee et al., 2010). It was observed that RPA2 is present in the SIRT1-PP4 complex (Figure 45A). Subsequently, the specific interaction between SIRT1 and RPA2 was detected upon stress conditions in CoIP experiments (Figure 45B).

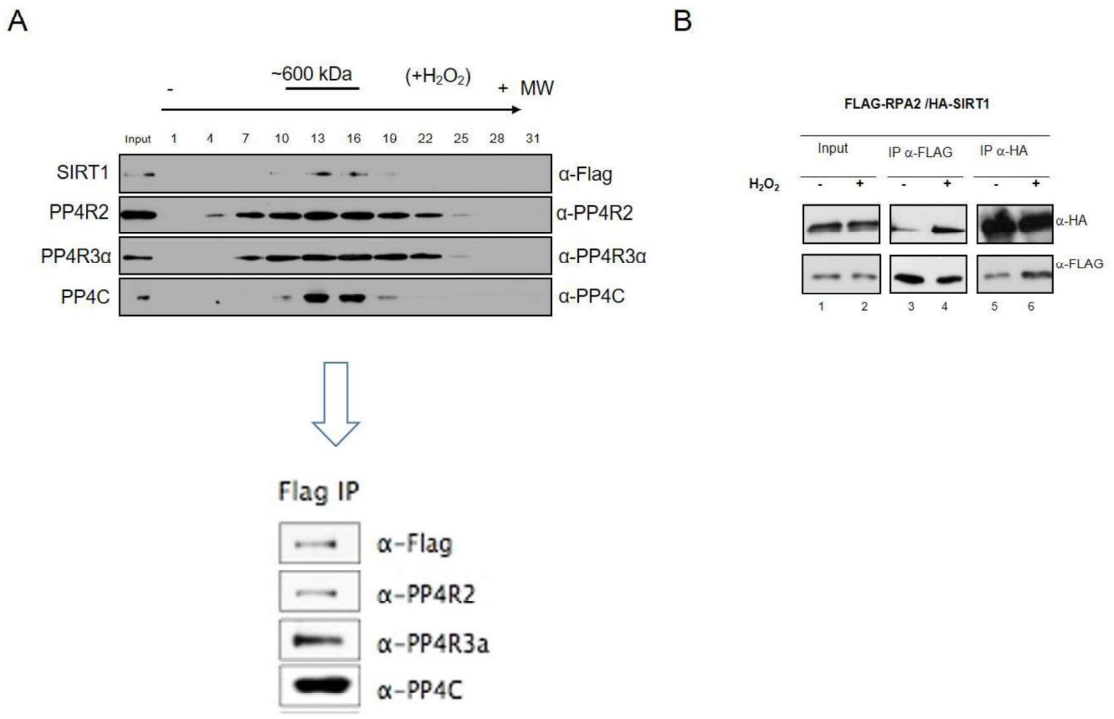

Figure 45. The SIRT1-PP4 complex contains RPA2. **(A)** Fractions 4-8 of the previously performed chromatography were pooled and immunoprecipitated using anti-FLAG antibody. The immunoprecipitated proteins were subjected to western blot using PP4C, PP4R2, PP4R3α and RPA2 antibodies. **(B)** HeLa cells expressing HA-SIRT1 and FLAG-RPA2 were treated with H_2O_2 and purified with either anti-HA or anti-FLAG antibodies. Precipitated proteins were detected with the indicated antibodies.

RESULTS

2.5. SIRT1 regulates de phosphorylation activity of PP4 complex

Based on these previous data, we aimed to study the functional significance of the interplay SIRT1-PP4 complex. Considering that both SIRT1 and PP4C are enzymes, our first question was whether PP4 activity is regulated by SIRT1. In order to achieve this objective, we overexpressed and purified whole PP4 complex (PP4C, PP4R2, and PP4R3 α and β) in HeLa cells and performed *in vitro* phosphatase assays in the presence or absence of SIRT1. We used γH2AX as a substrate, one of the best-known targets of the PP4 complex (Chowdhury et al.,2008). In the presence of NAD^+, SIRT1 completely inhibited the phosphatase activity of PP4 complex, indicating that PP4 activity was directly regulated by deacetylation of the complex (Figure 46A, lane 7). SIRT1 also

displayed a slight inhibitory effect in the absence of NAD^+, reflecting a catalytic-independent negative impact of SIRT1 binding to the PP4 complex (Figure 46A, lane 6).

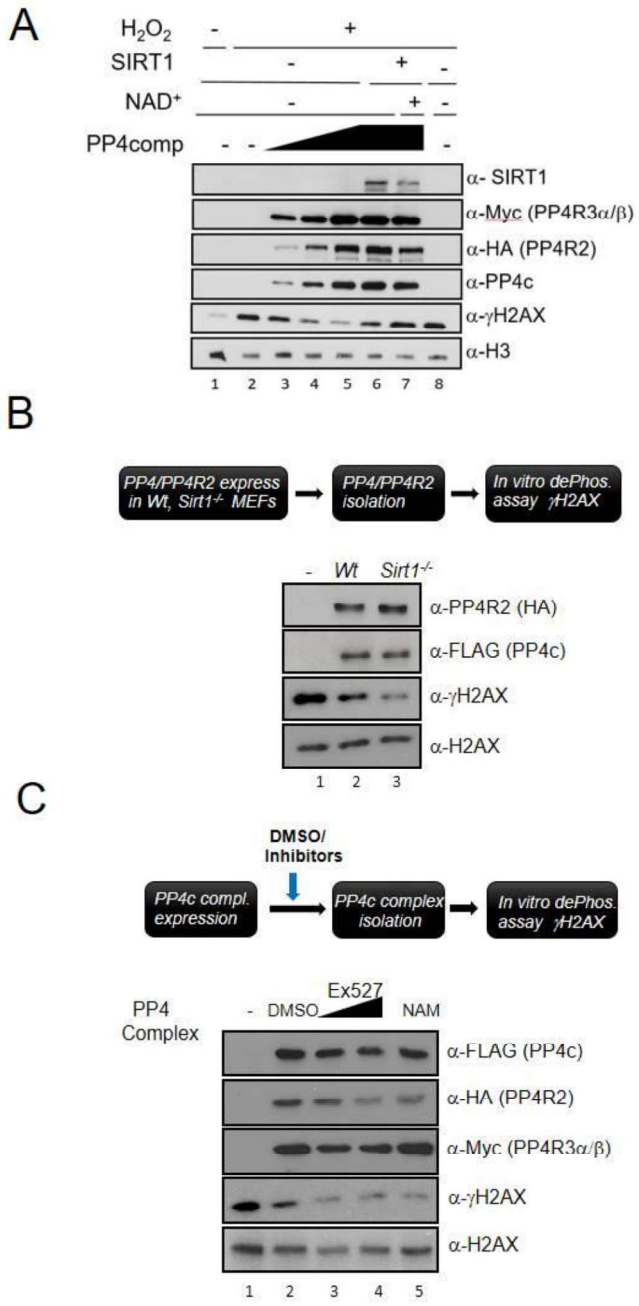

Figure 46. SIRT1 inhibits PP4 complex activity. **(A)** Different *in vitro* phosphatase assays were performed, where the SIRT1 was separately purified and then added to PP4 complex from Hela cells. **(B)** PP4 complexes purified from *Wt* and *Sirt1*$^{-/-}$ MEFs. **(C)** Purified PP4 complexes in the presence of selective inhibitor of SIRT1 (EX527, 1µM to 10 µM) and Sirtuins inhibitor Nicotinamide (NAM). The western blots are representative of three independent experiments.

Afterwards, we aimed to confirm our results in *Wt* vs *Sirt1*$^{-/-}$ MEFs cells. We transfected the core PP4 complex (PP4C and PP4R2), we purified the whole complex from either *Wt* and *Sirt1*$^{-/-}$ cells by affinity purification of PP4C, and we subsequently tested their activity in *in vitro* phosphatase assays using γH2AX-enriched histones as a substrate. We observed that the phosphatase activity of PP4 complex purified from *Sirt1*$^{-/-}$ cells was notably higher than the one purified from *Wt* cells (Figure 46B, lane3). These results confirmed the SIRT1 inhibitory effect over PP4 complex activity.

Next, we went further and tested whether the effect of SIRT1 is directly associated with its deacetylation activity. We analyzed the activity of the PP4 complex expressed in *Wt* and *Sirt1*$^{-/-}$ cells treated with DMSO, the SIRT1 selective inhibitor Ex-527 (1μM and 10 μM), or the general Sirtuin inhibitor NAM (1mM). We observed that inhibitory effect of EX527 or NAM strongly enhanced the phosphatase activity of PP4 in a similar magnitude which further supports the key role of SIRT1 activity in this regulation (Figure 46C).

2.6. SIRT1 regulates levels of γH2AX phosphorylation thorough modulation of PP4 complex activity

One of the most interesting previous observation on the role of SIRT1 in DNA damage signaling and repair was the significant decrease of γH2AX observed in *Sirt1*$^{-/-}$ mice (Wang et al., 2008). These observations could not be explained by the previously described mechanism regulated by SIRT1 in DSB repair. We next tested the possibility that this effect of SIRT1 on levels of γH2AX is mediated by PP4. For that purpose, we inhibited PP4 activity using Okadaic acid (OA), the most widely used inhibitor of phosphatases PP1 and PP2A, but it also inhibits strongly PP4, PP5 and likely PP6 (Swingle et al, 2007). We treated *Wt* and *Sirt1*$^{-/-}$ cells with either Okadaic acid (50 nM) or with DMSO (control) for 24 hours. We lysed the cells and obtained whole cell extract, subsequently they were subjected to SDS-PAGE. We observed, as expected, that inhibition of PP4 activity with OA resulted in increased levels of γH2AX in *Wt* cells. Interestingly, OA treatment in *Sirt1*$^{-/-}$ cells was able to partially restore the decreased levels of γH2AX due to SIRT1 loss (Figure 47). This data further supported a role for PP4

activity in SIRT1 dependent regulation of γH2AX in the context of DNA damage signaling and repair.

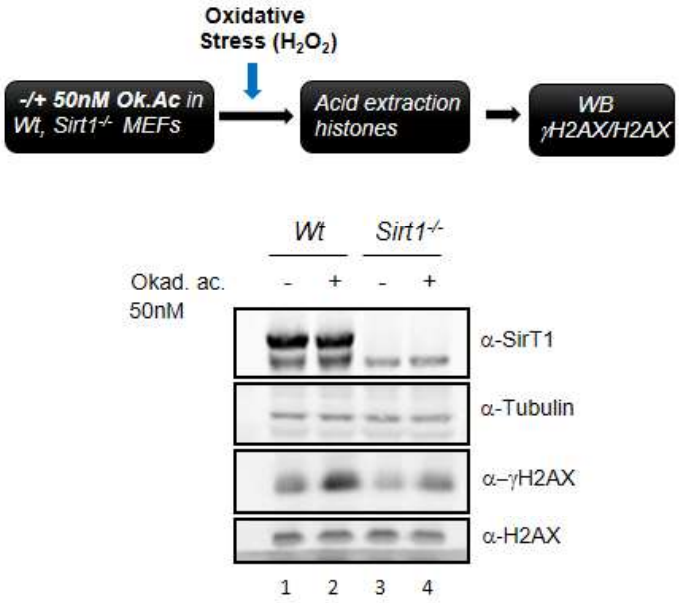

Figure 47. The effect of OA on PP4 complex activity. Top, schematic representation of the methodological steps in the assay. Bottom, *Wt* and *Sirt1*$^{-/-}$ cells were treated either with Okadaic acid (50 nM) or with DMSO (control) for 24 hours, then incubated with 2mM H_2O_2 for 1h. The cells were lysed and the whole cell extract were subjected to SDS-PAGE and the levels of γH2AX and H2AX were shown. The western blot is representative of three independent experiments.

2.7. Acetylation levels of PP4R3α and PP4R3β at K64 Regulate PP4 complex activity

We next aimed to examine the mechanism of PP4 inhibition through SIRT1-mediated deacetylation of the PP4 complex. In order to identify the nature of this modification and the residues involved, we purified the whole PP4 complex from *Wt* and *Sirt1*$^{-/-}$ cells. The elutions were resolved in an SDS-PAGE and after staining by colloidal coomassie, the bands were cut and analyzed by mass spectrometry. We detected acetylation of two lysine residues in the PP4R3α and PP4R3β in *Sirt1*$^{-/-}$ cells but not *Wt* cells (Figure 48A), one of them common to both PP4R3α and PP4R3β and the other one specific for each of the subunits. Thus, we detected acetylation in lysines 64 and 642 in PP4R3α, as well as in lysines 64 and 777 in PP4R3β. Interestingly, K64 is a conserved residue present in the WH1 N-terminal domain (also called EVH1), commonly present in the N-terminal

sequence of both PP4R3α and PP4R3β (Figure 48B). This evolutionary conserved protein domain plays an important role in protein–protein interactions. The EVH1/WH1 family of domains are involved in a wide number of eukaryotic signal transduction pathways including cytoskeleton organization, chromatin organization, cell motility, gene expression and cell cycle (Ball et al., 2002).

A

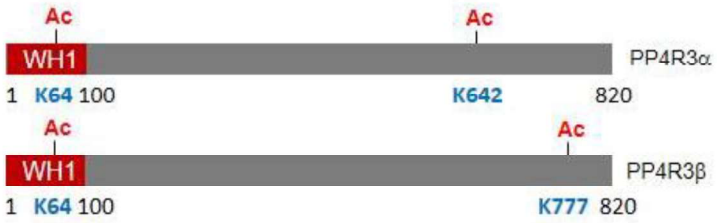

B

Protein	Sequence	Site	q-Value	PEP	MH+ [Da]	ΔM [ppm]
PP43A/P4R3B	INPNTAYQkQQDTLIVWSEAENYDLALSFQEK	K64	0,001	0,01479	3798,86533	4,07312741
P4R3A	ERQDNPkLDSMR	K642	0,008	0,149	1530,728685	-2,81630963
P4R3B	SVVSQTTPASSNVASSkTTSLATSVTATK	K777	0,001	0,02671	2853,458103	-3,768515118

Figure 48. Identification of SIRT1 targets in the PP4 complex. FLAG-PP4C and HA-PP4R2 subunits were overexpressed in *Wt* and *Sirt1*$^{-/-}$ MEFs and cells were treated with oxidative stress (2 mM H_2O_2, 1h). PP4 whole complex was purified using FLAG antibodies (endogenous PP4R3α and PP4R3β were immunoprecipitated by FLAG-PP4C). The elutions were loaded in an acrilamide gel that was stained with colloidal-coomassie-blue. The corresponding bands were cut and analyzed by mass spectrometry. **(A)** Schematic of the PP4R3α and PP4R3β protein domains. **(B)** List of peptides identified through mass spectrometry in Sirt1-/- but not Wt cells.

To study the effects of acetylation, we generated recombinant point mutants of PP4R3α and PP4R3β in these four residues in which lysine residues (K) were substituted by arginine (R) residues to mimic non-acetylated form of lysine (KR mutant), or glutamine (Q) to mimic acetylated form of lysine (KQ mutant). To examine if the

deacetylation of any of these residues could explain the inhibition of PP4 complex activity mediated by SIRT1, we overexpressed and purified the PP4 complex containing different combinations of these PP4R3α and PP4R3β Wt or mutants. We then examined the activity of the complex *in vitro* phosphatase assays in presence of γH2AX as substrate (Figure 49A). The analysis of the activity of complexes with single mutations in PP4R3α or PP4R3β did not render any specific effect (data not shown). Strikingly, we detected a significant inhibition of the phosphatase activity only when both PP4R3α and PP4R3β were mutated to K64R mutants (Figure 49B lanes 3,4). This suggested that both PP4R3α and PP4R3β may have a redundant role in the SIRT1 effect on PP4 complex activity and therefore that SIRT1 has to target both proteins to achieve the whole inhibitory effect. This effect was further confirmed by the increased activity detected in the PP4 complex containing both the PP4R3α and PP4R3β K64Q mutants (Figure 49A, lane 5). Taken all into account, we propose a functional antagonism between SIRT1 and the PP4 complex upon stress conditions, as SIRT1 is able to inhibit PP4 complex activity toward γH2AX by deacetylation of regulatory subunits of PP4 complex, PP4R3α and PP4R3β.

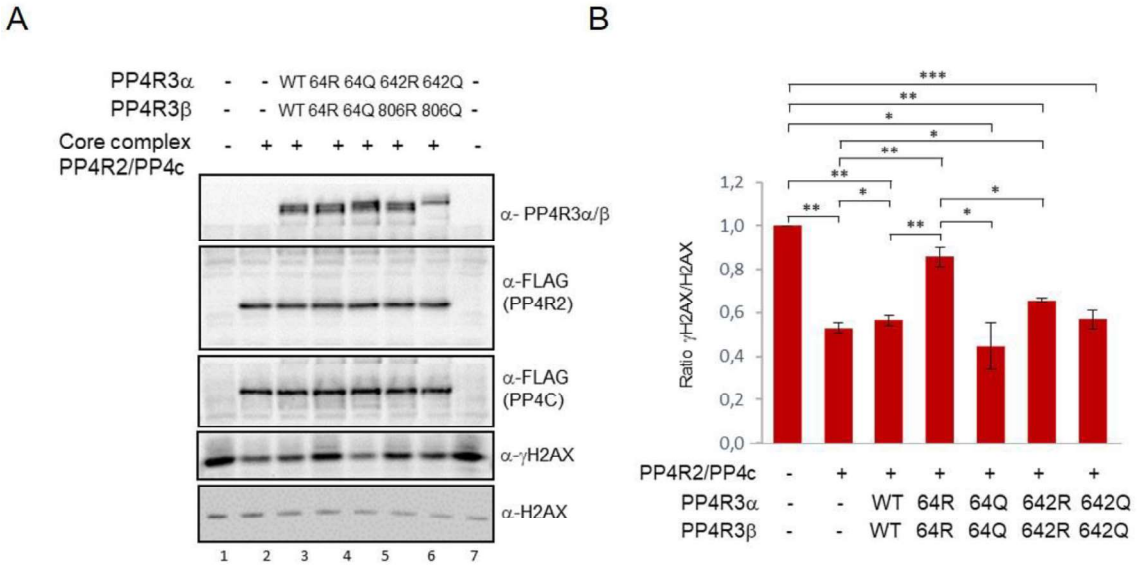

Figure 49. Acetylation of PP4R3α and PP4R3β at K64 affects PP4 complex activity. (A) Representative Western blot of three (n=3) independent experiments of *In vitro* phosphatase activity assay purifying PP4 complexes without PP4R3α and PP4R3β, or with Wt or different mutants of PP4R3α and PP4R3β. **(B)** Quantification of the protein levels of γH2AX and H2AX in the phosphatase assay. Data are expressed as mean ± SD (n = 3), Standard deviation is shown (*: p<0.05; **: p<0.005***: p<0.0005).

2.8. SIRT1 depletion alters RPA2 phosphorylation patterns

In order to characterize in more detail our observations about the antagonism between SIRT1 and PP4, we next analyzed the functional relationship between SIRT1 and RPA2. Thus, we treated *Wt* and *Sirt1*$^{-/-}$ MEF with hydrogen peroxide, to induce oxidative stress and IR to induce double strand breaks. We observed that in both cases, depletion of SIRT1 decreases foci formation of RPA2 upon damage which indicates that *Sirt1*$^{-/-}$ MEFs have impaired RPA2-foci formation under different stress conditions. This impairment tool place without affecting total RPA2 protein levels, which confirms the direct effect of SIRT1 activity on RPA2 functions (Figure 50).

2.9. Depletion of SIRT1 affects RPA2 phosphorylation

Based on our previous observations regarding the effect of SIRT1 in γH2AX regulation, we next aimed to examine whether SIRT1 also regulates phosphorylation levels of RPA2, a PP4-dependent key event in DNA repair dynamics and pathway choice (Lee et al., 2010). For that purpose, we induced DNA damage in *Wt* and *Sirt1*$^{-/-}$ MEFs by treatment of ionizing radiation (7.5 Gy) and we examined total levels of RPA2 and its corresponding phosphorylation. Supporting a direct effect of SIRT1, Western-blot of total RPA2 detected decreased levels of high molecular weight RPA2 in *Sirt1*$^{-/-}$ cells compared to *Wt* cells (Figure 51A). These higher MW forms of RPA2 have been shown to corrrespond to phosphorylated RPA2 (Nuss et al.,2005), which clearly demonstrate a similar effect as we observed with γH2AX. To confirm these results, we performed a similar experiment in *Wt* and *Sirt1*$^{-/-}$ MEFs (7.5 Gy IR) but this time we included a time course experiment to follow the dynamics of RPA2 phosphorylation through time and we performed the Western-blots using antibodies against specific mark phospho-RPA2 (S33). We collected the cells at 0, 24 and 48 hours after treatment. We observed that loss of SIRT1 correlate with a consistent decrease in the levels of phospho-RPA2 (S33) throughout the whole-time course from IR treatment to 48h post-irradiation. Strikingly, while *Wt* cells showed sustained levels this mark during the whole time course, this mark had completely disappeared in *Sirt1*$^{-/-}$ MEFs at 48h post-irradiation (Figure 51B). These observations confirmed that SIRT1 regulates RPA2 phosphorylation, which again links SIRT1 with PP4 function.

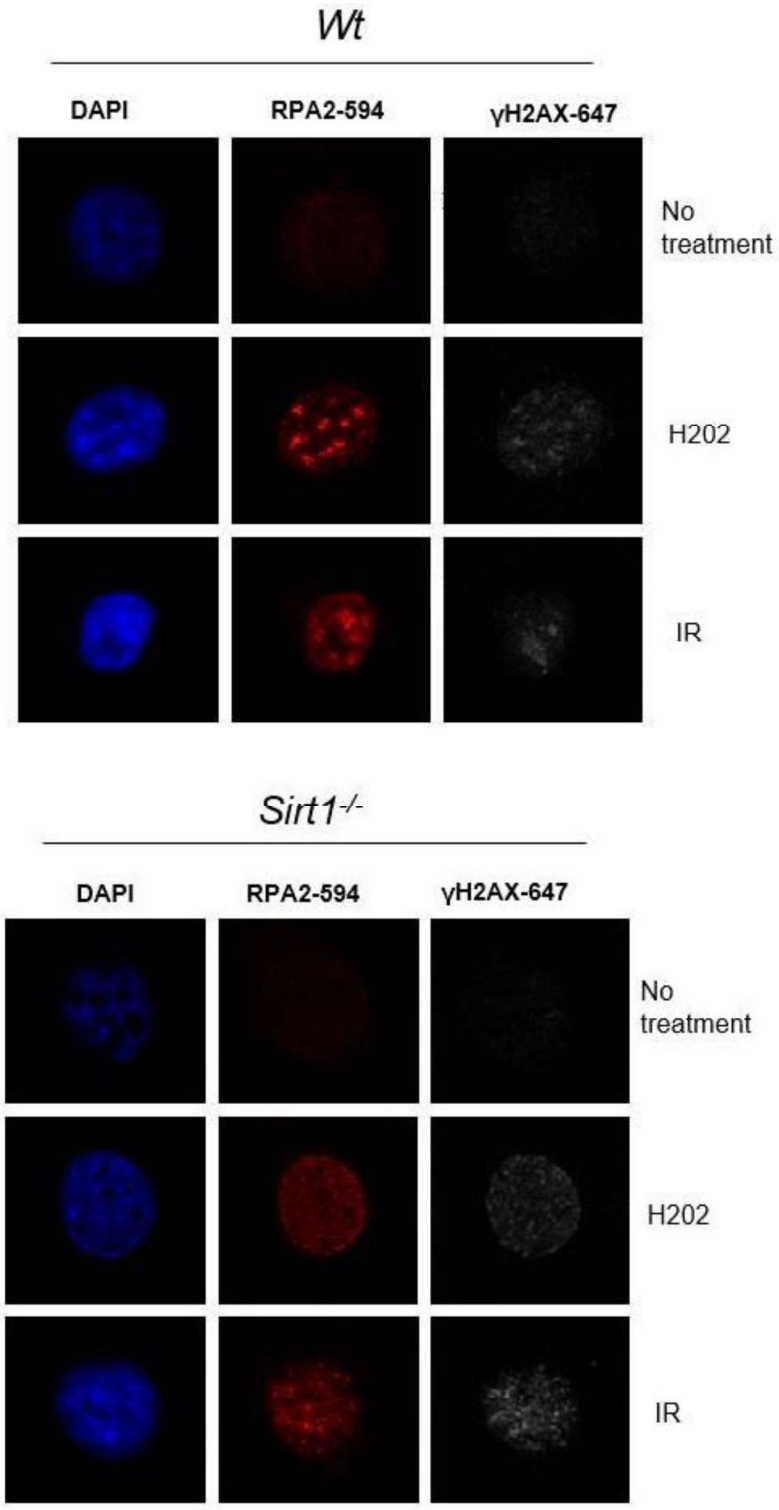

Figure 50. SIRT1 is required for RPA2 foci formation. Wild-type or *Sirt1*$^{-/-}$ MEF cells were treated with H_2O_2 for 1h, IR for 30 minutes, fixed and incubated with γH2Ax and RPA2 antibodies. RPA2 and γH2AX were stained with Alexa fluorescent dyes ® 594 and ® 647, respectively. Representative confocal images are representative of three independent experiments with similar results.

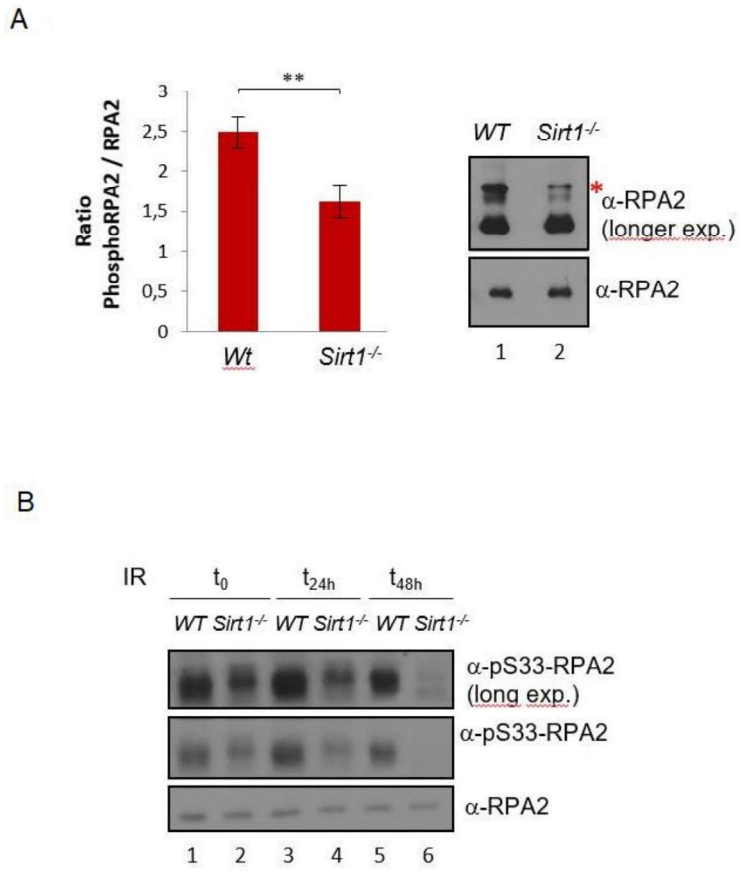

Figure 51. SIRT1 regulates RPA2 dephosphorylation. (A) *Wt* and *Sirt1*$^{-/-}$ MEFs were treated by IR (7.5 Gy) and the cells were lysed and subjected to westen blot analysis. The total levels of RPA2 and its corresponding phosphorylation were tested by RPA2 antibody. The Total RPA2 phosphorylation levels detected in compared *Wt* and *Sirt1*$^{-/-}$ were quantified. Data were obtained from three independent experiments, and values are represented as means ± Sd. **p < 0.05 vs *Wt*. **(B)** *Wt* and *Sirt1*$^{-/-}$ MEFs were treated by IR (7.5 Gy). the cells at 0, 24 and 48 hours after after treatment. The total levels of RPA2 and Phospho-RPA2 (S33) were tested by indicated antibodies. *Sirt1*$^{-/-}$ cells present decreased levels of phospho-RPA2 S33 after IR treatment compared to *Wt* cells. Representative Western blot of three (n=3) independent experiments.

2.10. SIRT1 regulates RPA2 phosphorylation through a PP4-dependent mechanism

In order to determine whether the effect of SIRT1 on phospho-RPA2 i) was direct, and ii) involved PP4 complex, we set up an experiment where we downregulated PP4C with ShRNA in *Wt* and *Sirt1*$^{-/-}$ and also set up a re-expression of SIRT1 in Sirt1$^{-/-}$ cells. For the experiment, we stressed or not these cell lines with IR (7.5 Gy).

While we observed a significant increase in phosphorylation levels of RPA2 (S33 or S4/8) upon IR upon PP4C downregulation in *Wt* MEFs, this effect was significantly reduced in

SIRT1-deficient MEFs. This observation was in agreement with a role of PP4 in SIRT1-dependent regulation of phospho-RPA2 (S33 and S4/8) (Figure 52). SIRT1 re-expression in *Sirt1*$^{-/-}$ cells partially restored the levels of phospho-RPA2, indicating that the decreased levels of these marks observed in *Sirt1*$^{-/-}$ MEFs were directly associated with SIRT1 protein (Figure 52, lane 12).

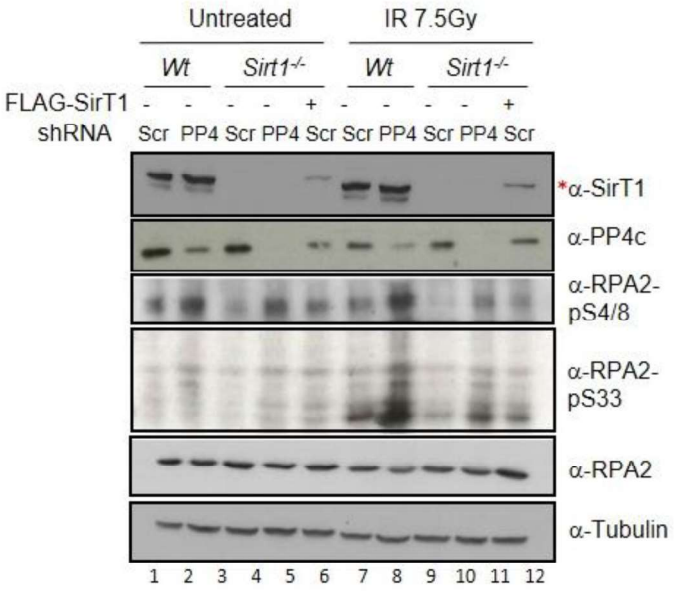

Figure 52. SIRT1 can partially rescue the levels of phospho-RPA2. *Wt* and *Sirt1*$^{-/-}$ cells were infected with ShScramble or ShPP4C, and SIRT1 was re-introduced in *Sirt1*$^{-/-}$ cells. The cells treated either with IR (7.5 Gy) or untreated (as control). Cell lines were collected after cold PBS wash by scraping in Lysis 2X SDS Buffer on ice. Lysates were sonicated at medium-high intensity for 10 seconds and subsequently boiled for 10 minutes at 90ºC. RPA2, phospho-RPA2(S33 and S4/8) were detected by indicated antibodies. Representative Western blot of three (n=3) independent experiments.

2.11. Depletion of SIRT1 affects RPA2 phosphorylation in other cell lines

To confirm our results generated in *Sirt1*$^{-/-}$ MEFs, we next examined RPA2 phosphorylation in Hela cells. We transfect the cells with siControl, siRNA SIRT1, or treated them with either SIRT1 inhibitor (EX527, 1µM), Nicotinamide (NAM, 5mM) or SIRT6 inhibitor (OSS128167, 200 µM) for 48 hours. Afterwards, the cells were stressed by Camptothecin (CPT, 1µM) for 1 hour, then released, and collected at 0h and 48h. We observed a reduction in RPA2 phosphorylation (S4/S8) after 48 hours of release in presence of either siSIRT1, SIRT1 inhibitor or NAM but not in the case of SIRT6 inhibitor.

This evidnce confirmed that SIRT1 specifically regulates phosphorylation levels of RPA2 upon DNA damage (Figure 53).

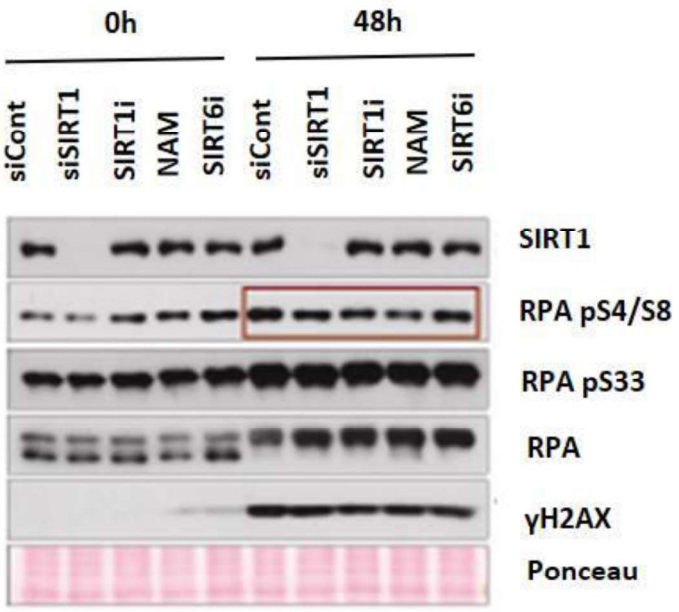

Figure 53. Depletion of SIRT1 affects RPA2 phosphorylation in Hela cells. The cells were grown in presence of either siControl, siRNA SIRT1, SIRT1 inhibitor (EX527,1µM), Nicotinamide (NAM, 5mM) or SIRT6 inhibitor (OSS128167,200 µM) for 48 hours. Subsequently, they were treated by CPT 1µM for 1h then released into fresh media during 0, and 48h. Representative Western blot of three (n = 3) independent experiments are shown.

2.12. Depletion of SIRT1 affects RPA2 phosphorylation through deacetylation of regulatory subunits of PP4 complex

Subsequently, we examined whether the regulation of RPA2 phosphorylation through SIRT1 involved deacetylation of regulatory subunits, PP4R3α and PP4R3β. We observed that the point mutation K64R in both PP4R3α and PP4R3β alters the ability of the PP4 complex to dephosphorylate phosphoRPA2. The results showed that, as in the case of γH2AX, inhibition of the phosphatase activity of PP4 complex toward phospho-RPA2, when both PP4R3α and PP4R3β were mutated to K64R mutants. Altogether, this data confirmed that SIRT1 plays a direct role in RPA2 dynamics by modulation of PP4 complex activity through deacetylation of PP4R3α and PP4R3β.

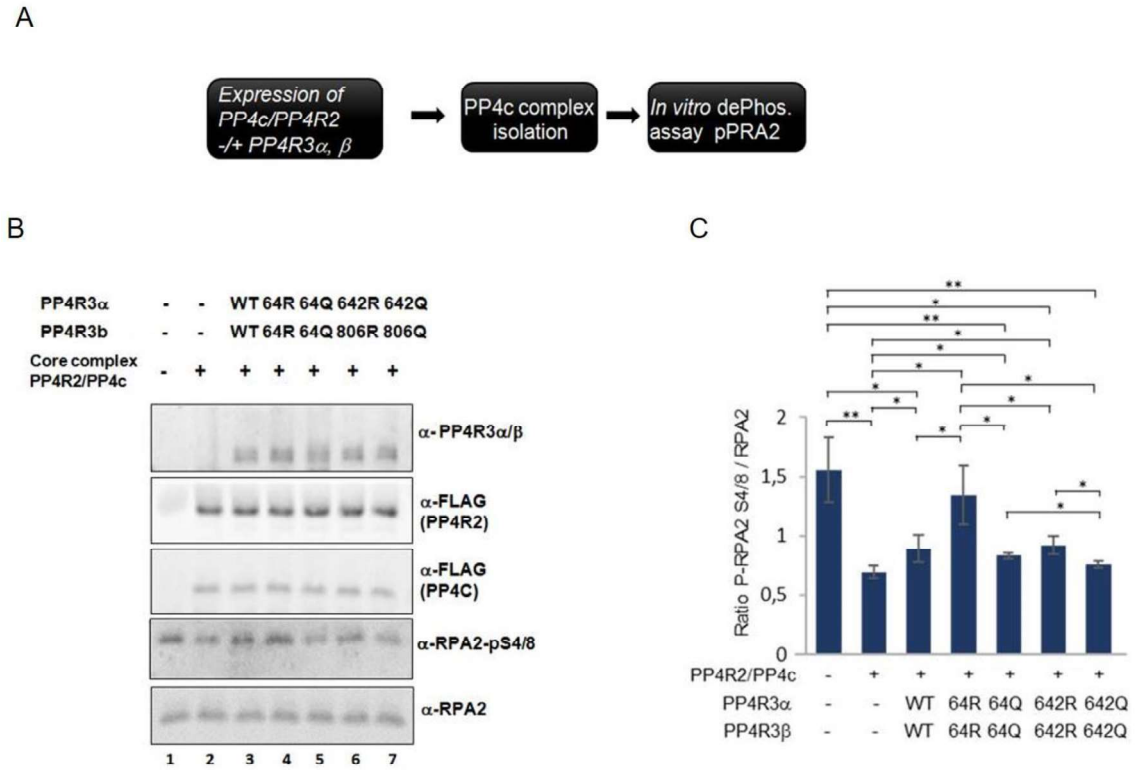

Figure 54. Acetylation levels of PP4R3α and PP4R3β at K64 impacts phospho-RPA2 levels. **(A)** Schematic of the *in vitro* phosphatase assay. Representative Western blot of three (n = 3) independent experiments is presented. **(B)** Phosphatase activity assay with purified PP4 complexes without regulatory subunits (PP4R3 α and β), or with WT or different combinations of mutants of PP4R3α and PP4R3β. **(C)** Quantifications of phospho-RPA2 and RPA2 levels in the phosphatase assay. Data are represented as mean ± SD (n = 3), Standard deviation is shown (*: p<0.05; **: p<0.005).

2.13. Depletion of SIRT1 affects γH2AX and RPA2 functions *in vivo*

In order to understand the functional antagonism between SIRT1 and PP4 in DSB repair, we next set up a time course experiment. We seeded *Wt* and *Sirt1*$^{-/-}$ MEFs in LabTek II chamber slides and we performed High throughput microscopy immunoflouoresence (See material and methods). We measured the levels of γH2AX and phospho-RPA2(S33) upon IR treatment in these cells.

A

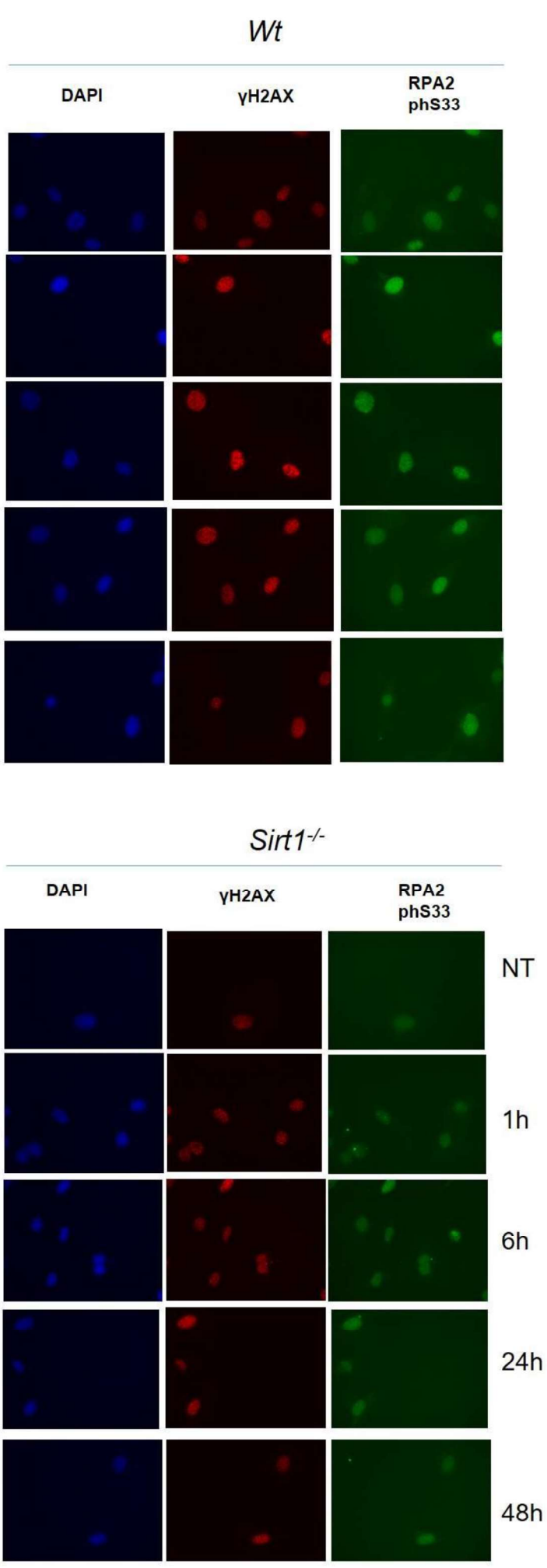
Wt
DAPI
γH2AX
RPA2 phS33
Sirt1-/-
DAPI
γH2AX
RPA2 phS33
NT
1h
6h
24h
48h

B

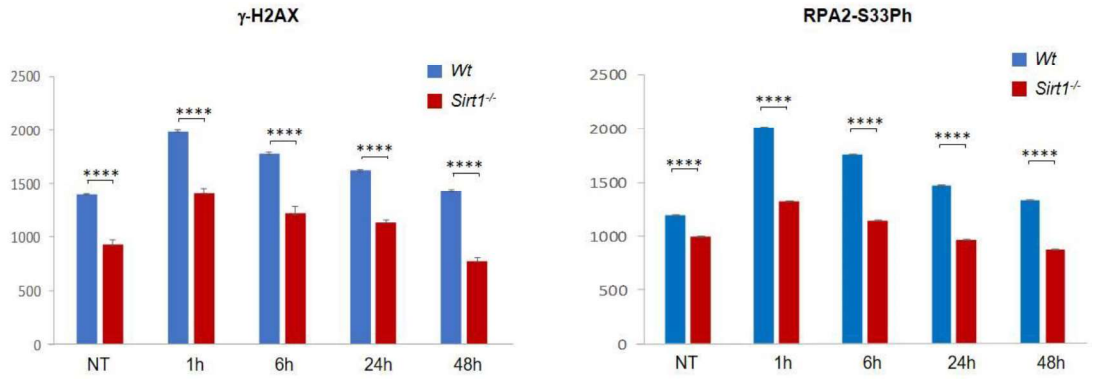

Figure 55. Immunofluorescence analysis by High throughput microscopy (HTM) of *Wt* and *Sirt1*$^{-/-}$ cells. **(A)** *Wt* and *Sirt1*$^{-/-}$ MEF cells were treated with/without IR for 1h and let for recovery for up to 48h, fixed and stained with γH2Ax and phospho-RPA2 (S33) antibodies. Representative confocal images are representative of three independent experiments. **(B)** Quantification of high throughput microscopy (HTM) analysis of phospho -RPA2 S33 and γH2AX in *Wt* and *Sirt1*$^{-/-}$ cells (with >5 γH2AX and RPA2 foci) during 48 hours. Data are representative of three independent experiments. The median is indicated and a two-tailed t-test was used for statistical analysis. At least 300 nuclei were analyzed and the mean with SEM is shown for independent cultures. Data are expressed as mean ± SD (n = 3), Standard deviation is shown (***: p<0.0005).

In agreement with the main function of SIRT1-PP4 axis, the major decrease in phospho-RPA2 (S33) levels was observed in *Sirt1*$^{-/-}$ MEFs compared with *Wt* observed 1 hour after the DNA damage (Figures 55A-B). Regarding γH2AX, the effect was more equivalently distributed, which may be due to the fact that *Sirt1*$^{-/-}$ MEFs have a remarkably lower levels of γH2AX from beginning (Figures 55A-B). These defects were accompanied by a predominant decrease in both γH2AX and RPA2 in *Sirt1*$^{-/-}$ MEFs foci evaluated by high throughput microscopy immunofluorescence. Overall, depletion of SIRT1 impairs γH2AX and RPA2 foci formation upon DNA damage.

2.14. SIRT1 loss is associated with levels of sister chromatin-exchange events that increase in a PP4-dependent manner

2.14.1. The Sister Chromatid Exchange (SCE) assay.

The most accepted means of detecting aberrant homologous recombination, whether in cells with low HR capacity, or in response to DNA damage, is the sister chromatid

exchange (SCE) assay which differentially stains sister chromatids using incorporated 5'-bromodeoxyuridine (BrdU), to allow microscopic detection of the physical exchange of DNA which occurs during homologous recombination crossover (Wilson et al., 2007). The chemical agents that produce inter-strand crosslinks, such as mitomycin C (MMC), which is DNA crosslinker that induces different types of damage and promotes repair through homologous recombination. They are SCE inducers, due to the fact that homologous recombination is required to repair the resultant blocked replication forks (Thompson et al., 2005). The protocol described in material and methods, used BrdU incorporation and fluorescence plus Giemsa (FPG) staining to make sister chromatin exchanges between sister chromatids visible under microscope (Figure57). BrdU is a nucleoside analog that is efficiently incorporated into replicating DNA (Wolff et al., 1996; Perry et al.,1974).

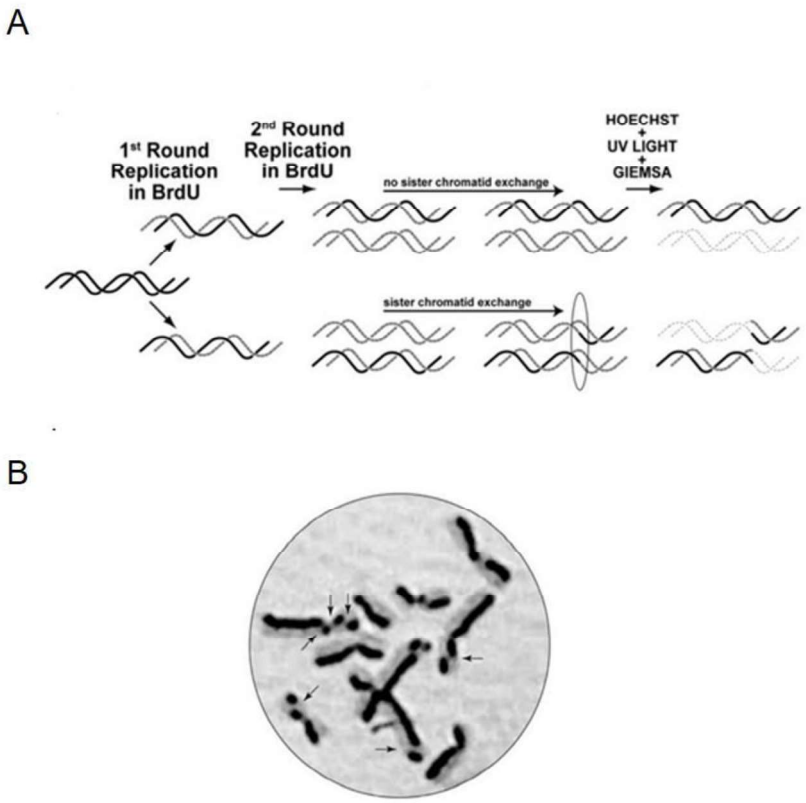

Figure57. Sister chromatid exchange (SCE) staining. **(A)** Schematic of two rounds of BrdU incorporation followed by Hoechst 33258 staining, exposure to UV light, and staining with Giemsa. Solid black lines: unsubstituted DNA single strand; dotted gray lines: BrdU-substituted DNA single strand; ellipse: point of physical SCE. **(B)** Results of the staining procedure on the cells. The exchanges indicated by arrows (adapted from Stults DM et al. 2020).

We aimed to confirm that the functional antagonism between SIRT1 and PP4 has a physiological impact. To monitor the effect of these factors we set up a sister chromatid exchange assay. To this end, we tested in *Wt* and *Sirt1*$^{-/-}$ the ability of MEFs, downregulated or not in PP4C by shRNA, to promote the exchange of DNA fragments upon treatment with MMC. We observed that while *Wt* MEFs sustained an average of 0.6 inter-chromatid recombination events, this ratio increased to 0.8 in MEFs that lacked SIRT1 (Figure 58B). The recombination rate in *Sirt1*$^{-/-}$ MEFs was partially restored by downregulation of PP4, implying that the interplay of the two factors is key to promoting efficient DNA repair.

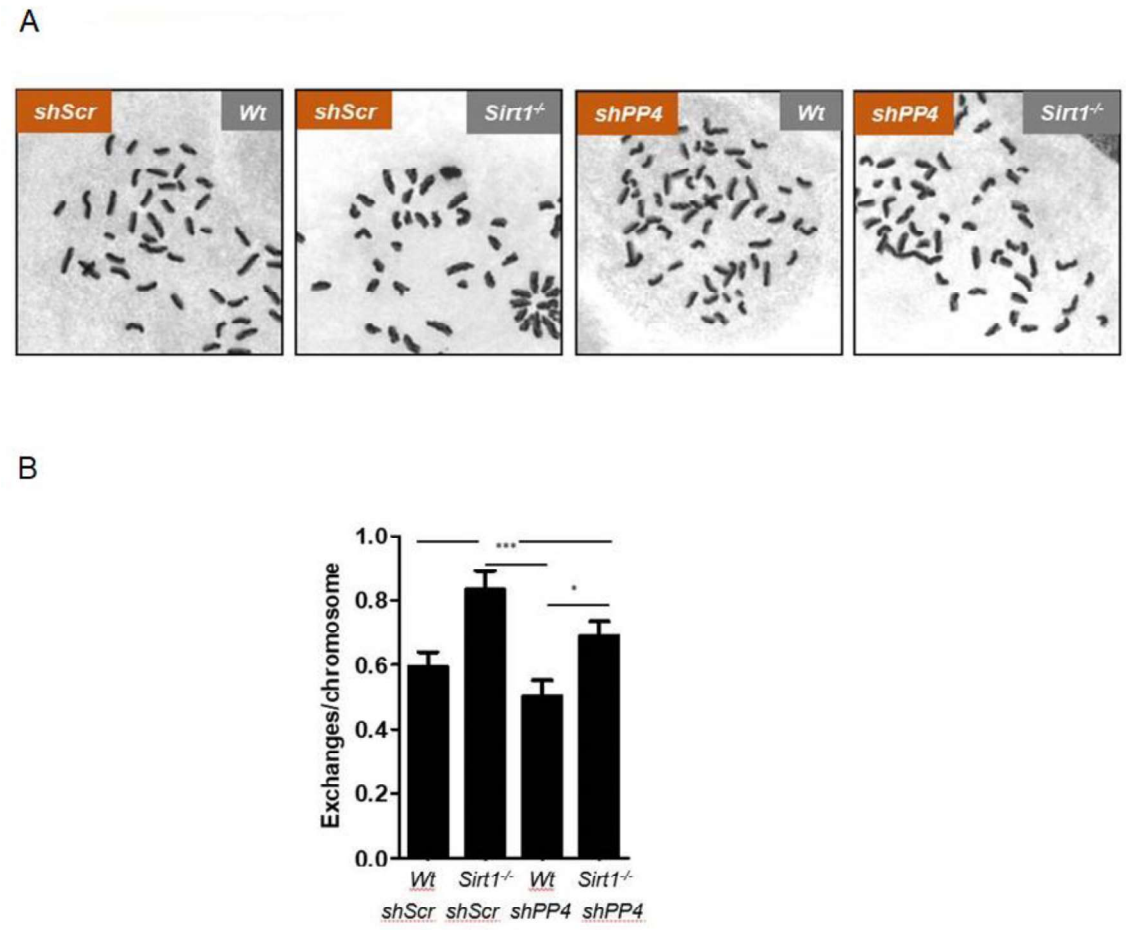

Figure 58. Sister chromatid exchanges (SCE). **(A)** The staining pattern of the metaphase chromosomes. **(B)** Quantification of SCE in *Sirt1*$^{-/-}$ cells expressing ShScramble or ShPP4C following replication stalling or DNA damage. A statistically significant increase in SCE levels was observed in control cells treated with 1µm mitomycin C (MMC), SCE rates in SIRT1 depleted cells were dramatically higher than all other conditions. Data are expressed as mean ± SD (n = 3), Standard deviation is shown (*: $p<0.05$;***: $p<0.0005$).

Overall, we identified and characterized the antagonistic interplay of SIRT1- PP4. While SIRT1 inhibits PP4 complex dephosphorylation activity toward γH2AX and RPA2, the PP4 complex can also reduce SIRT1 deacetylation activity in return. We conclude that the consequences of this interplay on DNA damage signaling and repair is key for a proper DNA repair.

DISCUSSION

The maintenance of genome stability and the control of transcriptional response to stress conditions are two of the key roles of Sirtuins. The importance of these functions is reflected by the well-established involvement of the members of the family in a variety of human diseases such as cancer, diabetes, neurodegenerative and aging related diseases. In this thesis, we have endeavored to investigate two major aspects of Sirtuin biology: In the one hand, the study of the factors that participate in the tumor suppressor role of SIRT6. In the other hand, the contribution of SIRT1 to the regulation of DNA damage signaling and repair.

Chapter I: Contribution of both HMTs Suv39h1 and G9a to the tumor suppressor activity of SIRT6

In the first objective, we have thoroughly studied the contribution of both Suv39h1 and G9a to the tumor suppressor activity of SIRT6. Our studies, which range from *in vitro* to *in vivo* xenograft analyses, reveal that the relationship between these two HMTs and SIRT6 is not the same. Both enzymes are key regulators of genome organization and stability and have been directly linked to tumorigenesis. In our study, we have demonstrated that although both enzymes interact with SIRT6, only Suv39h1 participates in in SIRT6-dependent regulation of several features associated to the cancer phenotype, such as cell proliferation, viability, independent colony assay formation and anchorage-independent growth (Figures 22-24). We further validated this important contribution of Suv39h1 to SIRT6 tumor suppression role in our mice xenograft assays (Figures 25-30). Our ChIP-seq studies suggest that Suv39h1 and SIRT6 synergize collaborates to regulate specifically a subset of genes. In contrast, although we found that G9a is functionally related to SIRT6, it seems to play a strong SIRT6-independent role as a tumor suppressor. Based on our studies, we propose a model for this interplay between SIRT6 and Suv39h1 (Figure 59). In normal conditions, we hypothesize that Suv39h1 regulates SIRT6 genomic distribution, which impacts in the silencing of a subset of genes involved in SIRT6-dependent tumor suppression, including genes involved in cell cycle control, inhibition of glycolysis and tumorigenesis suppression (Figure 59A). Based on our results, we also propose that other subsets of related genes are regulated by SIRT6 in a Suv39h1-independent manner (Figure 59B).

This hypothesis is ultimately based on our ChIP-seq analyses. The functional relevance of this interplay in the detected SIRT6-containing genes will be determined by currently ongoing studies, such as RNA-seq expression analyses of these cells derived of the tumors.

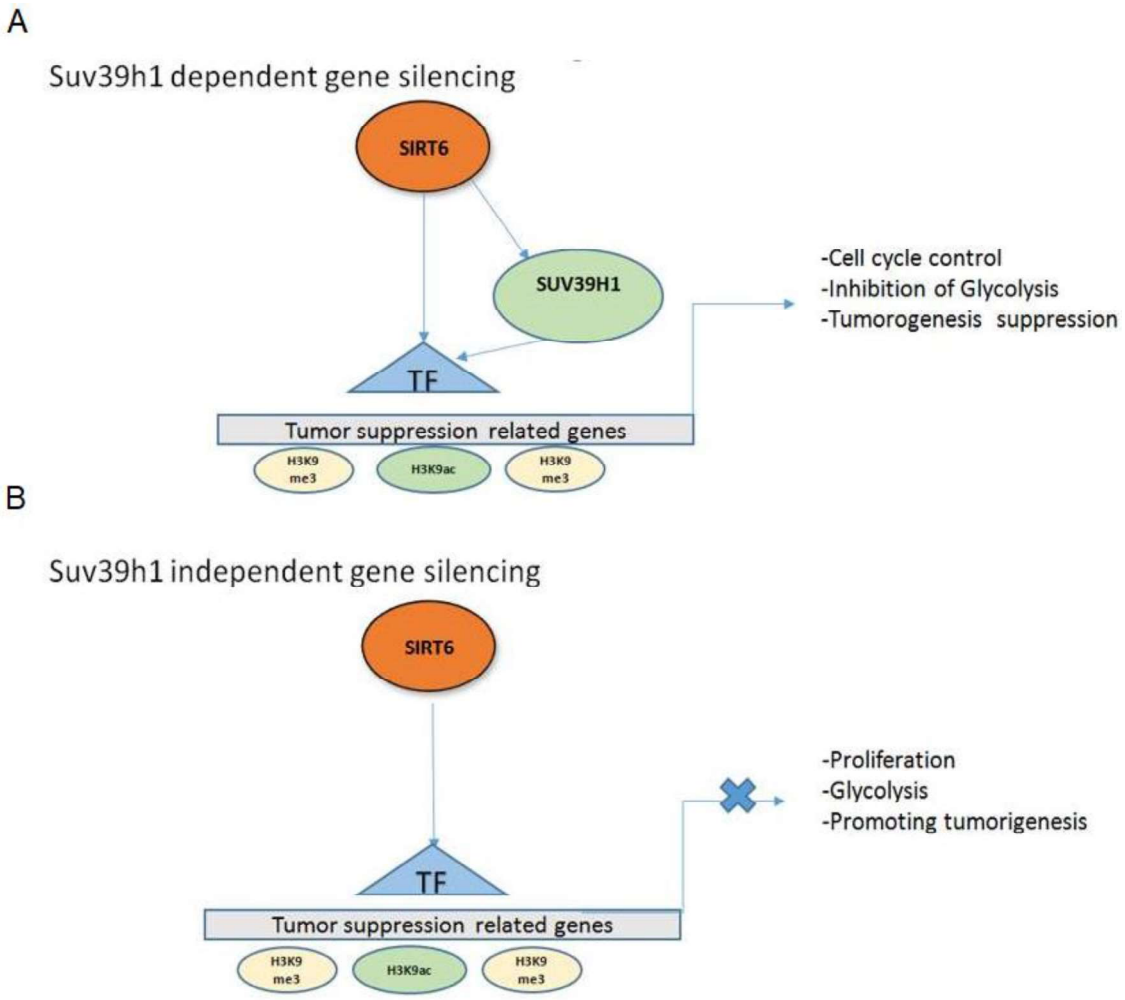

Figure 59. Suv39h1 collaborates with SIRT6 in its tumor suppressor activities. Proposed model for the regulation of the SIRT6 gene silencing, dependent or independent of Suv39h1. **(A)** SIRT6 promotes Suv39h1 activity through deacetylation of H3K9ac to allow H3K9me3 methylation by Suv39h1. SIRT6 is involved in cell cycle control, glycolysis inhibition and tumor suppression. **(B)** In the absence of Suv39h1, SIRT6 is not able to promote H3K9me3 methylation and perform its tumor suppressor activities. It may lead to promoting glycolysis, proliferation and tumorigenesis.TF (transcription factor).

Here we discuss several specific issues related to the work:

Suv39h1 and G9a as tumor promoters or tumor suppressors

In this study, we report a novel observation that depleting either Suv39h1 or G9a expression by shRNA in H-Ras (G12V)/Shp53 MEFs enhances tumor growth in xenograft model. As mentioned in the introduction, these HMTs have been found upregulated or downregulates in different cancer types. In a remarkable study, Kondo and colleagues demonstrated that knockdown of the Suv39h1 and G9a in PC3 prostate cancer cell line significantly inhibited cell growth and caused major morphological changes with depletion of telomerase activity and shortened telomeres (Kondo et al.,2008). Unexpectedly, our xenograft experiments showed that, contrary to earlier studies, not only G9a-depletion did not induce any apoptotic cell death *in vivo* and but also it enhanced the tumorigenic potential of transformed MEFs cells in nude mice (Figure 26). This highlights a possible dual role of Suv39h1 and G9a, thereby indicating that constitutive activation of Suv39h1 or G9a could be considered as a measure of either tumor progression or suppression based on specific features, such as cell type, the physiological/metabolic state or the factors involved in the transformation process. Since targeting tumor cells appears to be at least as efficient as targeting the host microenvironment, another possibility would be that Suv39h1 and G9a exert their tumor suppressor or tumor promoter activity effects respective of whether the host micro environmental cells or the tumor cells are targeted. This possibility is intriguing and will require further studies to define at which extent is an important factor in our observations.

Our findings probably also reflect the dual nature of the epigenetic marks H3K9me2/3 itself. While the loss of these marks is associated to genome instability and therefore to a higher probability to develop tumorigenesis, other studies have also demonstrated that for instance increased levels of H3K9me3 are associated to aggressive gastric and colorectal cancer phenotypes (Park et al., 2008; Yokoyama et al., 2013).

In our case, the use of MEFs immortalized with downregulation of p53 and overexpression of H-Ras (G12V) may be an important contributor to this effect. Endogenous expression of H-Ras (G12V) was connected to a higher mutation rate *in vivo* and they have a particularly high prevalence in skin papillomas (Schubbert et al., 2007).

Tumor initiation through H-Ras (G12V) requires an increase of signal output, which in papillomas and angiosarcomas is done via increased H-Ras-gene copy number (Chen et al.,2009). The specific alteration of these cells under our method of transformation may bias the final outcome towards mainly highlighting the key contribution of these factors to genome stability rather than altering tissue-specific pathways altered in a specific cell-type tumor. For instance, previous studies showed that Suv39h1/2 loss in mice results in chromosomal aberrations and B-cell lymphomas (Peters et al., 2001). While Suv39h1 expression and increased levels of H3K9me3 play an important role in HCC development and progression (Chiba et al., 2015). In contrast, low Suv39h1 expression characterizes cervical cancer migratory states (Rodrigues et al., 2019). On the other hand, G9a is over-expressed in many types of cancer and contributes to cancer aggressiveness. Another study has demonstrated that G9a exhibited its oncogenic function by dysregulating cellular iron hemostasis in breast cancer (Wang et al., 2017), epigenetically regulating metastatic genes in hypoxic condition in ovarian cancer (Kang et al.,2018), inducing angiogenic factors to promote angiogenesis in cervical cancer (Chen et al., 2017), modulating genes associated with DNA replication and RNA processing in hepatocellular carcinoma (Quin et al., 2018).

Therefore, targeting Suv39h1 or G9a for therapy may therefore be based on the origin of the tumor type or context. This can be critical when considering the cancer cells specifically because G9a is an essential mediator of apoptosis and cell death (Ho et al., 2017). Studies to identify the mechanisms of Suv39h1 and G9a's negative regulatory role may be useful in developing Suv39h1 and G9a-based therapeutics. Further investigation is still required to address the precise roles of Suv39h1 and G9a in tumor pathways and develop effective approaches for future cancer therapies.

Suv39h1 as a regulator of SIRT6 tumor suppressor activity

As explained in the introduction section, Sirtuins have been shown to play contradictory roles in carcinogenesis. While some of them are caretaker tumor suppressors that prevent cancer through protecting DNA from damage and oxidative stress, others play fundamental roles in maintenance of the malignant phenotype, mainly in cancer cell viability and cancer progression (reviewed in Zhao et al 2019). SIRT6

is a particularly relevant Sirtuin model of study as it has a well-established role as a tumor suppressor in different types of cancer through specific regulation of cell metabolism, chromatin structure and genome stability (Sebastian et al., 2012).
Although recently several studies have described few targets of SIRT6 in cancer, our knowledge about the associated mechanism involved in this tumor suppression function of SIRT6 has been, to this date, limited (Desantis et al.,2018). SIRT6 can act as negative regulator of Warburg effect by modulating activity of key signaling pathways, involved in cell proliferation, metabolism and DNA repair.

The discovery of Suv39h1 as an important contributor of SIRT6 tumor suppressor role opens the possibility to consider Suv39h1 as a marker of SIRT6-dependent tumor suppression, and as a possible therapeutic target of SIRT6-related cancers in combination with SIRT6 modulators or by itself. If this were the case, it would represent the first marker of this sort in the case of SIRT6 and one of the very few proposed for Sirtuins.

Although the mechanism behind this interplay is still undefined, the ChIP-seq analyses provide some clues. Our KEGG analysis show that loss of Suv39h1 results in the delocalization of SIRT6 from signaling pathway mostly enriched at MAPK signaling pathway to signaling pathways related to proteoglycans in cancer. MAPK signaling pathway is involved in proper physiological response including cellular proliferation, differentiation, and apoptosis in mammalian cells. In the other hand, proteoglycans provide a contact link between the cell membrane and the surrounding cell-extracellular matrix which plays an important role in promoting tumorigenesis. Another possibility to explain our results is what we previously described in our lab. SIRT6 can attenuate NF-κB pathway through a novel mechanism via Suv39h1 monoubiquitination (Santos-Barriopedro et al., 2018). NF-κB is a key signaling pathway associated with pathogenesis of different types of cancers. Uncontrolled activation of NFκB-signaling pathway has been described in various tumors (Xia et al., 2018). It is also very relevant, as the mechanism explains a role of SIRT6 in the global control of NF-kB pathway through regulation of IκBa expression. Thus, NF-κB pathway attenuation mediated by SIRT6 through Suv39h1 monoubiquitination can explain at least partially what we observed upon downregulation of Suv39h1 in *Wt* cells given the tumor-promoting role of

canonical NF-κB in cancer. Interestingly, our KEGG analysis showed that SIRT6 is enriched in the TNFα (tumor necrosis factor alfa) signaling pathway upon Suv39h1 depletion (Data not shown). TNFα is a key cytokine that activates NF-κB signaling in different cell types, such as activated B cells, through inducing NF-κB inhibitor, IkBα polyubiquitination which is responsible for controlling inflammation (Simon and Samuel, 2007; Gutierrez et al., 2008). We speculate that upon Suv39h1 downregulation, SIRT6 is not able to attenuate NF-κB pathway and its activation through TNFα may stimulate pathways has been implicated in tumorigenesis.

Our studies suggest that the interplay between both factors is relevant in the context of gene expression. However, we cannot exclude the possibility that it is also important in other functional contexts where both factors have been involved. For instance, both SIRT6 and Suv39h1 have been involved in DNA repair and the regulation constitutive pericentric and telomeric heterochromatin regions (Santos-Barriopedro et al., 2018; Michishita et al., 2008). Considering the well-established impact of both factors in genome integrity, the Suv39h1-dependent tumor suppression regulation by SIRT6 may be directly associated to these functions in addition to the silencing of subset of genes.

Suv39h1 in the control of SIRT6 genomic location

KEGG pathway analysis and GO analysis demonstrated that SIRT6 is most enriched in clusters associated to regulation of cell-matrix adhesion and regulation of cell migration involved in sprouting angiogenesis, both of which play a key role in tumor suppressing activities of SIRT6 (Edatt et al., 2020). Interestingly Suv39h1 downregulation resulted in the relocalization of SIRT6 to clusters related to negative regulation of cell differentiation and transcription (Figure 34B) which are crucial events in promoting sustained proliferation and enabling cells to acquire other hallmarks of cancer (Ke et al., 2018). In contrast, G9a downregulation resulted in enrichment in regulation of transcription from RNA polymerase II promoter and negative regulation of transcription, and no other significant signaling pathways (Figure 34C). These observations definitely support the crucial role of Suv39h1 for tumor suppressor activity of SIRT6 in contrast to G9a. Interestingly, KEGG and GO analysis didn't show significant gene changes in the case Suv39h1 upon depletion of SIRT6. The gene ontology analysis showed that Suv39h1

was enriched in both cases in biological functions related to cell-cell adhesion mediated by cadherin independently of SIRT6 (Figure 36A-B). This may not only indicate that the role of Suv39h1 in cadherin-related cell-cell adhesion is unrelated to SIRT6, but also confirms that Suv39h1 plays a much larger role in tumorigenesis than regulating SIRT6 or the maintenance of CH stability. This is a very interesting subject that deserves a deeper study as Suv39h1 has not been extensively studied beyond its role in CH.

The complex functional relationship between SIRT6 and G9a

Our *in vivo* evidence in mouse xenografts suggests that while knockdown of Suv39h1 or G9a promote tumor growth in *Sirt6*$^{-/-}$ cells, the observed growth rate in the case of G9a was considerably higher (Figure 26). However, while Suv39h1 downregulation decreased tumor growth in *Sirt6*$^{-/-}$ re-expressing SIRT6 upon doxocycline induction, loss of G9a in the same type of tumors behaved exactly as ShScramble (Figure 28). Overall, this suggested that G9a has a strong effect in tumor suppression independent of SIRT6. In agreement with that, pathological analysis of xenograft tumors demonstrated that SIRT6 re-expression in Suv39h1 depleted tumors had a minimal pathological alteration and displayed similar levels of polymorphism and necrosis while a similar analysis in G9a-depleted tumors showed increased differentiation levels suggesting that both SIRT6 and G9a play tumor suppressor roles independent of each other.

G9a plays a central role in carcinogenesis by mediating cell survival, growth, and differentiation. It is constitutively activated in several cancers. In general term, G9a may participate in tumorigenesis by either inhibition of tumor suppressors, like CDH1/E-Cadherin (Wozniak et al., 2007) and p53 (Huang et al., 2010), or induction of pro-oncogenic signaling pathways such as hypoxia response (Lee et al.,2011). It can also act through transcriptional repression of key tumor suppressors in a histone or non-histone dependent manner (Bachman et al., 2003; Casciello et al., 2015). It also has been showed that G9a is necessary for TGF-β-induced epithelial-to-mesenchymal transition (EMT) in head and neck squamous cell carcinoma (Tachibana et al., 2002). Another study showed that G9a induced invasion and metastasis through regulation of the epithelial cellular adhesion molecule (EpCAM) in lung cancer (Egger et al., 2004).

Contrary to its accepted tumor promoting role, we found G9a to be a negative regulator of growth in H-Ras (G12V) and Shp53 derived tumors. Although we have made

similar observations in xenografts of Suv39h1-deficient cells, the effect was observed in reduced magnitude compared to G9a xenografts. Interestingly, p53 is methylated and deactivated by G9a and GLP which indicates that G9a is a potential inhibitory target for cancer treatment (Huang et al., 2010). We speculate that our observations may be associated to the fact that to induce transformation we knocked down p53. This would mean that in this context, the reduction of G9a levels couldn't lead to a larger population of apoptotic cells and tumor suppression. If normal functioning of G9a is related to apoptosis and regression in tumor cells, G9a removal would raise the probability of an anti-apoptotic activity as its more appropriate function. This intricate balance between apoptotic and anti-apoptotic role of G9a in the functioning of the cells needs to be accurately defined before targeting tumors with G9a inhibitors.

Interestingly, KEGG pathway analysis and GO analysis showed that, upon SIRT6 depletion, G9a relocalized to genes involved in pathways linked tumorigenesis such as cell migration and metabolic processes (Figure 39B). These results together with the xenograft analysis may indicate that although we cannot detect a clear synergy between SIRT6 and G9a and tumorigenesis, SIRT6 can indeed control in part of G9a oncogenic associated gene expression events. Interestingly, these ChIP analyses showed that upon G9a downregulation, the signaling pathway with higher SIRT6 enrichment is Hippo signaling pathway (Figure 33C). The Hippo pathway plays an important role in contact inhibition and growth regulation by physical properties of cells. In fact, it may be the main place where different pathways that sense cell contact, cell shape and cell density are integrated to regulate cell survival and growth (Halder and Johnson, 2011; Tumaneng et al., 2012).

Suv39h1 as a close collaborator of Sirtuin function: SIRT1 vs SIRT6

SIRT6 is linked to gene silencing but the mechanism involved and the interplay with the rest of the transcriptional and chromatin regulatory machinery remain elusive. Here we describe that SIRT6 interacts with several factors, in particular, HTMs, Suv39h1 and G9a. Suv39h1 has been previously linked by the work of our group with Sirtuins. In particular, several seminal studies established the functional interplay between Suv39h1 and SIRT1 in the establishment and maintenance of constitutive and facultative heterochromatin (Vaquero et al., 2007; Bosch-Presegué et al., 2011) and with SIRT6 in

the regulation of NF-kB pathway (Santos-Barriopedro et al., 2018). The established differences between SIRT1 and SIRT6 on Suv39h1 are intriguing. SIRT1 and SIRT6 bind to Suv39h1 through different domains. SIRT1 interacts with N-terminal region of Suv39h1 while, SIRT6 does with C-terminal catalytic SET domain of Suv39h1. This indicates that both factors may bind simultaneously to the Suv39h1 molecule. Thus, while SIRT1 promotes Suv39h1 protein stabilization by inhibition of polyubiquitination of Suv39h1 N-terminal domain, SIRT6 induces the inactivation of Suv3h1 through monoubiquitination of PRESET domain of Suv39h1 in the promoter of the general repressor of the pathway IκBα (Santos-Barriopedro et al., 2018).

Interestingly, both Sirtuins participate in NF-kB regulation at different levels. SIRT6 not only controls IκBα expression through the aforementioned mechanism (Santos-Barriopedro et al., 2018), but also prevents excessive hyperactivation through deacetylation of H3K9ac in the promoters of NFκB regulated genes. On the other hand, SIRT1 also regulate RelA, one of the NF-kB transcription factors through deacetylation, but is unknown if it interacts with the Suv39h1 pools enriched on IκBα promoter (Yang et al.,2012).

Based on our results, we cannot exclude that Suv39h1 may also be an important contributor of SIRT1 tumor suppression role. Considering the close link between both Sirtuins and the regulation of NF-kB and other key stress-related pathways, this may be a very likely possibility. Future studies should define this hypothetic contribution and clarify possible redundant or opposite roles between SIRT1 and SIRT6 in their interplay with Suv39h1 in the context of tumorigenesis.

Chapter II: The role of SIRT1 in DNA damage signaling through its interaction with the PP4 complex.

In the second part of the thesis, we focused on the role of SIRT1 in DDR and repair signaling pathways. In this sense, the identification and characterization of the interplay between PP4 complex and SIRT1, provides a novel perspective about the way SIRT1 controls the DNA repair process, from the detection to the final repair of the damage sites. Until this work, all evidences had suggested that SIRT1 participate in specific

unconnected steps of the process, such as binding to (1) nibrin (NBS1), (2) Ku proteins, (3) Werner helicase (WRN) or (4) XRCC, and (5) deacetylation of H4K16ac to allow the establishment of H4K20me2, and others (Yousafzai et al., 2019; Jeong et al., 2007; Martínez-Redondo and Vaquero, 2013). However, we had not a clear consistent model to integrate the whole collection of observations accumulated on the role of SIRT1 in these processes thorough the years.

Considering together our evidence, we propose a novel integral regulatory mechanism for SIRT1 through PP4. This model also provides a new perspective on the Sirtuin-dependent control of DNA damage response through an interplay with phosphorylation/ dephosphorylation events. This mechanism may have further biological functions beyond DDR and DNA repair and could demonstrate a more complex interplay between SIRT1 and the PP4 complex (Figure 61).

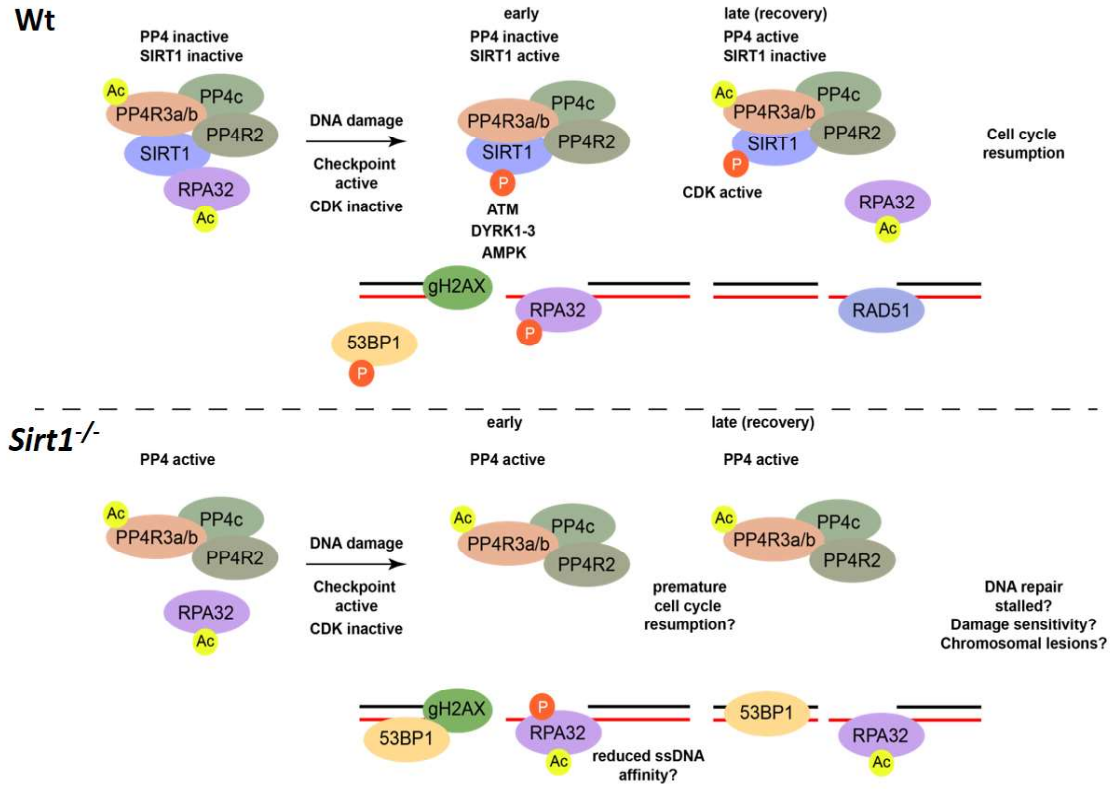

Figure 61. Proposed model of deacetylation-dependent deactivation of PP4 complex by SIRT1. In normal conditions, SIRT1 binds weakly to the regulatory subunits of the PP4 complex, which remain acetylated. Upon oxidative stress conditions, SIRT1 binds strongly to PP4 complex and deacetylates the PP4R3α and PP4R3β resulting in PP4 complex inhibition.

Future studies will be required to examine the way in which the acetylation status of regulatory subunits PP4R3α and PP4R3β affect PP4 dephosphorylation activity and to determine the relevance of this functional implications and its importance in SIRT1-dependent functions.

SIRT1 and γH2AX foci formation

As explained earlier, γ-H2AX is a histone modification that plays an essential role in DNA damage response of DSBs, as it acts as a recruitment site for diverse DNA repair proteins and other chromatin-remodeling complexes (Downs et al., 2004). The decreased levels of γH2AX observed in, *Sirt1*$^{-/-}$ cells in presence or absence of an external insult had been puzzling the Sirtuin field since it was reported in 2008 (Wang et al., 2008), as the underlying molecular mechanism was completely unknown. Interestingly, among the described γH2AX phosphatases, PP4 depletion results in elevated levels of γH2AX even in the absence of exogenous DNA damage, while the downregulation of other such as PP2A does not have any effect on this mark in the absence of an external insult. Based on these observations, it was proposed that PP4 is required for basal repair, and possibly linked to replicative stress (Chowdhury et al., 2005; Keogh et al., 2006). These observations are supported by our evidence and proposed hypothesis.

In the case of γH2AX, we hypothesize that while the stress is present, SIRT1 binding to PP4 complex guarantees that the signaling remains active until DNA repair to be completed and/or the damage signal disappears. This event cannot be related to the described deacetylation of NBS1 by SIRT1, since γH2AX is established earlier than NBS1 recruitment in DNA repair signaling (Yuan et al.,2007). Moreover, no significant differences in NBS1 foci formation could be detected between *Wt* and *Sirt1*$^{-/-}$ MEFs following IR treatment. Taken together, it suggests that acetylation of NBS1 does not play a role in the recruitment of MRN to γH2AX domains upon DSBs (Kobayshi et al., 2002; Yuan et al., 2007). Despite the importance of the PP4-SIRT1 interplay, our work suggests that SIRT1 can also regulate γ-H2AX levels through a PP4-independent mechanism, due to the γ-H2AX hyperphosphorylation observed upon PP4 downregulation or upon inhibition of its enzymatic activity using Okadaic acid, is also considerably reduced in *Sirt1*$^{-/-}$ background (Figure 47).

The interplay between SIRT1 and phosphorylation shapes the DNA damage response

The functional interplay between SIRT1 function and phosphorylation has been previously established at different levels. The first level is that phosphorylation is one of the most important activation mechanisms of SIRT1 function. SIRT1 is modified by posttranslational modifications, which are regulated by different stress stimuli (Figure 62). Mass spectrometry has identified at least 13 phosphorylation sites within SIRT1 (Sasaki et al.,2008). The c-Jun N-terminal kinase (JNK) is one of the kinases responsible of SIRT1 phosphorylation. JNK binds to and phosphorylates SIRT1 upon oxidative stress at Ser27, Ser47, and Thr530, leading to increased nuclear localization of SIRT1 (Nasrin et al., 2009). JNK belongs to the mitogen-activated protein kinase (MAPK) family and is responsive to different types of stress conditions, such as ultraviolet irradiation, heat shock, and osmotic shock (Vlahopoulos et al., 2004). This could explain, partially, how these stress stimuli result in an increase in SIRT1 activity on its nuclear targets.

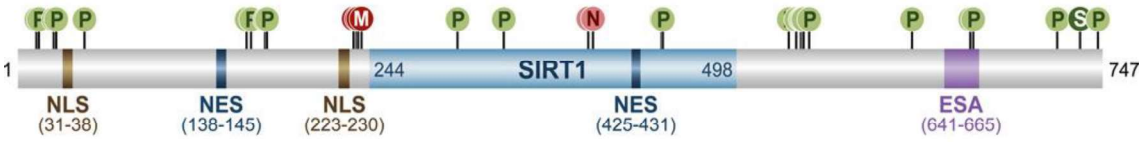

Figure 62. SIRT1 post-translational modifications. The human protein SIRT1 comprises several domains, including NLSs (nuclear localization signals), NESs (nuclear export signals), the ESA (essential for SIRT1 activity), and an enzymatic core (indicated in light blue) from residues 244 to 498. Residue numbers for each domain are shown under each domain name. SIRT1 is also subjected to a number of PTMs, including phosphorylation (P), methylation (M), nitrosylation (N), and SUMOylation (S) (adapted from Revollo and Li, 2013).

Interestingly, our observations suggest that PP4 also regulates SIRT1 activity through a mechanism requiring its phosphatase activity (Figure 44 and data not shown). Thus, an interesting possibility is that not only SIRT1 regulates PP4 in DDR, but also that PP4 controls SIRT1 activation by antagonizing its activation signals. This would involve a feedback regulatory mechanism ensuring the mutual control of both activities. As we discuss in the following section, the regulation of SIRT1 phosphorylation by PP4 complex may have important implications in other biological processes. Defining the precise mechanism involved and the extent of this functional SIRT1 inhibition by PP4 will be an important line of work in future studies.

Another important issue that we have not addressed in our work is how the interplay between PP4 and SIRT1 is linked to the previously described link of SIRT1 with the key kinases in these processes: ATM, ATR or DNA-PK. The first issue to remark is that contrary to the case of PP4, in the vast majority of these cases SIRT1 seems to be participate in a downstream position of these kinases. However, in specific cases, such as post-mitotic neurons, SIRT1 is an apical signal transducer of the DSB response, representing an important therapeutic option for the treatment of neurodegeneration (Dobbin et al., 2013). In this case, SIRT1 work together with ATM and HDAC1 to promote genome integrity in neurons. Thus, SIRT1 is recruited to DSBs in an ATM-dependent manner. In turn, SIRT1 induces ATM activity and stabilizes ATM at DSB sites (Dobbin et al., 2013). In these cells, upon DSB, SIRT1 also deacetylates HDAC1 enhancing its enzymatic activity, which is necessary for DSB repair by the NHEJ pathway.

In other cases, ATM seems to play the opposite effect on SIRT1. One of the best described cases is DBC1, the SIRT1 inhibitor both *in vivo* and *in vitro* through direct interaction (Kim et al.,2008). DBC1-dependent inhibition of SIRT1 activity results in an increase in p53 acetylation and subsequent upregulation of p53-dependent apoptotic activity (Zhao et al., 2008). Interestingly, the DBC1-SIRT1 interaction is boosted upon DNA damage by ATM-dependent phosphorylation of DBC1 at Thr454 which creates in DBC1 a second binding site for SIRT1 (Yuan et al., 2012). Thus, stress stimuli not only activate SIRT1 but can also suppress SIRT1 activity, proposing that the cells can fine-tune SIRT1 activity. On the other hand, SIRT1 also deacetylates XPA at residues Lys-63, Lys-67, and Lys-215 to promote interactions with ATR and promotes cAMP-induced DNA repair of UV damage. DNA-PK also cooperates with ATR and ATM to phosphorylate proteins involved in the DNA damage checkpoint (Jarrett et al., 2018).

The functional interplay between PP4 complex and SIRT1 beyond DDR

The functional connection between PP4 complex and SIRT1, seems to go further than DNA damage regulation as several evidence suggest that it may be also involved in other biological processes. However, in all these cases is not clear whether the interplay between PP4 and SIRT1 is a functional antagonism or the play synergic roles. One of the most interesting examples is glucose homeostasis. Despite that PP4 and SIRT1 both

seem to promote hepatic gluconeogenesis (GNG), evidence also suggest that they can act in opposing pathways. For example, it has been showed that PP4 is responsible for the dephosphorylation of CRTC2 at serine 171 residue, resulting in its the nuclear localization and subsequent GNG activation (Wang et al., 2012; Yoon et al., 2010). While SIRT1 activation promotes the opposite effect. As explained earlier, SIRT1 inhibits TORC2, a CREB-regulated transcription coactivator that is important for cAMP/CREB-dependent activation of gluconeogenesis genes, resulting in gluconeogenesis inhibition (Liu et al., 2008).

Another interesting example is the modulation of NF-κB signaling. SIRT1 activation suppresses NF-κB signaling and promotes oxidative metabolism and inflammation reduction through deacetylation of p65 subunit of NF-κB, which results in NF-κB transcription inhibition. Moreover, SIRT1 promotes oxidative energy production by the activation of AMPK, PPARα and PGC-1α, thus indirectly also inhibiting NF-κB, activation (Kauppinen et al., 2013). Interestingly, PP4 regulatory subunit 1 (PP4R1) acts as a negative regulator of NF-kB activity in T lymphocytes. PP4R1 belong to a specific PP4 holoenzyme and linked the key inhibitor of NF-κB , IKK complex and the PP4 complex, thus regulation the PP4 complex activity to dephosphorylate and inhibit the IKK complex (Brechman et al., 2012). These observations suggest that in this case, SIRT1 and PP4 may work together to control the activation of the NF-κB signaling and inflammation.

Another interesting link is also the response to TNF-α signaling, that as we explained earlier, is also connected to NF-κB activation. In this case, PP4 seems to also mediate part of the TNF-α regulatory effects since it specifically interacts with insulin receptor substrate 4 (IRS-4) following TNF-α stimulation and downregulates IRS-4 in a phosphatase activity-dependent manner (Mihindukulasuriya et al., 2004). In contrast, SIRT1 inhibits TNF-α-induced apoptosis of vascular adventitial fibroblasts partly through the deacetylation of FOXO1 (Wang et al., 2013).

The modulation of PP4 complex activity through deacetylation of conserved residue K64 in the WH1 domain of PP4R3α and PP4R3β

Another important finding of our work is the identification of regulatory subunits PP4R3α and PP4R3β as mediator of PP4 activity regulation by SIRT1. The identification

of conserved lysine residue K64 within the WH1 N-terminal domain of PP4R3α and PP4R3β as a direct target of SIRT1. It is an in important feature considering the role of this domain in recognizing and binding to the PP4 substrates (Ball et al., 2002). In fact, several studies suggest that the PP4R3 subunits can target PP4C to its substrates. For instance, human PP4R3α, also known as SMEK1, interacts with the cell polarity protein Par3, which results in its dephosphorylation in neuronal differentiation (Lyu et al., 2013). Moreover, the EVH1 domain of the regulatory subunit 3 of *Drosophila* PP4, Falafel (Flfl), directly interacts with the centromeric protein C (CENP-C) (Lipinszki et al., 2015). Interestingly, other studies have also suggested that in some cases, such as 53BP1 dephosphorylation in the context of DDR, the PP4C–PP4R3β complex does not require other regulatory subunits (like, PP4R2 or PP4R1) to promote a full functional effect (Lee et al., 2014). However, this is not always the case. In contrast, other studies demonstrated that both PP4R2 and PP4R3α are required to recruit PP4C to the centrosomes (Voss et al., 2013).

The fact that we had to mutate K64 in both PP4R3α and PP4R3β to observe a full inhibitory effect suggests that both subunits play a redundant role in this case. PP4R3α and PP4R3β are conserved throughout eukaryotic evolution. PP4R3β has 949 amino acid residues, 16 amino acids more than PP4R3α (833 aa). The *Saccharomyces cerevisiae* PP4R3 ortholog *Psy2* was identified previously in a screen for sensitivity to the DNA-damaging agent and anticancer drug cisplatin (Wu et al., 2004). Interestingly, a pull-down of PP4R3α confirmed the interaction with PP4C and PP4R2. No additional proteins were identified in the PP4R3α pull-down. Thus, with PP4C, PP4R2 appeared to be present in a complex with PP4R3α and/or PP4R3β. PP4R2, PP4R3α and PP4R3β Interact with PP4C but not with the related phosphatases, such as PP2AC or PP6C (Gingras et al., 2005). The sequence similarity between PP4R3α and PP4R3β and the conservation of WH1 domain in the N-terminal region of both proteins suggests that this is the case. Interestingly, our IP experiments seem to indicate that SIRT1 consistently interacts with PP4R3β more efficiently than PP4R3α. This suggests that PP4R3β may be the main mediator of SIRT1 action *in vivo* (Figure 43 and data not shown).

Other targets of SIRT1/PP4 regulatory axis in DNA repair

In this thesis, we have focused our studies on the two major targets of PP4 described in this context, γH2AX and RPA2. However, we cannot exclude the possibility that other key factors in DNA repair may also been targets of this regulatory interplay between SIRT1 and PP4. An obvious candidate is 53BP1 as it has been shown recently to be a target of PP4C (Isono et al., 2017). Interestingly, the acetylation levels of 53BP1 increased in SIRT1 knockout mouse cells (Kwon et al., 2019), which suggests that both factors may contribute to this regulation. Another interesting factor is KAP-1, a key regulator of stress response and DNA damage, and one of the best characterized targets of ATM (White et al., 2012). Some studies have suggested that PP4 regulate KAP-1 function. For instance, phosphorylation of S473 in KAP-1 regulates the G_2/M checkpoint response. Interestingly, depletion of KAP-1, overexpression of KAP-1 S473 mutant (S473D), or downregulation of PP4R3β results in a prolonged G_2/M checkpoint. Moreover, S824 phosphorylation in KAP-1 is required for repair of heterochromatic DNA damage. Thus, cells expressing phosphomimetic S824 mutant (S824D), or siRNA PP4R3β present prolonged relaxation of chromatin and releasing chromatin remodeler protein CHD3 (Lee et al., 2012). Interestingly, KAP-1 deacetylation by SIRT1 is an important regulatory mechanism that promotes NHEJ regulation (Lin et al., 2015), but whether PP4 is also involved in this mechanism has not been addressed yet.

SIRT1 and RPA2 phosphorylation

As for γ-H2AX dephosphorylation, PP4 role in dephosphorylating RPA2 is also crucial for a correct DNA repair. We have observed that SIRT1 is required to avoid RPA2 hyper-dephosphorylation by PP4 during the repair of a double-strand break, a process that impacts on the phosphorylation status of multiple protein involved in the DDR. Previously, it has been showed that depletion of PP4C or PP4R2 leads to increased levels of RPA2 phosphorylation, which in turn impedes HR-mediated DSB repair by affecting the recruitment of key factor RAD51 (Lee et al., 2020).

Interestinlgy the DNA-dependent protein kinase complex (DNA-PK), but not ATR or ATM, is the kinase responsible for the modifications for phosphorylation of S4, S8 in

RPA2 *in vivo*. RPA2 hyperphosphorylated at S4, S8 delays mitotic entry and seems to block unscheduled homologous recombination at collapsed DNA replication forks (Liaw et al., 2011). Our work suggests functional roles of the interplay of SIRT1 and PP4 for the modulation of RPA2 phosphorylation.

SIRT1 is not the only Sirtuin involved in DDR since SIRT6 and SIRT7, and to a lesser extent SIRT2, have been also involved in DNA repair mechanisms. Our laboratory previously showed that SIRT6 doesn't interact with PP4 complex. However, we cannot exclude at this point that PP4 is not associated to SIRT6 or the other Sirtuins in specific stress conditions. In fact, as many sirtuin activation pathways are common to many Sirtuin family members, PP4 may regulate the activation of other Sirtuins than SIRT1. Future studies should define whether this is the case and the contribution of PP4 to the global Sirtuin activity.

CONCLUSIONS

1) SIRT6 binds to both Suv39h1 and G9a. The binding of SIRT6 to Suv39h1 does not depend on any stress conditions. In contrast, the interaction between SIRT6 and G9a is specifically increased upon oxidative stress.

2) Loss of Suv39h1 decrease proliferation of *Wt* MEFs but does not have any change (compared to ShScramble) in the proliferative capacity of *Sirt6*$^{-/-}$ MEFs.

3) SIRT6 may regulate G9a and Suv39h1 post-translationally and also participate in the control of Suv39h1 RNA levels.

4) Xenografts studies of these transformed MEFs showed that loss of Suv39h1 or G9a increase the tumorigenic ability of *Wt* and KO cells.

5) Suv39h1 is a tumor suppressor directly involved in the tumor suppressor role of SIRT6. In contrast, G9a is a tumor suppressor with a very strong SIRT6-independent effect on tumorigenesis.

6) SIRT1 forms *in vitro* and *in vivo* a novel oxidative stress-dependent complex with the human protein phosphatase 4 (PP4), a multi-protein complex that targets the histone variant γH2AX and RPA2 during the repair of DNA double strand breaks (DSBs).

7) SIRT1 inhibits PP4 dephosphorylation activity towards γH2AX and phosphorylated RPA2 (S33 and S4/8).

8) SIRT1 regulates PP4 complex activity through deacetylation of residue K64 of PP4R3α and PP4R3β.

9) The SIRT1-PP4 complex contains the PP4 substrate replication protein A (RPA) subunit RPA2. SIRT1 loss alters the function and pattern of RPA2 function in Homologous recombination.

Overall, these results support a direct functional link between SIRT6 and Suv39h1 (compared to G9a) which directly involved in tumor suppressor activity of SIRT6. SIRT1-mediated oxidative stress response and the DNA repair proteins, PP4 complex and RPA2 provide a dynamic model of their regulation through SIRT1 to ensure genome stability.

REFERENCES

Aboussekhra A, Biggerstaff M, Shivji MK, Vilpo JA, Moncollin V, Podust VN, Protić M, Hübscher U, Egly JM, Wood RD. Mammalian DNA nucleotide excision repair reconstituted with purified protein components. Cell. 1995 Mar 24;80(6):859-68.

Accili D, Arden KC. FoxOs at the crossroads of cellular metabolism, differentiation, and transformation. Cell. 2004 May 14;117(4):421-6.

Ahmed MA, O'Callaghan C, Chang ED, Jiang H, Vassilopoulos A. Context-Dependent Roles for SIRT2 and SIRT3 in Tumor Development Upon Calorie Restriction or High Fat Diet. Front Oncol. 2020 Jan 8; 9:1462.

Ahuja N, Schwer B, Carobbio S, Waltregny D, North BJ, Castronovo V, Maechler P, Verdin E. Regulation of insulin secretion by SIRT4, a mitochondrial ADP-ribosyltransferase. J Biol Chem. 2007 Nov 16;282(46):33583-33592.

Alcendor RR, Gao S, Zhai P, Zablocki D, Holle E, Yu X, Tian B, Wagner T, Vatner SF, Sadoshima J. Sirt1 regulates aging and resistance to oxidative stress in the heart. Circ Res. 2007 May 25;100(10):1512-21.

ALLFREY VG, FAULKNER R, MIRSKY AE. ACETYLATION AND METHYLATION OF HISTONES AND THEIR POSSIBLE ROLE IN THE REGULATION OF RNA SYNTHESIS. Proc Natl Acad Sci U S A. 1964 May;51(5):786-94.

Anantha RW, Vassin VM, Borowiec JA. Sequential and synergistic modification of human RPA stimulates chromosomal DNA repair. J Biol Chem. 2007 Dec 7;282(49):35910-23.

Andrae J, Gallini R, Betsholtz C. Role of platelet-derived growth factors in physiology and medicine. Genes Dev. 2008 May 15;22(10):1276-312

Ansari A, Rahman MS, Saha SK, Saikot FK, Deep A, Kim KH. Function of the SIRT3 mitochondrial deacetylase in cellular physiology, cancer, and neurodegenerative disease. Aging Cell. 2017 Feb;16(1):4-16.

Ashton NW, Bolderson E, Cubeddu L, O'Byrne KJ, Richard DJ. Human single-stranded DNA binding proteins are essential for maintaining genomic stability. BMC Mol Biol. 2013 Apr 1;14:9.

Atsumi Y, Minakawa Y, Ono M, Dobashi S, Shinohe K, Shinohara A, Takeda S, Takagi M, Takamatsu N, Nakagama H, Teraoka H, Yoshioka K. ATM and SIRT6/SNF2H Mediate Transient H2AX Stabilization When DSBs Form by Blocking HUWE1 to Allow Efficient γH2AX Foci Formation. Cell Rep. 2015 Dec 29;13(12):2728-40.

Ayrapetov MK, Gursoy-Yuzugullu O, Xu C, Xu Y, Price BD. DNA double-strand breaks promote methylation of histone H3 on lysine 9 and transient formation of repressive chromatin. Proc Natl Acad Sci U S A. 2014 Jun 24;111(25):9169-74.

Baccelli I, Gareau Y, Lehnertz B, Gingras S, Spinella JF, Corneau S, Mayotte N, Girard S, Frechette M, Blouin-Chagnon V, Leveillé K, Boivin I, MacRae T, Krosl J, Thiollier C, Lavallée VP, Kanshin E, Bertomeu T, Coulombe-Huntington J, St-Denis C, Bordeleau ME, Boucher G, Roux PP, Lemieux S, Tyers M, Thibault P, Hébert J, Marinier A, Sauvageau G. Mubritinib Targets the Electron Transport Chain Complex I and Reveals the Landscape of OXPHOS Dependency in Acute Myeloid Leukemia. Cancer Cell. 2019 Jul 8;36(1):84-99. e8.

Bachman KE, Park BH, Rhee I, Rajagopalan H, Herman JG, Baylin SB, Kinzler KW, Vogelstein B. Histone modifications and silencing prior to DNA methylation of a tumor suppressor gene. Cancer Cell. 2003 Jan;3(1):89-95.

Balaban RS, Nemoto S, Finkel T. Mitochondria, oxidants, and aging. Cell. 2005 Feb 25;120(4):483-95.

Ball LJ, Jarchau T, Oschkinat H, Walter U. EVH1 domains: structure, function and interactions. FEBS Lett. 2002 Feb 20;513(1):45-52.

Bannister AJ, Kouzarides T. Regulation of chromatin by histone modifications. Cell Research. Nature Publishing Group; 2011 Feb 15;21(3):381–95.

Barski A, Cuddapah S, Cui K, Roh T-Y, Schones DE, Wang Z, et al. High-Resolution Profiling of Histone Methylations in the Human Genome. Cell. 2007 May;129(4):823–37.

Bascom G, Schlick T. Linking Chromatin Fibers to Gene Folding by Hierarchical Looping. Biophys J. 2017 Feb 7;112(3):434-445.

Batta K, Zhang Z, Yen K, Goffman DB, Pugh BF. Genome-wide function of H2B ubiquitylation in promoter and genic regions. Genes & Development. 2011 Nov 1;25(21):2254–65.

Baynton K, Otterlei M, Bjørås M, von Kobbe C, Bohr VA, Seeberg E. WRN interacts physically and functionally with the recombination mediator protein RAD52. J Biol Chem. 2003 Sep 19;278(38):36476-86.

Bedford MT, Richard S. Arginine methylation an emerging regulator of protein function. Molecular Cell. 2005 Apr 29;18(3):263–72.

Bednar J, Garcia-Saez I, Boopathi R, Cutter AR, Papai G, Reymer A, Syed SH, Lone IN, Tonchev O, Crucifix C, Menoni H, Papin C, Skoufias DA, Kurumizaka H, Lavery R, Hamiche A, Hayes JJ, Schultz P, Angelov D, Petosa C, Dimitrov S. Structure and Dynamics of a 197 bp Nucleosome in Complex with Linker Histone H1. Mol Cell. 2017 May 4;66(3):384-397.e8.

Bhandari D, Zhang J, Menon S, Lord C, Chen S, Helm JR, Thorsen K, Corbett KD, Hay JC, Ferro-Novick S. Sit4p/PP6 regulates ER-to-Golgi traffic by controlling the dephosphorylation of COPII coat subunits. Mol Biol Cell. 2013 Sep;24(17):2727-38.

Bhardwaj A, Das S. SIRT6 deacetylates PKM2 to suppress its nuclear localization and oncogenic functions. Proc Natl Acad Sci U S A. 2016 Feb 2;113(5):E538-47.

Binz SK, Sheehan AM, Wold MS. Replication protein A phosphorylation and the cellular response to DNA damage. DNA Repair (Amst). 2004 Aug-Sep;3(8-9):1015-24.

Binz SK, Wold MS. Regulatory functions of the N-terminal domain of the 70-kDa subunit of replication protein A (RPA). J Biol Chem. 2008 Aug 1;283(31):21559-70.

Bittencourt D, Wu DY, Jeong KW, Gerke DS, Herviou L, Ianculescu I, Chodankar R, Siegmund KD, Stallcup MR. G9a functions as a molecular scaffold for assembly of transcriptional coactivators on a subset of glucocorticoid receptor target genes. Proc Natl Acad Sci U S A. 2012 Nov 27;109(48):19673-8.

Bizhanova A, Kaufman PD. Close to the edge: Heterochromatin at the nucleolar and nuclear peripheries. Biochim Biophys Acta Gene Regul Mech. 2021 Jan;1864(1):194666.

Blander G, Bhimavarapu A, Mammone T, Maes D, Elliston K, Reich C, Matsui MS, Guarente L, Loureiro JJ. SIRT1 promotes differentiation of normal human keratinocytes. J Invest Dermatol. 2009 Jan;129(1):41-9.

Bode AM, Dong Z. Post-translational modification of p53 in tumorigenesis. Nat Rev Cancer. 2004 Oct;4(10):793-805.

Böhm L, Crane-Robinson C. Proteases as structural probes for chromatin: the domain structure of histones. Biosci Rep. 1984 May;4(5):365-86.

Bosch-Presegué L, Raurell-Vila H, Marazuela-Duque A, Kane-Goldsmith N, Valle A, Oliver J, Serrano L, Vaquero A. Stabilization of Suv39H1 by SirT1 is part of oxidative stress response and ensures genome protection. Mol Cell. 2011 Apr 22;42(2):210-23.

Bosch-Presegué L, Vaquero A. The dual role of sirtuins in cancer. Genes Cancer. 2011 Jun;2(6):648-62.

Bowater R, Doherty AJ. Making ends meet: repairing breaks in bacterial DNA by non-homologous end-joining. PLoS Genet. 2006 Feb;2(2):e8

Braithwaite SP, Stock JB, Lombroso PJ, Nairn AC. Protein phosphatases and Alzheimer's disease. Prog Mol Biol Transl Sci. 2012; 106:343-79.

Brandsma I, Gent DC. Pathway choice in DNA double strand break repair: observations of a balancing act. Genome Integr. 2012 Nov 27;3(1):9.

Brechmann M, Mock T, Nickles D, Kiessling M, Weit N, Breuer R, Müller W, Wabnitz G, Frey F, Nicolay JP, Booken N, Samstag Y, Klemke CD, Herling M, Boutros M, Krammer PH, Arnold R. A PP4 holoenzyme balances physiological and oncogenic nuclear factor-kappa B signaling in T lymphocytes. Immunity. 2012 Oct 19;37(4):697-708.

Brill SJ, Stillman B. Replication factor-A form Saccharomyces cerevisiae is encoded by three essential genes coordinately expressed at S phase. Genes Dev. 1991 Sep;5(9):1589-600.

Cai MY, Hou JH, Rao HL, Luo RZ, Li M, Pei XQ, Lin MC, Guan XY, Kung HF, Zeng YX, Xie D. High expression of H3K27me3 in human hepatocellular carcinomas correlates closely with vascular invasion and predicts worse prognosis in patients. Mol Med. 2011 Jan-Feb;17(1-2):12-20.

Cannan WJ, Pederson DS. Mechanisms and Consequences of Double-Strand DNA Break Formation in Chromatin. J Cell Physiol. 2016 Jan;231(1):3-14.

Casciello F, Al-Ejeh F, Kelly G, Brennan DJ, Ngiow SF, Young A, Stoll T, Windloch K, Hill MM, Smyth MJ, Gannon F, Lee JS. G9a drives hypoxia-mediated gene repression for breast cancer cell survival and tumorigenesis. Proc Natl Acad Sci U S A. 2017 Jul 3;114(27):7077-7082.

Casciello F, Windloch K, Gannon F, Lee JS. Functional Role of G9a Histone Methyltransferase in Cancer. Front Immunol. 2015 Sep 25; 6:487.

Chanut P, Britton S, Coates J, Jackson SP, Calsou P. Coordinated nuclease activities counteract Ku at single-ended DNA double-strand breaks. Nat Commun. 2016 Sep 19; 7:12889.

Chen L, Li Z, Zwolinska AK, Smith MA, Cross B, Koomen J, Yuan ZM, Jenuwein T, Marine JC, Wright KL, Chen J. MDM2 recruitment of lysine methyltransferases regulates p53 transcriptional output. EMBO J. 2010 Aug 4;29(15):2538-52

Chen RJ, Shun CT, Yen ML, Chou CH, Lin MC. Methyltransferase G9a promotes cervical cancer angiogenesis and decreases patient survival. Oncotarget. 2017 Jul 7;8(37):62081-62098.

Chen S, Seiler J, Santiago-Reichelt M, Felbel K, Grummt I, Voit R. Repression of RNA polymerase I upon stress is caused by inhibition of RNA-dependent deacetylation of PAF53 by SIRT7. Mol Cell. 2013 Nov 7;52(3):303-13.

Chen WY, Wang DH, Yen RC, Luo J, Gu W, Baylin SB. Tumor suppressor HIC1 directly regulates SIRT1 to modulate p53-dependent DNA-damage responses. Cell. 2005 Nov 4;123(3):437-48.

Chen X, Mitsutake N, LaPerle K, Akeno N, Zanzonico P, Longo VA, Mitsutake S, Kimura ET, Geiger H, Santos E, Wendel HG, Franco A, Knauf JA, Fagin JA. Endogenous expression of Hras(G12V) induces developmental defects and neoplasms with copy number imbalances of the oncogene. Proc Natl Acad Sci U S A. 2009 May 12;106(19):7979-84.
Chen Y, Liu X, Li Y, Quan C, Zheng L, Huang K. Lung Cancer Therapy Targeting Histone Methylation: Opportunities and Challenges. Comput Struct Biotechnol J. 2018 Jun 20; 16:211-223.

Cheng WH, Kusumoto R, Opresko PL, Sui X, Huang S, Nicolette ML, Paull TT, Campisi J, Seidman M, Bohr VA. Collaboration of Werner syndrome protein and BRCA1 in cellular responses to DNA interstrand cross-links. Nucleic Acids Res. 2006 May 19;34(9):2751-60.

Cheng WH, von Kobbe C, Opresko PL, Arthur LM, Komatsu K, Seidman MM, Carney JP, Bohr VA. Linkage between Werner syndrome protein and the Mre11 complex via Nbs1. J Biol Chem. 2004 May 14;279(20):21169-76.

Cheng X, Collins RE, Zhang X. Structural and sequence motifs of protein (histone) methylation enzymes. Annu Rev Biophys Biomol Struct. 2005; 34:267-94.

Chiang WC, Tishkoff DX, Yang B, Wilson-Grady J, Yu X, Mazer T, Eckersdorff M, Gygi SP, Lombard DB, Hsu AL. C. elegans SIRT6/7 homolog SIR-2.4 promotes DAF-16 relocalization and function during stress. PLoS Genet. 2012 Sep;8(9):e1002948.

Chiba T, Saito T, Yuki K, Zen Y, Koide S, Kanogawa N, Motoyama T, Ogasawara S, Suzuki E, Ooka Y, Tawada A, Otsuka M, Miyazaki M, Iwama A, Yokosuka O. Histone lysine methyltransferase SUV39H1 is a potent target for epigenetic therapy of hepatocellular carcinoma. Int J Cancer. 2015 Jan 15;136(2):289-98.

Chowdhury D, Keogh MC, Ishii H, Peterson CL, Buratowski S, Lieberman J. gamma-H2AX dephosphorylation by protein phosphatase 2A facilitates DNA double-strand break repair. Mol Cell. 2005 Dec 9;20(5):801-9.

Chowdhury D, Xu X, Zhong X, Ahmed F, Zhong J, Liao J, Dykxhoorn DM, Weinstock DM, Pfeifer GP, Lieberman J. A PP4-phosphatase complex dephosphorylates gamma-H2AX generated during DNA replication. Mol Cell. 2008 Jul 11;31(1):33-46.

Chowdhury D, Xu X, Zhong X, Ahmed F, Zhong J, Liao J, Dykxhoorn DM, Weinstock DM, Pfeifer GP, Lieberman J. A PP4-phosphatase complex dephosphorylates gamma-H2AX generated during DNA replication. Mol Cell. 2008 Jul 11;31(1):33-46.

Clark AR, Ohlmeyer M. Protein phosphatase 2A as a therapeutic target in inflammation and neurodegeneration. Pharmacol Ther. 2019 Sep;201:181-201.

Collins R, Cheng X. A case study in cross-talk: the histone lysine methyltransferases G9a and GLP. Nucleic Acids Res. 2010 Jun;38(11):3503-11.

Dali-Youcef N, Lagouge M, Froelich S, Koehl C, Schoonjans K, Auwerx J. Sirtuins: the 'magnificent seven', function, metabolism and longevity. Ann Med. 2007;39(5):335-45.

Davey CA, Sargent DF, Luger K, Maeder AW, Richmond TJ. Solvent mediated interactions in the structure of the nucleosome core particle at 1.9 a resolution. J Mol Biol. 2002 Jun 21;319(5):1097-113.

Dell'Aversana C, Lepore I, Altucci L. HDAC modulation and cell death in the clinic. Exp Cell Res. 2012 Jul 1;318(11):1229–44.

Deng CX. SIRT1, is it a tumor promoter or tumor suppressor? Int J Biol Sci. 2009;5(2):147-52.

Desantis V, Lamanuzzi A, Vacca A. The role of SIRT6 in tumors. Haematologica. 2018 Jan;103(1):1-4.

Dillon SC, Zhang X, Trievel RC, Cheng X. The SET-domain protein superfamily: protein lysine methyltransferases. Genome Biol. 2005;6(8):227.

Dizdaroglu M, Olinski R, Doroshow JH, Akman SA. Modification of DNA bases in chromatin of intact target human cells by activated human polymorphonuclear leukocytes. Cancer Res. 1993 Mar 15;53(6):1269-72

Dobbin MM, Madabhushi R, Pan L, Chen Y, Kim D, Gao J, Ahanonu B, Pao PC, Qiu Y, Zhao Y, Tsai LH. SIRT1 collaborates with ATM and HDAC1 to maintain genomic stability in neurons. Nat Neurosci. 2013 Aug;16(8):1008-15.

Dominy JE Jr, Lee Y, Jedrychowski MP, Chim H, Jurczak MJ, Camporez JP, Ruan HB, Feldman J, Pierce K, Mostoslavsky R, Denu JM, Clish CB, Yang X, Shulman GI, Gygi SP, Puigserver P. The deacetylase Sirt6 activates the acetyltransferase GCN5 and suppresses hepatic gluconeogenesis. Mol Cell. 2012 Dec 28;48(6):900-13.

Dominy JE Jr, Lee Y, Jedrychowski MP, Chim H, Jurczak MJ, Camporez JP, Ruan HB, Feldman J, Pierce K, Mostoslavsky R, Denu JM, Clish CB, Yang X, Shulman GI, Gygi SP, Puigserver P. The deacetylase Sirt6 activates the acetyltransferase GCN5 and suppresses hepatic gluconeogenesis. Mol Cell. 2012 Dec 28;48(6):900-13.

Douglas P, Moorhead G, Xu X, Lees-Miller S. Choreographing the DNA damage response: PP6 joins the dance. Cell Cycle. 2010 Apr 1;9(7):1221-2.

Douglas P, Ye R, Trinkle-Mulcahy L, Neal JA, De Wever V, Morrice NA, Meek K, Lees-Miller SP. Polo-like kinase 1 (PLK1) and protein phosphatase 6 (PP6) regulate DNA-dependent protein kinase catalytic subunit (DNA-PKcs) phosphorylation in mitosis. Biosci Rep. 2014 Jun 25;34(3):e00113.

Douglas P, Zhong J, Ye R, Moorhead GB, Xu X, Lees-Miller SP. Protein phosphatase 6 interacts with the DNA-dependent protein kinase catalytic subunit and dephosphorylates gamma-H2AX. Mol Cell Biol. 2010 Mar;30(6):1368-81.

Downs JA, Allard S, Jobin-Robitaille O, Javaheri A, Auger A, Bouchard N, Kron SJ, Jackson SP, Côté J. Binding of chromatin-modifying activities to phosphorylated histone H2A at DNA damage sites. Mol Cell. 2004 Dec 22;16(6):979-90.

Dryden SC, Nahhas FA, Nowak JE, Goustin AS, Tainsky MA. Role for human SIRT2 NAD-dependent deacetylase activity in control of mitotic exit in the cell cycle. Mol Cell Biol. 2003 May;23(9):3173-85.

Du J, Zhou Y, Su X, Yu JJ, Khan S, Jiang H, Kim J, Woo J, Kim JH, Choi BH, He B, Chen W, Zhang S, Cerione RA, Auwerx J, Hao Q, Lin H. Sirt5 is a NAD-dependent protein lysine demalonylase and desuccinylase. Science. 2011 Nov 11;334(6057):806-9.

Dusinská M, Dzupinková Z, Wsólová L, Harrington V, Collins AR. Possible involvement of XPA in repair of oxidative DNA damage deduced from analysis of damage, repair and genotype in a human population study. Mutagenesis. 2006 May;21(3):205-11.

Edatt L, Poyyakkara A, Raji GR, Ramachandran V, Shankar SS, Kumar VBS. Role of Sirtuins in Tumor Angiogenesis. Front Oncol. 2020 Jan 17; 9:1516.

Egger G, Liang G, Aparicio A, Jones PA. Epigenetics in human disease and prospects for epigenetic therapy. Nature. 2004 May 27;429(6990):457-63.

Eichhorn PJ, Creyghton MP, Bernards R. Protein phosphatase 2A regulatory subunits and cancer. Biochim Biophys Acta. 2009 Jan;1795(1):1-15.

Elhanati S, Ben-Hamo R, Kanfi Y, Varvak A, Glazz R, Lerrer B, Efroni S, Cohen HY. Reciprocal Regulation between SIRT6 and miR-122 Controls Liver Metabolism and Predicts Hepatocarcinoma Prognosis. Cell Rep. 2016 Jan 12;14(2):234-42.

Elhanati S, Kanfi Y, Varvak A, Roichman A, Carmel-Gross I, Barth S, Gibor G, Cohen HY. Multiple regulatory layers of SREBP1/2 by SIRT6. Cell Rep. 2013 Sep 12;4(5):905-12

Elhanati S, Kanfi Y, Varvak A, Roichman A, Carmel-Gross I, Barth S, Gibor G, Cohen HY. Multiple regulatory layers of SREBP1/2 by SIRT6. Cell Rep. 2013 Sep 12;4(5):905-12.

Estève PO, Patnaik D, Chin HG, Benner J, Teitell MA, Pradhan S. Functional analysis of the N- and C-terminus of mammalian G9a histone H3 methyltransferase. Nucleic Acids Res. 2005 Jun 6;33(10):3211-23.

Etchegaray JP, Zhong L, Li C, Henriques T, Ablondi E, Nakadai T, Van Rechem C, Ferrer C, Ross KN, Choi JE, Samarakkody A, Ji F, Chang A, Sadreyev RI, Ramaswamy S, Nechaev S, Whetstine JR, Roeder RG, Adelman K, Goren A, Mostoslavsky R. The Histone

Deacetylase SIRT6 Restrains Transcription Elongation via Promoter-Proximal Pausing. Mol Cell. 2019 Aug 22;75(4):683-699.e7.

Eymery A, Callanan M, Vourc'h C. The secret message of heterochromatin: new insights into the mechanisms and function of centromeric and pericentric repeat sequence transcription. Int J Dev Biol. 2009;53(2-3):259-68.

Fan DN, Tsang FH, Tam AH, Au SL, Wong CC, Wei L, Lee JM, He X, Ng IO, Wong CM. Histone lysine methyltransferase, suppressor of variegation 3-9 homolog 1, promotes hepatocellular carcinoma progression and is negatively regulated by microRNA-125b. Hepatology. 2013 Feb;57(2):637-47.

Fan J, Li L, Small D, Rassool F. Cells expressing FLT3/ITD mutations exhibit elevated repair errors generated through alternative NHEJ pathways: implications for genomic instability and therapy. Blood. 2010 Dec 9;116(24):5298-305.

Fanning E, Klimovich V, Nager AR. A dynamic model for replication protein A (RPA) function in DNA processing pathways. Nucleic Acids Res. 2006;34(15):4126-37.

Feldman JL, Baeza J, Denu JM. Activation of the protein deacetylase SIRT6 by long-chain fatty acids and widespread deacylation by mammalian sirtuins. J Biol Chem. 2013 Oct 25;288(43):31350-6.

Felsenfeld G, Groudine M. Controlling the double helix. Nature. 2003 Jan 23;421(6921):448-53.

Feng Q, Wang H, Ng HH, Erdjument-Bromage H, Tempst P, Struhl K, et al. Methylation of H3-lysine 79 is mediated by a new family of HMTases without a SET domain. Curr Biol. 2002 Jun 25;12(12):1052–8.

Feng XX, Luo J, Liu M, Yan W, Zhou ZZ, Xia YJ, Tu W, Li PY, Feng ZH, Tian DA. Sirtuin 6 promotes transforming growth factor-β1/H2O2/HOCl-mediated enhancement of hepatocellular carcinoma cell tumorigenicity by suppressing cellular senescence. Cancer Sci. 2015 May;106(5):559-66.

Finley LW, Haigis MC. Metabolic regulation by SIRT3: implications for tumorigenesis. Trends Mol Med. 2012 Sep;18(9):516-23

Fioriniello S, Marano D, Fiorillo F, D'Esposito M, Della Ragione F. Epigenetic Factors That Control Pericentric Heterochromatin Organization in Mammals. Genes (Basel). 2020 May 28;11(6):595.

Firestein R, Blander G, Michan S, Oberdoerffer P, Ogino S, Campbell J, Bhimavarapu A, Luikenhuis S, de Cabo R, Fuchs C, Hahn WC, Guarente LP, Sinclair DA. The SIRT1 deacetylase suppresses intestinal tumorigenesis and colon cancer growth. PLoS One. 2008 Apr 16;3(4): e2020.

Firestein R, Cui X, Huie P, Cleary ML. Set domain-dependent regulation of transcriptional silencing and growth control by SUV39H1, a mammalian ortholog of Drosophila Su(var)3-9. Mol Cell Biol. 2000 Jul;20(13):4900-9.

Flotho A, Melchior F. Sumoylation: a regulatory protein modification in health and disease. Annu Rev Biochem. 2013; 82:357-85.

Flynn RL, Zou L. Oligonucleotide/oligosaccharide-binding fold proteins: a growing family of genome guardians. Crit Rev Biochem Mol Biol. 2010 Aug;45(4):266-75.

Ford E, Voit R, Liszt G, Magin C, Grummt I, Guarente L. Mammalian Sir2 homolog SIRT7 is an activator of RNA polymerase I transcription. Genes Dev. 2006 May 1;20(9):1075-80.

Frescas D, Valenti L, Accili D. Nuclear trapping of the forkhead transcription factor FoxO1 via Sirt-dependent deacetylation promotes expression of glucogenetic genes. J Biol Chem. 2005 May 27;280(21):20589-95.

Fulco M, Schiltz RL, Iezzi S, King MT, Zhao P, Kashiwaya Y, Hoffman E, Veech RL, Sartorelli V. Sir2 regulates skeletal muscle differentiation as a potential sensor of the redox state. Mol Cell. 2003 Jul;12(1):51-62.

Fulco M, Schiltz RL, Iezzi S, King MT, Zhao P, Kashiwaya Y, Hoffman E, Veech RL, Sartorelli V. Sir2 regulates skeletal muscle differentiation as a potential sensor of the redox state. Mol Cell. 2003 Jul;12(1):51-62.

Fussner E, Strauss M, Djuric U, Li R, Ahmed K, Hart M, Ellis J, Bazett-Jones DP. Open and closed domains in the mouse genome are configured as 10-nm chromatin fibres. EMBO Rep. 2012 Nov 6;13(11):992-6.

Gan L, Ladinsky MS, Jensen GJ. Chromatin in a marine picoeukaryote is a disordered assemblage of nucleosomes. Chromosoma. 2013 Oct;122(5):377-86.

Garipler G, Mutlu N, Lack NA, Dunn CD. Deletion of conserved protein phosphatases reverses defects associated with mitochondrial DNA damage in Saccharomyces cerevisiae. Proc Natl Acad Sci U S A. 2014 Jan 28;111(4):1473-8.

Gavande NS, VanderVere-Carozza PS, Hinshaw HD, Jalal SI, Sears CR, Pawelczak KS, Turchi JJ. DNA repair targeted therapy: The past or future of cancer treatment? Pharmacol Ther. 2016 Apr; 160:65-83.

Giet R, Glover DM. Drosophila aurora B kinase is required for histone H3 phosphorylation and condensin recruitment during chromosome condensation and to organize the central spindle during cytokinesis. J Cell Biol. 2001 Feb 19;152(4):669-82.

Gillette R, Miller-Crews I, Skinner MK, Crews D. Distinct actions of ancestral vinclozolin and juvenile stress on neural gene expression in the male rat. Front Genet. 2015 Mar 2; 6:56.

Gillette WK, Esposito D, Abreu Blanco M, Alexander P, Bindu L, Bittner C, Chertov O, Frank PH, Grose C, Jones JE, Meng Z, Perkins S, Van Q, Ghirlando R, Fivash M, Nissley DV, McCormick F, Holderfield M, Stephen AG. Farnesylated and methylated KRAS4b: high yield production of protein suitable for biophysical studies of prenylated protein-lipid interactions. Sci Rep. 2015 Nov 2; 5:15916.

Gingras AC, Caballero M, Zarske M, Sanchez A, Hazbun TR, Fields S, Sonenberg N, Hafen E, Raught B, Aebersold R. A novel, evolutionarily conserved protein phosphatase complex involved in cisplatin sensitivity. Mol Cell Proteomics. 2005 Nov;4(11):1725-40.

Goellner EM, Putnam CD, Graham WJ 5th, Rahal CM, Li BZ, Kolodner RD. Identification of Exo1-Msh2 interaction motifs in DNA mismatch repair and new Msh2-binding partners. Nat Struct Mol Biol. 2018 Aug;25(8):650-659.

Gomes P, Fleming Outeiro T, Cavadas C. Emerging Role of Sirtuin 2 in the Regulation of Mammalian Metabolism. Trends Pharmacol Sci. 2015 Nov;36(11):756-768.

Goto H., Tomono, Y., Ajiro, K., Kosako, H., Fujita, M., Sakurai, M., Okawa, K., Iwamatsu, A., Okigaki, T., Takahashi, T., et al. 1999. Identification of a novel phosphorylation site on histone H3 coupled with mitotic chromosome condensation. J. Biol. Chem. 274**:** 25543–25549.

Greer EL, Shi Y. Histone methylation: a dynamic mark in health, disease and inheritance. Nat Rev Genet. 2012 Apr 3;13(5):343-57.

Grummt I, Ladurner AG. A metabolic throttle regulates the epigenetic state of rDNA. Cell. 2008 May 16;133(4):577-80.
Guarente L. Franklin H. Epstein Lecture: Sirtuins, aging, and medicine. N Engl J Med. 2011 Jun 9;364(23):2235-44.

Gurley LR, D'Anna JA, Barham SS, Deaven LL, Tobey RA. Histone phosphorylation and chromatin structure during mitosis in Chinese hamster cells. Eur J Biochem. 1978 Mar;84(1):1-15.

Gutierrez MG, Mishra BB, Jordao L, Elliott E, Anes E, Griffiths G. NF-kappa B activation controls phagolysosome fusion-mediated killing of mycobacteria by macrophages. J Immunol. 2008 Aug 15;181(4):2651-63.

Gutierrez RM, Hnilica LS. Tissue specificity of histone phosphorylation. Science. 1967 Sep 15;157(3794):1324-5.

Gyory I, Wu J, Fejér G, Seto E, Wright KL. PRDI-BF1 recruits the histone H3 methyltransferase G9a in transcriptional silencing. Nat Immunol. 2004 Mar;5(3):299-308.

Haigis MC, Mostoslavsky R, Haigis KM, Fahie K, Christodoulou DC, et al. SIRT4 inhibits glutamate dehydrogenase and opposes the effects of calorie restriction in pancreatic β cells. Cell. 2006; 126:941–954.

Haigis MC, Sinclair DA. Mammalian sirtuins: biological insights and disease relevance. Annu Rev Pathol. 2010; 5:253-95.

Halder G, Johnson RL. Hippo signaling: growth control and beyond. Development. 2011 Jan;138(1):9-22.

Hallows WC, Lee S, Denu JM. Sirtuins deacetylate and activate mammalian acetyl-CoA synthetases. Proc Natl Acad Sci U S A. 2006 Jul 5;103(27):10230-10235.

Hallows WC, Yu W, Smith BC, Devries MK, Ellinger JJ, Someya S, Shortreed MR, Prolla T, Markley JL, Smith LM, Zhao S, Guan KL, Denu JM. Sirt3 promotes the urea cycle and fatty acid oxidation during dietary restriction. Mol Cell. 2011 Jan 21;41(2):139-49.

Hariharan N, Maejima Y, Nakae J, Paik J, Depinho RA, Sadoshima J. Deacetylation of FoxO by Sirt1 Plays an Essential Role in Mediating Starvation-Induced Autophagy in Cardiac Myocytes. Circ Res. 2010 Dec 10;107(12):1470-82.

Hastie CJ, Carnegie GK, Morrice N, Cohen PT. A novel 50 kDa protein forms complexes with protein phosphatase 4 and is located at centrosomal microtubule organizing centres. Biochem J. 2000 May 1;347 Pt 3(Pt 3):845-55.

Hayashi K, Momoi Y, Tanuma N, Kishimoto A, Ogoh H, Kato H, Suzuki M, Sakamoto Y, Inoue Y, Nomura M, Kiyonari H, Sakayori M, Fukamachi K, Kakugawa Y, Yamashita Y, Ito S, Sato I, Suzuki A, Nishio M, Suganuma M, Watanabe T, Shima H. Abrogation of protein phosphatase 6 promotes skin carcinogenesis induced by DMBA. Oncogene. 2015 Aug 27;34(35):4647-55.

Heintzman ND, Stuart RK, Hon G, Fu Y, Ching CW, Hawkins RD, et al. Distinct and predictive chromatin signatures of transcriptional promoters and enhancers in the human genome. Nat Genet. 2007 Mar;39(3):311–8.

Heinz S, Benner C, Spann N, Bertolino E, Lin YC, Laslo P, Cheng JX, Murre C, Singh H, Glass CK. Simple combinations of lineage-determining transcription factors prime cis-regulatory elements required for macrophage and B cell identities. Mol Cell. 2010 May 28;38(4):576-89.

Hendriks IA, D'Souza RCJ, Yang B, Vries MV-D, Mann M, Vertegaal ACO. Uncovering global SUMOylation signaling networks in a site-specific manner. Nature Structural & Molecular Biology. Nature Publishing Group; 2014 Sep 14;21(10):927–36.

Hendzel MJ, Wei Y, Mancini MA, Van Hooser A, Ranalli T, Brinkley BR, Bazett-Jones DP, Allis CD. Mitosis-specific phosphorylation of histone H3 initiates primarily within pericentromeric heterochromatin during G2 and spreads in an ordered fashion coincident with mitotic chromosome condensation. Chromosoma. 1997 Nov;106(6):348-60.

Hershberger KA, Martin AS, Hirschey MD. Role of NAD^+ and mitochondrial sirtuins in cardiac and renal diseases. Nat Rev Nephrol. 2017 Apr;13(4):213-225.

Hervera A, Zhou L, Palmisano I, McLachlan E, Kong G, Hutson TH, Danzi MC, Lemmon VP, Bixby JL, Matamoros-Angles A, Forsberg K, De Virgiliis F, Matheos DP, Kwapis J, Wood MA, Puttagunta R, Del Río JA, Di Giovanni S. PP4-dependent HDAC3 dephosphorylation discriminates between axonal regeneration and regenerative failure. EMBO J. 2019 Jul 1;38(13):e101032.

Hirschey MD, Shimazu T, Goetzman E, Jing E, Schwer B, Lombard DB, Grueter CA, Harris C, Biddinger S, Ilkayeva OR, Stevens RD, Li Y, Saha AK, Ruderman NB, Bain JR, Newgard CB, Farese RV Jr, Alt FW, Kahn CR, Verdin E. SIRT3 regulates mitochondrial fatty-acid oxidation by reversible enzyme deacetylation. Nature. 2010 Mar 4;464(7285):121-5.

Hisahara S, Chiba S, Matsumoto H, Tanno M, Yagi H, Shimohama S, Sato M, Horio Y. Histone deacetylase SIRT1 modulates neuronal differentiation by its nuclear translocation. Proc Natl Acad Sci U S A. 2008 Oct 7;105(40):15599-604.

Ho JC, Abdullah LN, Pang QY, Jha S, Chow EK, Yang H, Kato H, Poellinger L, Ueda J, Lee KL. Inhibition of the H3K9 methyltransferase G9A attenuates oncogenicity and activates the hypoxia signaling pathway. PLoS One. 2017 Nov 16;12(11): e0188051.

Hoeijmakers JH. Genome maintenance mechanisms for preventing cancer. Nature. 2001 May 17;411(6835):366-74.

Horton JD, Goldstein JL, Brown MS. SREBPs: activators of the complete program of cholesterol and fatty acid synthesis in the liver. J Clin Invest. 2002 May;109(9):1125-31.

Hou T, Cao Z, Zhang J, Tang M, Tian Y, Li Y, Lu X, Chen Y, Wang H, Wei FZ, Wang L, Yang Y, Zhao Y, Wang Z, Wang H, Zhu WG. SIRT6 coordinates with CHD4 to promote chromatin relaxation and DNA repair. Nucleic Acids Res. 2020 Apr 6;48(6):2982-3000.

Huang J, Dorsey J, Chuikov S, Zhang X, Jenuwein T, Reinberg D, Berger SL. G9a and Glp methylate lysine 373 in the tumor suppressor p53. J Biol Chem. 2010 Mar 26;285(13):9636-9641.

Huang J, Xue L. Loss of flfl Triggers JNK-Dependent Cell Death in Drosophila. Biomed Res Int. 2015; 2015:623573.

Iftode C, Daniely Y, Borowiec JA. Replication protein A (RPA): the eukaryotic SSB. Crit Rev Biochem Mol Biol. 1999;34(3):141-80.

Imai S, Armstrong CM, Kaeberlein M, Guarente L. Transcriptional silencing and longevity protein Sir2 is an NAD-dependent histone deacetylase. Nature. 2000 Feb 17;403(6771):795-800.

Inoue T, Hiratsuka M, Osaki M, Oshimura M. The molecular biology of mammalian SIRT proteins: SIRT2 in cell cycle regulation. Cell Cycle. 2007 May 2;6(9):1011-8.

Isono M, Niimi A, Oike T, Hagiwara Y, Sato H, Sekine R, Yoshida Y, Isobe SY, Obuse C, Nishi R, Petricci E, Nakada S, Nakano T, Shibata A. BRCA1 Directs the Repair Pathway to Homologous Recombination by Promoting 53BP1 Dephosphorylation. Cell Rep. 2017 Jan 10;18(2):520-532.

Iyer RR, Pluciennik A, Burdett V, Modrich PL. DNA mismatch repair: functions and mechanisms. Chem Rev. 2006 Feb;106(2):302-23.

Izumi H, Inoue J, Yokoi S, Hosoda H, Shibata T, Sunamori M, Hirohashi S, Inazawa J, Imoto I. Frequent silencing of DBC1 is by genetic or epigenetic mechanisms in non-small cell lung cancers. Hum Mol Genet. 2005 Apr 15;14(8):997-1007.

Janssens V, Goris J. Protein phosphatase 2A: a highly regulated family of serine/threonine phosphatases implicated in cell growth and signalling. Biochem J. 2001 Feb 1;353(Pt 3):417-39.

Jarrett SG, Carter KM, Bautista RM, He D, Wang C, D'Orazio JA. Sirtuin 1-mediated deacetylation of XPA DNA repair protein enhances its interaction with ATR protein and promotes cAMP-induced DNA repair of UV damage. J Biol Chem. 2018 Dec 7;293(49):19025-19037.

Jeong J, Juhn K, Lee H, Kim SH, Min BH, Lee KM, Cho MH, Park GH, Lee KH. SIRT1 promotes DNA repair activity and deacetylation of Ku70. Exp Mol Med. 2007 Feb 28;39(1):8-13.

Jia H, Liu Y, Yan W, Jia J. PP4 and PP2A regulate Hedgehog signaling by controlling Smo and Ci phosphorylation. Development. 2009 Jan;136(2):307-16.

Jiang C, Pugh BF. Nucleosome positioning and gene regulation: advances through genomics. Nat Rev Genet. 2009 Mar;10(3):161-72.

Jiang H, Khan S, Wang Y, Charron G, He B, Sebastian C, Du J, Kim R, Ge E, Mostoslavsky R, Hang HC, Hao Q, Lin H. SIRT6 regulates TNF-α secretion through hydrolysis of long-chain fatty acyl lysine. Nature. 2013 Apr 4;496(7443):110-3.

Jokinen R, Pirnes-Karhu S, Pietiläinen KH, Pirinen E. Adipose tissue NAD^+-homeostasis, sirtuins and poly(ADP-ribose) polymerases -important players in mitochondrial metabolism and metabolic health. Redox Biol. 2017 Aug; 12:246-263.

Joo H-Y, Zhai L, Yang C, Nie S, Erdjument-Bromage H, Tempst P, et al. Regulation of cell cycle progression and gene expression by H2A deubiquitination. Nature. 2007 Oct 25;449(7165):1068–72.

Jung HR, Pasini D, Helin K, Jensen ON. Quantitative mass spectrometry of histones H3.2 and H3.3 in Suz12-deficient mouse embryonic stem cells reveals distinct, dynamic post-translational modifications at Lys-27 and Lys-36. Mol Cell Proteomics. 2010 May;9(5):838-50.

Kajino T, Ren H, Iemura S, Natsume T, Stefansson B, Brautigan DL, Matsumoto K, Ninomiya-Tsuji J. Protein phosphatase 6 down-regulates TAK1 kinase activation in the IL-1 signaling pathway. J Biol Chem. 2006 Dec 29;281(52):39891-6.

Kanfi Y, Naiman S, Amir G, Peshti V, Zinman G, Nahum L, Bar-Joseph Z, Cohen HY. The sirtuin SIRT6 regulates lifespan in male mice. Nature. 2012 Feb 22;483(7388):218-21.

Kanfi Y, Peshti V, Gil R, Naiman S, Nahum L, Levin E, Kronfeld-Schor N, Cohen HY. SIRT6 protects against pathological damage caused by diet-induced obesity. Aging Cell. 2010 Apr;9(2):162-73.

Kanfi Y, Shalman R, Peshti V, Pilosof SN, Gozlan YM, Pearson KJ, Lerrer B, Moazed D, Marine JC, de Cabo R, Cohen HY. Regulation of SIRT6 protein levels by nutrient availability. FEBS Lett. 2008 Mar 5;582(5):543-8.

Kasprzak KS, Jaruga P, Zastawny TH, North SL, Riggs CW, Olinski R, Dizdaroglu M. Oxidative DNA base damage and its repair in kidneys and livers of nickel(II)-treated male F344 rats. Carcinogenesis. 1997 Feb;18(2):271-7.

Kato H, Kurosawa K, Inoue Y, Tanuma N, Momoi Y, Hayashi K, Ogoh H, Nomura M, Sakayori M, Kakugawa Y, Yamashita Y, Miura K, Maemondo M, Katakura R, Ito S, Sato M, Sato I, Chiba N, Watanabe T, Shima H. Loss of protein phosphatase 6 in mouse keratinocytes increases susceptibility to ultraviolet-B-induced carcinogenesis. Cancer Lett. 2015 Sep 1;365(2):223-8.

Kaufmann T, Kukolj E, Brachner A, Beltzung E, Bruno M, Kostrhon S, Opravil S, Hudecz O, Mechtler K, Warren G, Slade D. SIRT2 regulates nuclear envelope reassembly through ANKLE2 deacetylation. J Cell Sci. 2016 Dec 15;129(24):4607-4621.

Kauppinen A, Suuronen T, Ojala J, Kaarniranta K, Salminen A. Antagonistic crosstalk between NF-κB and SIRT1 in the regulation of inflammation and metabolic disorders. Cell Signal. 2013 Oct;25(10):1939-48.

Kawahara TL, Michishita E, Adler AS, Damian M, Berber E, Lin M, McCord RA, Ongaigui KC, Boxer LD, Chang HY, Chua KF. SIRT6 links histone H3 lysine 9 deacetylation to NF-kappaB-dependent gene expression and organismal life span. Cell. 2009 Jan 9;136(1):62-74.

Kawahara TL, Rapicavoli NA, Wu AR, Qu K, Quake SR, Chang HY. Dynamic chromatin localization of Sirt6 shapes stress- and aging-related transcriptional networks. PLoS Genet. 2011Jun;7(6):e1002153.

Ke J, Wu R, Chen Y, Abba ML. Inhibitor of DNA binding proteins: implications in human cancer progression and metastasis. Am J Transl Res. 2018 Dec 15;10(12):3887-3910.

Keogh MC, Kim JA, Downey M, Fillingham J, Chowdhury D, Harrison JC, Onishi M, Datta N, Galicia S, Emili A, Lieberman J, Shen X, Buratowski S, Haber JE, Durocher D, Greenblatt JF, Krogan NJ. A phosphatase complex that dephosphorylates gammaH2AX regulates DNA damage checkpoint recovery. Nature. 2006 Jan 26;439(7075):497-501.

Keshav KF, Chen C, Dutta A. Rpa4, a homolog of the 34-kilodalton subunit of the replication protein A complex. Mol Cell Biol. 1995 Jun;15(6):3119-28.

Kim HS, Xiao C, Wang RH, Lahusen T, Xu X, Vassilopoulos A, Vazquez-Ortiz G, Jeong WI, Park O, Ki SH, Gao B, Deng CX. Hepatic-specific disruption of SIRT6 in mice results in fatty liver formation due to enhanced glycolysis and triglyceride synthesis. Cell Metab. 2010 Sep 8;12(3):224-36

Kim JA, Hicks WM, Li J, Tay SY, Haber JE. Protein phosphatases pph3, ptc2, and ptc3 play redundant roles in DNA double-strand break repair by homologous recombination. Mol Cell Biol. 2011 Feb;31(3):507-16.

Kim JE, Chen J, Lou Z. DBC1 is a negative regulator of SIRT1. Nature. 2008 Jan 31;451(7178):583-6.

Kim YJ, Wilson DM 3rd. Overview of base excision repair biochemistry. Curr Mol Pharmacol. 2012 Jan;5(1):3-13

Kloeker S, Reed R, McConnell JL, Chang D, Tran K, Westphal RS, Law BK, Colbran RJ, Kamoun M, Campbell KS, Wadzinski BE. Parallel purification of three catalytic subunits of the protein serine/threonine phosphatase 2A family (PP2A(C), PP4(C), and PP6(C)) and analysis of the interaction of PP2A(C) with alpha4 protein. Protein Expr Purif. 2003 Sep;31(1):19-33.

Kobayashi J, Tauchi H, Sakamoto S, Nakamura A, Morishima K, Matsuura S, Kobayashi T, Tamai K, Tanimoto K, Komatsu K. NBS1 localizes to gamma-H2AX foci through interaction with the FHA/BRCT domain. Curr Biol. 2002 Oct 29;12(21):1846-51.

Kobayashi Y, Furukawa-Hibi Y, Chen C, Horio Y, Isobe K, Ikeda K, Motoyama N. SIRT1 is critical regulator of FOXO-mediated transcription in response to oxidative stress. Int J Mol Med. 2005 Aug;16(2):237-43.

Kondo Y, Shen L, Ahmed S, Boumber Y, Sekido Y, Haddad BR, Issa JP. Downregulation of histone H3 lysine 9 methyltransferase G9a induces centrosome disruption and chromosome instability in cancer cells. PLoS One. 2008 Apr 30;3(4): e2037.

Kornberg RD. The molecular basis of eucaryotic transcription. Cell Death Differ. 2007 Dec;14(12):1989-97.

Krishnan J, Danzer C, Simka T, Ukropec J, Walter KM, Kumpf S, Mirtschink P, Ukropcova B, Gasperikova D, Pedrazzini T, Krek W. Dietary obesity-associated Hif1α activation in adipocytes restricts fatty acid oxidation and energy expenditure via suppression of the Sirt2-NAD+ system. Genes Dev. 2012 Feb 1;26(3):259-70.

Kugel S, Feldman JL, Klein MA, Silberman DM, Sebastián C, Mermel C, Dobersch S, Clark AR, Getz G, Denu JM, Mostoslavsky R. Identification of and Molecular Basis for SIRT6 Loss-of-Function Point Mutations in Cancer. Cell Rep. 2015 Oct 20;13(3):479-488.

Kugel S, Sebastián C, Fitamant J, Ross KN, Saha SK, Jain E, Gladden A, Arora KS, Kato Y, Rivera MN, Ramaswamy S, Sadreyev RI, Goren A, Deshpande V, Bardeesy N, Mostoslavsky R. SIRT6 Suppresses Pancreatic Cancer through Control of Lin28b. Cell. 2016 Jun 2;165(6):1401-1415.

Kulkarni S, Hicks DG. HER2-positive early breast cancer and trastuzumab: a surgeon's perspective. Ann Surg Oncol. 2008 Jun;15(6):1677-88.

Kwon J, Lee S, Kim YN, Lee IH. Deacetylation of CHK2 by SIRT1 protects cells from oxidative stress-dependent DNA damage response. Exp Mol Med. 2019 Mar 22;51(3):1-9.

Langan TA. Histone phosphorylation: stimulation by adenosine 3',5'-monophosphate. Science. 1968 Nov 1;162(3853):579-80.

Langie SA, Knaapen AM, Houben JM, van Kempen FC, de Hoon JP, Gottschalk RW, Godschalk RW, van Schooten FJ. The role of glutathione in the regulation of nucleotide excision repair during oxidative stress. Toxicol Lett. 2007 Feb 5;168(3):302-9.

Langmead B, Trapnell C, Pop M, Salzberg SL. Ultrafast and memory-efficient alignment of short DNA sequences to the human genome. Genome Biol. 2009;10(3):R25.

Latypov VF, Tubbs JL, Watson AJ, Marriott AS, McGown G, Thorncroft M, Wilkinson OJ, Senthong P, Butt A, Arvai AS, Millington CL, Povey AC, Williams DM, Santibanez-Koref MF, Tainer JA, Margison GP. Atl1 regulates choice between global genome and transcription-coupled repair of O(6)-alkylguanines. Mol Cell. 2012 Jul 13;47(1):50-60.

Lee A, Moon BI, Kim TH. *BRCA1*/*BRCA2* Pathogenic Variant Breast Cancer: Treatment and Prevention Strategies. Ann Lab Med. 2020 Mar;40(2):114-121.

Lee DH, Acharya SS, Kwon M, Drane P, Guan Y, Adelmant G, Kalev P, Shah J, Pellman D, Marto JA, Chowdhury D. Dephosphorylation enables the recruitment of 53BP1 to double-strand DNA breaks. Mol Cell. 2014 May 8;54(3):512-25.

Lee DH, Goodarzi AA, Adelmant GO, Pan Y, Jeggo PA, Marto JA, Chowdhury D. Phosphoproteomic analysis reveals that PP4 dephosphorylates KAP-1 impacting the DNA damage response. EMBO J. 2012 May 16;31(10):2403-15.

Lee DH, Pan Y, Kanner S, Sung P, Borowiec JA, Chowdhury D. A PP4 phosphatase complex dephosphorylates RPA2 to facilitate DNA repair via homologous recombination. Nat Struct Mol Biol. 2010 Mar;17(3):365-72.

Lee J, Adelmant G, Marto JA, Lee DH. Dephosphorylation of DBC1 by Protein Phosphatase 4 Is Important for p53-Mediated Cellular Functions. Mol Cells. 2015 Aug;38(8):697-704.

Lee MJ, Yaffe MB. Protein Regulation in Signal Transduction. Cold Spring Harb Perspect Biol. 2016 Jun 1;8(6):a005918.

Li H, Handsaker B, Wysoker A, Fennell T, Ruan J, Homer N, Marth G, Abecasis G, Durbin R; 1000 Genome Project Data Processing Subgroup. The Sequence Alignment/Map format and SAMtools. Bioinformatics. 2009 Aug 15;25(16):2078-9.

Li H, Ilin S, Wang W, Duncan EM, Wysocka J, Allis CD, Patel DJ. Molecular basis for site-specific read-out of histone H3K4me3 by the BPTF PHD finger of NURF. Nature. 2006 Jul 6;442(7098):91-5.

Li K, Casta A, Wang R, Lozada E, Fan W, Kane S, Ge Q, Gu W, Orren D, Luo J. Regulation of WRN protein cellular localization and enzymatic activities by SIRT1-mediated deacetylation. J Biol Chem. 2008 Mar 21;283(12):7590-8.

Li X, Wilmanns M, Thornton J, Köhn M. Elucidating human phosphatase-substrate networks. Sci Signal. 2013 May 14;6(275):rs10.

Li X, Zhang S, Blander G, Tse JG, Krieger M, Guarente L. SIRT1 deacetylates and positively regulates the nuclear receptor LXR. Mol Cell. 2007 Oct 12;28(1):91-106.

Li Z, Xu K, Zhang N, Amador G, Wang Y, Zhao S, Li L, Qiu Y, Wang Z. Overexpressed SIRT6 attenuates cisplatin-induced acute kidney injury by inhibiting ERK1/2 signaling. Kidney Int. 2018 Apr;93(4):881-892.

Liaw H, Lee D, Myung K. DNA-PK-dependent RPA2 hyperphosphorylation facilitates DNA repair and suppresses sister chromatid exchange. PLoS One. 2011;6(6): e21424.

Lim CS, Potts M, Helm RF. Nicotinamide extends the replicative life span of primary human cells. Mech Ageing Dev. 2006 Jun;127(6):511-4.

Lin S, Gregory RI. MicroRNA biogenesis pathways in cancer. Nat Rev Cancer. 2015 Jun;15(6):321-33.

Lin YH, Yuan J, Pei H, Liu T, Ann DK, Lou Z. PLoS One. 2015 Apr 23;10(4):e0123935.

Lipinszki Z, Lefevre S, Savoian MS, Singleton MR, Glover DM, Przewloka MR. Centromeric binding and activity of Protein Phosphatase 4. Nat Commun. 2015 Jan 6; 6:5894.

Liszt G, Ford E, Kurtev M, Guarente L. Mouse Sir2 homolog SIRT6 is a nuclear ADP-ribosyltransferase. J Biol Chem. 2005 Jun 3;280(22):21313-20.

Liu B, Wang Z, Zhang L, Ghosh S, Zheng H, Zhou Z. Depleting the methyltransferase Suv39h1 improves DNA repair and extends lifespan in a progeria mouse model. Nat Commun. 2013; 4:1868.

Liu CL, Kaplan T, Kim M, Buratowski S, Schreiber SL, Friedman N, Rando OJ. Single-nucleosome mapping of histone modifications in S. cerevisiae. PLoS Biol. 2005 Oct;3(10): e328.

Liu G, Chen H, Liu H, Zhang W, Zhou J. Emerging roles of SIRT6 in human diseases and its modulators. Med Res Rev. 2021 Mar;41(2):1089-1137.

Liu J, Xu L, Zhong J, Liao J, Li J, Xu X. Protein phosphatase PP4 is involved in NHEJ-mediated repair of DNA double-strand breaks. Cell Cycle. 2012 Jul 15;11(14):2643-9.

Liu Y, Dentin R, Chen D, Hedrick S, Ravnskjaer K, Schenk S, Milne J, Meyers DJ, Cole P, Yates J 3rd, Olefsky J, Guarente L, Montminy M. A fasting inducible switch modulates gluconeogenesis via activator/coactivator exchange. Nature. 2008 Nov 13;456(7219):269-73.

Lombard DB, Alt FW, Cheng HL, Bunkenborg J, Streeper RS, Mostoslavsky R, Kim J, Yancopoulos G, Valenzuela D, Murphy A, Yang Y, Chen Y, Hirschey MD, Bronson RT, Haigis M, Guarente LP, Farese RV Jr, Weissman S, Verdin E, Schwer B. Mammalian Sir2 homolog SIRT3 regulates global mitochondrial lysine acetylation. Mol Cell Biol. 2007 Dec;27(24):8807-14.

Loyola A, Tagami H, Bonaldi T, Roche D, Quivy JP, Imhof A, Nakatani Y, Dent SY, Almouzni G. The HP1alpha-CAF1-SetDB1-containing complex provides H3K9me1 for Suv39-mediated K9me3 in pericentric heterochromatin. EMBO Rep. 2009 Jul;10(7):769-75.

Lu J, Sun D, Liu Z, Li M, Hong H, Liu C, Gao S, Li H, Cai Y, Chen S, Li Z, Ye J, Liu P. SIRT6 suppresses isoproterenol-induced cardiac hypertrophy through activation of autophagy. Transl Res. 2016 Jun; 172:96-112.e6.

Luger K, Mäder AW, Richmond RK, Sargent DF, Richmond TJ. Crystal structure of the nucleosome core particle at 2.8 A resolution. Nature. 1997 Sep 18;389(6648):251-60.

Luo G, Jian Z, Zhu Y, Zhu Y, Chen B, Ma R, Tang F, Xiao Y. Sirt1 promotes autophagy and inhibits apoptosis to protect cardiomyocytes from hypoxic stress. Int J Mol Med. 2019 May;43(5):2033-2043.

Luo J, Nikolaev AY, Imai S, Chen D, Su F, Shiloh A, Guarente L, Gu W. Negative control of p53 by Sir2alpha promotes cell survival under stress. Cell. 2001 Oct 19;107(2):137-48.

Lyu J, Kim HR, Yamamoto V, Choi SH, Wei Z, Joo CK, Lu W. Protein phosphatase 4 and Smek complex negatively regulate Par3 and promote neuronal differentiation of neural stem/progenitor cells. Cell Rep. 2013 Nov 14;5(3):593-600.

Maeshima K, Hihara S, Eltsov M. Chromatin structure: does the 30-nm fibre exist in vivo? Curr Opin Cell Biol. 2010 Jun;22(3):291-7.

Maeshima K, Rogge R, Tamura S, Joti Y, Hikima T, Szerlong H, Krause C, Herman J, Seidel E, DeLuca J, Ishikawa T, Hansen JC. Nucleosomal arrays self-assemble into supramolecular globular structures lacking 30-nm fibers. EMBO J. 2016 May 17;35(10):1115-32.

Maeshima K, Rogge R, Tamura S, Joti Y, Hikima T, Szerlong H, Krause C, Herman J, Seidel E, DeLuca J, Ishikawa T, Hansen JC. Nucleosomal arrays self-assemble into supramolecular globular structures lacking 30-nm fibers. EMBO J. 2016 May 17;35(10):1115-32.

Mantel C, Broxmeyer HE. Sirtuin 1, stem cells, aging, and stem cell aging. Curr Opin Hematol. 2008 Jul;15(4):326-31.

Mao Z, Bozzella M, Seluanov A, Gorbunova V. DNA repair by nonhomologous end joining and homologous recombination during cell cycle in human cells. Cell Cycle. 2008 Sep 15;7(18):2902-6.

Mao Z, Bozzella M, Seluanov A, Gorbunova V. DNA repair by nonhomologous end joining and homologous recombination during cell cycle in human cells. Cell Cycle. 2008 Sep 15;7(18):2902-6.

Mao Z, Hine C, Tian X, Van Meter M, Au M, Vaidya A, Seluanov A, Gorbunova V. SIRT6 promotes DNA repair under stress by activating PARP1.

Martin L, Latypova X, Wilson CM, Magnaudeix A, Perrin ML, Yardin C, Terro F. Tau protein kinases: involvement in Alzheimer's disease. Ageing Res Rev. 2013 Jan;12(1):289-309.

MARTIN, Marcel. Cutadapt removes adapter sequences from high-throughput sequencing reads. EMBnet.journal, [S.l.], v. 17, n. 1, p. pp. 10-12, may 2011. ISSN 2226-6089.

Martínez-Redondo P, Vaquero A. The diversity of histone versus nonhistone sirtuin substrates. Genes Cancer. 2013 Mar;4(3-4):148-63.

Maselli GA, Slamovits CH, Bianchi JI, Vilarrasa-Blasi J, Caño-Delgado AI, Mora-García S. Revisiting the evolutionary history and roles of protein phosphatases with Kelch-like domains in plants. Plant Physiol. 2014 Mar;164(3):1527-41.

Masutani C, Kusumoto R, Iwai S, Hanaoka F. Mechanisms of accurate translesion synthesis by human DNA polymerase eta. EMBO J. 2000 Jun 15;19(12):3100-9.

Matsushita N, Yonashiro R, Ogata Y, Sugiura A, Nagashima S, Fukuda T, Inatome R, Yanagi S. Distinct regulation of mitochondrial localization and stability of two human Sirt5 isoforms. Genes Cells. 2011 Feb;16(2):190-202.

Matsuzaki H, Daitoku H, Hatta M, Aoyama H, Yoshimochi K, Fukamizu A. Acetylation of Foxo1 alters its DNA-binding ability and sensitivity to phosphorylation. Proc Natl Acad Sci U S A. 2005 Aug 9;102(32):11278-83.

McArthur K, Feng B, Wu Y, Chen S, Chakrabarti S. MicroRNA-200b regulates vascular endothelial growth factor-mediated alterations in diabetic retinopathy. Diabetes. 2011 Apr;60(4):1314-23.

McCord RA, Michishita E, Hong T, Berber E, Boxer LD, Kusumoto R, Guan S, Shi X, Gozani O, Burlingame AL, Bohr VA, Chua KF. SIRT6 stabilizes DNA-dependent protein kinase at chromatin for DNA double-strand break repair. Aging (Albany NY). 2009 Jan 15;1(1):109-21.

Melcher M, Schmid M, Aagaard L, Selenko P, Laible G, Jenuwein T. Structure-function analysis of SUV39H1 reveals a dominant role in heterochromatin organization, chromosome segregation, and mitotic progression. Mol Cell Biol. 2000 May;20(10):3728-41.

Melis JP, van Steeg H, Luijten M. Oxidative DNA damage and nucleotide excision repair. Antioxid Redox Signal. 2013 Jun 20;18(18):2409-19.

Mendoza MC, Booth EO, Shaulsky G, Firtel RA. MEK1 and protein phosphatase 4 coordinate Dictyostelium development and chemotaxis. Mol Cell Biol. 2007 May;27(10):3817-27.

Messner S, Altmeyer M, Zhao H, Pozivil A, Roschitzki B, Gehrig P, et al. PARP1 ADP-ribosylates lysine residues of the core histone tails. Nucleic Acids Research. Oxford University Press; 2010 Oct;38(19):6350–62.

Messner S, Hottiger MO. Histone ADP-ribosylation in DNA repair, replication and transcription. Trends in Cell Biology. Elsevier Ltd; 2011 Sep 1;21(9):534–42.

Mi J, Dziegielewski J, Bolesta E, Brautigan DL, Larner JM. Activation of DNA-PK by ionizing radiation is mediated by protein phosphatase 6. PLoS One. 2009;4(2): e4395.

Michishita E, McCord RA, Berber E, Kioi M, Padilla-Nash H, Damian M, Cheung P, Kusumoto R, Kawahara TL, Barrett JC, Chang HY, Bohr VA, Ried T, Gozani O, Chua KF. SIRT6 is a histone H3 lysine 9 deacetylase that modulates telomeric chromatin. Nature. 2008 Mar 27;452(7186):492-6

Michishita E, McCord RA, Boxer LD, Barber MF, Hong T, Gozani O, Chua KF. Cell cycle-dependent deacetylation of telomeric histone H3 lysine K56 by human SIRT6. Cell Cycle. 2009 Aug 15;8(16):2664-6

Mihindukulasuriya KA, Zhou G, Qin J, Tan TH. Protein phosphatase 4 interacts with and down-regulates insulin receptor substrate 4 following tumor necrosis factor-alpha stimulation. J Biol Chem. 2004 Nov 5;279(45):46588-94.

Miller J, Gordon C. The regulation of proteasome degradation by multi-ubiquitin chain binding proteins. FEBS Letters. 2005 Jun 13;579(15):3224–30.

Min L, Ji Y, Bakiri L, Qiu Z, Cen J, Chen X, Chen L, Scheuch H, Zheng H, Qin L, Zatloukal K, Hui L, Wagner EF. Liver cancer initiation is controlled by AP-1 through SIRT6-dependent inhibition of survivin. Nat Cell Biol. 2012 Nov;14(11):1203-11.

Min Z, Gao J, Yu Y. The Roles of Mitochondrial SIRT4 in Cellular Metabolism. Front Endocrinol (Lausanne). 2019 Jan 7; 9:783.

Ming M, Shea CR, Guo X, Li X, Soltani K, Han W, He YY. Regulation of global genome nucleotide excision repair by SIRT1 through xeroderma pigmentosum C. Proc Natl Acad Sci U S A. 2010 Dec 28;107(52):22623-8.

Morigi M, Perico L, Benigni A. Sirtuins in Renal Health and Disease. J Am Soc Nephrol. 2018 Jul;29(7):1799-1809.

Mostoslavsky R, Chua KF, Lombard DB, Pang WW, Fischer MR, Gellon L, Liu P, Mostoslavsky G, Franco S, Murphy MM, Mills KD, Patel P, Hsu JT, Hong AL, Ford E, Cheng HL, Kennedy C, Nunez N, Bronson R, Frendewey D, Auerbach W, Valenzuela D, Karow M, Hottiger MO, Hursting S, Barrett JC, Guarente L, Mulligan R, Demple B, Yancopoulos GD, Alt FW. Genomic instability and aging-like phenotype in the absence of mammalian SIRT6. Cell. 2006 Jan 27;124(2):315-29.

Mourtada-Maarabouni M, Kirkham L, Jenkins B, Rayner J, Gonda TJ, Starr R, Trayner I, Farzaneh F, Williams GT. Functional expression cloning reveals proapoptotic role for protein phosphatase 4. Cell Death Differ. 2003 Sep;10(9):1016-24.

Mozzetta C, Pontis J, Fritsch L, Robin P, Portoso M, Proux C, Margueron R, Ait-Si-Ali S. The histone H3 lysine 9 methyltransferases G9a and GLP regulate polycomb repressive complex 2-mediated gene silencing. Mol Cell. 2014 Jan 23;53(2):277-89.

Mumby M. PP2A: unveiling a reluctant tumor suppressor. Cell. 2007 Jul 13;130(1):21-4.

Murayama A, Ohmori K, Fujimura A, Minami H, Yasuzawa-Tanaka K, Kuroda T, Oie S, Daitoku H, Okuwaki M, Nagata K, Fukamizu A, Kimura K, Shimizu T, Yanagisawa J. Epigenetic control of rDNA loci in response to intracellular energy status. Cell. 2008 May 16;133(4):627-39.

Nakada S, Chen GI, Gingras AC, Durocher D. PP4 is a gamma H2AX phosphatase required for recovery from the DNA damage checkpoint. EMBO Rep. 2008 Oct;9(10):1019-26.

Nakagawa T, Kajitani T, Togo S, Masuko N, Ohdan H, Hishikawa Y, et al. Deubiquitylation of histone H2A activates transcriptional initiation via trans-histone cross-talk with H3K4 di- and trimethylation. Genes & Development. 2008 Jan 1;22(1):37–49.

Nasrin N, Kaushik VK, Fortier E, Wall D, Pearson KJ, de Cabo R, Bordone L. JNK1 phosphorylates SIRT1 and promotes its enzymatic activity. PLoS One. 2009 Dec 22;4(12):e8414.

Nestler EJ, Greengard P. Protein Phosphorylation is of Fundamental Importance in Biological Regulation. In: Siegel GJ, Agranoff BW, Albers RW, et al., editors. Basic Neurochemistry: Molecular, Cellular and Medical Aspects. 6th edition. Philadelphia: Lippincott-Raven; 1999.

Nielsen SJ, Schneider R, Bauer UM, Bannister AJ, Morrison A, O'Carroll D, Firestein R, Cleary M, Jenuwein T, Herrera RE, Kouzarides T. Rb targets histone H3 methylation and HP1 to promoters. Nature. 2001 Aug 2;412(6846):561-5.

Nishida Y, Rardin MJ, Carrico C, He W, Sahu AK, Gut P, Najjar R, Fitch M, Hellerstein M, Gibson BW, Verdin E. SIRT5 Regulates both Cytosolic and Mitochondrial Protein Malonylation with Glycolysis as a Major Target. Mol Cell. 2015 Jul 16;59(2):321-32.

Nishio H, Walsh MJ. CCAAT displacement protein/cut homolog recruits G9a histone lysine methyltransferase to repress transcription. Proc Natl Acad Sci U S A. 2004 Aug 3;101(31):11257-62.

Niu H, Erdjument-Bromage H, Pan ZQ, Lee SH, Tempst P, Hurwitz J. Mapping of amino acid residues in the p34 subunit of human single-stranded DNA-binding protein phosphorylated by DNA-dependent protein kinase and Cdc2 kinase in vitro. J Biol Chem. 1997 May 9;272(19):12634-41.

Nowak DE, Tian B, Brasier AR. Two-step cross-linking method for identification of NF-kappaB gene network by chromatin immunoprecipitation. Biotechniques. 2005 Nov;39(5):715-25.

Nuss JE, Patrick SM, Oakley GG, Alter GM, Robison JG, Dixon K, Turchi JJ. DNA damage induced hyperphosphorylation of replication protein A. 1. Identification of novel sites of phosphorylation in response to DNA damage. Biochemistry. 2005 Jun 14;44(23):8428-37.

Oberdoerffer P, Michan S, McVay M, Mostoslavsky R, Vann J, Park SK, Hartlerode A, Stegmuller J, Hafner A, Loerch P, Wright SM, Mills KD, Bonni A, Yankner BA, Scully R, Prolla TA, Alt FW, Sinclair DA. SIRT1 redistribution on chromatin promotes genomic stability but alters gene expression during aging. Cell. 2008 Nov 28;135(5):907-18.

Ohama T, Wang L, Griner EM, Brautigan DL. Protein Ser/Thr phosphatase-6 is required for maintenance of E-cadherin at adherens junctions. BMC Cell Biol. 2013 Sep 25;14:42.

O'Neill BM, Szyjka SJ, Lis ET, Bailey AO, Yates JR 3rd, Aparicio OM, Romesberg FE. Pph3-Psy2 is a phosphatase complex required for Rad53 dephosphorylation and replication fork restart during recovery from DNA damage. Proc Natl Acad Sci U S A. 2007 May 29;104(22):9290-5.

Ong MS, Richmond TJ, Davey CA. DNA stretching and extreme kinking in the nucleosome core. J Mol Biol. 2007 May 11;368(4):1067-74.

Osipovich O, Milley R, Meade A, Tachibana M, Shinkai Y, Krangel MS, Oltz EM. Targeted inhibition of V(D)J recombination by a histone methyltransferase. Nat Immunol. 2004 Mar;5(3):309-16.

Otterlei M, Bruheim P, Ahn B, Bussen W, Karmakar P, Baynton K, Bohr VA. (2006) Werner syndrome protein participates in a complex with RAD51, RAD54, RAD54B and

ATR in response to ICL-induced replication arrest. J Cell Sci. Dec 15;119(Pt 24): 5137-46.

Palazzo L, Mikoč A, Ahel I. ADP-ribosylation: new facets of an ancient modification. FEBS J. 2017 Sep;284(18):2932-2946.

Park J, Chen Y, Tishkoff DX, Peng C, Tan M, Dai L, Xie Z, Zhang Y, Zwaans BM, Skinner ME, Lombard DB, Zhao Y. SIRT5-mediated lysine desuccinylation impacts diverse metabolic pathways. Mol Cell. 2013 Jun 27;50(6):919-30.

Park JM, Yang SW, Yu KR, Ka SH, Lee SW, Seol JH, Jeon YJ, Chung CH. Modification of PCNA by ISG15 plays a crucial role in termination of error-prone translesion DNA synthesis. Mol Cell. 2014 May 22;54(4):626-38.

Park SH, Yu SE, Chai YG, Jang YK. CDK2-dependent phosphorylation of Suv39H1 is involved in control of heterochromatin replication during cell cycle progression. Nucleic Acids Res. 2014 Jun;42(10):6196-207.

Park YS, Jin MY, Kim YJ, Yook JH, Kim BS, Jang SJ. The global histone modification pattern correlates with cancer recurrence and overall survival in gastric adenocarcinoma. Ann Surg Oncol. 2008 Jul;15(7):1968-76.

Parthun MR. Hat1: the emerging cellular roles of a type B histone acetyltransferase. Oncogene. 2007 Aug 13;26(37):5319–28.

Paulson JR, Taylor SS. Phosphorylation of histones 1 and 3 and nonhistone high mobility group 14 by an endogenous kinase in HeLa metaphase chromosomes. J Biol Chem. 1982 Jun 10;257(11):6064-72.

Pawelczak KS, Bennett SM, Turchi JJ. Coordination of DNA-PK activation and nuclease processing of DNA termini in NHEJ. Antioxid Redox Signal. 2011 Jun 15;14(12):2531-43.

Pearson CK. ADP-ribosylation reactions. Principles of Medical Biology. 1995.

Perrone S, Lotti F, Geronzi U, Guidoni E, Longini M, Buonocore G. Oxidative Stress in Cancer-Prone Genetic Diseases in Pediatric Age: The Role of Mitochondrial Dysfunction. Oxid Med Cell Longev. 2016; 2016:4782426.

Perry P, Evans HJ. Cytological detection of mutagen-carcinogen exposure by sister chromatid exchange. Nature. 1975 Nov 13;258(5531):121-5.

Peters AH, Kubicek S, Mechtler K, O'Sullivan RJ, Derijck AA, Perez-Burgos L, Kohlmaier A, Opravil S, Tachibana M, Shinkai Y, Martens JH, Jenuwein T. Partitioning and plasticity of repressive histone methylation states in mammalian chromatin. Mol Cell. 2003 Dec;12(6):1577-89.

Peters AH, O'Carroll D, Scherthan H, Mechtler K, Sauer S, Schöfer C, Weipoltshammer K, Pagani M, Lachner M, Kohlmaier A, Opravil S, Doyle M, Sibilia M, Jenuwein T. Loss of

the Suv39h histone methyltransferases impairs mammalian heterochromatin and genome stability. Cell. 2001 Nov 2;107(3):323-37.

Petti E, Jordi F, Buemi V, Dinami R, Benetti R, Blasco MA, Schoeftner S. Altered telomere homeostasis and resistance to skin carcinogenesis in Suv39h1 transgenic mice. Cell Cycle. 2015;14(9):1438-46.

Picard F, Kurtev M, Chung N, Topark-Ngarm A, Senawong T, Machado De Oliveira R, Leid M, McBurney MW, Guarente L. Sirt1 promotes fat mobilization in white adipocytes by repressing PPAR-gamma. Nature. 2004 Jun 17;429(6993):771-6.

Ponugoti B, Kim DH, Xiao Z, Smith Z, Miao J, Zang M, Wu SY, Chiang CM, Veenstra TD, Kemper JK. SIRT1 deacetylates and inhibits SREBP-1C activity in regulation of hepatic lipid metabolism. J Biol Chem. 2010 Oct 29;285(44):33959-70.

Qiang L, Wang L, Kon N, Zhao W, Lee S, Zhang Y, Rosenbaum M, Zhao Y, Gu W, Farmer SR, Accili D. Brown remodeling of white adipose tissue by SirT1-dependent deacetylation of Pparγ. Cell. 2012 Aug 3;150(3):620-32.

Qin J, Li Q, Zeng Z, Wu P, Jiang Y, Luo T, Ji X, Zhang Q, Hao Y, Chen L. Increased expression of G9A contributes to carcinogenesis and indicates poor prognosis in hepatocellular carcinoma. Oncol Lett. 2018 Jun;15(6):9757-9765.

Rahman S, Islam R. Mammalian Sirt1: insights on its biological functions. Cell Commun Signal. 2011 May 8; 9:11.

Ran LK, Chen Y, Zhang ZZ, Tao NN, Ren JH, Zhou L, Tang H, Chen X, Chen K, Li WY, Huang AL, Chen J. SIRT6 Overexpression Potentiates Apoptosis Evasion in Hepatocellular Carcinoma via BCL2-Associated X Protein-Dependent Apoptotic Pathway. Clin Cancer Res. 2016 Jul 1;22(13):3372-82

Ran LK, Chen Y, Zhang ZZ, Tao NN, Ren JH, Zhou L, Tang H, Chen X, Chen K, Li WY, Huang AL, Chen J. SIRT6 Overexpression Potentiates Apoptosis Evasion in Hepatocellular Carcinoma via BCL2-Associated X Protein-Dependent Apoptotic Pathway. Clin Cancer Res. 2016 Jul 1;22(13):3372-82.

Rao VK, Ow JR, Shankar SR, Bharathy N, Manikandan J, Wang Y, Taneja R. G9a promotes proliferation and inhibits cell cycle exit during myogenic differentiation. Nucleic Acids Res. 2016 Sep 30;44(17):8129-43.

Rardin MJ, He W, Nishida Y, Newman JC, Carrico C, Danielson SR, Guo A, Gut P, Sahu AK, Li B, Uppala R, Fitch M, Riiff T, Zhu L, Zhou J, Mulhern D, Stevens RD, Ilkayeva OR, Newgard CB, Jacobson MP, Hellerstein M, Goetzman ES, Gibson BW, Verdin E. SIRT5 regulates the mitochondrial lysine succinylome and metabolic networks. Cell Metab. 2013 Dec 3;18(6):920-33.

Rea S, Eisenhaber F, O'Carroll D, Strahl BD, Sun ZW, Schmid M, Opravil S, Mechtler K, Ponting CP, Allis CD, Jenuwein T. Regulation of chromatin structure by site-specific histone H3 methyltransferases. Nature. 2000 Aug 10;406(6796):593-9.

Reddy P, Liu L, Ren C, Lindgren P, Boman K, Shen Y, Lundin E, Ottander U, Rytinki M, Liu K. Formation of E-cadherin-mediated cell-cell adhesion activates AKT and mitogen activated protein kinase via phosphatidylinositol 3 kinase and ligand-independent activation of epidermal growth factor receptor in ovarian cancer cells. Mol Endocrinol. 2005 Oct;19(10):2564-78.

Reed-Inderbitzin E, Moreno-Miralles I, Vanden-Eynden SK, Xie J, Lutterbach B, Durst-Goodwin KL, Luce KS, Irvin BJ, Cleary ML, Brandt SJ, Hiebert SW. RUNX1 associates with histone deacetylases and SUV39H1 to repress transcription. Oncogene. 2006 Sep 21;25(42):5777-86.

Reuter S, Gupta SC, Chaturvedi MM, Aggarwal BB. Oxidative stress, inflammation, and cancer: how are they linked? Free Radic Biol Med. 2010 Dec 1;49(11):1603-16.

Revollo JR, Li X. The ways and means that fine tune Sirt1 activity. Trends Biochem Sci. 2013 Mar;38(3):160-7.

Reyes-Turcu FE, Ventii KH, Wilkinson KD. Regulation and cellular roles of ubiquitin-specific deubiquitinating enzymes. Annu Rev Biochem. 2009; 78:363-97.

Rezazadeh S, Yang D, Biashad SA, Firsanov D, Takasugi M, Gilbert M, Tombline G, Bhanu NV, Garcia BA, Seluanov A, Gorbunova V. SIRT6 mono-ADP ribosylates KDM2A to locally increase H3K36me2 at DNA damage sites to inhibit transcription and promote repair. Aging (Albany NY). 2020 Jun 25;12(12):11165-11184.

Rezazadeh S, Yang D, Tombline G, Simon M, Regan SP, Seluanov A, Gorbunova V. SIRT6 promotes transcription of a subset of NRF2 targets by mono-ADP-ribosylating BAF170. Nucleic Acids Res. 2019 Sep 5;47(15):7914-7928.

Ribeiro-Mason K, Boulesteix C, Fleurot R, Aguirre-Lavin T, Adenot P, Gall L, Debey P, Beaujean N. H3S10 phosphorylation marks constitutive heterochromatin during interphase in early mouse embryos until the 4-cell stage. J Reprod Dev. 2012;58(4):467-75.

Rice JC, Briggs SD, Ueberheide B, Barber CM, Shabanowitz J, Hunt DF, Shinkai Y, Allis CD. Histone methyltransferases direct different degrees of methylation to define distinct chromatin domains. Mol Cell. 2003 Dec;12(6):1591-8.

Rodgers JT, Lerin C, Haas W, Gygi SP, Spiegelman BM, Puigserver P. Nutrient control of glucose homeostasis through a complex of PGC-1alpha and SIRT1. Nature. 2005 Mar 3;434(7029):113-8.

Rodrigues C, Pattabiraman C, Vijaykumar A, Arora R, Narayana SM, Kumar RV, Notani D, Varga-Weisz P, Krishna S. A SUV39H1-low chromatin state characterises and promotes migratory properties of cervical cancer cells. Exp Cell Res. 2019 May 15;378(2):206-216.

Rogakou EP, Pilch DR, Orr AH, Ivanova VS, Bonner WM. DNA double-stranded breaks induce histone H2AX phosphorylation on serine 139. J Biol Chem. 1998 Mar 6;273(10):5858-68.

Roopra A, Qazi R, Schoenike B, Daley TJ, Morrison JF. Localized domains of G9a-mediated histone methylation are required for silencing of neuronal genes. Mol Cell. 2004 Jun 18;14(6):727-38.

Ruan L, Wang L, Wang X, He M, Yao X. SIRT1 contributes to neuroendocrine differentiation of prostate cancer. Oncotarget. 2017 Dec 11;9(2):2002-2016.

Ryu D, Jo YS, Lo Sasso G, Stein S, Zhang H, Perino A, Lee JU, Zeviani M, Romand R, Hottiger MO, Schoonjans K, Auwerx J. A SIRT7-dependent acetylation switch of GABPβ1 controls mitochondrial function. Cell Metab. 2014 Nov 4;20(5):856-869.

Saksouk N, Simboeck E, Déjardin J. Constitutive heterochromatin formation and transcription in mammals. Epigenetics Chromatin. 2015 Jan 15; 8:3.

Sale JE, Lehmann AR, Woodgate R. Y-family DNA polymerases and their role in tolerance of cellular DNA damage. Nat Rev Mol Cell Biol. 2012 Feb 23;13(3):141-52.

Salminen A, Kaarniranta K. SIRT1: regulation of longevity via autophagy. Cell Signal. 2009 Sep;21(9):1356-60.

San José-Enériz E, Agirre X, Román-Gómez J, Cordeu L, Garate L, Jiménez-Velasco A, Vázquez I, Calasanz MJ, Heiniger A, Torres A, Prósper F. Downregulation of DBC1 expression in acute lymphoblastic leukaemia is mediated by aberrant methylation of its promoter. Br J Haematol. 2006 Jul;134(2):137-44.

Santos-Barriopedro I, Bosch-Presegué L, Marazuela-Duque A, de la Torre C, Colomer C, Vazquez BN, Fuhrmann T, Martínez-Pastor B, Lu W, Braun T, Bober E, Jenuwein T, Serrano L, Esteller M, Chen Z, Barceló-Batllori S, Mostoslavsky R, Espinosa L, Vaquero A. SIRT6-dependent cysteine monoubiquitination in the PRE-SET domain of Suv39h1 regulates the NF-κB pathway. Nat Commun. 2018 Jan 9;9(1):101.

Santos-Barriopedro I, Vaquero A. Complex role of SIRT6 in NF-κB pathway regulation. Mol Cell Oncol. 2018 May 24;5(4):e1445942.

Sasaki T, Maier B, Koclega KD, Chruszcz M, Gluba W, Stukenberg PT, Minor W, Scrable H. Phosphorylation regulates SIRT1 function. PLoS One. 2008;3(12): e4020.

Schärer OD. XPG: its products and biological roles. Adv Exp Med Biol. 2008; 637:83-92.

Scheffer MP, Eltsov M, Frangakis AS. Evidence for short-range helical order in the 30-nm chromatin fibers of erythrocyte nuclei. Proc Natl Acad Sci U S A. 2011 Oct 11;108(41):16992-7.

Scher MB, Vaquero A, Reinberg D. SirT3 is a nuclear NAD+-dependent histone deacetylase that translocates to the mitochondria upon cellular stress. Genes Dev. 2007 Apr 15;21(8):920-8.

Schubbert S, Shannon K, Bollag G. Hyperactive Ras in developmental disorders and cancer. Nat Rev Cancer. 2007 Apr;7(4):295-308.

Schubert HL, Blumenthal RM, Cheng X. Many paths to methyltransfer: a chronicle of convergence. Trends Biochem Sci. 2003 Jun;28(6):329-35.

Schwer B, Bunkenborg J, Verdin RO, Andersen JS, Verdin E. Reversible lysine acetylation controls the activity of the mitochondrial enzyme acetyl-CoA synthetase 2. Proc Natl Acad Sci U S A. 2006 Jul 5;103(27):10224-10229.

Sebastián C, Zwaans BM, Silberman DM, Gymrek M, Goren A, Zhong L, Ram O, Truelove J, Guimaraes AR, Toiber D, Cosentino C, Greenson JK, MacDonald AI, McGlynn L, Maxwell F, Edwards J, Giacosa S, Guccione E, Weissleder R, Bernstein BE, Regev A, Shiels PG, Lombard DB, Mostoslavsky R. The histone deacetylase SIRT6 is a tumor suppressor that controls cancer metabolism. Cell. 2012 Dec 7;151(6):1185-99.

Sedelnikova OA, Rogakou EP, Panyutin IG, Bonner WM. Quantitative detection of (125) IdU-induced DNA double-strand breaks with gamma-H2AX antibody. Radiat Res. 2002 Oct;158(4):486-92.

Shaltiel IA, Aprelia M, Saurin AT, Chowdhury D, Kops GJ, Voest EE, Medema RH. Distinct phosphatases antagonize the p53 response in different phases of the cell cycle. Proc Natl Acad Sci U S A. 2014 May 20;111(20):7313-8.

Shankar SR, Bahirvani AG, Rao VK, Bharathy N, Ow JR, Taneja R. G9a, a multipotent regulator of gene expression. Epigenetics. 2013 Jan;8(1):16-22.

Shen P, Feng X, Zhang X, Huang X, Liu S, Lu X, Li J, You J, Lu J, Li Z, Ye J, Liu P. SIRT6 suppresses phenylephrine-induced cardiomyocyte hypertrophy though inhibiting p300. J Pharmacol Sci. 2016 Sep;132(1):31-40.

Shi Y, Sawada J, Sui G, Affar el B, Whetstine JR, Lan F, Ogawa H, Luke MP, Nakatani Y, Shi Y. Coordinated histone modifications mediated by a CtBP co-repressor complex. Nature. 2003 Apr 17;422(6933):735-8.

Shiio Y, Eisenman RN. Histone sumoylation is associated with transcriptional repression. Proc Natl Acad Sci USA. National Acad Sciences; 2003 Nov 11;100(23):13225–30.

Shinkai Y, Tachibana M. H3K9 methyltransferase G9a and the related molecule GLP. Genes Dev. 2011 Apr 15;25(8):781-8.

Shoemaker CB, Chalkley R. An H3 histone-specific kinase isolated from bovine thymus chromatin. J Biol Chem. 1978 Aug 25;253(16):5802-7.

Simon R, Samuel CE. Activation of NF-kappaB-dependent gene expression by Salmonella flagellins FliC and FljB. Biochem Biophys Res Commun. 2007 Mar 30;355(1):280-5.

Simonet NG, Thackray JK, Vazquez BN, Ianni A, Espinosa-Alcantud M, Morales-Sanfrutos J, Hurtado-Bagès S, Sabidó E, Buschbeck M, Tischfield J, De La Torre C, Esteller M, Braun T, Olivella M, Serrano L, Vaquero A. SirT7 auto-ADP-ribosylation regulates glucose starvation response through mH2A1. Sci Adv. 2020 Jul 24;6(30):eaaz2590.

Simonet, N.G., Rasti, G., and Vaquero, A. Chapter 21 The Histone Code and Disease: Posttranslational Modifications as Potential Prognostic Factors for Clinical Diagnosis. Epigenetic Biomarkers and Diagnostics, (Elsevier), 2016 Dec pp. 417–445.

Smothers JF, Henikoff S. The HP1 chromo shadow domain binds a consensus peptide pentamer. Curr Biol. 2000 Jan 13;10(1):27-30.

Stefansson B, Brautigan DL. Protein phosphatase PP6 N terminal domain restricts G1 to S phase progression in human cancer cells. Cell Cycle. 2007 Jun 1;6(11):1386-92.

Stults DM, Killen MW, Marco-Casanova P, Pierce AJ. The Sister Chromatid Exchange (SCE) Assay. Methods Mol Biol. 2020; 2102:441-457.

Stünkel W, Peh BK, Tan YC, Nayagam VM, Wang X, Salto-Tellez M, Ni B, Entzeroth M, Wood J. Function of the SIRT1 protein deacetylase in cancer. Biotechnol J. 2007 Nov;2(11):1360-8.

Su YW, Chen YP, Chen MY, Reth M, Tan TH. The serine/threonine phosphatase PP4 is required for pro-B cell development through its promotion of immunoglobulin VDJ recombination. PLoS One. 2013 Jul 16;8(7): e68804.

Sundaresan NR, Gupta M, Kim G, Rajamohan SB, Isbatan A, Gupta MP. Sirt3 blocks the cardiac hypertrophic response by augmenting Foxo3a-dependent antioxidant defense mechanisms in mice. J Clin Invest. 2009 Sep;119(9):2758-71.

Sundaresan NR, Vasudevan P, Zhong L, Kim G, Samant S, Parekh V, Pillai VB, Ravindra PV, Gupta M, Jeevanandam V, Cunningham JM, Deng CX, Lombard DB, Mostoslavsky R,

Gupta MP. The sirtuin SIRT6 blocks IGF-Akt signaling and development of cardiac hypertrophy by targeting c-Jun. Nat Med. 2012 Nov;18(11):1643-50.

Sutton A, Immanuel D, Arndt KT. The SIT4 protein phosphatase functions in late G1 for progression into S phase. Mol Cell Biol. 1991 Apr;11(4):2133-48.

Swindell WR. Genes and gene expression modules associated with caloric restriction and aging in the laboratory mouse. BMC Genomics. 2009 Dec 7; 10:585.

Tachibana M, Sugimoto K, Fukushima T, Shinkai Y. Set domain-containing protein, G9a, is a novel lysine-preferring mammalian histone methyltransferase with hyperactivity and specific selectivity to lysines 9 and 27 of histone H3. J Biol Chem. 2001 Jul 6;276(27):25309-17.

Tachibana M, Sugimoto K, Nozaki M, Ueda J, Ohta T, Ohki M, Fukuda M, Takeda N, Niida H, Kato H, Shinkai Y. G9a histone methyltransferase plays a dominant role in euchromatic histone H3 lysine 9 methylation and is essential for early embryogenesis. Genes Dev. 2002 Jul 15;16(14):1779-91.

Tachibana M, Ueda J, Fukuda M, Takeda N, Ohta T, Iwanari H, Sakihama T, Kodama T, Hamakubo T, Shinkai Y. Histone methyltransferases G9a and GLP form heteromeric complexes and are both crucial for methylation of euchromatin at H3-K9. Genes Dev. 2005 Apr 1;19(7):815-26.

Tan M, Peng C, Anderson KA, Chhoy P, Xie Z, Dai L, Park J, Chen Y, Huang H, Zhang Y, Ro J, Wagner GR, Green MF, Madsen AS, Schmiesing J, Peterson BS, Xu G, Ilkayeva OR, Muehlbauer MJ, Braulke T, Mühlhausen C, Backos DS, Olsen CA, McGuire PJ, Pletcher SD, Lombard DB, Hirschey MD, Zhao Y. Lysine glutarylation is a protein posttranslational modification regulated by SIRT5. Cell Metab. 2014 Apr 1;19(4):605-17.

Tanner KG, Landry J, Sternglanz R, Denu JM. Silent information regulator 2 family of NAD- dependent histone/protein deacetylases generates a unique product, 1-O-acetyl-ADP-ribose. Proc Natl Acad Sci U S A. 2000 Dec 19;97(26):14178-82.

Tao R, Xiong X, DePinho RA, Deng CX, Dong XC. Hepatic SREBP-2 and cholesterol biosynthesis are regulated by FoxO3 and Sirt6. J Lipid Res. 2013 Oct;54(10):2745-53.

Tasselli L, Xi Y, Zheng W, Tennen RI, Odrowaz Z, Simeoni F, Li W, Chua KF. SIRT6 deacetylates H3K18ac at pericentric chromatin to prevent mitotic errors and cellular senescence. Nat Struct Mol Biol. 2016 May;23(5):434-40.

Tennen RI, Berber E, Chua KF. Functional dissection of SIRT6: identification of domains that regulate histone deacetylase activity and chromatin localization. Mech Ageing Dev. 2010 Mar;131(3):185-92.

Tennen RI, Bua DJ, Wright WE, Chua KF. SIRT6 is required for maintenance of telomere position effect in human cells. Nat Commun. 2011 Aug 16; 2:433.

Teperino R, Schoonjans K, Auwerx J. Histone methyl transferases and demethylases; can they link metabolism and transcription? Cell Metab. 2010 Oct 6;12(4):321-327.

Thompson LH, Hinz JM, Yamada NA, Jones NJ. How Fanconi anemia proteins promote the four Rs: replication, recombination, repair, and recovery. Environ Mol Mutagen. 2005 Mar-Apr;45(2-3):128-42.

Timinszky G, Till S, Hassa PO, Hothorn M, Kustatscher G, Nijmeijer B, Colombelli J, Altmeyer M, Stelzer EH, Scheffzek K, Hottiger MO, Ladurner AG. A macrodomain-containing histone rearranges chromatin upon sensing PARP1 activation. Nat Struct Mol Biol. 2009 Sep;16(9):923-9.

Timmons JA, Wennmalm K, Larsson O, Walden TB, Lassmann T, Petrovic N, Hamilton DL, Gimeno RE, Wahlestedt C, Baar K, Nedergaard J, Cannon B. Myogenic gene expression signature establishes that brown and white adipocytes originate from distinct cell lineages. Proc Natl Acad Sci U S A. 2007 Mar 13;104(11):4401-6.

Toiber D, Erdel F, Bouazoune K, Silberman DM, Zhong L, Mulligan P, Sebastian C, Cosentino C, Martinez-Pastor B, Giacosa S, D'Urso A, Näär AM, Kingston R, Rippe K, Mostoslavsky R. SIRT6 recruits SNF2H to DNA break sites, preventing genomic instability through chromatin remodeling. Mol Cell. 2013 Aug 22;51(4):454-68.

Tontonoz P, Spiegelman BM. Fat and beyond: the diverse biology of PPARgamma. Annu Rev Biochem. 2008; 77:289-312.

Torrens-Mas M, Oliver J, Roca P, Sastre-Serra J. SIRT3: Oncogene and Tumor Suppressor in Cancer. Cancers (Basel). 2017 Jul 12;9(7):90.

Toyo-oka K, Mori D, Yano Y, Shiota M, Iwao H, Goto H, Inagaki M, Hiraiwa N, Muramatsu M, Wynshaw-Boris A, Yoshiki A, Hirotsune S. Protein phosphatase 4 catalytic subunit regulates Cdk1 activity and microtubule organization via NDEL1 dephosphorylation. J Cell Biol. 2008 Mar 24;180(6):1133-47.

Tsai YC, Greco TM, Boonmee A, Miteva Y, Cristea IM. Functional proteomics establishes the interaction of SIRT7 with chromatin remodeling complexes and expands its role in regulation of RNA polymerase I transcription. Mol Cell Proteomics. 2012 May;11(5):60-76.

Tubbs JL, Latypov V, Kanugula S, Butt A, Melikishvili M, Kraehenbuehl R, Fleck O, Marriott A, Watson AJ, Verbeek B, McGown G, Thorncroft M, Santibanez-Koref MF, Millington C, Arvai AS, Kroeger MD, Peterson LA, Williams DM, Fried MG, Margison GP, Pegg AE, Tainer JA. Flipping of alkylated DNA damage bridges base and nucleotide excision repair. Nature. 2009 Jun 11;459(7248):808-13.

Tumaneng K, Russell RC, Guan KL. Organ size control by Hippo and TOR pathways. Curr Biol. 2012 May 8;22(9): R368-79.

Uhrig RG, Labandera AM, Moorhead GB. Arabidopsis PPP family of serine/threonine protein phosphatases: many targets but few engines. Trends Plant Sci. 2013 Sep;18(9):505-13.

Vaisman A, Woodgate R. Translesion DNA polymerases in eukaryotes: what makes them tick? Crit Rev Biochem Mol Biol. 2017 Jun;52(3):274-303.

Van Hoof C, Goris J. Phosphatases in apoptosis: to be or not to be, PP2A is in the heart of the question. Biochim Biophys Acta. 2003 May 12;1640(2-3):97-104.

Van Meter M, Kashyap M, Rezazadeh S, Geneva AJ, Morello TD, Seluanov A, Gorbunova V. SIRT6 represses LINE1 retrotransposons by ribosylating KAP1 but this repression fails with stress and age. Nat Commun. 2014 Sep 23; 5:5011.

Van Meter M, Simon M, Tombline G, May A, Morello TD, Hubbard BP, Bredbenner K, Park R, Sinclair DA, Bohr VA, Gorbunova V, Seluanov A. JNK Phosphorylates SIRT6 to Stimulate DNA Double-Strand Break Repair in Response to Oxidative Stress by Recruiting PARP1 to DNA Breaks. Cell Rep. 2016 Sep 6;16(10):2641-2650.

Vandel L, Nicolas E, Vaute O, Ferreira R, Ait-Si-Ali S, Trouche D. Transcriptional repression by the retinoblastoma protein through the recruitment of a histone methyltransferase. Mol Cell Biol. 2001 Oct;21(19):6484-94.

Vaquero A, Scher M, Erdjument-Bromage H, Tempst P, Serrano L, Reinberg D. SIRT1 regulates the histone methyl-transferase SUV39H1 during heterochromatin formation. Nature. 2007 Nov 15;450(7168):440-4.

Vaquero A, Scher M, Lee D, Erdjument-Bromage H, Tempst P, Reinberg D. Human SirT1 interacts with histone H1 and promotes formation of facultative heterochromatin. Mol Cell. 2004 Oct 8;16(1):93-105.

Vassilopoulos A, Fritz KS, Petersen DR, Gius D. The human sirtuin family: evolutionary divergences and functions. Hum Genomics. 2011 Jul;5(5):485-96.

Vaziri H, Dessain SK, Ng Eaton E, Imai SI, Frye RA, Pandita TK, Guarente L, Weinberg RA. hSIR2(SIRT1) functions as an NAD-dependent p53 deacetylase. Cell. 2001 Oct 19;107(2):149-59.

Vazquez BN, Thackray JK, Simonet NG, Kane-Goldsmith N, Martinez-Redondo P, Nguyen T, Bunting S, Vaquero A, Tischfield JA, Serrano L. SIRT7 promotes genome integrity and modulates non-homologous end joining DNA repair. EMBO J. 2016 Jul 15;35(14):1488-503.

Virshup DM, Shenolikar S. From promiscuity to precision: protein phosphatases get a makeover. Mol Cell. 2009 Mar 13;33(5):537-45.
Visconti R, Grieco D. New insights on oxidative stress in cancer. Curr Opin Drug Discov Devel. 2009 Mar;12(2):240-5.

Vlachopoulos, C., Tsekoura, D., Alexopoulos, N., Panagiotakos, D., Aznaouridis, K., Stefanadis, C., 2004. Type 5 phosphodiesterase inhibition bysildenafilabrogates acute smoking-induced endothelial dysfunction. Am. J. Hypertens. 17, 1040–1044.

Voss M, Campbell K, Saranzewa N, Campbell DG, Hastie CJ, Peggie MW, Martin-Granados C, Prescott AR, Cohen PT. Protein phosphatase 4 is phosphorylated and inactivated by Cdk in response to spindle toxins and interacts with γ-tubulin. Cell Cycle. 2013 Sep 1;12(17):2876-87.

Wan Y, Liu Y, Wang X, Wu J, Liu K, Zhou J, Liu L, Zhang C. Identification of differential microRNAs in cerebrospinal fluid and serum of patients with major depressive disorder. PLoS One. 2015 Mar 12;10(3):e0121975.

Wang D, Zhou J, Liu X, Lu D, Shen C, Du Y, Wei FZ, Song B, Lu X, Yu Y, Wang L, Zhao Y, Wang H, Yang Y, Akiyama Y, Zhang H, Zhu WG. Methylation of SUV39H1 by SET7/9 results in heterochromatin relaxation and genome instability. Proc Natl Acad Sci U S A. 2013 Apr 2;110(14):5516-21.

Wang F, Nguyen M, Qin FX, Tong Q. SIRT2 deacetylates FOXO3a in response to oxidative stress and caloric restriction. Aging Cell. 2007 Aug;6(4):505-14.

Wang H, Zhou X, Huang J, Mu N, Guo Z, Wen Q, Wang R, Chen S, Feng ZP, Zheng W. The role of Akt/FoxO3a in the protective effect of venlafaxine against corticosterone-induced cell death in PC12 cells. Psychopharmacology (Berl). 2013 Jul;228(1):129-41.

Wang L, Ma L, Pang S, Huang J, Yan B. Sequence Variants of SIRT6 Gene Promoter in Myocardial Infarction. Genet Test Mol Biomarkers. 2016 Apr;20(4):185-90.

Wang P, Chen T, Sakurai K, Han BX, He Z, Feng G, Wang F. Intersectional Cre driver lines generated using split-intein mediated split-Cre reconstitution. Sci Rep. 2012; 2:497.

Wang RH, Sengupta K, Li C, Kim HS, Cao L, Xiao C, Kim S, Xu X, Zheng Y, Chilton B, Jia R, Zheng ZM, Appella E, Wang XW, Ried T, Deng CX. Impaired DNA damage response, genome instability, and tumorigenesis in SIRT1 mutant mice. Cancer Cell. 2008 Oct 7;14(4):312-23.

Wang RH, Zheng Y, Kim HS, Xu X, Cao L, Luhasen T, Lee MH, Xiao C, Vassilopoulos A, Chen W, Gardner K, Man YG, Hung MC, Finkel T, Deng CX. Interplay among BRCA1, SIRT1, and Survivin during BRCA1-associated tumorigenesis. Mol Cell. 2008 Oct 10;32(1):11-20.

Wang YF, Zhang J, Su Y, Shen YY, Jiang DX, Hou YY, Geng MY, Ding J, Chen Y. G9a regulates breast cancer growth by modulating iron homeostasis through the repression of ferroxidase hephaestin. Nat Commun. 2017 Aug 17;8(1):274.

Watson GW, Wickramasekara S, Palomera-Sanchez Z, Black C, Maier CS, Williams DE, Dashwood RH, Ho E. SUV39H1/H3K9me3 attenuates sulforaphane-induced apoptotic signaling in PC3 prostate cancer cells. Oncogenesis. 2014 Dec 8;3(12):e131

Wei Y, Yu L, Bowen J, Gorovsky MA, Allis CD. Phosphorylation of histone H3 is required for proper chromosome condensation and segregation. Cell. 1999 Apr 2;97(1):99–109.

Weir HJ, Lane JD, Balthasar N. SIRT3: A Central Regulator of Mitochondrial Adaptation in Health and Disease. Genes Cancer. 2013 Mar;4(3-4):118-24.

Wengrod J, Wang D, Weiss S, Zhong H, Osman I, Gardner LB. Phosphorylation of eIF2α triggered by mTORC1 inhibition and PP6C activation is required for autophagy and is aberrant in PP6C-mutated melanoma. Sci Signal. 2015 Mar 10;8(367):ra27.

White D, Rafalska-Metcalf IU, Ivanov AV, Corsinotti A, Peng H, Lee SC, Trono D, Janicki SM, Rauscher FJ 3rd. The ATM substrate KAP1 controls DNA repair in heterochromatin: regulation by HP1 proteins and serine 473/824 phosphorylation. Mol Cancer Res. 2012 Mar;10(3):401-14.

Wilson AS, Power BE, Molloy PL. DNA hypomethylation and human diseases. Biochim Biophys Acta. 2007 Jan;1775(1):138-62.

Wolff DJ, Miller AP, Van Dyke DL, Schwartz S, Willard HF. Molecular definition of breakpoints associated with human Xq isochromosomes: implications for mechanisms of formation. Am J Hum Genet. 1996 Jan;58(1):154-60.

Woodcock CL. Chromatin fibers observed in situ in frozen hydrated sections. Native fiber diameter is not correlated with nucleosome repeat length. J Cell Biol. 1994 Apr;125(1):11-9.

Wozniak RJ, Klimecki WT, Lau SS, Feinstein Y, Futscher BW. 5-Aza-2'-deoxycytidine-mediated reductions in G9A histone methyltransferase and histone H3 K9 di-methylation levels are linked to tumor suppressor gene reactivation. Oncogene. 2007 Jan 4;26(1):77-90.

Wright DE, Wang CY, Kao CF. Histone ubiquitylation and chromatin dynamics. Front Biosci (Landmark Ed). 2012 Jan 1;17:1051-78.

Wu D, Li Y, Zhu KS, Wang H, Zhu WG. Advances in Cellular Characterization of the Sirtuin Isoform, SIRT7. Front Endocrinol (Lausanne). 2018 Nov 19;9:652.

Wu D, Qiu Y, Gao X, Yuan XB, Zhai Q. Overexpression of SIRT1 in mouse forebrain impairs lipid/glucose metabolism and motor function. PLoS One. 2011;6(6):e21759.

Wu HI, Brown JA, Dorie MJ, Lazzeroni L, Brown JM. Genome-wide identification of genes conferring resistance to the anticancer agents cisplatin, oxaliplatin, and mitomycin C. Cancer Res. 2004 Jun 1;64(11):3940-8.

Xia CH, Ma Z, Ciric R, Gu S, Betzel RF, Kaczkurkin AN, Calkins ME, Cook PA, García de la Garza A, Vandekar SN, Cui Z, Moore TM, Roalf DR, Ruparel K, Wolf DH, Davatzikos C, Gur RC, Gur RE, Shinohara RT, Bassett DS, Satterthwaite TD. Linked dimensions of psychopathology and connectivity in functional brain networks. Nat Commun. 2018 Aug 1;9(1):3003.

Yamamori T, DeRicco J, Naqvi A, Hoffman TA, Mattagajasingh I, Kasuno K, Jung SB, Kim CS, Irani K. SIRT1 deacetylates APE1 and regulates cellular base excision repair. Nucleic Acids Res. 2010 Jan;38(3):832-45.

Yamamoto H, Schoonjans K, Auwerx J. Sirtuin functions in health and disease. Mol Endocrinol. 2007 Aug;21(8):1745-55.

Yang B, Zwaans BM, Eckersdorff M, Lombard DB. The sirtuin SIRT6 deacetylates H3 K56Ac in vivo to promote genomic stability. Cell Cycle. 2009 Aug 15;8(16):2662-3.

Yang H, Zhang W, Pan H, Feldser HG, Lainez E, Miller C, Leung S, Zhong Z, Zhao H, Sweitzer S, Considine T, Riera T, Suri V, White B, Ellis JL, Vlasuk GP, Loh C. SIRT1 activators suppress inflammatory responses through promotion of p65 deacetylation and inhibition of NF-κB activity. PLoS One. 2012;7(9):e46364.

Yang L, Chen J. SirT1 and rRNA in the nucleolus: regulating the regulator. Oncoscience. 2014 Mar 15;1(2):111-2.

Yang T, Fu M, Pestell R, Sauve AA. SIRT1 and endocrine signaling. Trends Endocrinol Metab. 2006 Jul;17(5):186-91.

Yang W, Zheng Y, Xia Y, Ji H, Chen X, Guo F, Lyssiotis CA, Aldape K, Cantley LC, Lu Z. ERK1/2-dependent phosphorylation and nuclear translocation of PKM2 promotes the Warburg effect. Nat Cell Biol. 2012 Dec;14(12):1295-304.

Yang X-J, Seto E. HATs and HDACs: from structure, function and regulation to novel strategies for therapy and prevention. Oncogene. Nature Publishing Group; 2007 Aug 13;26(37):5310–8.

Ye X, Li M, Hou T, Gao T, Zhu WG, Yang Y. Sirtuins in glucose and lipid metabolism. Oncotarget. 2017 Jan 3;8(1):1845-1859.

Ye Y, Rape M. Building ubiquitin chains: E2 enzymes at work. Nature Reviews Molecular Cell Biology. 2009 Nov;10(11):755–64.

Yen K, Narasimhan SD, Tissenbaum HA. DAF-16/Forkhead box O transcription factor: many paths to a single Fork(head) in the road. Antioxid Redox Signal. 2011 Feb 15;14(4):623-34.

Yeung F, Hoberg JE, Ramsey CS, Keller MD, Jones DR, Frye RA, Mayo MW. Modulation of NF-kappaB-dependent transcription and cell survival by the SIRT1 deacetylase. EMBO J. 2004 Jun 16;23(12):2369-80.

Yokoyama M, Chiba T, Zen Y, Oshima M, Kusakabe Y, Noguchi Y, Yuki K, Koide S, Tara S, Saraya A, Aoyama K, Mimura N, Miyagi S, Inoue M, Wakamatsu T, Saito T, Ogasawara S, Suzuki E, Ooka Y, Tawada A, Otsuka M, Miyazaki M, Yokosuka O, Iwama A. Histone lysine methyltransferase G9a is a novel epigenetic target for the treatment of hepatocellular carcinoma. Oncotarget. 2017 Mar 28;8(13):21315-21326.

Yokoyama Y, Hieda M, Nishioka Y, Matsumoto A, Higashi S, Kimura H, Yamamoto H, Mori M, Matsuura S, Matsuura N. Cancer-associated upregulation of histone H3 lysine 9 trimethylation promotes cell motility in vitro and drives tumor formation in vivo. Cancer Sci. 2013 Jul;104(7):889-95.

Yoon YS, Lee MW, Ryu D, Kim JH, Ma H, Seo WY, Kim YN, Kim SS, Lee CH, Hunter T, Choi CS, Montminy MR, Koo SH. Suppressor of MEK null (SMEK)/protein phosphatase 4 catalytic subunit (PP4C) is a key regulator of hepatic gluconeogenesis. Proc Natl Acad Sci U S A. 2010 Oct 12;107(41):17704-9.

Youn HD, Liu JO. Cabin1 represses MEF2-dependent Nur77 expression and T cell apoptosis by controlling association of histone deacetylases and acetylases with MEF2. Immunity. 2000 Jul;13(1):85-94.

Yousafzai NA, Zhou Q, Xu W, Shi Q, Xu J, Feng L, Chen H, Shin VY, Jin H, Wang X. SIRT1 deacetylated and stabilized XRCC1 to promote chemoresistance in lung cancer. Cell Death Dis. 2019 May 1;10(5):363.

Yuan J, Luo K, Liu T, Lou Z. Regulation of SIRT1 activity by genotoxic stress. Genes Dev. 2012 Apr 15;26(8):791-6.

Yuan Z, Zhang X, Sengupta N, Lane WS, Seto E. SIRT1 regulates the function of the Nijmegen breakage syndrome protein. Mol Cell. 2007 Jul 6;27(1):149-62.

Yun M, Wu J, Workman JL, Li B. Readers of histone modifications. Cell Res. 2011 Apr;21(4):564-78.

Zeng K, Bastos RN, Barr FA, Gruneberg U. Protein phosphatase 6 regulates mitotic spindle formation by controlling the T-loop phosphorylation state of Aurora A bound to its activator TPX2. J Cell Biol. 2010 Dec 27;191(7):1315-32.

Zhang J, Xiang H, Liu J, Chen Y, He RR, Liu B. Mitochondrial Sirtuin 3: New emerging biological function and therapeutic target. Theranostics. 2020 Jul 9;10(18):8315-8342.

Zhang N, Li Z, Mu W, Li L, Liang Y, Lu M, Wang Z, Qiu Y, Wang Z. Calorie restriction-induced SIRT6 activation delays aging by suppressing NF-κB signaling. Cell Cycle. 2016;15(7):1009-18.

Zhang X, Ozawa Y, Lee H, Wen YD, Tan TH, Wadzinski BE, Seto E. Histone deacetylase 3 (HDAC3) activity is regulated by interaction with protein serine/threonine phosphatase 4. Genes Dev. 2005 Apr 1;19(7):827-39.

Zhang X-Y, Varthi M, Sykes SM, Phillips C, Warzecha C, Zhu W, et al. The putative cancer stem cell marker USP22 is a subunit of the human SAGA complex required for activated transcription and cell-cycle progression. Molecular Cell. 2008 Jan 18;29(1):102–11.

Zhang Y, Hu C, Hong J, Zeng J, Lai S, Lv A, Su Q, Dong Y, Zhou Z, Tang W, Zhao J, Cui L, Zou D, Wang D, Li H, Liu C, Wu G, Shen J, Zhu D, Wang W, Shen W, Ning G, Xu G. Lipid profiling reveals different therapeutic effects of metformin and glipizide in patients with type 2 diabetes and coronary artery disease. Diabetes Care. 2014 Oct;37(10):2804-12.

Zhang Y, Reinberg D. Transcription regulation by histone methylation: interplay between different covalent modifications of the core histone tails. Genes & Development. 2001 Sep 15;15(18):2343–60.

Zhang Z, Jones A, Joo HY, Zhou D, Cao Y, Chen S, et al. USP49 deubiquitinates histone H2B and regulates cotranscriptional pre-mRNA splicing. Genes & Development. 2013 Jul 19;27(14):1581–95.

Zhang ZZ, Cheng YW, Jin HY, Chang Q, Shang QH, Xu YL, Chen LX, Xu R, Song B, Zhong JC. The sirtuin 6 prevents angiotensin II-mediated myocardial fibrosis and injury by targeting AMPK-ACE2 signaling. Oncotarget. 2017 Aug 17;8(42):72302-72314.

Zhao G, Wang H, Xu C, Wang P, Chen J, Wang P, Sun Z, Su Y, Wang Z, Han L, Tong T. SIRT6 delays cellular senescence by promoting p27Kip1 ubiquitin-proteasome degradation. Aging (Albany NY). 2016 Sep 16;8(10):2308-2323.

Zhao W, Kruse JP, Tang Y, Jung SY, Qin J, Gu W. Negative regulation of the deacetylase SIRT1 by DBC1. Nature. 2008 Jan 31;451(7178):587-90.

Zhao Y, Onda K, Sugiyama K, Yuan B, Tanaka S, Takagi N, Hirano T. Antitumor effects of arsenic disulfide on the viability, migratory ability, apoptosis and autophagy of breast cancer cells. Oncol Rep. 2019 Jan;41(1):27-42.

Zhong L, D'Urso A, Toiber D, Sebastian C, Henry RE, Vadysirisack DD, Guimaraes A, Marinelli B, Wikstrom JD, Nir T, Clish CB, Vaitheesvaran B, Iliopoulos O, Kurland I, Dor

Y, Weissleder R, Shirihai OS, Ellisen LW, Espinosa JM, Mostoslavsky R. The histone deacetylase Sirt6 regulates glucose homeostasis via Hif1alpha. Cell. 2010 Jan 22;140(2):280-93

Zhou G, Mihindukulasuriya KA, MacCorkle-Chosnek RA, Van Hooser A, Hu MC, Brinkley BR, Tan TH. Protein phosphatase 4 is involved in tumor necrosis factor-alpha-induced activation of c-Jun N-terminal kinase. J Biol Chem. 2002 Feb 22;277(8):6391-8.